Origin of the Universe: statistical properties of primordial perturbations

by

Sabir Ramazanov

A THESIS SUBMITTED IN PARTIAL FULFILMENT
OF THE REQUIREMENTS OF

DOCTOR OF PHILOSOPHY
in
The Faculty of Sciences
(Niels Bohr International Academy)

THE UNIVERSITY OF COPENHAGEN
17 September 2012

Abstract

Recently, it has been proposed to relate properties of primordial scalar perturbations to the conformal invariance of some very early Universe models. A concrete realization of this idea is given in the context of the conformal rolling scenario. The main ingredient of the latter is the complex scalar field conformally coupled to gravity and rolling down the negative quartic potential. During the conformal rolling, phase perturbations acquire flat power spectrum, which can be converted into adiabatic perturbations at some later epoch by one of another mechanism. There are two sub-scenarios of the model depending on the behavior of the cosmologically interesting modes by the end of the rolling: one with superhorizon modes and the other with subhorizon ones. In the latter case, phase perturbations proceed to evolve at the intermediate stage between conformal rolling and conventional epoch. This evolution results into the small negative tilt, statistical anisotropy of all even multipoles starting from quadrupole of general structure and non-Gaussianity of the peculiar form. The signatures of the former sub-scenario are the quadrupole statistical anisotropy of both general and quadrupole types and the non-Gaussianity with a (fairly mild) singularity in the folded limit. We review analogous predictions in the context of the inflation and conclude that the conformal rolling scenario can be descriminated from the inflation in future experiments. We also discuss the novel cosmological scenario of the early Universe, where the potential role of conformal symmetries is understood from a much broader prospective. In this picture, proposed by Hinterbichler and Khoury, conformal rolling scenario is just a particular case in a myriad of possible models. We review the main novelties and assumptions of the general setup, and show that predictions made in the framework of the conformal rolling scenario hold for a broad class of models, e.g. the Galilean Genesis.

Starting from the particular prediction, the statistical anisotropy, we constrain the unique parameter h^2 of the conformal rolling scenario. For this purpose, we employ the quadratic maximum likelihood method, and apply it to the search of the statistical anisotropy in the seven-year WMAP data. We confirm the large quadrupole anisotropy detected in V and W bands, which has been argued to originate from systematic effects rather than from cosmology. We construct an estimator for the parameter h^2. In the case of the sub-scenario with the intermediate stage we set an upper limit $h^2 < 0.045$ at the 95% confidence level. The constraint on h^2 is much weaker in the case of another sub-scenario, where the intermediate stage is absent. We also comment on the statistical anisotropy recently detected in the CMB low multipoles. This anomaly is unlikely to be explained by the primordial physics. On the other hand, the uncounted foregrounds appear to be a natural source of the low multipoles correlations. We show that the strong quadrupole-octupole anomaly is, in principle, resolved by the account of the Kuiper belt. Simultaneously, the latter can provide the resolution to the parity asymmetry.

Acknowledgements

Firstly, I am indebted to my supervisor Pavel Naselsky for the introducing me to the CMB physics. Hope, the experience of work obtained under his guidance and his useful criticism will allow me to make further contributions to cosmology. I would like to thank the members of his group Martin Hansen, Anne Mette Frejsel and Jaseung Kim for the fruitful collaboration. I am indebted to the staff of the Niels Bohr International Academy and Niels Bohr Institute, namely, Poul Henrik Damgaard, Helle Killerich, Anna Maria Rey, Tarja Taarup and others, for the warm hospitality during my PhD study. I would like to express kind regards to my friends from the Niels Bohr Institute, Ara Martirossyan, Agnese Bissi, Yuki Sato, Lisa Glaser, my office mates Thomas Sondergaard and Hjalte Frellesvig, and others, who made my stay in Copenhagen extremely comfortable, and wish them success with their PhD defences.

It is a big pleasure for me to offer the gratitude to Valery Rubakov for the introducing me to various chapters of the theoretical physics. He was the supervisor of my Bachelor and Master defences and supported me during all these years. It is not a secret that the large part of this thesis is based on his inspiring ideas. Also I would like to thank my collaborators from the Institute for Nuclear Research, Grigory Rubtsov and Maxim Libanov.

My friends Ivan Grinin, Stanislav Evlashin, Pavel Inzhevatov, Alexander Zhiboedov, Andrey Zayakin, Dmitry Kirpichnikov, Sasha Kondakova and Marisya deserve gracious acknowledgements for the patiency and support. Not all of them are making on science currently. In any case, I wish them success in all their startings.

But most of all I am grateful to my parents Ramazan and Nasiyat and to my sister Sabina for the support from the very beginning.

Foreword

The present thesis collects the work of three publications by the author concerning theoretical and observational properties of the conformal rolling scenario, as well as the investigations of the statistical anisotropy in the CMB sky. All the results are original, unless otherwise stated. Chapters 4 and 6 are fully based on my articles [23, 112, 146] written with collaborators. In the Chapter 2, I review the state of affairs in the inflation and ekpyrotic models. The Chapter 3 is essentially the introduction to the topic of the conformal rolling scenario, while the Chapter 5 has been added to complete the discussion on the possible role of conformal symmetries in the theory of (very) early Universe.

Contents

1 Introduction

1.1 Problems of Hot Big Bang theory

With the advent of the WMAP data, the standard Big Bang theory has become the subject of rigorous experimental tests. As a result, the six-parametric ΛCDM model has been established as the best fit of the cosmological evolution starting from approximately $1s$ and till nowadays. In this picture, the Universe started from the extremely hot state and relatively small sizes in the far past. At these early times the radiation dominated epoch occured, which subsequently turned into the stage driven by the non-relativistic particles. Today, we live in the Universe undergoing the accelerated expansion with the almost constant Hubble rate. The content of the present Universe is quite well established, as well as some key properties like the homogeneity, the isotropy and flatness [1]. They are encoded in the form of the Friedmann–Robertson–Walker metric,

$$ds^2 = dt^2 - a^2(t)d\mathbf{x}^2 \ ,$$

where $a(t)$ is the scale factor. Clearly, these properties should be viewed as statistical, i.e. obtained as the average over the cosmological scales. The reality tells us that the Universe is locally inhomogeneous. These inhomogeneities start to emerge at distances as large as $\sim$ 100 Mpc, and result from the evolution of the cosmological perturbations. Assumed to be particularly small at the beginning of the hot epoch, they become enhanced during the evolution and move towards the Jeans instability at some point. This is essentially the mechanism of the structure formation. Cosmological perturbations are also interesting from the purely theoretical point of view. Indeed, their properties encoding the information about the far past epochs, are imprinted in the temperature fluctuations of the relic photons. The latter decouple from the baryons at the time $t \approx 350000$ years, and since this point on travel unaffected by interactions with the matter. Thus, study of the relic photons provides us with a deep insight into the properties of the cosmological perturbations at the early times. In particular, the prediction of the Big Bang theory about the oscillations in the baryon-photon plasma preceding the last scattering of photons was found to be in a remarkable agreement with the CMB data.

Though the tremendous success of the standard cosmology, there are several issues left unaddressed in the conventional picture. Probably, the most puzzling one is the nature of the dark energy driving the present accelerated expansion of the Universe. Formally, this amounts to adding the term with the positive Λ-constant to the Einstein–Hilbert action. This simple phenomenological construction, however, fails to explain the extremely small density associated with the dark energy as compared to the densities of the four known forces. If the dark energy is some uncounted fifth force or the General Relativity is inconcistent at large scales, is still unclear, though many proposals have been made on these issues. In particular,

it is unclear if the dark energy is indeed the constant or it is rather characterized in terms of some dynamical field, quintessence. Thus, we are in the situation, that no particular predictions about the future evolution of the Universe can be made.

The second problem is about the unnatural initial conditions set by hands at the beginning of the hot epoch. First, even the properties of the homogeneity and isotropy observed with a high accuracy, appear to be problematic for the Big Bang theory, since they require a huge fine-tuning of the initial data. The size of the Universe visible today is $l_{H,0} \approx 1.4 \cdot 10^4$Mpc. Let us draw back the evolution of the Universe to the times, when the last scattering of the photons occured. The size of the causally connected area at these times is

$$l_{H,1} = a(t_1) \int_{t_{Pl}}^{t_1} \frac{dt}{a(t)} \ .$$

Due to the expansion of the Universe, this size measured today is given by

$$l_{H,1} = a(t_1) \int_{t_{Pl}}^{t_1} \frac{dt}{a(t)} \ ,$$

which is rather small compared to the size of the visible Universe,

$$\frac{l_{H,0}}{l_{H,1}(t_0)} \sim 35 \ .$$

In particular, this implies that the CMB sphere visible today consists of the

$$\left(\frac{l_{H,0}}{l_{H,1}(t,0)} \right)^2 \sim 1000$$

patches, which have been disconnected at the times, when the last scattering occured. Thus, one naturally expects that the temperature anisotropies detected should be of the order unity, $\delta T(\mathbf{n})/T_0 \sim 1$. This natural prediction of the standard Big Bang theory is in a sharp contrast with the CMB data: $\delta T(\mathbf{n})/T_0 \sim 10^{-5}$.

From the viewpoint of the Big Bang theory, it is also challenging to explain, why the Universe is so flat. The general background metric in the homogeneous and isotropic Universe is given by

$$ds^2 = dt^2 - a^2(t) \left(\frac{dr^2}{1 - \kappa r^2} + r^2 d\Omega_2^2 \right) \ ,$$

where $\kappa = -1, 0, 1$ for an open, flat or closed Universe. According to the ΛCDM model, the Universe is filled with the radiation, which energy density scales as $\rho_r \sim a^{-4}$, the non-relativistic matter with $\rho_m \sim a^{-3}$ and the vacuum energy with the constant energy density. In the open and the closed Universes there is the additional contribution coming from the non-zero spatial curvature. Combining altogether, one writes the standard Friedmann equation

$$H^2 = \frac{8\pi G}{3} \rho - \frac{\kappa}{a^2} \qquad (1)$$

as follows

$$H^2 = H_0^2 \left(\Omega_{rad} \left(\frac{a_0}{a} \right)^4 + \Omega_m \left(\frac{a_0}{a} \right)^3 + \Omega_\Lambda + \Omega_{curv} \left(\frac{a_0}{a} \right)^2 \right) ,$$

where H_0 is the Hubble parameter measured today; Ω_{curv} is the current fractional contribution of the curvature given by

$$\Omega_{curv} = -\frac{\kappa}{a_0^2 H_0^2} .$$

It is strongly constrained by the seven-year WMAP data [1],

$$-0.0178 < \Omega_{curv} < 0.0063 .$$

As it follows, going backwards in time, the contribution of the curvature falls down during the radiation and matter dominated stages. Thus, the prediction of the standard Big Bang is that the contribution of the spatial curvature should be extremely small at early times. Say, at the Planckian times it is estimated as $|\Omega_{curv}| \lesssim 10^{-60}$. In the conventional cosmology, this tiny value is set by hands, which sounds very unnatural.

One more puzzle of the Big Bang theory is the entropy problem. The latter states that to achieve the present value of the entropy in the Universe, one should set the initial large value of the entropy by hands. This follows from the fact that the Universe is roughly in the equilibristic states at all the stages of the standard evolution. Thus, its entropy remains roughly constant. This translates into the large entropy of the small patch, from which the Universe has grown up.

The main focus of this thesis is, however, the problem of primordial scalar perturbations. Namely, there is no built-in mechanism for the structure formation in the Universe at later epochs, i.e. one sets the "seeds" of future structures "by hands". It sounds very unnatural, especially taking into account rather unusual properties of these "seeds". With a high accuracy, the latter are characterized by the unique quantity $\zeta(\mathbf{x})$, which remains frozen out at the superhorizon scales. In this situation, one deals with the adiabatic initial conditions[1]. Moreover, these primordial scalar perturbations are characterized by the flat power spectrum. To clarify this property, we introduce the correlation function of the product of two perturbations ζ,

$$\langle \zeta(\mathbf{x}) \zeta(\mathbf{y}) \rangle = \frac{1}{(2\pi)^3} \int d^3\mathbf{k} e^{i\mathbf{k}(\mathbf{x}-\mathbf{y})} P_\zeta(\mathbf{k}) . \tag{2}$$

The function $P_\zeta(\mathbf{k})$ is the power spectrum of the primordial scalar perturbations. The flatness of the spectrum implies the particular dependence on the momentum k, i.e. $P_\zeta(k) \sim k^{-3}$. It is convenient to introduce the power spectrum $\mathcal{P}_\zeta(k)$ defined by

$$\mathcal{P}_\zeta(k) = \frac{k^3}{2\pi^2} P_\zeta(k) . \tag{3}$$

[1]We give a more rigorous definition of the adiabatic initial conditions in the Appendix A.

With these notations the flatness implies the independence of the power spectrum on the momentum k, i.e. $\mathcal{P}_\zeta(k) = \text{const}$. The correlation function (2) taken at different equal spatial points $\mathbf{x} = \mathbf{y}$ is then reduced to

$$\langle \zeta^2(\mathbf{x}) \rangle = \int \frac{dk}{k} \mathcal{P}_\zeta(k) \ . \tag{4}$$

We prefer to work in terms of the power spectrum $\mathcal{P}_\zeta$ in what follows, unless the opposite is stated.

The problems mentioned above tell us clearly that the conventional cosmology is incomplete. There are several other (not so strong, however) features indicating the non-trivial extension of the ΛCDM model. We comment on some of them in the end of the Section 1.3, after we clarify basic notations of the CMB physics.

1.2 Models of (very) early Universe

1.2.1 Inflation

To address the problems of the unnatural initial conditions, one assumes that there must have been some epoch preceding the conventional Hot Big Bang. The most well-known candidate in this regard is the inflation, i.e. the epoch of the rapid accelerated expansion of the Universe. In this picture, the Universe observed today is just a small patch in the huge region, which became causally connected before the radiation dominated era started. The flatness is also addressed in the most elegant way. During the accelerated expansion the contribution of the spatial curvature falls down rapidly. Thus, we are left with the significantly flat Universe by the beginning of the conventional epoch.

Historically, the first model of the inflation was proposed by Starobinsky in [2]. Interestingly, his model addressed the problem of the conformal anomaly in the quantum gravity rather than the standard cosmological problems. Further, Mukhanov and Chibisov considered the mechanism responsible for the production of adiabatic perturbations and resulted with a flat spectrum [3]. The simple inflationary scenario with the scalar fields was proposed by Alan Guth in [4]. Guth's model played a profound role in establishing the inflation as the major cosmological paradigm. According to his scenario, inflation is an exponential expansion of the Universe in a supercooled false vacuum. Being metastable, the false vacuum decays into the bubbles of the true vacuum. The latter collide, and the Universe becomes hot. Later on it was understood that this simple picture dubbed as the "old inflation" suffered from the "graceful exit problem". The latter was avoided in the healthier scenario reffered to as the "new inflation" [5]. Still it suffered from the artic ficial assumptions about the thermodynamical equilibrium at the beginning of the inflation. These problems are absent in the chaotic scenario [6], which operates under rather general assumptions about the

underlying theory of the Nature at very early times and under very general initial conditions. The simplest versions of the chaotic inflation rely on the unique scalar field referred to as the inflaton. The special requirement to the form of the inflaton potential is that it should be flat enough, i.e. it obeys the so called slow roll conditions. The latter ensure that the Universe undergoes the epoch of the approximately de Sitter expansion, and this background is the dynamical attractor. The inflaton fluctuations evolving on the de Sitter background acquire the flat power spectrum, while the small deviations from the pure de Sitter encoded in the slow roll parameters leads to the slightly tilted spectrum [3, 7, 8]. Remarkably, the flat power spectrum of the primordial scalar perturbations has been confirmed in the experimental data, as well as the small tilt. Since this time on, the inflation became the leading candidate on the role of the very early Universe theory. Though the obvious success of the inflation, one should be careful, when treating it as the experimental fact. First, one needs to check if the desired properties of primordial perturbations are obtained in alternative frameworks.

Finally, the inflation also addresses the problem of the entropy. Once the inflaton field moves towards the minimum of its potential, the inflation finishes. At this time, the inflaton starts to oscillate around the minimum decaying into conventional particles. Since this process is highly non-equilibristic, the entropy grows and rapidly reaches the values required by the conventional cosmology. This process is referred to as the reheating and has been elaborated in the articles [9].

1.2.2 Bouncing and collapsing Universe

Searching for alternatives to the inflation, one naturally (but not necessarily) assumes that there has been the contracting stage previously to the standard Big Bang. This picture of the Universe immediately encounters several problems. First, the turn from the contraction to the expansion appears to be very problematic from the viewpoint of the quantum field theory. Indeed, at the contracting stage the Hubble parameter is negative, while it is positive during the expansion. Thus, to achieve the bounce, one claims that the derivative of the Hubble parameter is positive. This implies that the Universe must be dominated by the phantom energy near the bounce. Let us show this explicitly. Taking the derivative of the left and right handsides of the Friedmann equation and using the conservation law

$$\dot{\rho} + 3H(\rho + p) = 0 \ ,$$

one obtains

$$\dot{H} = -4\pi G(\rho + p) \ .$$

As it follows, $\dot{H} > 0$ implies $p < -\rho$. Note that the inequality $p \geq -\rho$, the Null Energy Condition (NEC)[2], is hardly violated in the quantum field theory. The naive way to construct the matter with the phantom properties is to consider the scalar field with the negative kinetic term,

$$\mathcal{L} = -\frac{1}{2}(\partial_\mu \phi)^2 - V(\phi) \ .$$

This naive theory, however, suffers from the ghost instabilities, i.e. one can infinitely lower the energy of the system by creating particles.

In the pre-Big Bang scenario (for a review see [10]) it is assumed that the transition occurs at energies so high that the effects of the quantum gravity become important. However, the theory of the quantum gravity or the superstring theory replacing the latter are not developed to address this issue. In particular, they fail to answer if the bounce is possible in principle. A very interesting proposal on the possibility of the NEC violation without the obvious pathologies has been made in the framework of the ghost condensate models [11]. Though they seem to suffer from several conceptual problems [12], they set the belief that the smooth bounce can be achieved in terms of some healthy theory. The ghost condensate phase has been incorporated as the necessary ingredient in some early Universe models. One example is represented in the starting-the-Universe picture [13]. It is also used in some versions of the ekpyrotic scenario [14], to which brief discussion we turn now, while postponing a more thorough analysis until the next Chapter.

The ekpyrotic models appeared first in the higher dimensional braneworld picture [15]. They, however, admit a four-dimensional description at the times far from the bounce. The ekpyrotic phase is then realized as the period of the slow contraction, when the Universe is driven by the matter with the super-stiff equation of state. Introducing the matter with this strange property is favored in a view of the other problem of bouncing cosmologies. Once the Universe contracts, it becomes more and more anisotropic. These anisotropies grow rapidly as the scale factor decreases, i.e. their energy density scales as $\rho_\sigma \sim 1/a^6$. This is the result from the article by Belinsky, Khalatnikov and Lifshitz [16]. Note that the energy density of the matter obeying the equation of state $p = w\rho$ scales as $\rho \sim a^{-2(1+3w)}$. Nothing to say that the contribution of the standard matter, relativistic or non-relativistic, becomes completely negligible as compared to the anisotropies at some point of the evolution. Thus, even if one managed to provide the transition through the bounce, it does not guarantee that the Universe is homogeneous and isotropic at the beginning of the conventional epoch. The problem is avoided, if the Universe is driven by the matter with $w > 1$ [17]. This is the case of the ekpyrotic phase. Consequently, the Universe smoothens provided that the contracting stage is long enough.

[2]The covariant formulation of the NEC is $T_{\mu\nu}n^\mu n^\nu \geq 0$, where $T_{\mu\nu}$ is the energy-momentum tensor, and n^μ is any non-spacelike vector.

The latter is also the requirement for the horizon problem to be resolved, in the sense that the Universe may become causally connected at large distances. Furthermore, during the ekpyrotic phase, the contribution of the spatial curvature falls down as compared to one of the dominating matter. Thus, if the duration of the slow contraction is long enough, the Universe becomes essentially flat. Hence, the flatness problem is also addressed in the ekpyrotic scenario. The conversion of the energy density during the ekpyrotic phase into the conventional matter can be designed in the same way as in the inflation. Thus, the entropy problem obtains the solution. The creation of the primordial scalar perturbations with the flat spectrum is rather challenging (but not impossible!) in the ekpyrotic models. We discuss this issue in details in the next Chapter. Here we just note, that even if the flatness of the spectrum is ensured, one cannot be sure that this property survives through the bounce. In this sense, the ekpyrotic models are currently at the stage of the development.

1.2.3 (Pseudo)-Conformal Universe

Our main concern in this thesis is the conformal rolling scenario first proposed in [18] and further developed in [19, 20, 21, 22, 23]. This model has been designed to address the problem of primordial scalar perturbations solely. The main assumption behind the conformal rolling scenario is that there must be some relation between the flatness of the primordial spectrum and conformal symmetries inherent in the early Universe theory [24]. The conformal rolling scenario is the concrete realization of this idea. Its basic ingredient is the complex scalar field ϕ conformally coupled to the gravity. During the evolution, it rolls down the slope of the negative quartic potential developing perturbations in the radial direction and in the orthogonal one. The latter, phase perturbations, are argued to acquire the flat spectrum before the conformal rolling stops. Once the phase perturbations are superhorizon at this point, they remain frozen out until the beginning of the hot epoch, when phase perturbations get converted into adiabatic ones. The particular predictions of this sub-scenario are the non-Gaussianity in the trispectrum and the quadrupole statistical anisotropy. If phase perturbations are still subhorizon at the end of the rolling, they proceed to evolve. In that case, the intermediate stage between the conformal rolling and the hot epoch is required. The evolution at the intermediate stage results into the trispectrum of a rather peculiar form and the statistical anisotropy of all even multipoles.

The other cosmological scenario incorporating conformal symmetries is the Galilean Genesis [25]. This model is based on the drastically different Lagrangian as compared to the conformal rolling scenario. However, the result is again the flat spectrum of the relevant perturbations. Note that the Galilean Genesis is also interesting in the different context. Due to the non-trivial higher derivetive structure, it allows for the strong violation of the NEC condition. This is to be compared with the ghost condensate, where this violation is rather mild [11]. The price is, however, superluminality.

Further, it has been understood by Hinterbichler and Khoury [26] that the similarity in the predictions of two different models is not the coincidence. They showed that the flatness of the spectrum of the primordial scalar perturbations is ensured provided that a few assumptions are satisfied: i) the background metric of the Universe is nearly of the Minkowski type; ii) the Universe is in the CFT state with a high accuracy, and among the field content of the Universe there are scalars with different conformal weights; iii) the conformal symmetry is spontaneously broken by the time-dependent values of the field(s) with the non-zero conformal weight(s); iv) there is a field with the zeroth conformal weight, which acquires the flat spectrum once the first three conditions are satisfied. These conditions are not restrictive at all, and in fact the speech is about the large class of models, of which the conformal rolling scenario and the Galilean Genesis are the particular cases. The models from this class represent the idea of the (pseudo)-Conformal Universe[3]. In particular, Hinterbichler and Khoury considered the dynamical scenario with the negative quartic potential, akin to the conformal rolling scenario. Interestingly, they resulted with the slowly contracting Universe, which is in the certain sense the incarnation of the ekpyrotic phase. More generally, the background evolution in the models of the (pseudo)-Conformal Universe is either the slow contraction or the slow expansion as represented in the Galilean Genesis. In any case, the Minkowskian evolution is the dynamical attractor of the (pseudo)-Conformal Universe.

1.3 Statistical properties of CMB

Since the growing number of early Universe models, it is of the particular importance to descriminate between them. The CMB data provides us with the opportunity to probe the primordial physics. In the 90's the COBE experiments supported the (nearly) flat spectrum of primordial scalar perturbations. The era of the precision cosmology started with the advent of the WMAP data, when it became possible to test the most intriguing puzzles of the Universe. Among the most fascinating results, the ΛCDM model has been established as the major paradigm of the cosmology starting from one second. Also, the non-Gaussian properties of primordial perturbations have been tested with the unprecedented accuracy.

The main idea, how one can probe the primordial physics from the CMB data is as follows. The CMB sphere is nothing but the sphere of the last scattering of photons. The latter decoupled at some initial stages of the conventional evolution of the Universe, i.e. deep in the matter dominated stage. At these early times the cosmologically interesting modes were essentially unaffected by the Jeans instability. Thus, they obeyed the linearized equations of motion and did not mix with each other. This allowed them to make a direct imprint on the CMB.

[3]The part "pseudo" stands for the slight violation of the conformal invariance by the gravitational effects. This, however, does not affect the main idea.

Among the signatures of the primordial physics in the CMB sky, the scalar tilt, tensor perturbations and the non-Gaussianity are ones most commonly discussed. The former implies that that the power of the primordial scalar perturbations may depend slightly on the wavenumber k. In fact, the small red tilt is even favored by the seven-year WMAP data [1],

$$n_s = 0.968 \pm 0.012$$

at the 68% confidence level, while the scale-invariant spectrum is ruled out at the 99.5% confidence level. Note that the slight violation of the scale invariance of the spectrum naturally arises within the inflation. Sometimes viewed as the strong argument in the support of the inflation, one should be aware that the red tilted spectrum may be easily predicted by the alternative frameworks. In this sense, the detection of the primordial tensor perturbations would be a much stronger argument in favor of the inflation. The reason is that the inflation predicts tensor modes, which can be as large as the current observational constraint. On the opposite, the common prediction of the alternative frameworks is the strongly blue tilted spectrum of the tensor perturbations. In particular, this implies they are suppressed at the cosmological scales.

One more standard prediction of the inflation is the tiny level of the non-Gaussianities of the primordial perturbation $\zeta(\mathbf{x})$. More precisely, this concerns the slow roll inflation driven by the scalar with the canonical kinetic term [27]. Large non-Gaussianities may arise in more complicated inflationary frameworks as well as in the alternative ones. Thus, the level of non-Gaussianities itself cannot descriminate between the models of the early Universe. However, it is a useful tool in a view of descriminating from the simplest versions of the inflation. In this sense, the best motivated non-Gaussianity is one of the local type defined in the real space by

$$\zeta = \zeta_g + \frac{3}{5} f_{NL} (\zeta_g^2 - \langle \zeta_g^2 \rangle) \ , \tag{5}$$

where ζ_g is the Gaussian field, and f_{NL} is the constant, which measures the non-Gaussianity. The parameter f_{NL} is constrained by the seven-year WMAP data [1],

$$-11 < f_{NL} < 74 \tag{6}$$

at the 95% confidence level. With the advent of the PLANCK data, this constraint is promised to be improved up to $|f_{NL}| \simeq 5$ (in the case of the non-observation).

In principle, the non-Gaussianity may have the non-trivial shape. Namely, the three-point function $\langle \zeta_{\mathbf{k}_1} \zeta_{\mathbf{k}_2} \zeta_{\mathbf{k}_2} \rangle$ may have a peculiar dependence with respect to the peculiar dependence on the momenta $\mathbf{k}_1$, $\mathbf{k}_2$ and $\mathbf{k}_3$. Due to the translational invariance, the latter satisfy the triangle relation $\mathbf{k}_1 + \mathbf{k}_2 + \mathbf{k}_3 = 0$. According to this, one naturally deals with the following configurations in the momentum space:
i) the squeezed configuration with one of the momenta, say, k_3 much less than the other two;

ii) the equilateral one with three momenta of the same order of magnitude.
There is its own physics standing behind each of the configurations. Thus, testing the shape of the primordial bispectrum provides us with a powerful tool to probe the models of the early Universe.

More interesting observables are given by the connected part of the four-point function, the trispectrum. This is clear from the fact that the number of possible non-trivial configurations is larger in this case. Note, however, that the price for this diversity of the potential signatures is the lower sensitivity of the experiments.

One more potential observable in the CMB sky is the statistical anisotropy. This implies the correlation of the CMB coefficients a_{lm} defined by

$$a_{lm} = \int d\Omega_{\mathbf{n}} \delta T(\mathbf{n}) Y^{\star}_{lm}(\mathbf{n}) \ .$$

Nowadays it is assumed that the covariance of the coefficients a_{lm},

$$\langle a_{lm} a_{l'm'} \rangle = C_{lm;l'm'} \ ,$$

is diagonal, i.e. $C_{lm;l'm'} = C_l \delta_{ll'} \delta_{mm'}$. Violation of this property implies the statistical anisotropy. From the viewpoint of the early Universe physics this means the direction-dependence of the primordial power spectrum. However, the origin of the statistical anisotropy can be completely different. To clarify the situation, it is reasonable to divide the range of multipole numbers into low l's corresponding to $l \lesssim 30$ and large $l \sim 100$. In particular, this separation is justified from the viewpoint of several CMB anomalies observed at the 2.5σ-4σ confidence level in the WMAP data. These are the low quadrupole power, the quadrupole-octupole alignment, the "axis of evil", cold spots, parity asymmetry and others [28, 29, 30, 31, 32, 33, 34, 35, 36, 37]. Some of them, e.g. the quadrupole-octupole strong correlation indicate that the statistical anisotropy is broken at low multipoles. If this and other anomalies have the cosmological origin and, thus, indicate the non-trivial extension of the conventional ΛCDM model, or they are due to the residuals of the foregrounds [38], or, perhaps, one deals with yet unknown systematic errors, is still not clear. In this thesis, we elaborate on the second opportunity, i.e. we assume that the quardrupole-octupole alignment (and, simultaneously, the parity asymmetry) is explained by the uncounted foregrounds. On the other hand, we insist that the statistical anisotropy at higher multipoles, if not due to the systematics, is most likely to be described in terms of the primordial physics.

Statistical anisotropy of CMB is going to be the key observable for us in what follows.

1.4 Organization of the thesis

This thesis is organized as follows. In the Chapter 2 we give a brief overview of the inflation. This we do for several reasons. First, the inflation provides with the best established mechanism of the primordial perturbations creation. Second, several ideas conventionally discussed

in infaltion are in fact generic ones and applied in different frameworks. In particular, this concerns the mechanisms of converting isocurvature perturbations into the adiabatic ones, as in the curvaton models. Thirdly and most importantly, we have to give the picture of inflationary predictions, as broad as possible. These are to be compared with ones of the conformal rolling scenario. In the end of the Chapter 2 we discuss the state of affairs in the ekpyrotic models as one of the most widely developed alternatives to inflation nowadays.

In the Chapter 3, we turn to the topic of the primary interest, namely the conformal rolling scenario. There we discuss the basic ideas underlying this model. At some point it is natural to divide the model in two sub-scenarios depending on the evolution of the cosmological modes by the end of the rolling. These are referred to as the sub-scenario A with superhorizon modes by the end of rolling and the sub-scenario B with subhorizon ones. The behaviour of the relevant perturbations in the former sub-scenario is fully captured by the dynamics at the conformal rolling, and we discuss it therein. On the other side, the sub-scenario B requires some additional assumptions and results into the different predictions. Thus, it makes the sense to consider it in the separate Chapter.

As pointed out above, the conformal rolling scenario is just the particular case in the myriad of ways to realize the flatness of the spectrum using the conformal symmetries. Thus, our discussion would be incomplete without a brief review of the general setup. We fill in this gap in the Chapter 5. There we also discuss the dynamical models of the Universe and the set of possible predictions. In particular, we show that the most important signatures of the conformal rolling scenario are in fact generic for a much broader class of models.

In the Chapter 6 we discuss the signatures of the conformal rolling scenario in the CMB sky. From the non-observation of the (cosmological) statistical anisotropy, we establish the first constraint on the parameter of the conformal rolling scenario. There we also discuss the non-primordial sources of the statistical anisotropy in low multipoles. We consider the particular model, which could stand for the strong quadrupole-octupole correlations. The basic ingredient of this model is the Kuiper belt treated as the new foreground. Simultaneously, we address the problem of the parity asymmetry recently observed in the WMAP data.

2 Perturbations in inflation and ekpyrotic models

2.1 Single-field slow roll inflation

Nowadays, the inflation is realized in a very broad range of models. We will mostly focus on the particular class of models representing the inflationary paradigm in a very simple way, i.e. ones obeying the slow roll conditions [2, 5, 6]. Assume that the Universe is dominated by the scalar field ϕ. During the evolution, it slowly rolls down the slope of its potential $V(\phi)$. Then, under rather general conditions, namely, slow roll conditions, the Universe undergoes the period of a rapid (approximately) de Sitter expansion. Despite the simplicity, the slow roll inflation provides the solution to (almost) all problems of the Hot Big Bang as outlined in the Introduction. In particular, it provides the mechanism for the primordial scalar perturbations creation with (almost) flat power spectrum. The latter property has been favored by the COBE and WMAP missions, and established inflation as the most promising candidate on the role of very early Universe theory. For the time being, we will specify to the single-field versions of the slow roll models, of which the "new inflation" [5], chaotic inflation [6] and even historically first Starobinsky's model [2] are the particular examples[4].

To achieve the accelerated expansion, the evolution of the Universe should be driven by the matter with the negative pressure, or, more precisely,

$$p < -\frac{1}{3}\rho \, .$$

Let us show, how this requirement can be satisfied in the model with the single scalar field. The action for the latter is given by

$$S = \int d^4x\sqrt{-g}\left(\frac{1}{2}g^{\mu\nu}\partial_\mu\phi\partial_\nu\phi - V(\phi)\right) \, .$$

In this Section, we focus on the classical evolution of the field ϕ. Assuming that the latter is homogeneous and provided that the metric is spatially flat, we obtain the following equation of motion,

$$\ddot{\phi} + 3H\dot{\phi} + V_\phi = 0 \, . \tag{7}$$

The energy-momentum tensor is given by

$$T^\mu_\nu = g^{\mu\lambda}\partial_\lambda\phi\partial_\nu\phi - \delta^\mu_\nu\left(\frac{1}{2}g^{\lambda\rho}\partial_\lambda\phi\partial_\rho\phi - V(\phi)\right)$$

[4]The R^2-based model of Starobinsky admits the effective description in terms of the scalar field (referred to as scalaron) with the exponential potential. In this treatment, it represents the example of the large-field slow roll inflation.

In particular, the energy density of the homogeneous field ϕ simply reads from this energy-momentum tensor,

$$\rho \equiv T_0^0 = \frac{1}{2}\dot{\phi}^2 + V(\phi) \ ,$$

while the pressure is given by

$$p = \frac{1}{2}\dot{\phi}^2 - V(\phi) \ .$$

The second equation, which describes the evolution of the field ϕ, is the Friedmann law,

$$H^2 = \frac{8\pi}{3M_{Pl}^2}\left(\frac{1}{2}\dot{\phi}^2 + V(\phi)\right) \ .$$

As it follows from the latter, if the potential term dominates upon the kinetic one,

$$\frac{\dot{\phi}^2}{2V(\phi)} \ll 1 \ , \tag{8}$$

the equation of state is of the vacuum type, i.e. $p \approx -\rho$, and the Universe undergoes the period of the (approximately) de Sitter expansion. The slow roll inflation also implies that the second term in the Eq. (7) (Hubble-"friction") dominates upon the first one,

$$\frac{\ddot{\phi}}{3H\dot{\phi}} \ll 1 \ . \tag{9}$$

With this condition obeyed, the de Sitter background turns out to be the dynamical attractor of the equations of motion. If the requirements (8) and (9) are satisfied, the system of equations takes the following simple form,

$$\dot{\phi} = -\frac{1}{3H}V_\phi \tag{10}$$

and

$$H = \frac{1}{M_{Pl}}\left(\frac{8\pi V}{3}\right)^{1/2} \ . \tag{11}$$

It is convenient to express the conditions (8) and (9) as the restrictions on the form of the potential $V(\phi)$. For this purpose, we substitute the Hubble parameter from the Eq. (11) into the Eq. (10) and use the requirement (8). This gives

$$\epsilon \equiv \frac{M_{Pl}^2}{16\pi}\left(\frac{V_\phi}{V}\right)^2 \ll 1 \ . \tag{12}$$

Providing similar manipulations, we obtain the second condition

$$\eta = \frac{M_{Pl}^2}{8\pi}\frac{V_{\phi\phi}}{V} \ll 1 \ . \tag{13}$$

In literature, the conditions (12) and (13) are dubbed as the slow roll conditions, while the parameters ϵ and η are referred to as the slow roll parameters. In particular, the conditions (12) and (13) imply that the slow roll inflation occurs provided the potential $V(\phi)$ is sufficiently flat. In what follows, we will also use the expressions for the derivatives of the Hubble parameter and the inflaton field in terms of the slow roll parameters,

$$\frac{\dot{\phi}^2}{2V} = \frac{\epsilon}{3} , \quad \frac{\dot{H}}{H^2} = -\epsilon , \quad \frac{\ddot{\phi}}{H\dot{\phi}} = \epsilon - \eta .$$

Now, let us show how the cosmological problems are resolved within the slow roll inflation. In this Section, we consider the horizon and flatness problems. For concreteness, we specify to the chaotic inflation [6], and the power law potential

$$V = g\phi^n .$$

For this type of the potential the slow roll conditions are always obeyed provided that the values of the inflaton are very large,

$$\phi \gg \frac{nM_{Pl}}{4\sqrt{3\pi}} .$$

Let us discuss the realistic scenario of the beginning of inflation in this particular setup. It is natural to assume that at very early times the Universe is highly inhomogeneous and curved at Planckian scales. Assume further that we know the underlying theory of Nature at these superhigh energies, and that there is the scalar ϕ with flat potential among the field content of the theory. The field ϕ is, generally speaking, inhomogeneous, and there is also the contribution of the curvature to the Friedmann equation. However, both these contributions scale as $1/a^2$. The natural expectation is that some region of the Universe has the size larger than Planckian. As a result, the contribution of the gradient terms and of the curvature become smaller than the potential term. This region starts to expand and rapidly tends to the inflationary regime. We live in one of these bubbles.

During the inflation, the scale factor grows exponentially. Take, for instance, the time, when the field value equals to some ϕ. Since this time and until the end of inflation, the scale factor grows in e^{N_e} times, where N_e is the so called number of e-folds defined by

$$N_e(\phi) = \int_{t_\phi}^{t_e} H(t)dt .$$

After the chain of the algebraic manipulations,

$$N_e(\phi) = \int_{\phi}^{\phi_e} H(\phi)\frac{d\phi}{\dot{\phi}} = \int_{\phi_e}^{\phi} 3H^2\frac{d\phi}{V_\phi} = \frac{8\pi}{M_{Pl}^2}\int_{\phi_e}^{\phi}\frac{V}{V_\phi}d\phi ,$$

we obtain the expression for the number of e-folds

$$N_e(\phi) = \frac{4\pi}{n}\frac{\phi^2}{M_{Pl}^2}$$

(still the power law potentials are considered). At the beginning of inflation, the natural value of the potential density is of the Planckian order, $V(\phi_i) \sim M_{Pl}^4$. Then, the initial value of the inflaton field is estimated as $\phi_i \sim g^{-1/n} M_{Pl}^{4/n}$. The total number of e-folds then reads

$$N_e^{(tot)} = \frac{4\pi}{n}\left(\frac{M_{Pl}^{(4-n)}}{g}\right)^{2/n} .$$

Taking the conreteness the quartic potential, $V(\phi) = \lambda\phi^4$, we obtain

$$N_e^{(tot)} \simeq \frac{2\pi}{\sqrt{\lambda}}$$

The inflationary mechanism of the primordial perturbations creation requires a particularly small value of the coupling constant, i.e. $\lambda \sim 10^{-13}$. This will become clear in what follows. Then, the number of e-folds is estimated as $N_e^{(tot)} \sim 10^7$. Given this large value, the Universe becomes causally connected at distances much exceeding the current visible size. Thus, the horizon problem is addressed in the extremely successful way. Simultaneously, the inflation resolves the flatness problem. The contribution of the spatial curvature scales as $1/a^2$ during the inflation and, hence, falls down rapidly. Thus, we are left with the significantly flat Universe, before the conventional hot epoch starts. Note, that in the inflationary framework the present constraint on the spatial curvature appears to be very conservative. Hence, any deviation from the flatness will be a serious challenge for inflationary models.

2.2 Primordial perturbations during inflation

The merit of inflation is that it provides the mechanism for the primordial scalar perturbations creation. This issue has been first addressed by Mukhanov and Chibisov in [3] and further elaborated in [7, 8]. We discuss the fluctuation of the inflaton on the homogeneous background,

$$\phi(\mathbf{x}, t) = \phi(t) + \varphi(\mathbf{x}, t) ,$$

where $\varphi(\mathbf{x}, t)$ is the inflaton fluctuation. It is instructive to study the evolution of the perturbations at the qualitative level first. We perform the quantitave analysis in the end of this Section.

During the inflation, the Hubble parameter varies very slowly with the time. Thus, in the zeroth order in the slow roll parameters ϵ and η, we are allowed to consider the background

space-time with the pure de-Sitter metric. Also, in this approximation, we can neglect the effective mass of the inflaton.

In general, quantization procedure in curved space-time is involved. But the things are not so complicated if the background metric is spatially flat. The reason is that in the conformal time the spatially flat metric is conformally related to the Minkowski one. Remind that the conformal time is defined by

$$a(\eta)d\eta = dt \ .$$

With this notation, the metric of every spatially flat space-time takes the form

$$ds^2 = a^2(\eta)(d\eta^2 - d\mathbf{x}^2) \ .$$

In the particular case of the de Sitter space-time, the scale factor is given by

$$a(\eta) = -\frac{1}{H\eta} \ , \quad H = \text{const} \ ,$$

with the understanding that the conformal time is negative, $\eta < 0$.

We should be aware of the potential problem with the evolution on the time-dependent curved background. The difficulty is that the vacuum state may be ill-defined in this case. Indeed, the background time-dependent metric can be viewed as the external field. It is well-known that presence of the latter may lead to the particle creation and annihilation. However, we are on the safe side, since the effects of the background de Sitter metric become weak in the asymptotic past. This is true if we consider the modes with the momenta k, which are subhorizon at very early times. The reason is that the corresponding wavelengths are much smaller than the horizon size and, thus, the effects of the space-time curvature are negligible. In particular, this implies that at very early times we can work on the effectively Minkowski background. The vacuum in this case is well-defined, at least for the modes with small wavelengths (as compared to the horizon size at this time). We assume that this asymptotic past exists at least for all cosmologically interesting modes.

The action for the massless scalar field on the spatially flat background is given by

$$S_\varphi = \frac{1}{2}\int d^4x a^2(\eta)[(\partial_\eta\varphi)^2 - (\partial_i\varphi)^2] \ . \tag{14}$$

To establish the closer relation to the Minkowski space-time, we introduce the field χ,

$$\chi = a(\eta)\varphi \ . \tag{15}$$

In terms of the new variable χ the action (14) takes the form

$$S_\chi = \frac{1}{2}\int d^3x d\eta \left[\chi'^2 - (\partial_i\chi)^2 + \frac{a''}{a}\chi^2\right] \ , \tag{16}$$

The equation of motion for the field χ reads

$$\chi'' + k^2\chi - \frac{2}{\eta^2}\chi = 0 \ . \tag{17}$$

In the asymptotic past, $\eta \to -\infty$ the third term on the left hand side is negligible. Then, at very early times the field χ behaves as the free massless scalar field on the Minkowski background. With this said, the quantization of the field χ is the straightforward procedure. We write

$$\chi(\mathbf{x},\eta) = \int \frac{d^3k}{(2\pi)^{3/2}} \left(e^{-i\mathbf{kx}} \chi_k^{(+)} A_{\mathbf{k}}^\dagger + e^{i\mathbf{kx}} \chi_k^{(-)} A_{\mathbf{k}} \right) \ , \tag{18}$$

where $A_{\mathbf{k}}^\dagger$ and $A_{\mathbf{k}}$ are the creation and the annihilation operators obeying the canonical commutation relation,

$$[A_{\mathbf{k}}, A_{\mathbf{k}}^\dagger] = \delta(\mathbf{k} - \mathbf{k}') \ .$$

The amplitudes $\chi_k^{(-)}$ and $\chi_k^{(+)}$ are the negative and positive frequency solutions of the Eq. (17), respectively. The reality of the field $\chi(\mathbf{x},\eta)$ implies that

$$\chi_k^{(-)} = [\chi_k^{(+)}]^\star \ .$$

In the WKB approximation the negative frequency solution in the asymptotic past is given by

$$\chi_k^{(-)}(\eta) = \frac{1}{\sqrt{2w_k}} e^{-i\int^\eta w_k d\eta} \ ,$$

where $w_k = \sqrt{k^2 - \frac{2}{\eta^2}}$. Taking into account only the leading non-trivial term, we write

$$\chi_k^{(-)} = \frac{1}{\sqrt{2k}} e^{-ik\eta} \left(1 - \frac{i}{k\eta} \right) \ .$$

At all the times we can write the general solution,

$$\chi_k^{(-)} = \sqrt{-\eta}(C_1 H_{3/2}(-k\eta) + C_2 H_{3/2}^\star(-k\eta)) \ .$$

This general solution respects the early times asymptotics. provided that $C_1 = -\sqrt{\frac{\pi k}{4}}$ and $C_2 = 0$. Here we used the behaviour of the Hankel function $H_\beta(x)$ at $x \to \infty$,

$$H_\beta(x) \to \sqrt{\frac{2}{\pi x}} \exp\left[i \left(x - \frac{\beta\pi}{2} - \frac{\pi}{4} \right) \right] \ , \tag{19}$$

where the upper sign in the argument of the exponent corresponds to the first Hankel function, and vice versa. In the opposite regime, $x \to 0$, the asymptotics of the Hankel function reads

$$H_\beta \to -\frac{i}{\pi} \Gamma(\beta) \left(\frac{x}{2} \right)^{-\beta} \ . \tag{20}$$

As it follows from the latter, after the mode with momentum k exits the horizon, i.e. in the regime $k|\eta| \ll 1$, the amplitude is given by

$$\chi_k^{(-)} = -\frac{1}{\sqrt{2k}} \left(\frac{i}{k\eta}\right) \ .$$

Substituting this late-time solution into the expression (18), and using the relation between the fields χ and φ, we obtain the late time solution for the latter in the form

$$\varphi(\mathbf{x}, \eta) = \int \frac{d^3k}{(2\pi)^{3/2}\sqrt{2k}} \frac{H}{k} (e^{-i\mathbf{kx}} \tilde{A}_{\mathbf{k}}^{\dagger} + e^{i\mathbf{kx}} \tilde{A}_{\mathbf{k}}) \ , \tag{21}$$

where the operators $\tilde{A}_{\mathbf{k}}$ and $\tilde{A}_{\mathbf{k}}^{\dagger}$ differ from $A_{\mathbf{k}}$ and $A_{\mathbf{k}}^{\dagger}$ by the irrelevant phase factors. From (21), it is straightforward to compute the power spectrum of the inflaton fluctuations in the superhorizon regime,

$$\langle \phi^2(\mathbf{x}) \rangle = \int \frac{dk}{k} \frac{H^2}{(2\pi)^2} \ ,$$

where the integration is performed over the superhorizon modes. This implies the following amplitude of the inflaton fluctuations

$$\Delta_{\phi} = \sqrt{\mathcal{P}_{\phi}} = \frac{H}{2\pi} \ .$$

In the superhorizon regime, the amplitude of the inflaton fluctuations stays constant until the time, when it reenters the horizon at the Big Bang stage. Though the amplitude stays constant behind the horizon, the corresponding wavelengths grow exponentially during the inflation. Now, let us estimate the minimal duration of the inflation provided the flatness of the power spectrum is satisfied for all cosmologically interesting modes. The mode with the conformal momentum k becomes superhorizon provided that

$$\frac{k}{a(\eta_k)} \sim H \ ,$$

where η_k is the time of the horizon exit. Our aim is to estimate the minimal number of e-folds $N_e^{min} = \ln \frac{a_e}{a(\eta_k)}$ starting from the time η_k and until the end of the inflation. To do it, let us perform physical momentum at the time η_k as follows,

$$\frac{k}{a(\eta_k)} = \frac{k}{a_0} \frac{a_0}{a_{reh}} \frac{a_{reh}}{a_e} \frac{a_e}{a(\eta_k)} \ ,$$

where a_e is the scale factor at the end of the inflation, a_{reh} is some characteristic value of the scale factor during the reheating, and a_0 is the present scale today. Assume that the

Hubble parameter is not much smaller than the Planck mass during the inflation. Then, the estimate for the minimal number of e-folds takes the form,

$$\ln \frac{a_e}{a(\eta_k)} \simeq \ln \frac{M_{Pl}}{q_0} - \ln \frac{a_0}{a_{reh}} - \ln \frac{a_{reh}}{a_e} \ ,$$

where q_0 is the physical momentum corresponding to the conformal momentum k measured today. To simplify the estimates assume that the scale factor does not change significantly from the end of the inflation and until the end of the reheating. Note also that the temperature during the Big Bang scales as $T \sim 1/a$. Assuming further that the temperature of the reheating can be as large as the Planck mass, i.e. $T_{reh} \sim M_{Pl}$, we obtain the following estimate for the minimal number of e-folds during the inflation,

$$N_e^{min} = \ln \frac{a_e}{a(\eta_k)} \sim \ln \frac{T_0}{q_0} \sim 60 \ .$$

Here we used some characteristic momentum $q_0 = 0.002\text{Mpc}^{-1}$. In our estimates we completely neglected the evolution during the reheating. However, more correct estimates are not much different from the one given above,

$$N_e^{min} \simeq 50 - 60 \ .$$

Now, let us estimate the primordial density perturbations generated by the inflationary mechanisms. To do it, we use the picture of the local Universes. At the inflationary stage, different patches of the Universe with size larger than the de Sitter horizon evolve like separate Universes. Due to the perturbations of the inflaton with wavelengths larger than the de Sitter horizon, the full inflaton field is approximately homogeneous in each patch, but takes slightly different values in different patches. Hence, different patches undergo different stages of the evolution. The time delay is given by

$$\dot{\phi}\delta t = \delta\phi \ . \tag{22}$$

Due to this time delay, "local Universes" exit the inflation at slightly different time. Then, the energy density in these patches is different: in those regions, which exit the inflation earlier, the energy density is lower, and vice versa. It is this physical mechanism which stands for the primordial density perturbations formation. The estimate of the energy density perturbations in these regions is given by

$$\delta\rho \sim \dot{\rho}\delta t \ . \tag{23}$$

After the exit from the inflation, the energy density decreases accordingly to

$$\dot{\rho} \sim -H\rho \ ,$$

Substituting the latter into the (23) and using (22), we obtain for the energy density perturbations,

$$\frac{\delta\rho}{\rho} \sim \frac{H}{\dot{\phi}}\delta\phi \ .$$

This estimate is in a remarkable agreement with the correct result. Note, however, that the perturbation of the energy-density is gauge-dependent with respect to the associated fluctuations of the metric. Commonly, the curvature perturbation ζ is used for the gauge-invariant description of the primordial fluctuations [43, 8, 44]. For details and definitions, we refer the reader to the Appendix A, or (more prefferably), to very nice reviews and textbooks [39, 40, 41, 42]. Here we just recall that in the general theory of one scalar field with the canonical kinetic term, the combination

$$u = a\left(\varphi - \frac{a\phi'}{a'}\Psi\right),$$

dubbed as the Mukhanov–Sasaki variable [45], is gauge-invariant. Here Ψ is the scalar potential referred to the excitation of the spatial metric. The quantity u satisfies the equation

$$u'' - \Delta u - \frac{z''}{z}u = 0 \ , \tag{24}$$

where

$$z = \frac{a^2\phi'}{a'} \ . \tag{25}$$

It is straightforward to show that in the slow roll approximation $z''/z = 2/\eta^2$, and, therefore, the Eq. (24) coincides with one of the massless scalar field on the de Sitter background. Thus, following the same evolution and starting from the vacuum initial conditions, we simply write down the answer for the amplitude of u/a in the superhorizon regime,

$$\mathcal{P}_{u/a} = \frac{H}{2\pi} \ .$$

Furthemore, in the superhorizon regime the curvature perturbation ζ and the Mukhanov–Sasaki variable are related to each other by

$$u = -z\zeta \ .$$

The power spectrum for the quantity ζ then reads

$$\mathcal{P}_\zeta = \frac{H^2}{2\pi|\dot{\phi}|} \ . \tag{26}$$

The curvature perturbations ζ stays frozen out until the end of the inflation, survives through the reheating and serves as the initial condition for the scalar perturbations at the beginning of the conventional hot epoch.

If we go beyond the approximation of the massless scalar field evolving on the de Sitter background, the power spectrum becomes slightly tilted. To show this, we replace the power spectrum obtained above with the following one,

$$\mathcal{P}_\zeta \to \mathcal{P}_\zeta(k) = \frac{H_k^2}{2\pi|\dot{\phi}_c(\eta_k)|} \,. \tag{27}$$

The subscript k here implies that the Hubble parameter is different at times, when different modes k exit the horizon. Clearly, this effect is described in terms of the slow roll parameter $\epsilon = -\frac{\dot{H}}{H^2}$. The second effect captured by the formula (27) is the variation of the inflaton derivative. This is due to the non zero effective mass of the inflaton, $V_{\phi\phi}$, and described in terms of the slow roll parameter η. The deviation from the flatness is normally characterized by the scalar tilt defined as follows

$$n_s - 1 = \frac{d\ln\mathcal{P}_\zeta}{d\ln k} \,.$$

After not very tricky calculations, one obtains the following expression for the spectral tilt [39, 40, 41, 42]:

$$n_s - 1 = 2\eta - 6\epsilon \,.$$

The last term on the right hand side is always negative, since $\epsilon > 0$. Thus, taken separately it sources the red spectrum. On the other hand, the first term may be either positive or negative in dependence of the effecive mass squared of the inflaton, and stands for the blue or red tilt, respectively.

The slightly tilted spectrum of primordial scalar perturbations is the most well-known prediction of the inflation. It is, however, not a particularly strong signature, since it is easily achieved in the alternative frameworks, e.g. models of the (pseudo)-Conformal Universe [19, 26]. It appears that tensor perturbations are much more interesting in this regard.

2.2.1 Tensor perturbations

One more issue commonly discussed within the inflation, is the creation of primordial tensor perturbations. Though this issue is out of the scope of this thesis, it is of the particular importance from the observational point of view. In fact, primordial tensor perturbations serve as the potential "anti-smoking gun" for a broad row of cosmological models. As we will see shortly, the standard inflation predicts the tensor perturbations, which may be naturally of the detectable size. This may not be the case in different cosmological frameworks. In particular, the tiny tensor perturbations are naturally predicted by curvaton mechanisms (see discussion in Section 2.3 and references therein), or in the frameworks alternative to the inflation.

During inflation, the tensor perturbations satify the same equation as the Mukhanov–Sasaki variable. Then, if they start from the vacuum initial state in the de Sitter space-time, they follow the same evolution. Consequently, in the superhorizon horizon regime they acquire the flat spectrum. First this has been shown in the context of Starobinsky's model [2].

We decompose the tensor perturbation h_{ij}^{TT} as follows

$$h_{ij}^{TT} = \sum_{A=1,2} e_{ij}^{A} h^{A} \ ,$$

where e_{ij}^{A} are the basic symmetric traceless tensors, see Appendix A for more details. Note that the fields h^A are not canonically normalized. Thus, it is more convenient to work with the field, $\phi^A = \sqrt{\frac{M_{Pl}^2}{32\pi}} h^A$, or, more precisely with the variable $\tilde{\phi}^A = a(\eta)\phi^A$. Since the fields $\tilde{\phi}^A$'s are canonically normalized and obey the same equation as the field χ, the power spectrum of the fields ϕ^A in the superhorizon regime reads

$$\mathcal{P}_{\phi^A}(k) = \frac{H_k^2}{(2\pi)^2} \ .$$

Returning to the variables h^A, we obtain the power spectrum of tensor perturbations,

$$\mathcal{P}_T = \frac{16}{\pi} \frac{H_k^2}{M_{Pl}^2} \ .$$

Here we take into account the fact that there are two tensor polarizations. As it follows, the tensor perturbations have flat power spectrum to the zeroth order in the slow roll parameters. With the slow roll conditions obeyed, one writes the power spectrum as follows,

$$\mathcal{P}_T = \frac{128}{3} \frac{V}{M_{Pl}^4} \ ,$$

and the tensor-to-scalar ratio reads,

$$r \equiv \frac{\mathcal{P}_T}{\mathcal{P}_{\mathcal{R}}} = \frac{1}{\pi} \frac{M_{Pl}^2 V_\phi^2}{V^2} = 16\epsilon \ .$$

The present constraint is [1]

$$r < 0.20$$

at the 95% confidence level. As it follows, the small (relatively large) parameter ϵ implies in turn the small (relatively large) magnitude of the tensor perturbations. This correspondence existing in the minimal versions of the inflation does not necessarily hold in more complicated scenarios, e.g. ones incorporating higher derivative terms [59, 60, 61].

The power spectrum of tensor perturbations is also slightly tilted. In the minimal inflation, the tensor tilt is given by,

$$n_T \equiv \left.\frac{d\ln \mathcal{P}_T}{d\ln k}\right|_{k=k_\star} = -2\epsilon \ .$$

This provides us with the model-independent prediction of the single field slow roll inflationary models,

$$n_T = -\frac{r}{8} \ .$$

The detection of the tensor perturbations with parameters obeying this relation, will be a strong argument in favor of the inflation in its minimal versions. More generally, the observation of any primordial tensor perturbations would be a very big problem for the alternative frameworks. In particular, this concerns the conformal rolling scenario and other models of the (pseudo)-Conformal Universe.

2.3 Curvaton model

2.3.1 Basic ideas

So far we discussed the single-field slow roll inflation. The attractive feature of this type of models is that the problems of the Hot Big Bang are resolved in the unique manner, i.e. by introducing the single field, the inflaton. In this framework, the Hot Big Bang starts from the initial conditions described in terms of the adiabatic perturbation ζ, which obeys the essentially Gaussian statistics. Though these properties are favored by the current experiments, even small deviations from the adiabaticity and Gaussianity detected in the forthcoming PLANCK data, would be a strong argument against the simplest models of inflation. This is one of the motivations to develope alternative mechanisms of primordial perturbations creation. In this Section we focus on the simple mechanism provided in the curvaton scenario [46, 47, 49, 48]; our discussion will mostly follow the Refs. [47, 49, 50]. Note that our main motivation here is somewhat different from one mentioned above. As it will become clear shortly, the ideas, which appeared first in the context of curvaton models, are generic ones in the sense that they do not rely on the assumption of the inflationary stage. In particular, this concerns the important issue of conversion entropic perturbations into adiabatic ones. We will encounter this problem in the context of the conformal rolling scenario. Moreover, it appers in almost all known alternatives to the inflation. The reason is that relevant perturbations are commonly generated by the subdominant field(s) there and, therefore, they are of the isocurvature type at the very beginning of the conventional cosmological epoch. The purpose of the discussion below is to ensure the reader that this situation is not hopeless at all.

Let us assume that primordial cosmological perturbations are produced from fluctuations of the scalar field σ (different from the inflaton) during a period of inflation, in the case when the perturbations of the inflaton are considered to be negligible. The curvaton is supposed to be the subdominant component of the Universe during the inflation. Hence, its fluctuations are initially of the isocurvature type. To do not go into contradiction with the experimental data, one should think of the mechanism converting isocurvature perturbations into adiabatic ones. We postpone this discussion until the next Subsection. Here we focus on the evolution of the curvaton during the inflation. The unperturbed curvaton field satisfies the equation of motion

$$\sigma'' + 2\frac{a'}{a}\sigma' + a^2 V_\sigma = 0 \ .$$

Next, we expand the curvaton field up to the first order in the perturbations around the homogeneous background as

$$\sigma(\mathbf{x}, \eta) = \sigma(\eta) + \delta\sigma(\mathbf{x}, \eta) \ ,$$

The linear perturbations satisfy the following equation on the large scales

$$\delta\sigma'' + 2\frac{a'}{a}\delta\sigma' + a^2 V_{\sigma\sigma}\delta\sigma = 0 \ .$$

This is essentially the same equation as of the inflaton fluctuation on the superhorizon scales[5]. Hence, the fluctuation $\delta\sigma$ on superhorizon scales will be Gaussian distributed and they will have a nearly scale-invariant spectrum

$$\mathcal{P}_{\delta\sigma} \approx \frac{H_k^2}{(2\pi)^2} \ .$$

This is true provided that the effective mass of the curvaton is small as compared to the Hubble parameter during the inflation, i.e. $m_{eff}^2 = V_{\sigma\sigma} \ll H^2$. The subscript k denotes that the Hubble parameter may vary between the horizon-exit of modes with different momenta k. The spectral tilt is then given by

$$n_\sigma - 1 \equiv \frac{d\ln\mathcal{P}_\sigma}{d\ln k} = 2\frac{\dot{H}}{H^2} + \frac{2}{3}\frac{V_{\sigma\sigma}}{H^2} \ .$$

We assume that this spectral tilt is inherited by the adiabatic perturbations generated after the curvaton decay. For the quadratic potential we then obtain the slightly blue spectrum of primordial perturbations. This may not be the case for the general potential since the effective mass-squared $m_{eff}^2 = V_{\sigma\sigma}$ may be either positive or negative.

[5]To establish the better correspondence with the discussion in Section 2.2, one chooses to work with the variable $\delta\tilde{\sigma} = a\delta\sigma$.

2.3.2 Conversion into adiabatic perturbations

After the end of the inflation the curvaton perturbation $\delta\sigma$ the classical value σ and, hence, their ratio $\delta\sigma/\sigma_c$ stay constant for some time. Once the Hubble parameter drops below the mass of the curvaton m_{eff}, the oscillations about the minimum of the potential $V(\sigma)$ (taken, say, at $\sigma = 0$) start. Provided that the potential is quadratic, the curvaton perturbation to its classical value ratio stays constant in the oscillatory regime, since they obey one and the same equation in this case. Even if the curvaton potential is not quadratic, after some Hubble times one can make the approximation $V \approx \frac{1}{2}m^2\sigma^2$. The fractional field perturbation then has some constant value

$$\left(\frac{\delta\sigma}{\sigma}\right) = q\left(\frac{\delta\sigma}{\sigma}\right)_\star ,$$

where the constant q equals to unity in the case of the initially quadratic potential, while in the opposite case $q < 1$. For simplicity, we will always assume that $q = 1$. The energy density in the oscillating field is given by

$$\rho_\sigma(\eta, \mathbf{x}) = \frac{1}{2}m_\sigma^2\sigma^2(\mathbf{x}, \eta) ,$$

where $\sigma(\mathbf{x}, \eta)$ is the amplitude of the oscillation. We define the fractional energy density keeping also the quadratic term,

$$\frac{\delta\rho_\sigma}{\rho_\sigma} \approx 2\frac{\delta\sigma}{\sigma} + \frac{(\delta\sigma)^2}{\sigma^2} . \tag{28}$$

The non-linear term may not be particularly small, thus giving rise to the significant non-Gaussianity.

During the oscillatory stage, the energy density of the curvaton field scales as non-relativistic matter $\rho_\sigma \sim a^{-3}$. This observation is crucial from the viewpoint of converting isocurvature perturbations into adiabatic ones. Indeed, since the radiation scales with the scale factor as $\rho_\gamma \sim a^{-4}$, the curvaton field may give the significant contribution to the total energy density or even dominate the latter at some point. Thus, its isocurvature perturbations may be converted into adiabatic ones.

Let us study this mechanism in more details. The convenient way to do it is to introduce the gauge-invariant curvature perturbation ζ_i associated with each individual energy density component. The weighted sum during the oscillations of the curvaton field can be written as follows,

$$\zeta = (1 - f)\zeta_\gamma + f\zeta_\sigma , \tag{29}$$

where the quantity f is given by

$$f = \frac{\rho'_\sigma}{\rho'} = \frac{3\rho_\sigma}{4\rho_\gamma + 3\rho_\sigma} .$$

Let us work in the approximation of the sudden decay of the curvaton field, i.e. we assume that the decay effects can be neglected right until some point in time, when the decay width Γ becomes of the order of the Hubble parameter. At this point, all the energy of the curvaton field instantaneously gets converted into the energy of the radiation. Before the sudden decay, the curvaton and the radiation energy densities satisfy the energy conservation equation separately,

$$\rho'_\gamma = -4\frac{a'}{a}\rho_\gamma \ , \quad \rho'_\sigma = -3\frac{a'}{a}\rho_\sigma \ ,$$

and the curvature perturbation ζ_i of each component remains constant on superhorizon scales until the decay of the curvaton. In the curvaton scenario, the inflaton field is supposed to give a negligible contribution to the primordial scalar perturbations formation. Under this assumption, the initial curvature perturbation in radiation is negligible. Then, well before the epoch of the curvaton decay, the total curvature perturbation is given by

$$\zeta_{tot} = f\zeta_\sigma^{in} \ , \quad \zeta_\gamma = 0 \ .$$

Before the oscillations start, the contribution of the curvaton field to the total energy density is small. Hence, the quanity f is also small. Thus, the perturbations at this stage are of the purely isocurvature type, i.e. the total curvature perturbation is negligible. They evolve in the superhorizon regime due to the evolution of the quanity f. During the oscillatory regime, the contribution of the curvaton field to the total energy density grows. Hence, the quantity f also grows. Extrapolating the Eq. (29) to the time of the curvaton decay, we obtain the total curvature perturbation at this time,

$$\zeta_{tot} = f_D\zeta_\sigma^{in} \ . \tag{30}$$

After the curvaton decay, the total energy density is due to the radiation solely. Thus, it is of the adiabatic type and characterized by the unique curvature perturbation ζ. Strictly speaking, the sudden decay approximation is applied provided that the curvaton field dominates the evolution of the Universe at the time of the decay, i.e. provided that the decay constant $f_D \approx 1$. This is the result of the numerical calculations made in [50]. In the opposite case, the constant f_D should be replaced by the ratio

$$r \approx \left(\frac{\rho_\sigma}{\rho}\right)_D$$

defined at the time of the decay.

2.3.3 Non-Gaussianity in curvaton scenario

It is interesting to speculate about the possible values of the parameter r. At the theoretical level, it can be arbitrarily small. This corresponds to the case of the arbitrarily large curvaton

perturbation. Going into the particularly small values of r, however, strikes the observational constraint, see (6). Indeed, shortly we will see that the small parameter r implies the large non-Gaussianity, namely $f_{NL} \sim \frac{1}{r}$.

In more details, the initial curvature perturbation corresponding to the curvaton field evaluated on the unperturbed hypersurfaces ($\Psi = 0$) is given by

$$\zeta_\sigma = \frac{1}{3}\frac{\delta\rho_\sigma}{\rho_\sigma} \ . \tag{31}$$

Now, we substitute the fractional energy density from the Eq. (28) and keep only the linaer term for the time being. This results into the purely Gaussian total curvature perturbation

$$\zeta_g = \frac{2r}{3}\frac{\delta\sigma}{\sigma} \ .$$

Here we made use of the Eq. (30), where we replaced the decay constant f_D by the ratio r. Expressing the relative curvaton perturbation from this formula and substituting it into the Eq. (28), and then substitung the relative energy density perturbation with the non-linear term included back into the formula (31) and again making use of the Eq. (30), we obtain

$$\zeta = \zeta_g + \frac{3}{4r}\zeta_g^2 \ .$$

Comparing the latter formula with the Eq. (5), one finally obtains the non-Gaussianity parameter [49]

$$f_{NL} = \frac{5}{4r} \ .$$

Thus, very small values of r (and, in turn, very large curvaton perturbation) are in a contradiction with the experimantal data. The "disadvantage" of this result is that curvaton fluctuations are not allowed to be arbitrarily large, since the constraint (6). In the Chapter 3, this will turn into the constraint on the unique parameter of the conformal rolling scenario. The pleasant feature is that the non-Gaussianities generated by the curvaton (or analogous) mechanisms can serve as the descriminator between models of the early Universe, i.e between minimal versions of inflation and different frameworks. We will strengthen this statement in the following Section, where a bit broader picture of the possible primordial non-Gaussianities is given.

2.4 Shapes and magnitudes of non-Gaussianities during inflation: general case

2.4.1 Bispectrum

It may happen so that no significant tensor modes are detected in the PLANCK experiment. The scalar tilt appears to be a very weak descriminator between the models of the early

Universe. Hopefully, there are other interesting signatures: the non-Gaussianity and the statistical anisotropy. In this Section we focus on the former one.

Clearly, the non-Gaussianity in the spectrum of primordial perturbations originates from the non-linearities in the equations of motion of fields sourcing the adiabatic mode. If these non-linearities are suppressed, the spectrum of resulting perturbations is Gaussian with a high accuracy. This is the case, e.g. of the minimal inflationary models [27]. On the other side, non-linearities, and, hence, non-Gaussianities can be large enough in the curvaton scenario. These two examples, however, do not give the complete picture of non-linearities, which may arise in the inflationary framework. Any thorough discussion of this issue could be the subject of the separate thesis. Here we just give a very brief picture of the possible non-Gaussianities generated by the inflationary mechanisms.

It is instructive to start with the simplest models of the inflation. To calculate the non-Gaussianities there, one expands the cosmological perturbation theory up to the second order in the inflaton-metric fluctuations. This analysis is very involved, and we refer the interested reader to a very nice summary on these issues in [51]. We will, however, show on rather general grounds that non-Gaussianity in the single-field slow roll inflation is tiny. In particular, the magnitude of the non-Gaussianity is well below the sensitivity of the WMAP and PLANCK experiments. In the first iteration, one naively estimates the level of non-linearities accounting for the inflaton fluctuations only. This, however, leads to a wrong estimate: the parameter of the non-Gaussianity reads in this case $f_{NL} = \mathcal{O}(\epsilon^2, \eta^2)$, [52]. The leading contribution comes from the non-linearities in the fluctuations of the metric, and estimated as $f_{NL} = \mathcal{O}(\epsilon, \eta)$, [53]. There is an elegant way to demonstrate this statement following the argument presented by Maldacena in his work [27]. For this purpose, let us specify to the so called squeezed limit, which implies that one of the three momenta, say k_1, is much smaller than the other two. Then, $k_2 \sim k_3$. The fluctuation $\zeta_{\mathbf{k_1}}$ is frozen by the time the other two momenta cross the horizon. So, its only effect is to rescale the other two momenta, so that we get a contribution propotional to the violation in scale invariance of the two-point function with large momenta. Thus, we conclude that the effect should be propotional to the tilt of the scalar perturbations,

$$\langle \zeta_{\mathbf{k_1}} \zeta_{\mathbf{k_2}} \zeta_{\mathbf{k_3}} \rangle \sim \langle \zeta_{\mathbf{k_1}} \zeta_{-\mathbf{k_1}} \rangle k \frac{d}{dk} \langle \zeta_{\mathbf{k_2}} \zeta_{\mathbf{k_3}} \rangle = -(n_s - 1) \langle \zeta_{\mathbf{k_2}} \zeta_{\mathbf{k_3}} \rangle \langle \zeta_{\mathbf{k_1}} \zeta_{-\mathbf{k_1}} \rangle \ .$$

To avoid the confusion, note that the non-Gaussianity of the standard inflation is not captured fully by the squeezed limit. However, the result for the full bispectrum is in agreement with the estimate $f_{NL} = \mathcal{O}(\epsilon, \eta)$. The qualification here is that the non-Gaussianity in the minimal inflation is not of the local type, but has a more generic structure. Hence, the parameter f_{NL} is not a constant but a function of the momenta $\mathbf{k}_1$ and $\mathbf{k}_2$. Note also that the primordial non-Gaussianity calculated in [27] is not the one, which could be, in principle, measured in the CMB experiments. There is also the contribution due to the non-linear

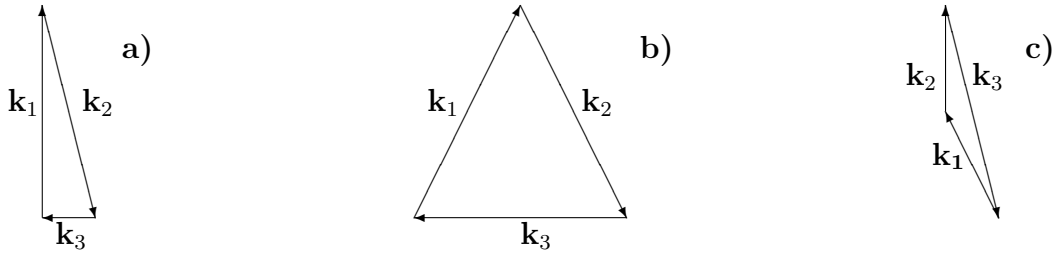

Figure 1: The momenta $\mathbf{k}_i$ describing the bispectrum satisfy the triangle relation: $\mathbf{k}_1 + \mathbf{k}_2 + \mathbf{k}_3 = 0$. Three interesting configurations with respect to the triangle relation are: a) the squeezed configuration; b) the equilateral one; c) the flattened triangle.

evolution of the gravitational potentials at the conventional cosmological epoch resulting into the significant improvement of the parameter f_{NL}, so that the latter is estimated as $f_{NL} \sim 1$ at the times of the last scattering. Still, this value is below the sensitivity of the PLANCK experiments, $|f_{NL}| \simeq 5$. Clearly also, this improvement is inherent to the physics at the hot epoch rather than to any features of the primordial physics. Thus, it is not the descriminator between the early Universe models at all. In what follows, we focus on the primordial non-Gaussianities.

In principle, the non-Gaussianity may have a rich structure as in the minimal versions of the inflation and a large value as in the curvaton models. The general form of the three-point function in the Fourier representation is given by

$$\langle \zeta_{\mathbf{k_1}} \zeta_{\mathbf{k_2}} \zeta_{\mathbf{k_3}} \rangle = (2\pi)^3 \delta \left(\sum_i \mathbf{k}_i \right) F_\zeta(\mathbf{k}_1, \mathbf{k}_2, \mathbf{k}_3) \, .$$

The δ-function standing here preserves the translation invariance; $F_\zeta(\mathbf{k}_1, \mathbf{k}_2, \mathbf{k}_3)$ is the bispectrum. As it follows, all the possible configurations in the momentum space satisfy the triangle relation $\mathbf{k}_1 + \mathbf{k}_2 + \mathbf{k}_3 = 0$. Thus, it is possible to describe the trispectrum in terms of the variables k_1, k_2 and k_3. Interesting configurations following from the triangle relation appear in the limits listed below:
i) the squeezed limit, when one of the three momenta, say k_3, is much less than the other two;
ii) equilateral one, when all three momenta have equal magnitude;
iii) flattened triangle, which corresponds the degenerate configuration with $k_1 = k_2 = \frac{1}{2} k_3$.
This classification is well motivated from the physical point of view. Accordingly to [54], the squeezed bispectrum corresponds to the situation, when the evolution outside the horizon dominates. This situation is natural in the context of the curvaton models [46, 47, 48], the inflation with multiple light scalars (see e.g. [57] and references therein) or in the modulated decay scenario [56, 55]. The equilateral configuration corresponds to the non-Gaussianity

generated at the horizon-crossing. The flattened triangle configuration is less widely discussed, and it corresponds to the non-Gaussianity generated in the subhorizon regime [62]. This occurs, if the inflaton fluctuations start from initial conditions different from the vacuum ones. The consistensy of this scenario is questionable, and we omit it in our discussion.

In line with the classification of Babich, Creminelli and Zaldarriaga [54], the local type bispectrum peaks in the squeezed limit. Indeed, once we go into the Fourier space, the Eq. (5) implies the function F_ζ of the form

$$F(\mathbf{k}_1, \mathbf{k}_2, \mathbf{k}_3) \propto \frac{f_{NL}\mathcal{P}_\zeta^2}{\Pi_{i=1}^3 k_i^3} \cdot \sum_i k_i^3 \ .$$

The dependence on the momenta k_i encoded in this formula, translates into the enhancement of the bispectrum $F_\zeta(k_1, k_2, k_3)$ in the squeezed limit, in accord with the expectations of the Ref. [54].

The equilateral configuration is provided, once the correlation is among the modes with comparable wavelengths, which exit the horizon nearly at the same time. This opportunity is realized if the non-Gaussianity is generated by derivative interactions: these interactions become exponentially irrelevant, when the modes exit the horizon because both time and spatial derivatives become small, so that all the correlation is among the modes freezing almost at the same time. The examples of this type are obtained if we add higher derivative operators [58]. Provided that the latter are crucial for the inflaton dynamics as is the case of the k-inflation [59], the DBI inflation [61] or the ghost inflation [60], one's natural prediction is the non-Gaussianity peaking in the equilateral limit. On the other hand, the corresponding bispectrum is suppressed in the squeezed limit. This statement is true for the generic single-field inflation and holds if no other fields apart from the inflaton play a significant role in the primordial perturbations creation [63]. The reason is essentially the same as in the minimal versions of the inflation. Thus, the suppression is again of the order of the scalar tilt. Consequently, the behaviour of the bispectrum in the squeezed limit is the key to understanding if the primordial seeds of the structure formation are sourced by the (unique) inflaton field or not. So, the enhancement of the squeezed configuration would imply the presence of the additional degrees of freedom like those of the curvaton models [46, 47, 49], modulated decay scenario [56, 55] etc. This opportunity is also natural in the alternative frameworks. On the other hand, the detection of the equilateral type bispectrum (suppressed in the other limits) in the future experiments would be a strong argument in favor of the inflation. Indeed, in most alternative frameworks, e.g. ones we consider in this thesis, the three-point function peaks at best at the squeezed configuration. This is clear from the discussion above: the equilateral bispectrum implies the low correlation between modes with different momenta. This opportunity is natural, once the scale factor changes rapidly, i.e. in the inflation.

2.4.2 Trispectrum

The richer phenomenolgy is given, once we turn to the non-Gaussianity in the four-point function of the primordial fluctuations. Commonly it is described in terms of the function T_ζ, the trispectrum, defined from

$$\langle\zeta(\mathbf{k}_1)\zeta(\mathbf{k}_2)\zeta(\mathbf{k}_3)\zeta(\mathbf{k}_4)\rangle_c = (2\pi)^3\delta(\mathbf{k}_1+\mathbf{k}_2+\mathbf{k}_3+\mathbf{k}_4)T_\zeta(\mathbf{k}_1,\mathbf{k}_2,\mathbf{k}_3,\mathbf{k}_4)\ ,$$

where only the connected part of the four-point function on the left hand side is considered. Unlike the bispectrum, the trispectrum typically depends on the relative orientations of the $\mathbf{k}_i$ in addition to their magnitudes. It is convenient to use the momenta k_1, k_2, k_3, k_4, $k_{12} = |\mathbf{k}_1+\mathbf{k}_2|$ and $k_{14} = |\mathbf{k}_1+\mathbf{k}_4|$ as the independent variables. In what follows, it is more convenient to work with the trispectra $\mathcal{T}$ defined from,

$$T(k_1,k_2,k_3,k_4,k_{12},k_{14}) = \frac{\mathcal{P}_\zeta^3}{\Pi_{i=1}^4 k_i^3}\mathcal{T}(k_1,k_2,k_3,k_4,k_{12},k_{14})\ .$$

The configurations of interest are listed below [64].

- Squeezed limit configuration. In this case, one of the external momenta is small as compared to the others, say, $k_1 \ll k_2 \sim k_3 \sim k_4$.
- Equilateral configuration: all the external momenta have the same magnitude, i.e. $k = k_1 = k_2 = k_3 = k_4$.
- Folded limit configuration corresponds to the situation, when two momenta with the equal magnitude have the opposite direction, say, $k_{12} \to 0$, and, respectively, $k_1 = k_2$, $k_3 = k_4$.
- Specialized planar limit configuration. In this case, one has $k_1 = k_3 = k_{14}$, and

$$k_{12} = \left[k_1^2 + \frac{k_2k_4}{2k_1^2}\left(k_2k_4 + \sqrt{(4k_1^2-k_2^2)(4k_1^2-k_4^2)}\right)\right]^{1/2}\ .$$

- Near double limit configuration: the tetahedron is now a planar quadrangle and $k_3 = k_4 = k_{12}$.

Let us look at the local type non-Gaussianities from the viewpoint of these configurations. Commonly, the following parametrization is used to describe the locally non-Gaussian perturbation in the real space [65, 66]

$$\zeta = \zeta_g + \frac{3}{5}f_{NL}(\zeta_g^2 - \langle\zeta_g^2\rangle) + \frac{9}{25}g_{NL}(\zeta_g^3 - 3\zeta_g\langle\zeta_g^2\rangle)\ ,$$

where f_{NL} and g_{NL} are generically independent parameters. We separate the reduced trispectrum into the sum of two contributions [69],

$$\mathcal{T}_{\zeta}^{local} = f_{NL}^2 \mathcal{T}_1^{local} + g_{NL} \mathcal{T}_2^{local} \ .$$

In the momentum representation,

$$\mathcal{T}_1^{local} = \frac{9}{50} \left(\frac{k_1^3 k_3^3 + k_1^3 k_4^3 + k_2^3 k_3^3 + k_2^3 k_4^3}{k_{12}^3} + \{\mathbf{k}_2 \leftrightarrow \mathbf{k}_3\} + \{\mathbf{k}_2 \leftrightarrow \mathbf{k}_4\} \right) \ .$$

and

$$\mathcal{T}_2^{local} = \frac{27}{100} \sum_{i=1}^{4} k_i^3 \ .$$

There are two interesting degenerate configurations, where a non-Gaussianity of the local form maximizes the trispectrum. The first is again the squeezed limit, with one of the three momenta taken to zero. In this limit, the quadrilateral, formed by the momentum vectors $\mathbf{k}_i$ degenerates into a triangle. For instance, taking $k_4 \ll k_1, k_2, k_3$ one obtains

$$\mathcal{T}_{\zeta}^{local} = \left(\frac{9}{25} f_{NL}^2 + \frac{27}{100} g_{NL} \right) \sum_i k_i^3 \ .$$

Thus, τ_{NL} and g_{NL} contribute equally to the trispectrum in this limit. The second interesting limit occurs, when the magnitude of the sum of two momenta is taken to zero, so that $k_{ij} = |\mathbf{k}_i + \mathbf{k}_j| \to 0$ for some $i \neq j$, i.e. in the folded case. The local trispectrum simplifies in this limit. By taking $k_{12} \ll k_1 \approx k_2, k_3 \approx k_4$ one obtains

$$\mathcal{T}_{\zeta}^{local}(\mathbf{k}_1, \mathbf{k}_2, \mathbf{k}_3, \mathbf{k}_4) = \frac{18}{25} \frac{k_2^3 k_4^3}{k_{12}^3} f_{NL}^2 \ .$$

Thus, only f_{NL} contributes to the trispectrum in this limit.

Once again, the trispectrum of the local type is the natural prediction of models, where the fields different from the inflaton play a significant role in the primordial scalar perturbations creation, as it occurs in the curvaton scenario or by the modulated decay mechanisms. Clearly, the trispectrum generated in this way does not necessarily rely on the assumptions of the de Sitter expansion. Hence, common predictions may arise in the different frameworks. Interested in the intrinsic large non-Gaussianities, one again turns to the inflation incorporating higher derivative terms[6] [68]. To account properly for the possible non-linearities in that case, the effective field theory approach is commonly employed. For the inflation, it

[6]As in the case of the bispectrum, non-Gaussianities at the level of the four-point function are of the undetectable size for the minimal versions of inflation and, thus, the object of the purely theoretical considerations [67].

has been proposed in [70] and further extended in [64, 71, 72, 73, 74, 75]. Basing on this approach, generic conclusions have been made. In particular, the trispectrum of the single-field inflation must be finite in the folded limit, $k_{12} \to 0$, see [64]. This is in contrast to the predictions of the conformal rolling scenario [7] [21, 22], where the trispectrum has a (fairly mild) singularity as $k_{12} \to 0$. On the other hand, the trispectrum there is distinct from one of the local type. We postpone the further discussion until the next Chapter.

2.5 Statistical anisotropy

In a view of the future results, let us discuss the issue of the statistical anisotropy, which may appear in the context of the inflation. Remind that at the level of the primordial scalar perturbations, the violation of the statistical isotropy implies the direction dependence of their power spectrum. This translates into the non-zero correlations of the CMB temperature coefficients a_{lm} with different l's. To generate the primordial statistical anisotropy, one naturally assumes that the rotational invariance is partially broken during the inflation [76]. Then, the inflaton fluctuations evolving on this background acquire the direction dependent spectrum. Note, however, that the anisotropic ("hairy") background is hardly achieved during the inflation. First of all, it is challenging because of the cosmic no-hair conjecture [77]. The latter states that the initially expanding homogeneous cosmological models in the presence of a positive cosmological constant will rapidly approach a de Sitter solution, if the other matter fields obey the dominant and the strong energy conditions. Therefore, the statistical isotropy is favored by the inflation. There is, however, a line of researches showing that the cosmic non-hair theorem may be avoided in the inflationary framework, see e.g. [78] and references therein.

Indeed, several proposals have been made in literature, where the statistical anisotropy is achieved by introducing vector fields [79, 80, 81, 82]. In this framework, the issue of the statistical anisotropy is akin to the problem of generating primordial magnetic fields during the inflation. Originally, this issue was discussed in [84] (see also [83]), and it was argued there that only tiny magnetic fields can be generated by the inflationary mechanisms. Further, it was understood that this statement can be circuvemented [85], see also [86] for more recent discussions. Interestingly, the backreation of generated vector fields may affect the background, so that it may become slightly anisotropic. Consequently, the inflaton fluctuations may acquire the direction-dependent power spectrum. The qualification here is that vector fields must have rather peculiar properties in order to source the statistical anisotropy. Clearly, the standard Maxwellian fields are not appropriate for this purpose, since their contribution falls rapidly in the inflationary Universe, thus, leaving the negligible imprint on the background evolution. The example of statistical isotropy violated in terms

[7] The speech is about the version with superhorizon modes, see Chapter 3.

of vector fields is given in the model by Ackerman, Carroll and Wise (ACW model) [79], which attracted much attention recently. There the authors introduced the spacelike massive vector with the fixed norm, which created the slightly anisotropic background. The authors concluded with the following power spectrum of the primordial scalar perturbations,

$$\mathcal{P}_\zeta = \mathcal{P}_0(1 + g_\star(\mathbf{d}\hat{\mathbf{k}})^2) \ . \tag{32}$$

This is the statistical anisotropy of the special quadrupole type. It is characterized by the amplitude $g_\star$ and two direction of the unit vector $\mathbf{d}$. Though being the most widely discussed, the ACW model suffers from the instability problem. Moreover, pathologies have been found in models characterized by, [87]:
i) a potential $V(A^2)$ for the vector A_μ, i.e. the inflation with massive vector fields;
ii) a fixed spatial norm of the vector, enforced by a lagrange multiplier;
iii) a nonminimal coupling of the vector to the scalar curvature.
In all three cases the ghost instabilities have been uncovered. Pathological is the longitudinal degree of freedom, which is dynamical because of the broken $U(1)$ symmetry. Though it is so, the direction dependence of the special quadrupole type holds in the healthy scenarios[8], e.g. in [81]. The main idea of this model is the gauge field with the non-standard kinetic term,

$$S = -\frac{1}{4}\int d^4x\sqrt{-g}f^2_{ab}(\phi)F^{a\mu\nu}F^b_{\mu\nu} \ ,$$

where $F^a_{\mu\nu} = \partial_\mu A^a_\nu - \partial_\nu A^a_\mu$, and f_{ab} is the gauge kinetic function. Clearly, this specific way of coupling of the gauge fields preserves the $U(1)$ symmetry. Thus, the argument of [87] is not applied. Indeed, and the model [81] is free of pathologies [88]. Further, for a broad range of the gauge kinetic functions, the conditions, at which the cosmic no-hair theorem is obeyed, may be circuvemented. Consequently, there is a chance to obtain the direction dependence of the power spectrum. Indeed, as it has been shown in the anisotropic background metric

$$ds^2 = dt^2 - e^{2Ht}\left[e^{-2\Sigma t}dx^2 + e^{2\Sigma t}(dy^2 + dz^2)\right] \ , \tag{33}$$

is the attractor solution for a wide range of kinetic functions. Here H and Σ describe the average expansion rate and the anisotropic expansion rate, respectively. Further, the inflaton perturbations evolving on the anisotropic background (33) obtain the direction dependent power spectrum of the ACW form (32). The issue of naturalness in the model [81] is also addressed in the sense that the gauge fields with the peculiar couplings naturally arise in the bosonic sector of the supergravitational theory.

[8]It appears that the model [80] with the vector coupled to the waterfall field of the hybrid inflation is also free of pathologies, but the imprint of the vector field on the background remains ubiquitos in that case, at it has been pointed out by Soda himself in [82]

The other class of models, still involving vector fields, is presented in the framework of the vector curvaton paradigm [89]. However, the prediction is again the power spectrum of the ACW form. Different predictions about the form of the power spectrum may arise in the inflation extended by the scalar fields with the non-minimal kinetic terms [90]. In this case, the quadrupole statistical anisotropy is absent at all. There have been also studies relying on the inhomogeneities during the inflationary stage at the times, when the inflaton fluctuations are deep subhorizon and characterized by the trans-Planckian momenta, see [91]. More exotic scenarios are ones relying on the non-commutative geometry [92, 93].

To conclude, we note that the statistical anisotropy appears to be a marginal prediction of the inflationary framework, since it requires many efforts and encounters a lot of problems. On the other hand, it is easily obtained in the conformal rolling scenario [**?**, 23]. This is one of the crucial differences between two setups, which in turn implies different predictions about the correlations of the CMB temperature coefficients. Hence, the statistical anisotropy may be viewed as the powerful tool in descriminating between the inflation and the conformal rolling scenario.

2.6 Alternatives to inflation: ekpyrotic scenario

Before we turn to the conformal rolling scenario, let us give a brief overview of the ekpyrotic models. Among the other alternatives to the inflation, they are ones most widely discussed nowadays.

Our main motivation in this Section is as follows. Dynamical scenarios of the (pseudo)-Conformal Universe, which are the subject of our primary interest in the present thesis, result into a very slow contraction/expansion at very early times. The first opportunity is in the certain sense the incarnation of the ekpyrotic phase, as we discuss it below. It is realized, e.g. in the conformal rolling scenario treated as the dynamical model. Thus, the latter shares some problems of the ekpyrotic models. Hopefully, some ot them are absent.

Originally, the ekpyrotic cosmology is based on the braneworld picture of the Universe, in which spacetime is effectively five-dimensional, but the fifth dimension is not infinite, but being a line segment [15]. The endpoints of this line segment (orbifold) are two $(3 + 1)$-dimensional boundary branes. Our Universe is identified with one of the branes. Futher, there is the attractive force between the branes, which causes them to collide at some point. This collision is associated with the Big Bang. Being highly inelastic process, this collision produces the matter and the radiation on the branes, where the now standard cosmology takes the place. Remarkably, far from this collision the ekpyrotic models admit a fully four-dimensional description. In this effective picture the effects of the fifth dimension are captured by the scalar field ϕ, the radion, associated with the distance between the branes. Once the scalar field drives the evolution of the Universe, the latter undergoes the stage of the slow contraction. As we will see shortly, the latter condition is enough to solve one of

the most challenging problem of the contracting Universe, i.e. the problem of the growing anisotropies.

Let us consider the contribution of the anisotropies in the contracting Universe. This problem has been addressed a long time ago in the Ref. [16]. Here we briefly recall the main results of this article. In the synchronous gauge, one writes the metric as follows

$$ds^2 = dt^2 - g_{ij}(x^\mu)dx^i dx^j \ .$$

As it follows from the Ref. [16], in the contracting Universe spatial gradients become quickly irrelevant compared to the time gradients, so that one results with the simplified metric

$$ds^2 = dt^2 - a^2(t)\sum_i e^{2\beta_i(t)}dx^i dx^j \ ,$$

which is of Kasner type and one can require $\sum \beta_i = 0$. In this case, the Einstein equations reduce to the following ones

$$H^2 = \frac{1}{6}\sum_i \dot{\beta_i}^2 + \frac{8\pi G}{3}\rho$$

and

$$\ddot{\beta}_i + 3H\dot{\beta}_i = 0 \ .$$

The latter gives $\dot{\beta}_i = \frac{d_i}{a^3}$, so that

$$H^2 = \frac{\sigma^2}{a^6} + \frac{8\pi G}{3}\rho \ ,$$

where $\sigma^2 = \sum_i d_i^2$. Once the Universe approaches the singularity, it becomes more and more anisotropic. Thus, the picture of the Universe driven by the matter with $p < \rho$ encounters severe problems (see, however, [13] for discussions). On the other side, this problem is absent in the Universe filled with the matter characterized by the super-stiff equation of state, i.e. one with $p = w\rho$ and $w > 1$, see [17].

In the ekpyrotic models, the super-stiff equation of state is achieved by introducing the scalar field with the negative steep potential. The concrete example is the exponential potential, so that the action is given by

$$S = \int d^4x\sqrt{-g}\left(\frac{1}{2}g^{\mu\nu}\partial_\mu\phi\partial_\nu\phi + V_0 e^{-c\phi}\right) \ ,$$

where $V_0 > 0$ and the constant $c \gg 1$. In this situation, the Friedmann equation admits the following solution for the scale factor

$$a = (-t)^p \ , \quad p = \frac{2}{c^2} \ , \quad \phi = \frac{2}{c}\ln\left(-\sqrt{c^2V/2}t\right) \ . \tag{34}$$

Thus, we deal with a very slowly contracting Universe. The equation of state is given by

$$p = w\rho \ , \quad w = \frac{2}{3p} - 1 \gg 1 \ ,$$

and the scaling of the energy density is then simply read from the conservation equation

$$\rho \sim a^{-2(1+3w)} \ .$$

Thus, we expect that the contribution of the anisotropies to the total energy density becomes completely diluted at rather late times.

The flatness problem is also addressed in the context of the ekpyrotic models. Indeed, the contribution of the curvature to the Friedmann equation,

$$\Omega_{curv} = -\frac{\kappa}{a^2 H^2} \ ,$$

falls down rapidly during the phase of the slow contraction. The ratio of the curvatures at the end and the beginning of the ekpyrotic phase is

$$\frac{\Omega_{curv}(t_{end})}{\Omega_{curv}(t_{beg})} = \frac{a^2(t_{beg})H^2(t_{beg})}{a^2(t_{end})H^2(t_{end})} \ .$$

In the limit $c \to \infty$ (and, respectively, $p \to 0$), this ratio is reduced to the following one

$$\frac{\Omega_{curv}(t_{end})}{\Omega_{curv}(t_{beg})} = \frac{|t_{beg}|^2}{|t_{end}|^2} \ .$$

One naturally takes the initial value $\Omega_{curv}(t_{beg}) \sim 1$. Keeping the end time of the ekpyrotic phase of the Planckian scale, $|t_{end}| \sim M_{Pl}^{-1}$, one estimates the curvature at the onset of the ekpyrosis as $|\Omega_{curv}| \sim 10^{-60}$. Thus, the flatness problem is resolved, provided that the duration of the slow contraction is large enough

$$|t_{beg}| = 10^{30}|t_{end}| \sim 10^{30} M_{Pl}^{-1} \sim 10^{-13} s \ .$$

Clearly that the horizon problem can be also resolved, once the duration of the ekpyrotic phase is long.

As pointed out in the Introduction, there is one specific problem in the models of the collapsing Universe. This is the transition from the contraction to the conventional expansion. Remind that the main difficulty here is to violate the Null Energy Condition (NEC) in terms of the healthy quantum field theory. In this sense, the theories of the big crunch/smooth bounce are currently at the stage of the development. There are, however, at least two proposals indicating that the smooth transition is possible in principle. One is to introduce the ghost condensate phase [11], where the NEC is *mildly* violated. This idea is used in the "new

ekpyrotic models" [14]. The different proposal on the *strong* violation of the NEC has been made recently, with the advent of the Galileon theories [95, 96]. The latter are incorporated, e.g. in the G-bounce, which is the novel scenario of the smooth transition [97].

Let us briefly discuss the design of the "new ekpyrotic models"[9]. Far from the bounce they behave essentially as in the standard four-dimensional picture. In the vicinity of the bounce, they are described in terms of the ghost condensate phase. The main ingredient of the latter is the scalar field with the non-canonical kinetic term, namely the relevant term in the Lagrangian is given by

$$\mathcal{L} = \sqrt{-g} M^4 P(X) \ ,$$

where

$$X = \frac{1}{2m^4}(\partial\phi)^2$$

is the standard canonical term; M and m are two mass scales that must be determined by the underlying microscopic theory and that have to satisfy certain consistency conditions [14]. The feature is that the function $P(X)$ is rather non-trivial. Thus, it may have the extremum at some finite point, say, $X_0 = 1/2$. The solution to the ghost condensate field then reads

$$\phi = -m^2 t \ .$$

Note, that the ghost condensate field ϕ itself does not violate the NEC, since it has the same equation of state as the cosmological constant. Hence, it does not provide the desired transition. However, the fluctuations around the extremum can violate the NEC. One defines the fluctuations π via

$$\phi = -m^2 t + \pi \ .$$

Their dynamics can be expressed by the effective Lagrangian

$$\mathcal{L} \sim 2X_0 P_{XX}(X_0)\dot{\pi}^2 \ ,$$

which shows that the kinetic term has the correct sign if the extremum is a minimum. Expanding then the expression for the energy density, $\rho = M^4(2P_X X - P)$, to linear order in π, one obtains $\rho = -KM^4\dot{\pi}/m^2$. One can provoke such a fluctuation by adding a potential V, implying that the energy density and the pressure are now approximately given by

$$\rho \approx -\frac{KM^2}{m^2}\dot{\pi} + V \ , \quad p = -V \ ,$$

where $K = P_{XX}(X_0) > 0$ and $P(X_0) = 0$. This immediately implies that

$$\dot{H} \approx \frac{KM^4}{2m^2}\dot{\pi} \ ,$$

[9]Since this poin on, our discussion parallels with one of the Ref. [94].

and hence, since $\dot{\pi}$ can take either sign, we now have the possibility of the NEC violating. The idea behind the "new ekpyrotic models" is to join the ekpyrotic phase with the NEC violating phase. In the first reference of [14] this is achieved by assuming that the function $P(X)$ is linear during the ekpyrotic phase and then quadratic around the minimum. Also, the potential V has to become positive at the onset of the bounce phase in order to push the equation of state parameter w below -1. There are two sources of the instabilities in the "new ekpyrotic models". One is the Jeans type instability and the second is a gradient instability. Both of these instabilities are harmless, if the bounce phase is rather fast, see the Refs. [14] for more thorough discussions.

To conclude this Subsection, we note that the ghost condensate models are likely to suffer from several conceptual problems [12]. We provided the discussion above in order to show that the bounce impossible at all. Whether, it is designed in terms of the ghost condensate or Galileon theories, is not our concern in this thesis. In what follows, we assume that the transition is smooth, perturbations generated at the contracting stage remain unaffected through the bounce and serve as the source of primordial fluctuations at the beginning of the conventional epoch [98].

2.6.1 Scalar perturbations in ekpyrotic models: one field case

In the ekpyrotic models, creation of primordial scalar perturbations is, generally speaking, quite challenging. The naive approach is to consider the unique scalar field dominating the slow contraction and study its fluctuations up until the horizon-exit. The perturbations are of the adiabatic type in this case. It is straightforward to check directly that they have the flat spectrum in the superhorizon regime. Indeed, the corresponding equation of motion reads[10]

$$\ddot{\delta\phi} + k^2\delta\phi + V_{\phi\phi}\delta\phi = 0 \ .$$

Using the zero energy condition for the classical background, we obtain $V_{\phi\phi} = c^2 V = -c^2\dot{\phi}^2/2 = -2/t^2$. Consequently, we obtain the same equation as in the case of the inflaton perturbations. Thus, we conclude with the flat spectrum of the field ϕ fluctuations.

Remind that in the inflationary context, the relevant fluctuations remained flat, once the gravity was turned on. This is not the case during the ekpyrotic phase. It turns out that with the gravitational effects included, one results with the blue spectrum of the gauge-independent curvature perturbation ζ [99]. This is in a sharp contrast with the CMB observations. To show this explicitly, we employ the Mukhanov–Sasaki variable introduced in the Section 2.2 (see also the Appendix A for more details). Remind that the equation (24) is generic and does not rely on any assumptions about the background evolution. Thus, we

[10]The approximation of the Minkowski background is used here. This is allowed if the constant c is large

can use it here. During the ekpyrotic phase, the quantity z defined by the Eq. (25) reads

$$z = -c[-(1-p)\eta]^{\frac{p}{1-p}} \ .$$

Here we made use of (34). Note that the relation between the proper time and the conformal time at the ekpyrotic stage is as follows,

$$-t = [-(1-p)\eta]^{\frac{1}{1-p}} \ . \tag{35}$$

Then, the equation of motion for the Mukhanov–Sasaki variable u in the momentum representation is given by

$$u'' + k^2 u - \frac{p(2p-1)}{(1-p)^2\eta^2} u = 0 \ .$$

At very early times, the amplitude of the negative frequency solution behaves as

$$u_k^{(-)} = \frac{1}{\sqrt{2k}} e^{-ik\eta} \ , \quad \text{where} \quad \eta \to -\infty \ .$$

The solution at all the times is then given by

$$u_k^{(-)} = \sqrt{-\eta}\left(C_1 H_\beta(-k\eta) + C_2 H_\beta^\star(-k\eta)\right) \ ,$$

where the constant β is given by

$$\beta = \sqrt{\frac{z''}{z}\eta^2 + 1/4} \ .$$

Using the expression for the Hankel function in the asymptotic past, the Eq. (19), one fixes the constant C_1,

$$C_1 = \frac{\sqrt{\pi}}{2} \exp\left[\frac{i\pi\beta}{2} + i\frac{\pi}{4}\right] \ ,$$

while the other constant $C_2 = 0$. Consequently, the late-time solution for the negative-frequency amplitude reads

$$u_k^{(-)} = \sqrt{-\frac{\eta}{4\pi}} \left(-\frac{k\eta}{2}\right)^{-\beta} \exp\left[\frac{i\pi\beta}{2} - \frac{i\pi}{4}\right] \ ,$$

where we make use of (20). Once we deal with the super-stiff equation of state, the parameter p is naturally very small, and the constant β tends to $1/2$ in this limit. Thus, in the late-time regime we obtain

$$u_k^{(-)} = \frac{1}{\sqrt{2\pi k}} \ .$$

This implies a very blue spectrum of the adiabatic perturbations [99]. In principle, this prediction can be avoided in the ekpyrotic scenarios with the rapidly changing equation of

state, [100]. In this model, the adiabatic perturbations evolving on the dynamical attractor solution acquire the flat spectrum. Further, it was argued in [101] that this scenario does not work because of the breakdown of the perturbation theory at small scales. This problem was circuvemented in [102] by altering of the potential such that the power is suppressed on small scales.

2.6.2 Scalar perturbations in ekpyrotic scenario: the case of two fields

There is the other way to handle the situation. That is to introduce the second scalar field with the negative quartic potential [103, 104]. In this situation, scalar perturbations can be decomposed into the sum of adiabatic perturbations and isocurvature ones. The latter are argued to have the flat power spectrum. The potential term for the system of two scalars is

$$V = -\sum_i V_i e^{-c_i \phi_i} \ .$$

In this assisted ekpyrotic collapse the solution for the scale factor is

$$a \sim (-t)^p \ , \quad \text{where} \quad p = \sum_i \frac{2}{c_i^2} \ . \tag{36}$$

This represents the evolution along the effective exponential potential, which is less steep than any of the individual potentials from which it was constructed, $c^2 < c_i^2$, where the constant c is defined from

$$\frac{2}{c^2} = \sum_i \frac{2}{c_i^2} \ .$$

Let us stress on the potential danger with the scaling solution (36). The problem is that in a collapsing Universe, the field with the steepest potential comes to dominate at late times, i.e. the solution (36) is unstable [105]. To show this explicitly, we turn from the fields ϕ_1 and ϕ_2 to the adiabatic field σ and the isocurvature one, χ,

$$\sigma = \frac{c_2\phi_1 + c_1\phi_2}{\sqrt{c_1^2 + c_2^2}} \ , \quad \chi = \frac{c_1\phi_1 - c_2\phi_2}{\sqrt{c_1^2 + c_2^2}} \ .$$

In terms of the fields σ and χ, the total potential can be written as follows,

$$V = -U(\chi) e^{-c\sigma} \ .$$

The dependence of the potential U on the orthogonal field is given by

$$U(\chi) = V_1 e^{(c_1/c_2)c\chi} + V_2 e^{(c_2/c_1)c\chi} \ .$$

Close to its minimum, one can expand the function as follows,

$$U(\chi) = U_0 \left[1 + \frac{c^2}{2}(\chi - \chi_0)^2 + ... \right] \ .$$

As it folllows, there is a classical trajectory for the two fields in which χ remains fixed, $\chi = \chi_0$, while the adiabatic field σ rolls down a steep exponential potential

$$V|_{\chi=\chi_0} = -U_0 e^{-c\sigma} \ .$$

However, the isocurvature field χ has a negative mass-squared, $m_\chi^2 = c^2 V < 0$, whcih implies the tachionic instability [105]. The linear perturbation in the fields orthogonal to the background trajectory are decoupled from the first-order metric perturbations,

$$\ddot{\delta\chi} + 3H\dot{\delta\chi} + \left(\frac{k^2}{a^2} + m_\chi^2\right)\delta\chi = 0 \ .$$

In terms of the rescaled field $v = a\delta\chi$, the equation takes the form

$$v'' + \left[k^2 - \frac{a''}{a} + m_\chi^2 a^2\right] v = 0 \ .$$

Omitting the last term on the right hand side, this equation coincides with one of Mukhanov–Sasaki variable and has been considered in the last Subsection. On the stable background, the effective mass-squared of the field χ is negligible as compared to the Hubble rate. In this (natural) situation, we obtain the strongly blue spectrum. The different story occurs, if we turn to the unstable scaling solution (36). In that case, the mass term dominates instead. Moreover, is has the form of the massless scalar field evolving on the de Sitter background. Hence, the flat spectrum of the relevant perturbations [103, 104]. In fact, it has a small blue tilt,

$$n_{\delta\chi} - 1 \approx 2p \ .$$

As it follows, the flatness of the spectrum in the ekpyrotic models requires the fine-tuning of the initial data[11]. In contrast, this problem is absent in models of the (pseudo)-Conformal Universe. In that case, relevant perturbations evolving on the *dynamical attractor* background acquire the flat spectrum.

2.6.3 Tensor perturbations in ekpyrotic models

Without much efforts, we can derive the spectrum of tensor perturbations in the ekpyrotic models. For this purpose, it is convenient to introduce the gauge-invariant canonical variable $\tilde{\phi}^A = a(\eta)\phi^A$. where $\phi^A = \sqrt{\frac{M_{Pl}^2}{32\pi}} h^A$ (see the discussion in the Appendix A). Making the redefinition $\tilde{\phi}^A = \frac{\phi_A}{a}$, we obtain the equation of motion for the field $\tilde{\phi}^A$,

$$(\tilde{\phi}^A)'' + \left(k^2 - \frac{a''}{a}\right)\tilde{\phi}^A = 0 \ .$$

[11] This fine-tuning can be automatic in the cyclic models [106]

In fact, it is the same equation as for the Mukhanov–Sasaki variable u introduced in the inflationary context and already used in the case of ekpyrotic models. This becomes particularly clear once we note that

$$\frac{a''}{a} = \frac{z''}{z} = \frac{p(2p-1)}{(1-p)^2\eta^2} \, .$$

Thus, the behaviour of the field $\tilde{\phi}_A$ coincides with one of the Mukhanov–Sasaki variable u. Hence, we immediately conclude with the strongly blue spectrum of the tensor perturbations

$$n_T - 1 \approx 2 \, .$$

This blue spectrum implies that the tensor perturbations are non-observable at the cosmological scales. Note that this is a common prediction of the alternatives to the inflation. This clarifies the point made in the beginning of the Subsection 2.2.1, that the detection of strong tensor perturbations in the forthcoming experiments will serve as the "anti-smoking gun" for the alternative frameworks, e.g. conformal rolling scenario.

3 Conformal rolling scenario

3.1 Flat power spectrum from conformal invariance

The inflationary mechanism [3, 7, 8] generates almost Gaussian scalar perturbations whose power spectrum is almost flat due to the slow evolution of relevant parameters (the Hubble parameter and time derivative of the inflaton field). Similar situation occurs in the inflationary scenario with the curvaton mechanism [46, 47, 48]; in either case, the approximate flatness of the spectrum is a direct consequence of the approximate de Sitter symmetry of the inflating background.

In quest for an alternative symmetry behind the flat scalar spectrum one naturally turns to conformal invariance [18, 25, 26]. Conformal symmetry implies scale invariance, which in the end may be responsible for the scale-invariant scalar spectrum [24]. An assumption of conformal invariance at the time the primordial perturbations are generated is in line with the viewpoint that the underlying theory of Nature may have conformal phase, and that the Universe may have started off from, or passed through that phase.

In this Chapter, we focus on the concrete realization of this idea, namely conformal rolling scenario proposed in Ref. [18]. Besides conventional Einstein gravity and some matter that dominates the cosmological evolution, its main ingredient is a complex scalar field ϕ conformally coupled to gravity. We assume that the field ϕ is a spectator which does not affect the cosmological evolution. For this reason, the mixing between this field and gravitational degrees of freedom is negligible. Conformal invariance implies that the scalar potential is quartic, while the dynamics is non-trivial if its sign is negative,

$$V(\phi) = -h^2|\phi|^4 \,, \tag{37}$$

where h is a small parameter. One assumes that the background space-time is homogeneous, isotropic and spatially flat,

$$ds^2 = a^2(\eta)(d\eta^2 - d\mathbf{x}^2) \,.$$

We do not make the special assumptions about the scale factor $a(\eta)$ standing here. The Universe can undergo the inflationary expansion, the phase of the contraction etc. The only qualification here is that the evolution should be long so, that the horizon problem is already resolved. In particular, this implies that the conformal rolling scenario cannot operate during the Hot Big Bang epoch, where there is simply no enough time. Due to the conformal coupling of the field ϕ to gravity, the model is invariant under Weyl transformations supplemented by transformations of the field ϕ,

$$g_{\mu\nu} \to g'_{\mu\nu} = e^{-2\sigma(\mathbf{x},\eta)} g_{\mu\nu} \,, \phi \to e^{\sigma(\mathbf{x},\eta)}\phi \,.$$

Taking $e^{\sigma(\mathbf{x},\eta)} = a(\eta)$, we result with the Minkowski background. The dynamics of the field

$$\chi(\eta, \mathbf{x}) = a(\eta)\phi(\eta, \mathbf{x}) \tag{38}$$

is the same as in flat space-time. As it rolls down its potential $V(\chi) = -h^2|\chi|^4$, it approaches the late time attractor

$$\chi_c(\eta) = \frac{1}{h(\eta_* - \eta)} \ . \tag{39}$$

We take χ_c real without loss of generality with the understanding that the action is $U(1)$-invariant. Here $\eta_\star$ is the arbitrary real parameter, which has the meaning of the end-of-roll time. The point of Ref. [18] is that the behavior of the phase[12] $\theta = \sqrt{2}$ Arg ϕ in the background (39) is very similar to what happens at inflation to the fluctuations of a massless scalar field minimally coupled to gravity (e.g., inflaton itself). The phase perturbations $\delta\theta$ start off as vacuum fluctuations and eventually freeze out. To the leading order in h, the resulting phase perturbations are Gaussian and have flat power spectrum [18]

$$\mathcal{P}_\theta = \frac{h^2}{(2\pi)^2} \ . \tag{40}$$

After this brief introduction to the topic, let us discuss the evolution of fields during conformal rolling in more details. At this stage, the theory is described by the action

$$S = S_{G+M} + S_\phi \ ,$$

where S_{G+M} is the action for gravity and some matter that dominates the evolution of the Universe, and

$$S_\phi = \int d^4x\sqrt{-g}\left[g^{\mu\nu}\partial_\mu\phi^*\partial_\nu\phi + \frac{R}{6}\phi^*\phi - V(\phi)\right]$$

is the action for the scalar field we are going to discuss. Here the scalar potential is given by (37). After introducing the field $\chi = \mathrm{Re}\chi + i\mathrm{Im}\chi$ as in (38), one obtains its action in conformal coordinates in the Minkowskian form,

$$S[\chi] = \int \ d^3x \ d\eta \ \left[\eta^{\mu\nu}\partial_\mu\chi^*\partial_\nu\chi + h^2|\chi|^4\right] \ . \tag{41}$$

In terms of the radius and phase of the field $\chi = \rho e^{i\frac{\theta}{\sqrt{2}}}$ this action takes the form

$$S[\rho,\theta] = \int d^3x d\eta \left[\eta^{\mu\nu}\partial_\mu\rho\partial_\nu\rho + \frac{1}{2}\rho^2(\partial_\mu\theta)^2 + h^2\rho^4\right] \ . \tag{42}$$

Let us first study the classical background, χ_c. One further assumes that the classical field χ_c is homogeneous. In terms of the radius and phase, $\chi_c = \rho e^{i\frac{\theta}{\sqrt{2}}}$, one of the equations is the conservation of the current,

$$\frac{d}{d\eta}\left(\rho^2\theta'\right) = 0 \ .$$

[12]The normalization here is chosen for future convenience.

As the value of ρ increases, the phase θ freezes out, and the evolution proceeds in the radial direction. Without loss of generality, we take χ_c to be real at that time. This allows us to use the notation χ_c instead of ρ in what follows. Then, the first integral of the equation of motion is

$$\chi_c^{'2} - h^2\chi_c^4 = \epsilon \ ,$$

where ϵ is the constant of integration. The solution to this equation tends to the dynamical attractor independent of the constant ϵ and given by (39).

Now we turn to the evolution of the phase perturbations on the background (39). It is convenient to work with the imaginary part of the field χ, or, more precisely, with the quantity $\delta\chi_2 = \sqrt{2}\mathrm{Im}\chi$. We introduce the factor $\sqrt{2}$, so that the field $\delta\chi_2$ is canonically normalized. In terms of the field $\delta\chi_2$, the phase perturbations are given by

$$\theta = \frac{\delta\chi_2}{\chi_c} \ ,$$

up to the corrections $\mathcal{O}(\theta^3)$. We keep the notation θ for the phase perturbation as for the overall phase. We are allowed to do that, since its classical value is tuned to zero. It is straightforward to derive the equation of motion for the field $\delta\chi_2$ from the action (41),

$$(\delta\chi_2)'' + k^2\delta\chi_2 - 2h^2\chi_c^2\delta\chi_2 = 0 \ . \tag{43}$$

At early times, when $k(\eta_\star - \eta) \gg 1$, the second term dominates, and $\delta\chi_2$ oscillates like free scalar field in Minkowski space-time. At later times, the third term dominates instead. In more details, Eq. (43) reads

$$(\delta\chi_2)'' + k^2\delta\chi_2 - \frac{2}{(\eta_\star - \eta)^2}\delta\chi_2 = 0 \ .$$

Formally this is the same equation of perturbations of minimally coupled massless scalar field in de Sitter space-time. Hence, the spectrum of $\delta\chi_2$ is the same flat spectrum. We are interested in the solution that behaves at early times as

$$\chi_2^{(-)} = \frac{1}{(2\pi)^{3/2}\sqrt{2k}}e^{ik(\eta_\star - \eta)} \ .$$

The solution is expressed through the Hankel function.

$$\chi_2^{(-)} = \frac{1}{4\pi}\sqrt{\frac{\eta_\star - \eta}{2}}\mathrm{H}_{3/2}[k(\eta_\star - \eta)] \tag{44}$$

At $k(\eta_\star - \eta) \ll 1$ this solution is

$$\chi_2^{(-)} = \frac{i}{2\pi^{3/2}}\frac{1}{k^{3/2}(\eta_\star - \eta)} \ .$$

The dependence on the momentum k standing here implies that the perturbations of the imaginary part have flat power spectrum in the super-"horizon" regime,

$$\Delta_{\delta\chi_2} = \frac{1}{2\pi(\eta_\star - \eta)} \, .$$

Consequently, phase perturbations are described by the flat power spectrum (40) up to the higher order corrections [18]. The phase perturbations are the source of the adiabatic perturbations in this scenario, which proceeds as follows. At large field values, the potential $V(|\phi|)$ is assumed to be different from (37) and to have a minimum at $|\phi| = f_0$; we assume that $f_0 \ll M_{\rm PL}$ (see also the discussion in Section 4.2), so that the contribution of the field ϕ to the effective Planck mass is always negligible. At $|\phi| \sim f_0$, conformal symmetry is broken, the radial field $|\phi|$ interacts with other fields, and its oscillations about the minimum get damped quickly enough. To be on the safe side, we assume that the field ϕ is a spectator at this and earlier stages, i.e., its energy density ρ_ϕ is small compared to the energy density $\rho_{\rm tot}$ of matter that dominates the cosmological evolution. This is the case provided that

$$|\rho_\phi| \sim h^2 f_0^4 \ll \rho_{\rm tot} = \frac{3}{8\pi} M_{\rm PL}^2 H^2 \, . \tag{45}$$

Then the decay products of the field $|\phi|$ do not affect the evolution of the Universe and, furthermore, the perturbations of $|\phi|$, that exist before the end of rolling and disappear after $|\phi|$ gets relaxed to the minimum of $V(|\phi|)$, do not produce substantial density perturbations in the Universe.

The scenario cannot work at the conventional hot cosmological epoch, for the following reason. The vacuum state of the phase perturbations θ is well defined at early times provided that these perturbations evolve in the WKB regime, which implies

$$k(\eta_* - \eta) \gg 1 \, , \qquad \text{early times} \, , \tag{46}$$

where k is conformal momentum. On the other hand, the property that these perturbations are frozen out at late times holds if

$$k(\eta_* - \eta) \ll 1 \, , \qquad \text{late times} \, . \tag{47}$$

So, the scenario requires that both of these inequalities are satisfied at conformal rolling stage. This can only happen if the duration of that stage in conformal time is greater than k^{-1}. For conformal momenta of cosmological significance this means that conformal rolling lasts longer (in conformal time) than the entire hot stage until the present epoch. Thus, the mechanism can only work at some pre-hot epoch at which the horizon problem is solved, at least formally [18]. This is similar to most other mechanisms of the generation of cosmological perturbations (see, however, Ref. [107]).

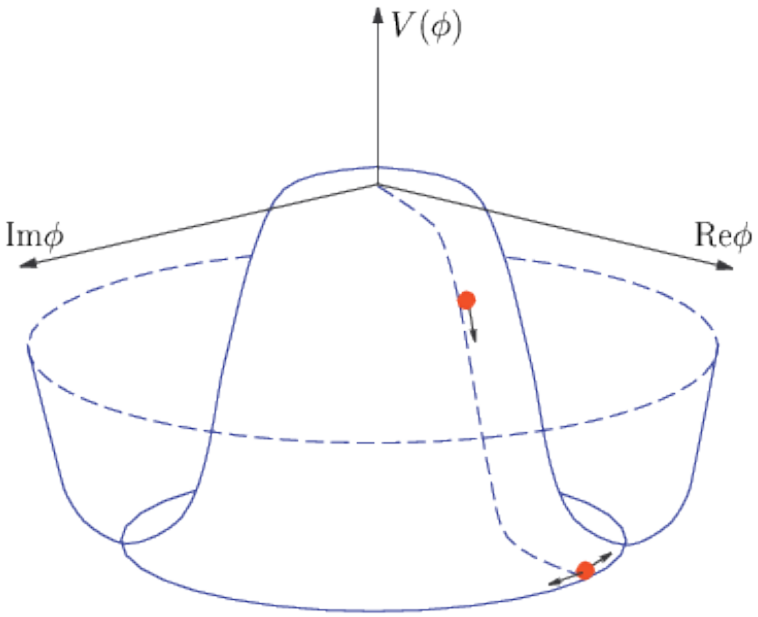

Figure 2: Evolution of the field ϕ during conformal rolling

At the conformal rolling stage, the dynamics of the phase perturbations θ is governed solely by their interaction with the background field (39) (as well as with the radial perturbations $\delta|\chi|$, see below); the evolution of the scale factor $a(\eta)$ is irrelevant. After the end of conformal rolling, the situation is reversed. Once the radial field $|\phi|$ has relaxed to the minimum of the scalar potential, the phase θ is a massless scalar field minimally coupled to gravity (this is true for any Nambu–Goldstone field [108]). Since we are talking about a yet unknown pre-hot epoch, it is legitimate to ask what happens to the perturbations of the phase right after the end of conformal rolling. Barring fine tuning, there are two possibilities for the perturbations θ: (i) they are already superhorizon in the conventional sense at that time, or (ii) they are still subhorizon. The version (i) of the scenario has been considered in Refs. [20, 21, 22]; in that case, the phase perturbations do not evolve after the end of the conformal rolling stage, and the properties of the adiabatic perturbations are determined entirely by the dynamics at conformal rolling (modulo possible non-Gaussianity generated at the conversion epoch; the latter is not specific to the conformal rolling scenario). To subleading orders in h, this dynamics is fairly non-trivial, and the resulting effects include certain types of statistical anisotropy [20] and non-Gaussianity [21, 22]. In what follows, we refer to this version as to the sub-scenario A, and consider its phenomenological consequences in the end of this Chapter.

The version (ii) of the conformal rolling scenario requires a long intermediate stage between the end of roll and the beginning of the conventional epoch [23]. We discuss this

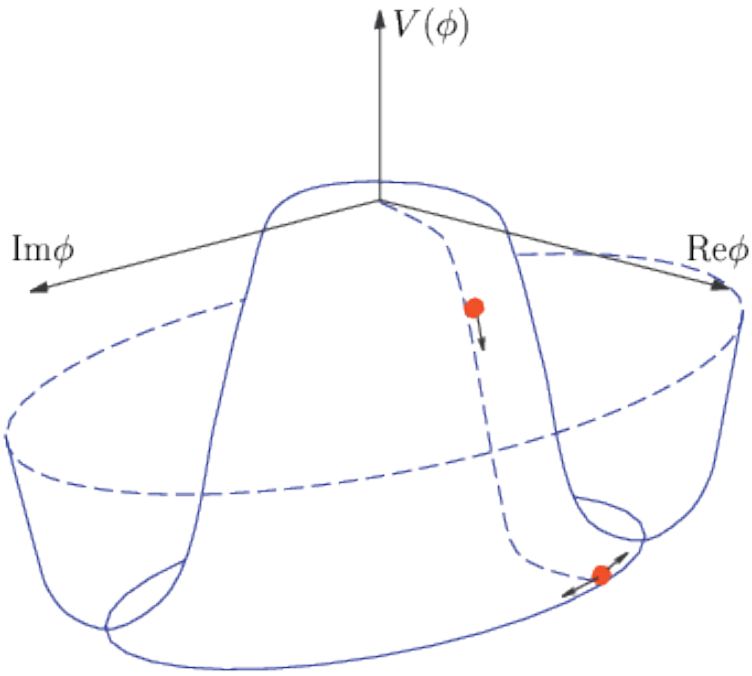

Figure 3: Curvaton-type conversion mechanism requires the small effective mass of the phase perturbation. The harmless way to satisfy this claim is to introduce the small breaking of the $U(1)$ invariance, which, in turn, can be realized via the small tilt of the potential $V(\phi)$

opportunity in details in the forthcoming Chapter.

3.2 Conversion mechanisms

Once the radial field $|\phi|$ settles down to f_0, what remains are the perturbations of the phase, which at this point are isocurvature perturbations. Thus, one should take care about reprocessing phase perturbations into adiabatic ones at much later epoch. We already encountered this situation when discussed the curvaton mechanism. Then, the similarity between the curvaton field and the phase after the end of the conformal rolling gives us the idea how to provide the conversion into the adiabatic perturbations. Following [18], we demand that the global $U(1)$ symmetry is broken near $|\phi| = f_0$, so that the phase acquires the non-zero.[13] From this point on, the phase serves as the pseudo-Nambu-Goldstone field, and our discussion parallels to one presented in [48]. Provided that the Hubble parameter is larger than the effective mass of the phase, the latter stays constant for some time. Once the Hubble rate drops below the mass, the phase rolls to the nearest minimum of its potential and os-

[13]We assume that the corresponding scale of breaking is small as compared to f_0. Thus, we can safely neglect the effects of $U(1)$ symmetry breaking during the conformal rolling.

cillates there decaying into radiation. With no loss of generality, we can assume that the minimum is located at $\theta = 0$. Simultaneously we shift the classical value of the phase during the conformal rolling to some non zero value θ_c. Following the discussion of Section, we see that the correspondence with the curvaton case is established by the obvious replacements $\theta \leftrightarrow \delta\sigma$, $\theta_c \leftrightarrow \sigma_c$. Thus, we write the result for the amplitude of the adiabatic perturbations ζ generated during the decay epoch,

$$\Delta_\zeta \equiv \sqrt{\mathcal{P}_\zeta} = \frac{rh}{3\pi\theta_c} \, . \tag{48}$$

Remind that the constant r is the ratio of the phase field energy density to the total energy of the Universe at the time of the decay. This constant cannot be arbitrarily small, since otherwise it gives rise to a huge non-Gaussianity. From the current constraint on the bispectrum constant, see the Eq. (6), it follows that $r > 0.017$. Taking into account the amplitude of the adiabatic perturbation, $\Delta_\zeta \simeq 5 \times 10^{-5}$, this translates into the constraint on the ratio,

$$\frac{h}{\theta_c} \lesssim 3 \times 10^{-2} \, . \tag{49}$$

This means that the value of the coupling constant is allowed to be as large as $h \sim 0.1$. This value is achieved provided that the phase starts rolling to the minimum from the value $\theta_c \simeq \pi$. Let us speculate about the upper constraint on the coupling constant h in the case of the non-observation of the primordial non-Gaussianity in the PLANCK data. This would imply that the parameter f_{NL} is at most on the level os the sensitivity of the PLANCK experiment, i.e. $|f_{NL}| \lesssim 5$. Then the constraint on the constant h would read $h \lesssim 0.007$. This constraint applies, once we insist on the curvaton-type conversion mechanism.

Alternatively, perturbations θ may be converted into adiabatic perturbations by the modulated decay mechanism [55, 56]. One assumes that the phase θ interacts with some heavy particles in such a way that the masses and/or widths of the latter depend on θ,

$$M = M_0 + \epsilon_M \theta \quad \text{and/or} \quad \Gamma = \Gamma_0 + \epsilon_\Gamma \theta \, . \tag{50}$$

One assumes further that these particles survive at the Hot Big Bang epoch until they are non-relativistc and domonate the cosmological expansion. When these particles decay, the perturbations in θ, and hence in M and/or Γ, induce adiabatic perturbations,

$$\zeta \simeq \frac{\delta M}{M} = \frac{\epsilon_M \theta}{M_0 + \epsilon_M \theta_c} \tag{51}$$

and/or

$$\zeta \simeq \frac{\delta \Gamma}{\Gamma} = \frac{\epsilon_\Gamma \theta}{\Gamma_0 + \epsilon_\Gamma \theta_c} \, . \tag{52}$$

The shape of the adiabatic perturbations is again the same as that of the initial power spectrum of θ. The modulated decay mechanism also induces non-Gaussianity in the adiabatic perturbations. However, once the dependence of the mass/width on θ is linear, the non-Gaussian part of the adiabatic perturbations is of the order $(\delta M/M)^2, \quad (\delta\Gamma/\Gamma)^2 \sim \zeta^2$. In other words, irrespectively of the coupling h, the non-Gaussianity is fairly small,

$$f_{NL} \sim 1 \, . \tag{53}$$

Thus, the modulated decay mechanism by itself does not imply any bound on h.

3.3 Radial perturbations

Searching for the non-trivial phenomenolgical properties of the conformal rolling scenario, one should consider the radial perturbations about the classical background. As we will see in what follows, the interaction of the phase perturbations and the radial ones results into the statistical anisotropy and the non-Gaussianity in trispectrum. Though we are focused on the conformal rolling scenario, the results obtained in this particular framework are generic for a broader class of models [25, 26], as we discuss it in the Chapter 5. Let us fix the notations. We proceed to work in terms of the radius and the imaginary part of the field χ. It is convenient because the equation of motion of the imaginary part for a fixed radius is always linear, and all the non-linearities are transferred to the equation of motion for the radius. To the leading order in h, perturbations[14] $\delta\chi_1 = \sqrt{2}\delta\chi_c$ and $\delta\chi_2 = \sqrt{2}\mathrm{Im}\,\chi$ decouple from each other, and we can study their evolution separately.

The radial perturbations obey the linearized field equation, which in the momentum representation reads

$$(\delta\chi_1)'' + p^2\delta\chi_1 - 6h^2\chi_c^2\delta\chi_1 \equiv (\delta\chi_1)'' + p^2\delta\chi_1 - \frac{6}{(\eta_* - \eta)^2}\delta\chi_1 = 0 \, , \tag{54}$$

We denote the conformal momentum of the radial perturbation by $\mathbf{p}$ and reserve the notation $\mathbf{k}$ for the conformal momentum of the phase perturbation. The properly normalized solution to Eq. (54) is

$$\delta\chi_1 = \frac{1}{4\pi}\sqrt{\frac{\eta_* - \eta}{2}}H_{5/2}\left[p(\eta_* - \eta)\right] \cdot \hat{B}_{\mathbf{p}} + h.c. \, , \tag{55}$$

where $\hat{B}_{\mathbf{p}}$, $\hat{B}^\dagger_{\mathbf{p}}$ are annihilation and creation operators obeying the standard commutational relation $[\hat{B}_{\mathbf{p}}, \hat{B}^\dagger_{\mathbf{p}'}] = \delta(\mathbf{p} - \mathbf{p}')$, $H_{5/2}$ is the Hankel function, and here and in what follows in this Section we omit irrelevant phase factors. At late times the solution approaches the asymptotics

$$\delta\chi_1 = \frac{3}{4\pi^{3/2}}\frac{1}{p^{5/2}(\eta_* - \eta)^2} \cdot \hat{B}_{\mathbf{p}} + h.c. \, .$$

[14] We proceed to use the same notation for the perturbed radial solution as for the classical field χ_c. To avoid the confusion, we will indicate the spatial dependence of the perturbed radius, where necessary.

At very late times the perturbations $\delta\chi_1$ become so large that they ruin the linearized analysis. There is a way to avoid this difficulty. This is to impose the requirement that the field χ_1 is approximately homogeneous over the whole visible Universe at the time when the scales of interest exit the "horizon" [18]. This requirement reads

$$\Delta_{\delta\chi_1}(k_{min}, \eta_{max}) \ll \chi_1(\eta_{max}) \ ,$$

where the time η_{max} is defined by

$$k_{max}(\eta_\star - \eta_{max}) \sim 1 \ .$$

These conditions translate into the severe constraint on the parameter of the model,

$$h \ll \frac{k_{min}}{k_{max}} \sim 10^{-4} \ .$$

There is, however, the alternative approach to the problem. First, we notice that the super-"horizon" perturbations $\delta\chi_1$ of the field χ_1 can be absorbed into the redefinition of the end-of-roll time $\eta_\star$, so that we can write the full radial solution as follows [18],

$$\chi_c(\eta, \mathbf{x}) = \frac{1}{h[\eta_*(\mathbf{x}) - \eta]} \ , \tag{56}$$

where

$$\eta_*(\mathbf{x}) = \eta_* + \delta\eta_*(\mathbf{x})$$

The inhomogeneous shift $\delta\eta_\star(\mathbf{x})$ is the random Gaussian field chosen in such a way that it matches the late-time solution in the regime, when the linear approximation is valid,

$$\delta\eta_*(\mathbf{x}) = \frac{3h}{4\sqrt{2}\pi^{3/2}} \int \frac{d^3p}{p^{5/2}} \left(\mathrm{e}^{i\mathbf{px}} \cdot \hat{B}_\mathbf{p} + h.c. \right) \ .$$

Note that this field has red power spectrum,

$$\mathcal{P}_{\delta\eta_*} = \frac{9h^2}{8\pi^2} \frac{1}{p^2} \ . \tag{57}$$

One can view this trick as the convenient book-keeping tool. The things are in fact deeper. The clarify the situation, we write the exact equation of motion for the radius of the field χ,

$$\eta^{\mu\nu}\partial_\mu\partial_\nu\chi_c - \frac{\chi_c}{2}\eta^{\mu\nu}\partial_\mu\theta\partial_\nu\theta - 2h^2\chi_c^3 = 0 \ . \tag{58}$$

Let us omit the backreaction of the phase perturbations, i.e. the second term here. We comment on this point in the end of the Section. Being interested in the effects due to very long wavelengths, we neglect the spatial variation of the end-of-roll time $\eta_\star(\mathbf{x})$. In this

situation, the solution (56) satisfies the Eq. (58). This proves that the corresponding effects are indeed harmless, since they can be summed up into the shift of the end-of-roll time. Clearly, this homogeneous shift is irrelevant from the physical point of view. Interesting effects appear, once we account for the spatial variation of the end-of-roll time $\eta_\star(\mathbf{x})$. It is convenient to introduce the notation

$$v_i = -\partial_i \eta_\star \ , \tag{59}$$

while keeping the standard notation for the second order derivative, $\partial_i \partial_j \eta_\star$. Notably, derivatives v_i and $\partial_i \partial_j \eta_\star$ have flat and blue power spectra, respectively. Thus, corresponding corrections are safe for us. In fact, the correstion linear in v_i is already included in (56). Indeed, still keeping very long wavelengths, one expands the end-of-roll time, i.e. $\eta_\star(\mathbf{x}) = \eta_\star - v_i x_i$. Substituting the latter into (56), we see that the background (56) still satisfies the Eq. (58). This is true up to the corrections of the order v^2 and $\partial_i \partial_j \eta_\star / k$. To account for the latter, we use the following ansatz for the radial background

$$\chi_c(\eta, \mathbf{x}) = \frac{1}{h(\eta_\star(\mathbf{x}) - \eta)} + \frac{\alpha v^2}{h(\eta_\star(\mathbf{x}) - \eta)} + \beta \frac{\partial_i \partial_j \eta_\star}{h} \ .$$

The constants α and β standing here are defined by substituting the ansatz into the Eq. (58). We find that $\alpha = -1/2$ and $\beta = 1/6$. The coefficient in front of v^2 is not accidental. It should be viewed as the "remnant" of the Lorentz factor $\gamma = (1 - v^2)^{-1/2}$. Though keeping corrections coming from the distortion of the boost factor is not legitimate, we write the background solution as follows [20],

$$\chi_c(\eta, \mathbf{x}) = \frac{1}{h\gamma(\eta_\star(\mathbf{x}) - \eta)} + \frac{\partial_i \partial_j \eta_\star}{6h} \ , \tag{60}$$

where the linearization in v^2 is understood. In a view of the future results, note that wavelengths of the radial perturbations relevant for us in what follows are such that much exceed the cosmologically interesting scales, i.e. $p \ll k$. In particular, this implies that at cosmologically interesting scales we can expand the end-of-roll time as follows,

$$\eta_\star(\mathbf{x}) = \eta_\star - v_i x_i + \frac{1}{2} \partial_i \partial_j \eta_\star x_i x_j \ .$$

The only exception is the non-Gaussianity as discussed in the end of this Chapter. In other cases we are allowed to study the evolution of phase perturbations on the background (60), when the radial perturbations are in the super-"horizon" regime. Assuming this mode separation, one can show that the backreaction of the phase perturbations is negligible in the approximation we work in. In more details, let us consider the contribution of sub-"horizon" wavelengths, i.e.

$$k(\eta_\star - \eta) \gg 1 \tag{61}$$

and ones, $k(\eta_\star - \eta) \ll 1$ separately. Obviously, the sub-"horizon" phase perturbations oscillate like massless Minkowskian field. For this reason, their contribution to the radial field equation is negligible (formally, it is zero). The contribution of the super-"horizon" modes is estimated as

$$\chi_c \langle \partial_i \theta \partial_i \theta \rangle \sim \frac{h k_{max}^2}{\eta_\star - \eta}$$

The momentum k_{max} is estimated at most as $k_{max}(\eta_\star - \eta) \sim 1$. The contribution of the order v^2 correction is estimated as $\frac{h \ln \Lambda}{(\eta_\star - \eta)^3}$. The latter is logarithmically amplified by the infrared physics encoded in the parameter Λ. Hence, keeping corrections of the order v^2 is legitimate. This may not hold in the case of the second correction on the right handside of Eq. (60). The similar arguments lead to the constraint on the momentum range of the radial perturbations,

$$h \ll p_{max}(\eta_\star - \eta) \ll 1$$

If the constant h is not particularly small, the left inequality may break down at very late times. This is, however, not of the special importance for us. The reason is that the correction to the background due to the second derivative does not lead to any observable effects.

3.4 Corrections to phase perturbations

3.4.1 Order v

Let us now turn to the perturbations $\delta\chi_2$ of the imaginary part, and account for their interaction with radial perturbations. As we will see in what follows, relevant perturbations $\delta\eta_*$ have wavelengths much longer than the wavelengths of the phase perturbations, i.e. the inequality (61) holds. Because of this separation of scales, it is legitimate to use the expression (60), valid in the late-time regime $p(\eta_* - \eta) \ll 1$, when considering the dynamics of $\delta\chi_2$, and treat the field (60) as the background. For the time being we omit the corrections of the orders v^2 and $\partial_i\partial_j/k$, and account only for the order v effects encoded in (56). We present the expressions valid to these orders and $\partial_i\partial_j\eta_\star/k$ and v^2 in the following Subsection. With this qualification, the linearized field equation for $\delta\chi_2$ reads

$$(\delta\chi_2)'' - \partial_i\partial_i\delta\chi_2 - 2h^2\chi_c^2(\eta, \mathbf{x}) \cdot \delta\chi_2 \equiv (\delta\chi_2)'' - \partial_i\partial_i\delta\chi_2 - \frac{2}{[\eta_*(\mathbf{x}) - \eta]^2}\delta\chi_2 = 0 \, . \qquad (62)$$

At early times, when $k(\eta_* - \eta) \gg 1$, we get back to the Minkowskian massless equation, and the solutions are spatial Fourier modes that oscillate in time. Hence, the solution to Eq. (62) has the following form,

$$\delta\chi_2(\mathbf{x}, \eta) = \int \frac{d^3k}{(2\pi)^{3/2}\sqrt{2k}} \left(\delta\chi_2^{(-)}(\mathbf{k}, \mathbf{x}, \eta)\hat{A}_\mathbf{k} + h.c. \right) \, ,$$

where $\delta\chi_2^{(-)}(\mathbf{k},\mathbf{x},\eta)$ tends to $\mathrm{e}^{i\mathbf{kx}-ik\eta}$ as $\eta\to-\infty$ and $\hat{A}_\mathbf{k}$, $\hat{A}^\dagger_\mathbf{k}$ is another set of annihilation and creation operators. It is straightforward to see that to the linear order in h and modulo corrections proportional to $\partial_i\partial_j\eta_*(\mathbf{x})$, the solution with this initial condition is

$$\delta\chi_2^{(-)}(\mathbf{k},\mathbf{x},\eta)=-\mathrm{e}^{i\mathbf{kx}-ik\eta_*(\mathbf{x})-i\mathbf{kv}(\eta_*-\eta)}\cdot\sqrt{\frac{\pi}{2}q[\eta_*(\mathbf{x})-\eta]}\;H^{(1)}_{3/2}[q(\eta_*(\mathbf{x})-\eta)]\;, \qquad (63)$$

where $q=k+\mathbf{kv}$. This is basically the Lorentz boost of the solution that one would find for $\eta_*=\mathrm{const}$.

At small $\eta_*(\mathbf{x})-\eta$, one has $\delta\chi_2\propto[\eta_*(\mathbf{x})-\eta]^{-1}$, i.e., the same behaviour as in (56). So, the phase perturbation freezes out [20]:

$$\theta(\mathbf{x},\eta)=\frac{\delta\chi_2(\mathbf{x},\eta)}{\mathrm{Re}\,\chi(\mathbf{x},\eta)}=\int\frac{d^3k}{\sqrt{k}}\frac{h}{4\pi^{3/2}(k+\mathbf{kv})}\;\mathrm{e}^{i\mathbf{kx}-ik\eta_*(\mathbf{x})}\hat{A}_\mathbf{k}+h.c.\;, \qquad (64)$$

where we again omit an irrelevant constant phase factor. Note that for η_* constant in space (and hence $\mathbf{v}=0$), i.e., to the leading order in h, the phase perturbations are Gaussian random field with flat power spectrum (40). The interaction with the radial perturbations makes the situation less trivial. However, at the conformal rolling stage corresponding effects of the order v are washed out. Indeed, let us consider the two-point correlation function of the phase perturbation. Accordingly to (64), in the late-time regime,

$$\langle\theta(\mathbf{x}_1)\theta(\mathbf{x}_2)\rangle=\frac{h^2}{16\pi^3}\int\frac{d^3k}{kq^2}e^{i\mathbf{q}(\mathbf{x}_1-\mathbf{x}_2)}+c.c.$$

We now change the integration variable from $\mathbf{k}$ to $\mathbf{q}$. Since, the integration measure $\frac{d^3k}{k}$ is Lorentz-invariant, we obtain

$$\langle\theta(\mathbf{x}_1)\theta(\mathbf{x}_2)\rangle=h^2\int\frac{d^3q}{16\pi^3q^3}e^{i\mathbf{q}(\mathbf{x}_1-\mathbf{x}_2)}+c.c.$$

This is precisely the two-point function to the leading order in h. The latter argument is straightforwardly generalized to multiple correlators: for a given realization of the random field $\eta_\star(\mathbf{x})$, they are all expressed in terms of the two-point correlation function. In other words, the infrared effects are removed by the field redefinition,

$$\hat{\mathcal{A}}_\mathbf{q}=e^{-ik\eta_\star(0)}\sqrt{\frac{k}{q}}\hat{A}_\mathbf{k}\;.$$

Consequently, the order v corrections do not make any imprint on the observables, once the behaviour of the phase perturbations is fully captured by their dynamics at the rolling stage. This is true in the case of the sub-scenario A with superhorizon modes by the end of roll. On the opposite, the most interesting phenomenological consequences of the sub-scenario with the intermediate stage, i.e. the statistical anisotropy and the non-Gaussianity, follow from the order v correction.

3.4.2 Orders $\partial_i\partial_j\eta_\star/k$ and v^2. Final formula

Finally, we should calculate the phase perturbations in the orders $\partial_i\partial_j\eta_\star/k$ and v^2. The former one is quite tedious and we refer the interested reader to the Appendix B, where we reproduce the computations of the Ref. [20]. Otherwise, see the result below. It is much easier to derive the correction of the order v^2. This is expected to complete the analysis of the deep infrared effects on the phase perturbations. Remind, that the quantity $\mathbf{v}$ has the flat power spectrum and, therefore, the quantity v^2 is logarithmically amplified due to the deep infrared modes. Using the analogy with the Lorentz boost, one immediately obtains, instead of (63),

$$\delta\chi_2^{(-)}(\mathbf{k},\mathbf{x},\eta) = \mathrm{e}^{iq_{||}\gamma(x_{||}+v\eta)+i\mathbf{q}^T\mathbf{x}^T-iq\gamma\eta_*(0)}\cdot\sqrt{\frac{\pi}{2}\gamma q[\eta_*(\mathbf{x})-\eta]}\;H^{(1)}_{3/2}[\gamma q(\eta_*(\mathbf{x})-\eta)]\;,$$

where the indices $||$ and T refer to components parallel and normal to $\mathbf{v}$, respectively, the boosted momenta are

$$q_{||} = \gamma(k_{||}+kv)\;,\quad \mathbf{q}^T = \mathbf{k}^T\;,\quad q = \gamma(k+k_{||}v)\;,$$

and, consistently neglecting the second derivatives of $\delta\eta_*(\mathbf{x})$, we have used $\eta_*(\mathbf{x}) = \eta_*(0)-\mathbf{vx}$. In the limit $q(\eta_*(\mathbf{x})-\eta)\to 0$ one obtains the late-time expression for the phase, which can be written in a form. Let us write the final expression for the phase perturbations generated by the end of the conformal rolling [20],

$$\delta\theta(\mathbf{x},\eta) = \int\frac{d^3k}{\sqrt{k}}\frac{h}{4\pi^{3/2}\gamma(k+\mathbf{kv})}\,\mathrm{e}^{i\mathbf{kx}-ik\eta_*(\mathbf{x})}\left(1-\frac{\pi}{2k}\frac{k_ik_j}{k^2}\partial_i\partial_j\eta_\star+\frac{\pi}{6k}\partial_i\partial_j\eta_\star\right)\hat{A}_{\mathbf{k}}+h.c.\;. \tag{65}$$

This formula encodes all the necessary information about the statistical anisotropy in the sub-scenario A, i.e. one with cosmological mode superhorizon by the end of the conformal rolling. In this case the phase perturbations are frozen at the value (65). We assume that at the beginning of the Hot Big Bang the conversion into the adiabatic perturbations occurs, and the latter inherit the form of the phase perturbations generated (up to the possible non-Gaussianities of the local type). In the sub-scenario B the phase perturbations further evolve as they are still subhorizon at the end of the conformal rolling. In this case the value (65) serves as the initial condition for the evolution at the intermediate stage.

An important remark is in order. Even though we illustrated the conformal rolling mechanism by making use of the concrete model [18], the results are characteristic of the entire class of conformal models. As an example, the above formulas are valid [22], modulo field redefinition, in the Galilean Genesis model [25] based on conformal Galilean field with higher derivative action [95]. In fact, these formulas hold [26], provided that the theory has the general properties at the conformal rolling stage. We discuss them in the Chapter 5.

3.5 Conformal rolling: sub-scenario A

Now, let us discuss the version of the conformal rolling with the cosmologically interesting modes superhorizon by the end of the conformal rolling. In principle, all the basics of the sub-scenario A have been discussed in the previous Chapter. Here we just accumulate this knowledge to derive its phenomelogical properties. Namely, one can show that the sub-scenario A results into the quadrupole statistical anisotropy and non-Gaussianity in trispectrum [20, 21, 22]. Remarkably, these predictions are not specific to the conformal rolling scenario. The same ones are inherent in the much broader class of models, based on drastically different Lagrangians [25, 26], Hope, this will become clear from the discussion in the Chapter 5. Also note that the sub-scenario A is natural from the dynamical point of view. Namely, the field ϕ, which we assumed to be a spectator so far, can be pushed to drive the evolution of the Universe. This is actually not the case of the aternative sub-scenario, namely, the conformal rolling scenario with the intermediate stage.

3.5.1 Statistical anisotropy

The interaction of the phase perturbations with the radial ones at the conformal rolling stage leads to non-trivial effects in the spectrum of the primordial perturbations. In particular, it gives rise to the statistical anisotropy. Indeed, let us consider the two-point product $\delta\theta(\mathbf{x})\delta\theta(\mathbf{x}')$ and average it over the realizations of the operators $A_{\mathbf{k}}$ and $A^{\dagger}_{\mathbf{k}}$. To the leading order, we obtain the flat and isotropic power spectrum. The directional dependence appears once we take into account corrections coming from the derivatives of the end-of-roll time $\eta_*(\mathbf{x})$ and keep only those modes of $\delta\eta_*(\mathbf{x})$ which are still superhorizon today (shorter modes of $\delta\eta_*(\mathbf{x})$ give rise to the non-Gaussianity rather than statistical anisotropy [21, 22]). For so long modes of $\delta\eta_*(\mathbf{x})$, it does not make sense to average over the realizations of the operators $B_{\mathbf{p}}$, $B^{\dagger}_{\mathbf{p}}$ at this stage. In this way one obtains the power spectrum of the primordial perturbations $\zeta(\mathbf{k})$ [20]:

$$\mathcal{P}_{\zeta}(\mathbf{k}) = \mathcal{P}_0(k)\left(1 + Q_1(\mathbf{k}) + Q_2(\mathbf{k})\right) \ ; \tag{66}$$

(remind that we assume $\zeta \sim \theta$ up to the constant factor). The directional dependence is encoded in the functions $Q_1(\mathbf{k})$ and $Q_2(\mathbf{k})$, which originate from the corrections to the linear and next-to-linear orders in the parameter h, respectively,

$$Q_1(\mathbf{k}) = -\frac{\pi}{k}\hat{k}_i\hat{k}_j\left(\partial_i\partial_j\eta_\star - \frac{1}{3}\delta_{ij}\partial_k\partial_k\eta_\star\right) \ , \tag{67}$$

$$Q_2(\mathbf{k}) = -\frac{3}{2}(\hat{\mathbf{k}}\mathbf{v})^2 \ , \tag{68}$$

where $\hat{\mathbf{k}} = \mathbf{k}/k$. First, let us consider the leading order contribution $Q_1(\mathbf{k})$. We expand it in spherical harmonics,

$$Q_1(\mathbf{k}) = a(k) \sum_{LM} q_{LM} Y_{LM}(\hat{\mathbf{k}}) \; , \tag{69}$$

where

$$a(k) = k^{-1} \; . \tag{70}$$

By comparing (67) with (69), one concludes that the anisotropic coefficients q_{LM} are Gaussian variables, since they are linearly related to the derivatives of the end-of-roll time $\eta_\star(\mathbf{x})$, which is the Gaussian field. We keep very long modes of $\delta\eta_*(\mathbf{x})$ with $p < H_0$, where H_0 is the present value of the Hubble parameter. At shorter wavelengths the field $\delta\eta_\star(\mathbf{x})$ gets averaged out. Therefore, the expression in parenthesis in (67) should be treated as a constant tensor throughout our part of the Universe; retaining its dependence on $\mathbf{x}$ would result in effects suppressed by H_0/k. For this reason, only the quadrupole of the general type survives in Eq. (69). Neither its direction nor precise magnitude can be predicted because of the cosmic variance. Yet its variance in the ensemble of Universes like ours is calculable and given by

$$\langle q_{2M} q^\star_{2M'} \rangle = \frac{\pi h^2 H_0^2}{25} \delta_{MM'} \; . \tag{71}$$

For similar reason, the second contribution $Q_2(\mathbf{k})$ also represents the quadrupole statistical anisotropy, but of the special type. It can be expanded in the same fashion as in (69). As compared to the previous case, the amplitude $a(k)$ is independent of the wavenumber k. We will see that this fact is crucial from the viewpoint of the CMB observations. The other important distinction is that the quantities q_{2M} are not Gaussian now. Therefore, it will be convenient to work with the components of the "velocity" $\mathbf{v}$, which are Gaussian variables with zero means and variances

$$\langle v_i^2 \rangle = \frac{3h^2}{8\pi^2} \ln \frac{H_0}{\Lambda} \; . \tag{72}$$

Here the present value of the Hubble parameter and the constant Λ appear as the ultraviolet and infrared cutoffs, respectively. The quantities q_{2M} are then given by

$$q_{2M} = -\frac{4\pi v^2}{5} Y^\star_{2M}(\hat{\mathbf{v}}) \; , \tag{73}$$

where $\hat{\mathbf{v}} = \mathbf{v}/v$ is the unit vector in the direction of the "velocity" $\mathbf{v}$.

Equations (70), (71), (72) and (73) are the starting point of our analysis of the statistical anisotropy in the CMB within the sub-scenario A.

3.5.2 Non-Gaussianity

The statistical anisotropy appears to be a weak signature of the sub-scenario A, since it is suppressed either by the factor H_0/k or by the power of the coupling constant h. In quest for

more relevant signatures of the sub-scenario A, one turns to the non-Gaussianity. First to note, the non-Gaussianity at the level of bispectrum is not particularly interesting. So, the intrinsic bispectrum vanishes for the symmetry reasons. This is clear from the action (42), which is invariant under the change of sign of the phase θ, i.e. under the transformation $\theta \to -\theta$. Hence, all the correlators of odd number of phase perturbations vanish. Further, as discussed in Section, the non-Gaussianity generated at the conversion epoch is not specific to the conformal scenario. Thus, bispectrum alone cannot descriminate between conformal scenario and, say, inflation equipped with the curvaton mechanism [46, 47, 49, 48, 50].

Fortunately, the intrinsic non-Gaussianity of a rather peculiar form is non-zero at the level of the trispectrum [21, 22]. Probably, the most striking feature of the trispectrum calculated there, is the singularity in the limit where tmo momenta are equal in absolute value and have opposite directions (folded limit). The singular part of the connected four-point function is given by

$$\langle \zeta_{\mathbf{k_1}} \zeta_{\mathbf{k_2}} \zeta_{\mathbf{k_3}} \zeta_{\mathbf{k_4}} \rangle = \mathrm{const} \delta \left(\sum_{i=1}^{n} \right) \frac{1}{k_{12} k_1^4 k_3^4} \left[1 - 3 \left(\frac{\mathbf{k_{12}} \mathbf{k}_1}{k_{12} k_1} \right)^2 \right] \left[1 - 3 \left(\frac{\mathbf{k_{12}} \mathbf{k_3}}{k_{12} k_3} \right)^2 \right] , \qquad (74)$$

where

$$\mathbf{k_{12}} = \mathbf{k_1} + \mathbf{k_2} \to 0 , \qquad (75)$$

i.e., the trispectrum blows up as k_{12}^{-1}. The singularity in the folded limit is due to the enhancement of the perturbations $\delta\chi_c$. To account this effect properly, one needs to go beyond the techiques applied so far. The reason is that the momenta p relevant for the non-Gaussianity can be as large as the cosmologically interesting momenta k.

Interestingly, the single-field inflation predicts the trispectrum finite in the limit $k_{12} \to 0$. This sets a belief that the conformal rolling scenario can be distinguished from the broad class of the inflationary models. Remind that the local type non-Gaussianity is also singular in the folded limit, i.e. it peaks as k_{12}^{-3} as $k_{12} \to 0$. This is, however, not a sort of worry for us. In the Ref. [22], the trispectrum of the conformal rolling scenario was compared with the local one. As it follows from the Figs. 4-6, the corresponding shapes are essentially different in various limits. Hopefully, this statement holds at the level of the CMB observations.

Remarkably, the trispectrum calculated in [21, 22] is not specific to the conformal rolling scenario only. The lowest order interaction between the phase and the radial perturbation $\delta\chi_c$ is described by the interaction Hamiltonian,

$$\mathcal{H}_I = -\mathcal{L}_{int} = -\chi_c \delta\chi_c (\partial_\mu \theta)^2 . \qquad (76)$$

Let us borrow the intuition developed in the Ref. [26], and view the radius χ_c and the phase θ as two separate fields. In this treatment, χ_c is the conformal weight-one field, θ is the weight-zero field, while the expression (76) represents the minimal interaction between

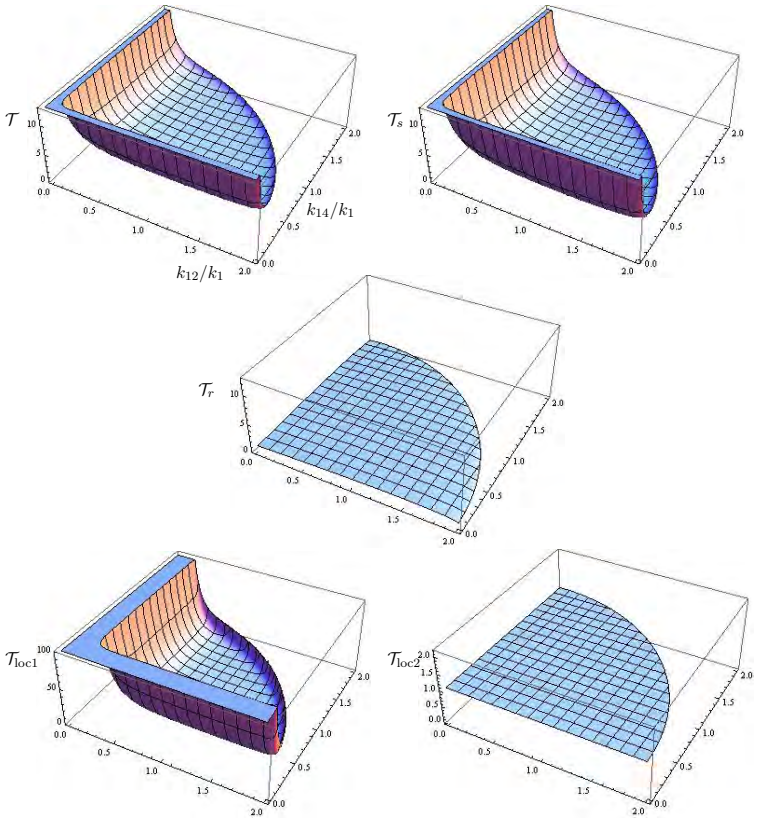

Figure 4: Complete trispectrum $\mathcal{T}$ (upper left pannel), its singular part $\mathcal{T}_s$ (upper right panel), its regular part $\mathcal{T}_r$ (middle panel), trispectrum of the local form $\mathcal{T}_{loc1}$ (lower left panel) and trispectrum of another local form $\mathcal{T}_{loc2}$ (lower right panel) in equilateral limit. The picture is reproduced with the permission of the authors [22]

these fields preserving the conformal invariance. The similar picture occurs in the Galilean Genesis [25]. The qualification is that the weight-zero degree of freedom *a la* the phase of the conformal rolling scenario is set by hands in this model. The behaviour of the Galilean field, the weight-one conformal field, is essentially the same as of the radius χ_c. Thus, not surprisingly that predictions of two models coincide. This remarkable statement has been first made in [22] and further proved clarified on much more general grounds in [26]. In particular, this means that the trispectrum of the Galilean Genesis has the same shape as one calculated in [22]. We further elaborate on these points in the Chapter 5.

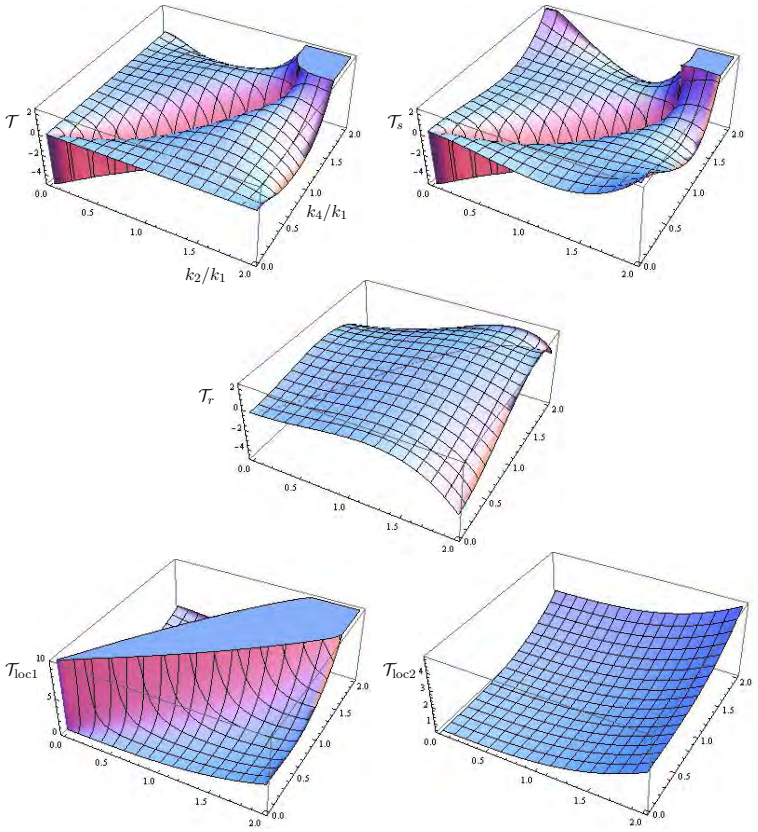

Figure 5: Same as in the Fig. 4 but in the specialized planar limit. The picture is reproduced with the permission of the authors [22]

3.6 Scalar tilt from broken conformal invariance

So far we avoided the discussion of one more important signature of the primordial physics, i.e. the scalar tilt. Remind that the latter is favored by the current experiments. Not aiming to go into the contradiction with the WMAP data, one should think about the sources of the scalar tilt inherent in the model under the consideration. Unfortunately, the prediction of the conformal rolling scenario as it stands is the exactly flat spectrum. Thus, to sustain the consistency with the data, one (or some) of the assumptions underlying the model should be mildly avoided. To understand what are these assumptions, let us return to the discussion of the scalar tilt in the inflation. The deviation from the flatness there is due to the two effects: the small effective mass of the inflaton and the slight breaking of the background de Sitter symmetry. In the context of the conformal rolling scenario, the former would correspond to the slightly broken $U(1)$ symmetry. This is achieved without any efforts in the general setup of Hinterbichler and Khoury [26] rather than in the conformal rolling scenario [18].

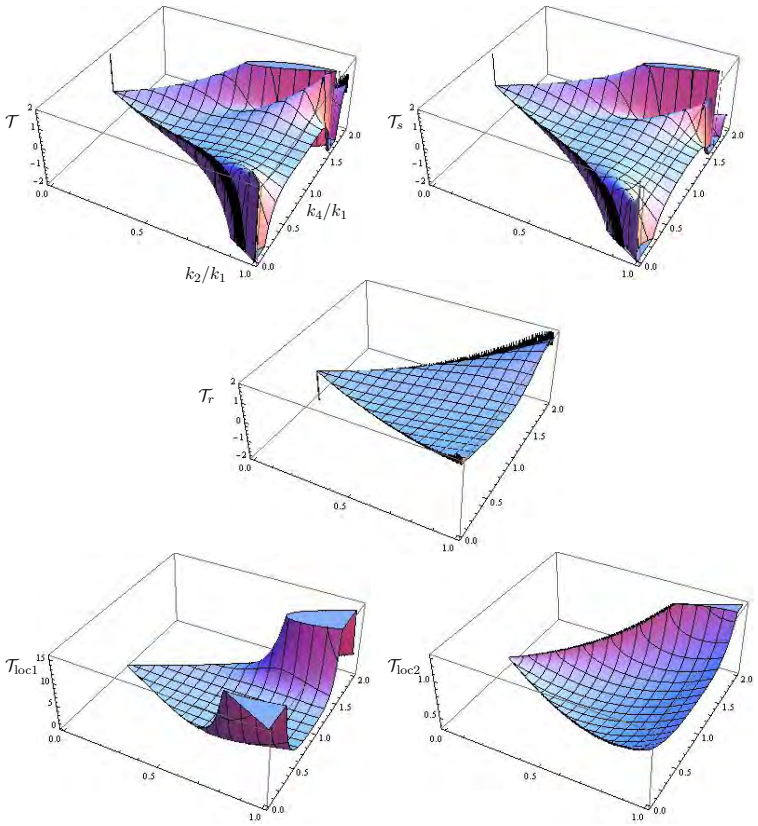

Figure 6: Same as in the Fig. 4, but in the near double-squeezed limit. The picture is reproduced with the permission of the authors [22]

We postpone this discussion until the Chapter 5. There is the other way to obtain the scalar tilt, i.e. by the explicit breaking of the conformal invariance. This idea has been proposed in [19].

The easiest way to break conformal invariance is to assume that the potential of the conformal rolling is slightly different from the quartic one,

$$V(\phi) = -h^2|\phi|^{4+\alpha} \ ,$$

where the parameter α is assumed to be small, i.e. $\alpha \ll 1$. If the conformal symmetry is broken, then the scale factor does not drop out from the field equation, and we have to specify the cosmological model. Following [19], one chooses the contracting Universe filled with matter with stiff equation of state $w > 1$ as the background, as given, e.g. in the ekpyrotic models with the negative exponential potential. In terms of conformal time, the evolution of the scale factor is

$$a(\eta) = \mathcal{A}(-\eta)^p,$$

where $p = \frac{2}{1+3w}$, $\mathcal{A} = \text{const}$. The evolution of phase perturbations on this background results into the slightly tilted power spectrum characterized by the spectral index [19]

$$n_s - 1 = \alpha(1 + p) \ . \tag{77}$$

Hence, the tilt is blue or red if the constant α is positive or negative, respectively. This expression completes the set of predictions of the sub-scenario A. As it follows, violation of the conformal invariance is the unique source of the scalar tilt in this case. The situation is different in the sub-scenario with the intermediate stage, to which discussion we turn shortly. However, the additional contribution to the scalar tilt appearing there is rather weak [23], since it relies on the coupling constant h^2. Thus, the spectral tilt as given by the formula (77) seems to be the major source also in the sub-scenario B. One more option of getting the spectral tilt is to break the $U(1)$-invariance, so that the phase obtains the effective mass term. We consider this opportunity in the Chapter 5, where the general point of view on the conformal rolling scenario is review.

4 Conformal rolling scenario with intermediate stage

4.1 Setup and phenomenology

In this Chapter we assume that there is a long enough period of time after the end of conformal rolling, at which the phase perturbations remain subhorizon in the conventional sense [23]. Their behavior between the end of conformal rolling and horizon exit depends strongly on the evolution of the scale factor at this intermediate stage. In order that the flat power spectrum (40) be not grossly modified at this epoch, the scale factor should evolve in such a way that the dynamics of θ is effectively nearly Minkowskian. Although this requirement sounds prohibitively restrictive, there are at least two cosmological scenarios in which it is obeyed. One is the bouncing Universe, with matter at the contracting stage having super-stiff equation of state, $p \gg \rho$. It is worth noting in this regard that stiff equation of state is preferred at the contracting stage for other reasons [17, 94] and is inherent, e.g., in a scalar field theory with negative exponential potential, like in the ekpyrotic model [15]. It is known [99] that in models with super-stiff matter at contracting stage, the resulting power spectrum of scalar perturbations is almost the same as that of massless scalar field in Minkowski space, $\mathcal{P}(k) \propto k^2$. This implies that the dynamics of the scalar field perturbations is almost Minkowskian in these models. In tractable bouncing models like those of Refs. [13, 14], our phase perturbations exit the horizon at the contracting stage, pass through the bounce unaffected (cf. Ref. [98]), remain superhorizon early at the hot expansion epoch and get reprocessed into adiabatic perturbations by one or the other mechanism [56, 55, 48].

The similar situation occurs in the framework of the (pseudo)-Conformal Universe [26], of which the conformal rolling scenario and the Galilean Genesis [25] are the particular examples. This will become clear in the next Chapter. Now, let us state that the (nearly) Minkowskian background is the dinamical background of the Universe undergoing the conformal phase. In the concrete example of Hinterbichler-Khoury [26] the evolution of the Universe is akin to one in the ekpyrotic scenarios with the negative exponential potential, i.e. the Universe slowly contracts at very early times. In Galilean Genesis, the Universe is initially spatially flat and nearly static, stays in this nearly Minkowskian state for long time, then its expansion quickly speeds up and eventually the conventional hot epoch begins. If our conformal rolling stage ends up well before the start of rapid expansion, the evolution of the phase perturbations is again nearly Minkowskian up until the horizon exit.

In both scenarios the relevant range of momenta is wide, provided that f_0 is small enough (but not unrealistically small). We discuss this point in Section 4.2. So, it is legitimate to approximate the evolution of the phase perturbations as Minkowskian in the time interval[15] $\eta_* - \epsilon < \eta < \eta_1$, where η_1 is some time after the horizon exit, and $(\eta_* - \epsilon)$ is the time when

[15]For the reason that will become clear shortly, we drop here the superscript (0) in the notation of η_*.

the radial field relaxes to the minimum of $V(|\phi|)$ and the conformal rolling stage ends. We set $\epsilon = 0$ in what follows to simplify notations; keeping $\epsilon \neq 0$ would not change our results (recall that the phase perturbations are frozen out well before $\eta = \eta_*$). The field $\theta(\mathbf{x}, \eta_*)$, determined by the dynamics at the conformal rolling stage, serves as the initial condition for further Minkowskian evolution from η_* to η_1. Barring fine tuning, the case of interest for us is[16]

$$k(\eta_1 - \eta_*) \gg 1 \, .$$

Our purpose is to study the properties of the phase perturbations at $\eta = \eta_1$, as these properties are inherited by the adiabatic perturbations.

To the leading order in h, we find nothing new: the phase perturbations at $\eta = \eta_1$ are Gaussian and have flat power spectrum. Subleading orders in h are more interesting. A simple way to understand what is going on is to notice that the end-of-roll time η_*, instead of being a constant parameter, is actually a Gaussian random field [18], $\eta_*(\mathbf{x}) = \eta_* + \delta\eta_*(\mathbf{x})$ with $\delta\eta_* \propto h$. This is due to the fact that not only the phase θ but also the radial field $|\chi|$ acquire perturbations at the conformal rolling stage; after freeze out, perturbations $\delta|\chi|$ can be interpreted as perturbations $\delta\eta_*(\mathbf{x})$. The effect of the perturbations $\delta\eta_*$ on the phase perturbations θ is twofold. First, the perturbations $\delta\eta_*$ modify the dynamics of θ at the conformal rolling stage, as it follows from Ref. [20]. The new point is that the resulting field $\theta(\mathbf{x}, \eta_*(\mathbf{x}))$ serves as the initial condition for the Minkowskian evolution. Second, this initial condition is now imposed at the non-trivial hypersurface $\eta = \eta_*(\mathbf{x})$. This is illustrated in Fig. 7. The net result is that the perturbation $\theta(\mathbf{x})$ at the time η_1 is a combination of two Gaussian random fields originating from vacuum fluctuations of the phase θ and radial field $|\chi|$, respectively (better to say, from vacuum fluctuations of imaginary and real parts of χ, with our convention of real background χ_c). This leads to several potentially observable effects.

At the level of the two-point correlation function of the phase perturbation $\theta(\mathbf{x}, \eta_1)$, and hence of the adiabatic perturbation ζ, we have found two effects. The first one is negative scalar tilt [23]

$$n_s - 1 = -\frac{3h^2}{4\pi^2} \, . \tag{78}$$

We note in passing that this is not a particularly strong result, as small scalar tilt in our scenario may also originate from weak violation of conformal invariance at the conformal rolling stage [19], see the Eq. (77) and/or not exactly Minkowskian evolution of θ at the intermediate stage. The second effect is the statistical anisotropy: the power spectrum has the form [23]

$$\mathcal{P}_\zeta(\mathbf{k}) = \mathcal{P}_\zeta(k) \left[1 + Q(\hat{\mathbf{k}})\right] \, , \tag{79}$$

[16] In the opposite case, the phase perturbations do not evolve between η_* and η_1, and we are back to the version (i) above.

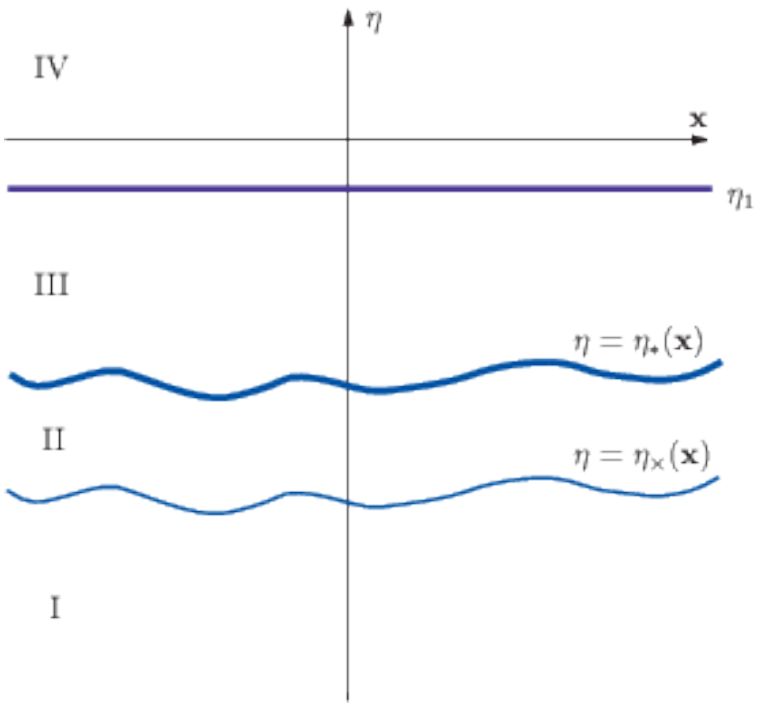

Figure 7: Due to the perturbations of the radial field, the evolution of phase perturbations proceeds in inhomogeneous background. Perturbations θ oscillate in time at early stage (region I), freeze out at time $\eta = \eta_\times(\mathbf{x})$ and temporarily stay constant (region II) until the end of conformal rolling that occurs at $\eta = \eta_*(\mathbf{x})$. Then they evolve again, now in nearly Minkowskian regime (region III), until the horizon exit time η_1. Later on (region IV), perturbations θ are superhorizon and stay constant.

where $\mathcal{P}_\zeta$ is independent of the direction of momentum (nearly flat spectrum with small tilt), $\hat{\mathbf{k}} = \mathbf{k}/k$ is the unit vector along the momentum and $Q(\hat{\mathbf{k}})$ is itself a random field, which depends on the direction of $\mathbf{k}$ only. Unlike the statistical anisotropy discussed in the inflationary context [79, 82, 81, 82, 89], and also in the version A of the conformal rolling scenario [20], the function $Q(\hat{\mathbf{k}})$ contains all even angular harmonics, starting from quadrupole. We give here the expression for $Q(\hat{\mathbf{k}})$ which accounts for the quadrupole component only (see Section 4.4 for the results valid for all multipoles)

$$Q(\hat{k}) = \mathcal{Q} \cdot w_{ij} \left(\hat{k}_i \hat{k}_j - \frac{1}{3}\delta_{ij} \right) , \tag{80}$$

where w_{ij} is a general symmetric traceless tensor normalized to unity, $w_{ij}w_{ij} = 1$, and the variance of the quadrupole component (in the sense of an ensemble of universes) is

$$\langle \mathcal{Q}^2 \rangle = \frac{225h^2}{32\pi^2} \tag{81}$$

Of course, the precise values of the multipoles of $Q(\hat{\mathbf{k}})$ in our patch of the Universe are undetermined because of the cosmic variance.

Due to the interaction with the perturbations $\delta\eta_*$, the resulting phase perturbations $\theta(\mathbf{x}, \eta_1)$ and their descendant perturbations ζ are non-Gaussian (we leave aside here the non-Gaussianity that may be generated at the epoch of conversion of the phase perturbations into adiabatic ones; our scenario is not special in this respect). Their three-point correlation function vanishes identically due to the discrete symmetry $\theta \to -\theta$ (cf. Ref. [20]), while the four-point correlation function has a peculiar form [23]

$$\langle\zeta(\mathbf{k})\zeta(\tilde{\mathbf{k}})\zeta(\mathbf{k}')\zeta(\tilde{\mathbf{k}}')\rangle = \frac{\mathcal{P}_\zeta(k)}{4\pi k^3}\frac{\mathcal{P}_\zeta(k')}{4\pi k'^3}\delta(\mathbf{k}+\tilde{\mathbf{k}})\delta(\mathbf{k}'+\tilde{\mathbf{k}}')\cdot\left[1+F_{NG}(\hat{\mathbf{k}},\hat{\mathbf{k}}')\right] + (\mathbf{k}\leftrightarrow\mathbf{k}') + (\tilde{\mathbf{k}}\leftrightarrow\mathbf{k}') \,. \tag{82}$$

The leading term in (82) (unity in square brackets) is the Gaussian part, while the non-Gaussianity is encoded in $F_{NG} = O(h^2)$. Note that the structure of the non-Gaussian part is fairly similar to that of the disconnected four-point function. Note also that F_{NG} depends on the angle between $\mathbf{k}$ and $\mathbf{k}'$ only. For reasons we discuss in Section 4.5, the notion of non-Gaussianity is appropriate if the angle between $\mathbf{k}'$ and $\mathbf{k}$ is small, i.e., $|\hat{\mathbf{k}} - \hat{\mathbf{k}}'| \ll 1$. In this regime, the leading behaviour of F_{NG} is

$$F_{NG} = \frac{3h^2}{\pi^2}\log\frac{\text{const}}{|\hat{\mathbf{k}}-\hat{\mathbf{k}}'|} \,,$$

where constant in the argument of logarithm cannot be reliably calculated because of the cosmic variance. The logarithmic behavior does not hold for arbitrarily small $|\hat{\mathbf{k}} - \hat{\mathbf{k}}'|$: the function $F_{NG}(\hat{\mathbf{k}} - \hat{\mathbf{k}}')$ flattens out most likely at $|\hat{\mathbf{k}} - \hat{\mathbf{k}}'| \sim [k(\eta_1 - \eta_*)]^{-1/2}$, and certainly at $|\hat{\mathbf{k}} - \hat{\mathbf{k}}'| \sim [k(\eta_1 - \eta_*)]^{-1}$. So, the parameter $(\eta_1 - \eta_*)$ is detectable in principle (but, probably, not in practice).

It is tempting to speculate that the negative scalar tilt $n_s - 1 \simeq -0.04$, favoured by the data [113], has its origin in the dynamics we discuss in this paper. If so, our only free parameter h is determined from (78), $h^2 \simeq 0.5$, while the small amplitude of the adiabatic perturbations is to be attributed to the mechanism that reprocesses the phase perturbations into adiabatic ones. In that case the statistical anisotropy is roughly of order 1, which is probably inconsistent with the data. On the other hand, if one attributes the small observed amplitude of primordial scalar perturbations, $\sqrt{\mathcal{P}_\zeta} \simeq 5 \cdot 10^{-5}$ [114], entirely to the smallness of h, i.e., identifies $\mathcal{P}_\theta$ with $\mathcal{P}_\zeta$, then $h^2 \sim 10^{-7}$, and the statistical anisotropy is at the level $Q \sim 10^{-3}$, while the non-Gaussianity is probably unobservable. This gives an idea of the range of predictions of our model.

4.2 Momentum scales

Before discussing field perturbations in detail, let us consider momentum scales for which our scenario, outlined in previous Subsection, is valid. According to this scenario, conformal rolling stage ends up when the radial field $|\phi|$ becomes of order f_0. This occurs at time η_f such that

$$\frac{1}{a(\eta_f)h(\eta_f - \eta_*^{(0)})} \sim f_0 \ .$$

Hence, the shortest waves obeying (47) have present momenta

$$\frac{k_{\max}}{a_0} \sim h f_0 \cdot \frac{a(\eta_f)}{a_h} \cdot \frac{a_h}{a_0} \ ,$$

where a_0 and a_h are the present value of the scale factor and its value at the beginning of the hot stage, respectively. On the other hand, we assume that the relevant modes are subhorizon right after η_f,

$$\frac{k}{a(\eta_f)} > H(\eta_f) \ . \tag{83}$$

We recall our requirement (45) and find that the longest waves obeying (83) satisfy

$$\frac{k}{a_0} > \frac{k_{\min}}{a_0} \sim \frac{h f_0^2}{M_{\rm PL}} \cdot \frac{a(\eta_f)}{a_h} \cdot \frac{a_h}{a_0} \ . \tag{84}$$

We see that the relevant range of momenta is

$$\frac{f_0}{M_{Pl}} \cdot k_{\max} < k < k_{\max} \ .$$

It is wide enough, provided that the energy scale f_0 is sufficiently low. As an example, for $k_{\max}/k_{\min} \sim (10\text{kpc})^{-1}/(10\text{Gpc})^{-1}$ we need $f_0 < 10^{-6} M_{Pl}$.

If our mechanism is supposed to work at contracting stage in the bouncing Universe scanario with the hot epoch starting immediately after bounce, the inequality (84) implies much stronger bound on f_0. Indeed, $a(\eta_f)/a_h > 1$ in this scenario, while $a_h/a_0 \gtrsim T_0/T_h > T_0/M_{Pl}$. We require that $k_{\min}/a_0$ is lower than the present Hubble scale H_0 and obtain

$$\sqrt{h} \cdot f_0 < M_{Pl} \left(\frac{H_0}{T_0}\right)^{1/2} \sim 10^{-15} M_{Pl} \ . \tag{85}$$

Even for $h \sim 10^{-4}$ this implies $f_0 < 10^6$GeV. Interestingly, fully consistent with this scenario is the scale $f_0 \sim$ TeV.

On the contrary, $a(\eta_f)/a_h$ can be large in the Galilean Genesis scenario [25]. Therefore, no bound similar to (85) can be established in that case.

4.3 Evolution at the intermediate stage

4.3.1 Cauchy problem

As outlined in Subsection 4.1, our scenario involves the evolution of the phase perturbations θ from the hypersurface $\eta = \eta_*(\mathbf{x})$ to the hypersurface $\eta = \eta_1 = \text{const}$. At this intermediate stage, the radial field stays at the minimum of the scalar potential, while the phase field is minimally coupled to gravity, and evolves in the subhorizon regime. At time η_1, the phase perturbations become superhorizon and freeze out again. The evolution of the phase must be nearly Minkowskian at this stage, otherwise its power spectrum would be grossly modified, see also Appendix A. So, the quantity of interest is $\theta(\mathbf{x}, \eta_1)$, and it has to be evaluated by solving the Minkowskian equation

$$\Box\theta \equiv (\theta)'' - \partial_i\partial_i\theta = 0 \; . \tag{86}$$

The initial condition $\theta(\mathbf{x}, \eta_*(\mathbf{x}))$ at the hypersurface $\eta = \eta_*(\mathbf{x})$ is determined by the dynamics at the conformal rolling stage. In this Section we perform the calculation to the linear order in v, so the explicit expression is given by (64). The second initial condition is that the perturbation θ is frozen out by the end of the conformal rolling stage, so that

$$\partial_N\theta = 0 \qquad \text{at} \;\; \eta = \eta_*(\mathbf{x}) \; , \tag{87}$$

where ∂_N denotes the normal derivative to the hypersurface $\eta = \eta_*(\mathbf{x})$. As pointed out in the beginning of the Chapter, the case of interest is $k(\eta_1 - \eta_*) \gg 1$, so the evolution is long.

4.3.2 Leading order: effects of the background cosmological evolution

Let us discuss the free propagation of the phase θ to the leading order in the constant h. The only possible source of non-trivialities in this case is due to the background evolution, which we choose to be the slow contraction driven by the matter with the super-stiff equation of state, $p = w\rho$, $w \gg 1$. Our point here is to show that in the limit $w \to \infty$ the propagation is effectively Minkowskian all the way down to $a(\eta) \to 0$.

For constant w, the scale factor evolves in conformal time as follows,

$$a = |\eta|^\beta \; , \qquad \eta < 0 \; ,$$

where

$$\beta = \frac{2}{1+3w} \; .$$

In terms of the field $\sigma = a\theta$, the field equation reads

$$\sigma'' + k^2\sigma - \frac{a''}{a}\sigma = \sigma'' + k^2\sigma - \frac{\beta(1-\beta)}{\eta^2}\sigma = 0 \; . \tag{88}$$

For large w and hence small β, the last term in the left hand side of Eq. (88) is negligible before the horizon exit time, $\eta_{ex} \sim -\sqrt{\beta}/k$, while there is simply no time to evolve even in Minkowski space in the time interval $(\eta_{ex}, 0)$. This is why one can make use of the Minkowskian evolution to evaluate the value of the field θ as $\eta \to 0$, i.e., deep in the super-horizon regime.

To substantiate this claim, let us consider the Cauchy problem. Namely, let the initial value θ_i be specified at $\eta = \eta_* = \text{const}$ with $|\eta_*| \gg k^{-1}$, and another initial condition is $\theta' = 0$ at $\eta = \eta_*$. Let us compare the values of θ obtained at $\eta = 0$ by solving the Minkowskian evolution equation $\Box\theta = 0$ and by evolving the field according to Eq. (88). The Minkowski evolution gives the solution for the negative frequency mode: $\theta^{Mink}(\eta, k) = \theta_i(\eta, k)e^{-k(\eta-\eta_*)}$, so that

$$\theta^{Mink}(\eta \to 0) = \theta_i e^{ik\eta_*} \ .$$

The solution to Eq. (88) with the above initial conditions imposed at $|\eta_*| \gg k^{-1}$ is

$$\sigma(\eta) = \theta_i |\eta_*|^\beta \sqrt{\frac{\pi}{2} k|\eta|} u H_\nu^{(1)}(-k\eta) \ ,$$

where $\nu = 1/2 - \beta$,

$$u = \mathrm{e}^{ik\eta_* + i\frac{\pi}{2}(1-\beta)}$$

and $H_\nu^{(1,2)}$ are Hankel functions. The asymptotics of $\theta = \sigma/a$ as $\eta \to 0$ for $\beta < 1/2$ is

$$\theta(\eta \to 0) = \theta_i e^{i\left(k\eta_* - \frac{\pi\beta}{2}\right)} \left(\frac{k|\eta_*|}{2}\right)^\beta \frac{\Gamma(1/2-\beta)}{\Gamma(1/2)} \ .$$

We see that the Minkowskian result indeed coincides with the exact one in the limit $w \to \infty$, i.e., $\beta \to 0$. The main effect for finite but large w is the induced tilt in the power spectrum. The phase $\pi\beta/2$ is irrelevant as it cancels out in the correlation functions. Keeping in mind this possible imprint of the background, we further deal with the purely Minkowskian evolution.

4.3.3 The case of $\mathbf{v} = \text{const}$

It is instructive to consider the unrealistic case

$$\eta_*(\mathbf{x}) = \eta_* - \mathbf{v}\mathbf{x}$$

with constant $\mathbf{v}$. This means that the Cauchy hypersurface is flat and boosted with respect to the cosmic frame. Let us consider the solution to Eq. (86) obeying the initial condition (cf. (64))

$$\theta_{\mathbf{k}}(\mathbf{x}, \eta_*(\mathbf{x})) = \mathrm{e}^{i\mathbf{k}\mathbf{x} - ik\eta_*(\mathbf{x})} \ , \quad \partial_N \theta_{\mathbf{k}} = 0 \ .$$

By going to the boosted reference frame back and forth, one finds that the solution, to the first order in v (and hence in h), can be written as follows,

$$\theta_{\mathbf{k}}(\mathbf{x},\eta) = \mathrm{e}^{i(\mathbf{k}+k\mathbf{v})[\mathbf{x}+\mathbf{v}(\eta-\eta_*)]-ik\eta_*}\cos[(k+\mathbf{kv})(\eta+\mathbf{vx}-\eta_*)]\ .$$

Equivalently,

$$\theta_{\mathbf{k}}(\mathbf{x},\eta) = \frac{1}{2}\left[\mathrm{e}^{i(\mathbf{k}+2k\mathbf{v})\mathbf{x}+i(k+2\mathbf{kv})\eta-2i(k+\mathbf{kv})\eta_*} + \mathrm{e}^{i\mathbf{kx}-ik\eta}\right]\ . \tag{89}$$

The first lesson is that the solution is the sum of waves traveling along $\mathbf{k}$ and (almost) in the opposite direction; we will see in what follows that this situation is generic. Furthermore, for large enough $(\eta-\eta_*)$ the two terms in (89) have very different phases at given $\mathbf{x}$, so their interference is negligible when integrated over $\mathbf{k}$ with any smooth function. The second lesson is that the wave moving along $\mathbf{k}$ has momentum $\mathbf{k}$, while the momentum of the wave moving in the opposite direction is $(\mathbf{k}+2k\mathbf{v})$. We interpret this as the Doppler shift. Indeed, let us go to the reference frame $(\tau,\mathbf{y})$ that moves with velocity $\mathbf{v}$ with respect to the cosmic frame, i.e.,

$$\mathbf{x} = \mathbf{y}-\mathbf{v}\tau\ , \qquad \eta = \tau - \mathbf{vy}$$

(recall that we work to the first order in v). The Cauchy hypersurface $\eta=\eta_*(\mathbf{x})$ corresponds to $\tau=\eta_*=\mathrm{const}$, and the mode at this hypersurface is

$$\theta_{\mathbf{k}}(\mathbf{y}) = \mathrm{e}^{i\mathbf{kx}-ik\eta_*(\mathbf{x})} = \mathrm{e}^{i(\mathbf{k}+k\mathbf{v})\mathbf{y}}\cdot\mathrm{e}^{-i(k+\mathbf{kv})\eta_*}\ .$$

The last factor here is merely a constant phase, while the first factor describes the wave with momentum $(\mathbf{k}+k\mathbf{v})$ in the new reference frame. In the cosmic frame, this momentum gets shifted by $-k\mathbf{v}$ and $k\mathbf{v}$ for waves moving along $\mathbf{k}$ and opposite to $\mathbf{k}$, respectively. Hence the result (89). We will see that this situation is also generic: to the first non-trivial order in h, the main effect due to the intermediate stage is precisely the Doppler shift and the lack of interference between waves coming in the directions of $\mathbf{k}$ and $-\mathbf{k}$.

4.3.4 General formula and saddle point calculation

The general solution to the Cauchy problem for Eq. (86) with the field and its normal derivative specified at hypersurface Σ is

$$\theta(x) = \int_\Sigma d\Sigma^\mu \left\{ D^{ret}(x,y)\partial_\mu\theta(y) - \left[\frac{\partial}{\partial y^\mu}D^{ret}(x,y)\right]\theta(y)\right\}\ , \tag{90}$$

where D^{ret} is the retarded Green's function of Eq. (86), x collectively denotes the coordinates $(\eta,\mathbf{x})$, and the normal to the hypersurface is directed towards future. In our case the first term in the integrand is absent because of (87). We make use of the explicit expression (valid in the case $x^0>y^0$ we are interested in)

$$D^{ret}(x,y) = \frac{1}{2\pi}\delta[(x-y)^2]\ , \tag{91}$$

perform the integration over the radial variable and obtain for large $(\eta_1 - \eta_*)$ (see Appendix C for details)

$$\theta(x) = \int \frac{d\Omega_{\mathbf{n}}}{4\pi} \frac{1}{1 - \mathbf{nv}} r \partial_r \theta \ , \tag{92}$$

where we still use the notation $v_i = -\partial_i \eta_*$. Here $\mathbf{n}$ is unit radius-vector, integration runs over the unit sphere parametrized by $\mathbf{n}$, and $r = r(\mathbf{n})$ is the spatial distance that light travels from the hypersurface $\eta = \eta_*(\mathbf{y})$ to the point $x = (\eta_1, \mathbf{x})$. It obeys the following equation:

$$r = \eta_1 - \eta_*(\mathbf{x} + \mathbf{n}r) \ . \tag{93}$$

The function $\theta = \theta(r, \mathbf{n})$ in the right hand side of (92) is the field value at the Cauchy hypersurface,

$$\theta(r, \mathbf{n}) = \theta(\mathbf{y}, \eta_*(\mathbf{y}))$$

with

$$\mathbf{y} = \mathbf{x} + \mathbf{n}r \ .$$

The formula (92) is exact for large r (for arbitrary r and general Cauchy data with non-vanishing $\partial_N \theta$, its generalization is Eq. (211) in Appendix B).

We now make use of (64) and obtain

$$\theta(\mathbf{x}, \eta_1) = \frac{h}{4\pi^{3/2}} \int \frac{d^3k}{\sqrt{k}} \mathrm{e}^{i\mathbf{kx}} A_{\mathbf{k}} \cdot I + h.c. \ , \tag{94}$$

where I is the integral over unit sphere,

$$I = i \int \frac{d\Omega_{\mathbf{n}}}{4\pi} \mathrm{e}^{i\psi(\mathbf{n})} \cdot r \cdot \frac{(\mathbf{k} + k\mathbf{v})\mathbf{n}}{(1 - \mathbf{nv})(k + \mathbf{kv})} \tag{95}$$

with

$$\psi = \mathbf{kn}r - k\eta_*(\mathbf{x} + \mathbf{n}r) = \mathbf{kn}\eta_1 - (\mathbf{kn} + k)\eta_*(\mathbf{x} + \mathbf{n}r) \ . \tag{96}$$

All quantities in the integrand of (95) (including $\mathbf{v}$) are to be evaluated at $\mathbf{y} = \mathbf{x} + \mathbf{n}r$. Corrections to the integrand are of order v^2 and $\partial v / k$.

The exponential factor $\mathrm{e}^{i\psi}$ in (95) is, generally speaking, a rapidly oscillating function of $\mathbf{n}$, since ψ is proportional to the large parameter kr. Therefore, the integral (95) can be calculated by the saddle point method, adapted to our problem. When performing the calculation, we have to keep in mind one point. Namely, even though we deal with soft modes in $\delta\eta_*(\mathbf{x})$ (with momenta $p \ll k$), the term $k\eta_*(\mathbf{x} + \mathbf{n}r)$ in ψ also gives rise to a rapidly oscillating factor, since r is large. So, we cannot neglect the second derivatives $\partial^2 \eta_*$ in the exponent ψ.

The saddle points are extrema of $\psi(\mathbf{n})$, where $\mathbf{n}$ is *a unit vector*. To find them, let us formally consider $\mathbf{n}$ as an arbitrary vector, and ψ formally as a function of this vector. Then the extremum on unit sphere is the point where $\partial\psi/\partial\mathbf{n}$ is parallel to $\mathbf{n}$, i.e.,

$$\frac{\partial\psi}{\partial\mathbf{n}} = \lambda kr\mathbf{n} \tag{97}$$

with yet to be determined λ (the factor kr on the right hand side is introduced for further convenience; in fact, λkr is nothing but the Lagrange multiplier). We use Eq. (93) to find, to the first order in v,

$$\frac{\partial r}{\partial\mathbf{n}} = \mathbf{v}r$$

and, therefore,

$$\frac{\partial\psi}{\partial\mathbf{n}} = [\mathbf{k} + (\mathbf{kn} + k)\mathbf{v}]\, r \ . \tag{98}$$

We see that there are two saddle points, one near the unit vector $\hat{\mathbf{k}} = \mathbf{k}/k$ directed along the momentum, and another near $(-\hat{\mathbf{k}})$. These saddle points correspond to waves moving from the Cauchy hypersurface in directions opposite to $\mathbf{k}$ and along $\mathbf{k}$, respectively, in accord with the discussion in Section 4.3.3.

The contributions of the two saddle points to the integral (95) are calculated in Appendix D to the first order in v and ∂v. They sum up to

$$I = \frac{1}{2k}\left\{\mathrm{e}^{i\psi_+}\left[1 - \hat{\mathbf{k}}\mathbf{v}^{(+\hat{\mathbf{k}})} + r(\delta_{ij} - \hat{k}_i\hat{k}_j)\partial_i v_j^{(+\hat{\mathbf{k}})}\right] + \mathrm{e}^{i\psi_-}\left(1 - \hat{\mathbf{k}}\mathbf{v}^{(-\hat{\mathbf{k}})}\right)\right\} \ , \tag{99}$$

where

$$\psi_+ = \psi_+(\mathbf{x}, \hat{\mathbf{k}}) = k\eta_1 - 2k\eta_*(\mathbf{x} + \hat{\mathbf{k}}r) \ ,$$
$$\psi_- = -k\eta_1 \ ,$$

and superscripts $(+\hat{\mathbf{k}})$ and $(-\hat{\mathbf{k}})$ indicate that the corresponding quantities are to be evaluated at

$$\mathbf{y}^{(+)} = \mathbf{x} + \hat{\mathbf{k}}r \tag{100a}$$

and

$$\mathbf{y}^{(-)} = \mathbf{x} - \hat{\mathbf{k}}r \ , \tag{100b}$$

respectively. The terms in (99) marked by $+$ and $-$ come from the saddle points $\mathbf{n} \approx \hat{\mathbf{k}}$ and $\mathbf{n} \approx -\hat{\mathbf{k}}$, respectively; they are analogs of the two terms in (89) (the factor $(k + \mathbf{kv})^{-1} = k^{-1}(1 - \hat{\mathbf{k}}\mathbf{v})$ in the integrand in (64) was ignored in Section 4.3.3). Note that there is no symmetry between the two contributions; technically, this is because the dependence on $\delta\eta_*$ is absent in the phase (96) for $\mathbf{n} = -\hat{\mathbf{k}}$, but present for $\mathbf{n} = \hat{\mathbf{k}}$. Note also that the saddle point value ψ_+ depends on $\mathbf{x}$ already to the linear order in h, while the second saddle point

value ψ_- does not. This is precisely what we observed in Section 4.3.3: the momentum of perturbation corresponding to the first contribution in (99) is $\mathbf{k}+\partial\psi_+/\partial\mathbf{x} = \mathbf{k}+2k\mathbf{v}$, like in the first term in (89). Note finally that since we consider the case $kr \gg 1$, it is legitimate to neglect the correction of order $\partial^2\eta_*/k = \partial v/k$, indicated in (64), while keeping the correction of order $r\partial v$ in (99).

One more remark is in order. Our notation $\mathbf{v}^{(\pm\hat{\mathbf{k}})}$ suggests that these quantities are functions of the direction of momentum only, i.e., that they are independent of the length of the vector $\mathbf{k}$. This is true, but within our approximation only. The reason is that the horizon exit time η_1 is different for different k, so the arguments $\mathbf{y}^{(\pm)}$ of $\mathbf{v}^{(\pm\hat{\mathbf{k}})}$ depend on k through $r = \eta_1 - \eta_*$. This is irrelevant for us, since $|\eta_1(k) - \eta_1(k')|$ is at most of order $1/k$ or $1/k'$ (in fact, it is even smaller), so the effect we discuss is of order $\partial v/k$. Also, one may worry that the phases $\psi_\pm$ depend on k through η_1. This is irrelevant as well, for the following reason. When calculating the correlation functions of the field $\delta\theta$, one neglects the interference between the contributions due to the first and second saddle points, since the interference term oscillates in k as e^{2ikr} and is negligible when integrated with any smooth function of $\mathbf{k}$. Then the factor, say, $\mathrm{e}^{ik\eta_1}$ is merely a phase factor that can be absorbed into the redefinition of $A_\mathbf{k}$. In other words, $\mathbf{x}$-independent phases cancel out in the correlation functions of $\delta\theta$, so the dependence on k through η_1 does not appear. These observations apply to all calculations in this paper, so we neglect the dependence of η_1 on k in what follows.

We conclude this Section by the discussion of the range of validity of our saddle point calculation. It follows from (96) that the relevant region of angular integration in (95) near each of the saddle points is $\Delta\vartheta \sim (kr)^{-1/2}$. The saddle-point calculation makes sense if $\eta_*(\mathbf{x}+\mathbf{n}r)$ does not change dramatically at this angular scale. Hence, by the saddle point method we can only treat the interaction of the phase perturbations with the modes of $\delta\eta_*$ whose momentum p obeys $pr\Delta\vartheta \lesssim 1$, i.e.,

$$p \lesssim \sqrt{\frac{k}{r}}\,. \tag{101}$$

The momenta p relevant for the statistical anisotropy do obey this inequality, see Section 4.4, while the requirement (101) restricts the angular scales at which we can reliably study non-Gaussianity. The latter point is further discussed in the end of Section 4.5.

4.4 Statistical anisotropy

We see from Eqs. (94) and (99) that the resulting phase perturbation $\theta(\mathbf{x},\eta_1)$ is a combination of two random fields, one associated with operators $A_\mathbf{k}$ and $A^\dagger_\mathbf{k}$ and another being $\delta\eta_*(\mathbf{x})$. Let us discuss the two-point product $\theta(\mathbf{x})\theta(\mathbf{x}')$ averaged over the realizations of $A_\mathbf{k}$ and $A^\dagger_\mathbf{k}$ for *one realization* of $\delta\eta_*$, still to the linear order in h (in this Section we consider solely the

resulting perturbations $\theta(\mathbf{x}, \eta_1)$ and omit the argument η_1 in the notation). As discussed in the end of Section 4.3.4, we neglect interference between terms with $\mathrm{e}^{i\psi_+}$ and $\mathrm{e}^{i\psi_-}$. Then the two-point function reads

$$\langle\theta(\mathbf{x})\theta(\mathbf{x}')\rangle = \frac{h^2}{16\pi^3}\left\{\frac{1}{4}\int \frac{d^3k}{k^3}\mathrm{e}^{i(\mathbf{k}+2k\mathbf{v}^{(+\hat{\mathbf{k}})})(\mathbf{x}-\mathbf{x}')}\cdot\left[1-2\hat{\mathbf{k}}\mathbf{v}^{(+\hat{\mathbf{k}})}+2r(\delta_{ij}-\hat{k}_i\hat{k}_j)\partial_i v_j^{(+\hat{\mathbf{k}})}\right]\right.$$
$$\left.+\frac{1}{4}\int \frac{d^3k}{k^3}\mathrm{e}^{i\mathbf{k}(\mathbf{x}-\mathbf{x}')}\cdot\left(1-2\hat{\mathbf{k}}\mathbf{v}^{(-\hat{\mathbf{k}})}\right)\right\}\ , \tag{102}$$

where we made use of the fact that, to the first order in v,

$$\psi_+(\mathbf{x},\hat{\mathbf{k}})-\psi_+(\mathbf{x}',\hat{\mathbf{k}}) = 2k\mathbf{v}^{(+\hat{\mathbf{k}})}(\mathbf{x}-\mathbf{x}')\ .$$

Since we consider the long-ranged component of the field $\mathbf{v}$, i.e., $p \ll k$, we neglect the terms of order $|\mathbf{x}-\mathbf{x}'|\cdot\partial v$. In particular, we do not distinguish between $\mathbf{v}(\mathbf{x}'+\hat{\mathbf{k}}r)$ and $\mathbf{v}(\mathbf{x}+\hat{\mathbf{k}}r)$ in the right hand side of (102).

We now see explicitly that the actual momentum corresponding to the first term in (102) equals $\mathbf{k}+2k\mathbf{v}$, whereas the momentum in the second integrand equals $\mathbf{k}$. To obtain the standard form of the Fourier expansion, we change the variable to $\tilde{\mathbf{k}} = \mathbf{k}+2k\mathbf{v}$ in the first integral. To the first orger in h, the Jacobian of this change of variables is

$$\left(\det\frac{\partial\tilde{k}_i}{\partial k_j}\right)^{-1} = 1-2\hat{\mathbf{k}}\mathbf{v}^{(+\hat{\mathbf{k}})}-2k\frac{\partial v_i^{(+\hat{\mathbf{k}})}}{\partial k_i} = 1-2\hat{\mathbf{k}}\mathbf{v}^{(+\hat{\mathbf{k}})}-2\partial_j v_i^{(+\hat{\mathbf{k}})}\cdot r(\delta_{ij}-\hat{k}_i\hat{k}_j)\ ,$$

where we recalled that $\mathbf{v}^{(+\hat{\mathbf{k}})} = \mathbf{v}(\mathbf{x}+\hat{\mathbf{k}}r)$. It is worth noting that the last term here cancels out the last term in square brackets in (102). So, omitting tilde over $\tilde{\mathbf{k}}$, we obtain that for given realization of $\mathbf{v}(\mathbf{x})$, the power spectrum, with the correction of the first order in h, has the following form:

$$\mathcal{P}_\theta(\mathbf{k}) = \mathcal{P}_0\left[1+\hat{k}_i\left(v_i^{(+\hat{\mathbf{k}})}-v_i^{(-\hat{\mathbf{k}})}\right)\right] \equiv \mathcal{P}_0\left[1+Q(\hat{\mathbf{k}})\right]\ , \tag{103}$$

where

$$\mathcal{P}_0 = \frac{h^2}{8\pi^2}$$

is the power spectrum to the leading order in h (it is twice smaller than the power spectrum at conformal rolling stage after freeze-out of the phase perturbations; this is because the contributions of the two saddle points do not sum up coherently at $\eta = \eta_1$). Note that the non-trivial term in (103) depends on the *direction* of momentum $\mathbf{k}$. Note also that the power spectrum (103) is symmetric under $\mathbf{k}\to-\mathbf{k}$, so the two-point function (102) is invariant under $\mathbf{x}\leftrightarrow\mathbf{x}'$, as it should. Low angular harmonics of $\mathbf{v}^{(\pm\hat{\mathbf{k}})}$, viewed as a function on unit sphere in momentum space, take certain values in our patch of the Universe. Hence, they

induce statistical anisotropy; in particular, the lowest multipole of the expression in the right hand side of (103) (quadrupole) gives rise to the power spectrum of the form (79), (80).

In more detail, the right hand side of (103) contains all even multipoles,

$$Q(\hat{\mathbf{k}}) = \sum_{LM} q_{LM} Y_{LM}(\hat{\mathbf{k}}) \ , \tag{104}$$

where Y_{LM} are spherical harmonics. Making use of the definition $\mathbf{v}^{(\pm\hat{\mathbf{k}})} = \mathbf{v}(\mathbf{y}^{(\pm)})$, where $\mathbf{y}^{(\pm)}$ are given in (100), we find for $L \neq 0$ that the multipole coefficients are given by

$$q_{LM} = -i \int d^3p \delta\eta_*(\mathbf{p}) \int d\Omega_{\hat{\mathbf{k}}} Y^*_{LM}(\hat{\mathbf{k}}) \cdot \mathbf{p}\hat{\mathbf{k}} \left(e^{ir\mathbf{p}\hat{\mathbf{k}}} - e^{-ir\mathbf{p}\hat{\mathbf{k}}} \right) \ , \tag{105}$$

where we omitted an irrelevant $\hat{\mathbf{k}}$-independent phase. It is worth noting that for low multipoles, the relevant range of integration over $\mathbf{p}$ is roughly $p \sim r^{-1}$: at larger p the integrand rapidly oscillates, while at smaller p the expression in the inner integrand in (105) decays as p^2 while according to (57) the amplitude of $\delta\eta_*(\mathbf{p})$ behaves as $\sqrt{\mathcal{P}_{\delta\eta_*}} \propto p^{-1}$. At large L, the relevant momenta are of order $p \sim Lr^{-1}$. Thus, our approximation $p \ll (k/r)^{1/2}$ is justified at least for low multipoles.

The calculation of the variance of q_{LM} is performed in much the same way as the calculation of the CMB anisotropy multipoles. This is done in Appendix E with the result

$$\langle q_{LM} q^*_{L'M'} \rangle = \frac{3h^2}{\pi} \frac{1}{(L-1)(L+2)} \delta_{LL'} \delta_{MM'} \ , \qquad \text{even} \quad L \neq 0 \ . \tag{106}$$

Note that we use different normalization here and in (80). To establish the correspondence, we calculate the angular integral of the variance of the quadrupole term in (80):

$$\int d\Omega_{\hat{\mathbf{k}}} \langle \left[\mathcal{Q} \cdot w_{ij} \left(\hat{k}_i \hat{k}_j - \frac{1}{3}\delta_{ij} \right) \right]^2 \rangle = \frac{8\pi}{15} \langle \mathcal{Q}^2 \rangle \ ,$$

while the same integral of the quadrupole term in (104) is given by

$$\int d\Omega_{\hat{\mathbf{k}}} \langle \mid \sum_{M=-2}^{2} q_{2M} Y_{2M}(\hat{\mathbf{k}}) |^2 \rangle = \sum_{M=-2}^{2} \langle |q_{2M}|^2 \rangle \ .$$

Hence the extra factor $75/8\pi$ in (81) as compared to (106).

4.5 Non-Gaussianity

The statistical anisotropy is an appropriate notion for describing the effect due to the variation of $\mathbf{v}^{(\pm\hat{\mathbf{k}})}$ over *large* angular scales in momentum space. On the other hand, the effect of fluctuations of $\mathbf{v}^{(\pm\hat{\mathbf{k}})}$ at *small* angular scales is naturally interpreted, we believe, in terms of

non-Gaussianity. Indeed, in the latter case it makes sense to treat $\mathbf{v}^{(\pm\hat{\mathbf{k}})}$ as genuine random field and perform averaging over its realizations, having in mind multiplicity of patches in the $\hat{\mathbf{k}}$-sphere.

It is worth noting that even though we are going to consider $\mathbf{v}^{(\pm\hat{\mathbf{k}})}$ at small angular scales $\Delta\vartheta$ in momentum space, the relevant momenta $\mathbf{p}$ of the field $\delta\eta_*$ are still small, $p \sim (r\Delta\vartheta)^{-1}$. So, our approximation $p \ll (k/r)^{1/2}$ is still valid, provided that $\Delta\vartheta$ is not very small, see the discussion in the end of this Section.

Let us consider higher order correlation functions of $\theta(\mathbf{x})$ (we again omit the argument η_1 in this Section). Since this field has the general structure (94), where I does not contain the operators $A_{\mathbf{k}}$, $A^\dagger_{\mathbf{k}}$, the three-point function vanishes identically. For calculating the non-Gaussian part of the four-point function, the expression (99), valid to the first order in v, is sufficient. Proceeding in the same way as in the beginning of Section 4.4, we obtain

$$\langle\theta(\mathbf{k})\theta(\tilde{\mathbf{k}})\theta(\mathbf{k}')\theta(\tilde{\mathbf{k}}')\rangle = \frac{1}{4\pi k^3}\frac{1}{4\pi k'^3}\mathcal{P}_0^2\,\delta(\mathbf{k}+\tilde{\mathbf{k}})\delta(\mathbf{k}'+\tilde{\mathbf{k}}') \times\Big[1+G_{NG}(\hat{\mathbf{k}},\hat{\mathbf{k}}')+G_{NG}(-\hat{\mathbf{k}},\hat{\mathbf{k}}')+G_{NG}(\hat{\mathbf{k}},-\hat{\mathbf{k}}')+G_{NG}(-\hat{\mathbf{k}},-\hat{\mathbf{k}}')\Big] + (\mathbf{k}\leftrightarrow\mathbf{k}')+(\tilde{\mathbf{k}}\leftrightarrow\mathbf{k}')\,, \qquad (107)$$

where the non-Gaussianity is encoded in

$$G_{NG}(\hat{\mathbf{k}},\hat{\mathbf{k}}') = \langle\hat{k}_i\left(v_i^{(+\hat{\mathbf{k}})}-v_i^{(-\hat{\mathbf{k}})}\right)\cdot\hat{k}'_l\left(v_l^{(+\hat{\mathbf{k}}')}-v_l^{(-\hat{\mathbf{k}}')}\right)\rangle\,. \qquad (108)$$

Fluctuations of $\mathbf{v}^{(\pm\hat{\mathbf{k}})}$ at small angular scales in momentum space show up when $\mathbf{k}$ and $\mathbf{k}'$ are either nearly parallel, or nearly antiparallel, the latter case being related to the former by the interchange $\mathbf{k}\leftrightarrow\tilde{\mathbf{k}}$. So, it suffices to consider nearly parallel $\mathbf{k}$ and $\mathbf{k}'$, i.e.,

$$|\hat{\mathbf{k}}-\hat{\mathbf{k}}'|\ll 1\,.$$

Since the power spectrum of the random field $\mathbf{v}(\mathbf{x})$ is flat, the leading term is logarithmic in $|\hat{\mathbf{k}}-\hat{\mathbf{k}}'|$.

The expression in (108) involves the combination

$$\mathbf{v}^{(+\hat{\mathbf{k}})}-\mathbf{v}^{(-\hat{\mathbf{k}})} = \mathbf{v}(\mathbf{x}+\hat{\mathbf{k}}r)-\mathbf{v}(\mathbf{x}-\hat{\mathbf{k}}r)\,.$$

Therefore, the integral over momenta of the field $\mathbf{v}$ is cut off in the infrared at $p\sim r^{-1}$. We cannot quantitatively treat the modes of these momenta anyway, since they are plagued by cosmic variance. So, we consider modes with $p > r^{-1}$, recall the expression (57) for the power spectrum of $\delta\eta_*$ and write

$$G_{NG} = 2\langle\hat{k}_i v_i^{(+\hat{\mathbf{k}})}\cdot\hat{k}'_j v_j^{(+\hat{\mathbf{k}}')}\rangle_{p\gtrsim r^{-1}} = 2\cdot\frac{9h^2}{8\pi^2}\int_{p\gtrsim r^{-1}}\frac{d^3p}{4\pi p^5}\hat{k}_i\hat{k}'_j p_i p_j\;\mathrm{e}^{i\mathbf{p}(\hat{\mathbf{k}}-\hat{\mathbf{k}}')r}\,.$$

The angular integral here is straightforwardly evaluated. We make use of the fact that $\hat{\mathbf{k}}(\hat{\mathbf{k}}-\hat{\mathbf{k}}') = O((\hat{\mathbf{k}}-\hat{\mathbf{k}}')^2)$ and obtain

$$G_{NG} = -\frac{9h^2}{4\pi^2}\int_{x\gtrsim|\hat{\mathbf{k}}-\hat{\mathbf{k}}'|}\frac{dx}{x^2}\left(\frac{\sin x}{x}\right)' ,$$

where $x = rp|\hat{\mathbf{k}}-\hat{\mathbf{k}}'|$. This is a logarithmic integral, and in the leading logarithmic approximation we immediately get

$$G_{NG} = \frac{3h^2}{4\pi^2}\log\frac{\text{const}}{|\hat{\mathbf{k}}-\hat{\mathbf{k}}'|} .$$

The constant here is of order 1; it cannot be reliably calculated, since the contribution of the region $p \sim r^{-1}$ is undetermined because of the cosmic variance. Finally, we notice that the right hand side of (108) is symmetric under $\mathbf{k} \to -\mathbf{k}$, so the four terms in (107) give equal contributions. Thus, the four-point function at $|\hat{\mathbf{k}}-\hat{\mathbf{k}}'| \ll 1$ is

$$\langle\theta(\mathbf{k})\theta(\tilde{\mathbf{k}})\theta(\mathbf{k}')\theta(\tilde{\mathbf{k}}')\rangle = \frac{1}{4\pi k^3}\frac{1}{4\pi k'^3}\mathcal{P}_0^2\,\delta(\mathbf{k}+\tilde{\mathbf{k}})\delta(\mathbf{k}'+\tilde{\mathbf{k}}')\cdot\left[1+F_{NG}(\hat{\mathbf{k}}-\hat{\mathbf{k}}')\right] + (\mathbf{k}\leftrightarrow\mathbf{k}') + (\tilde{\mathbf{k}}\leftrightarrow\mathbf{k}') ,$$

where

$$F_{NG}(\hat{\mathbf{k}}-\hat{\mathbf{k}}') = \frac{3h^2}{\pi^2}\log\frac{\text{const}}{|\hat{\mathbf{k}}-\hat{\mathbf{k}}'|} . \tag{109}$$

Note that our analysis is valid provided that we can treat the range $x \equiv rp|\hat{\mathbf{k}}-\hat{\mathbf{k}}'| \sim 1$ within our approximation $p \ll (k/r)^{-1/2}$, see (101). So, the logarithmic behaviour (109) persists until $|\hat{\mathbf{k}}-\hat{\mathbf{k}}'| \gtrsim (kr)^{-1/2}$. At even smaller angles between $\hat{\mathbf{k}}$ and $\hat{\mathbf{k}}'$, the function $F_{NG}(\hat{\mathbf{k}}-\hat{\mathbf{k}}')$ most likely flattens out. The logarithmic behaviour is definitely absent for $|\hat{\mathbf{k}}-\hat{\mathbf{k}}'| \lesssim (kr)^{-1}$, since momenta p higher than k do not contribute to the effect. These observations suggest that the value of r is potentially measurable.

We conclude by writing the expression for the trispectrum of the primordial scalar perturbations predicted by the scenario with the intermediate stage,

$$\mathcal{T}_\zeta(\mathbf{k},\tilde{\mathbf{k}},\mathbf{k}',\tilde{\mathbf{k}}' \propto \frac{h^2}{\mathcal{P}_\zeta}\left[\delta(\mathbf{k}+\tilde{\mathbf{k}})\tilde{k}^3\tilde{k}^3\log\frac{\text{const}}{|\hat{\mathbf{k}}-\hat{\mathbf{k}}'|} + (\mathbf{k}\leftrightarrow\mathbf{k}') + (\tilde{\mathbf{k}}\leftrightarrow\mathbf{k}')\right] , \tag{110}$$

up to the irrelevant phase factor. The direct comparison of our trispectrum with the local one seems to be ubiquitos because of the delta-functions standing here. Hopefully, the things become more clear, once we study their imprint on the CMB temperature coefficients. We leave the further investigation of this trispectum for the future (more precisely, until the advent of the PLANCK data).

4.6 Scalar tilt

Once the interactions of the phase field with the radial one are not neglected, the power spectrum of the phase perturbations obtains a small tilt. The reason is that for larger k, there are more modes of $\delta\eta_*$ with $p < k$ which affect the properties of the phase perturbations. We will see that the effect is logarithmic because of the flat spectrum of $\mathbf{v}$.

To this end, let us come back to the two-point correlation function $\langle\theta(\mathbf{x})\theta(\mathbf{x}')\rangle$. Even though the integral (92) is again saturated near $\mathbf{n} = \pm\hat{\mathbf{k}}$, the saddle point calculation like that performed in Section 4.3.4 is no longer appropriate, since we are going to consider all modes of $\delta\eta_*$ of momenta $p \ll k$ and not necessarily very large wavelength modes obeying (101). The problem is not notoriously difficult, nevertheless, since we are interested in logarithmically enhanced effect. Imagine that one calculates $\langle\theta(\mathbf{x})\theta(\mathbf{x}')\rangle$ by expanding in $\delta\eta_*$ the complete expression (92), with θ in the integrand given by (65). In principle, large logarithms could come from the expectation values $\langle\delta\eta_* \cdot \partial_i\partial_j\delta\eta_*\rangle$ and $\langle v_i \cdot v_j\rangle$. We reiterate, however, that the overall time shift is irrelevant for our problem, so the terms of the former type do not appear explicitly (for the same reason, there are no terms involving correlation functions of $\delta\eta_*$ with itself and with $\mathbf{v}$, which would yield power law corrections). Thus, it is legitimate to ignore the correction of order $\partial_i\partial_j\delta\eta_*$ in (65). Moreover, we can formally consider the velocity $\mathbf{v}$ in (65) as a constant which is independent of spatial coordinates. So, we effectively deal with the Lorentz-boosted hypersurface $\eta_* = \eta_*(\mathbf{y}_\pm) - \mathbf{v}(\mathbf{y} - \mathbf{y}_\pm)$, where $\mathbf{y}_\pm = \mathbf{x} \pm \hat{\mathbf{k}}r$. The qualification here is that the velocity is to be evaluated at $\mathbf{y} = \mathbf{y}_\pm$, and that $\mathbf{v}(\mathbf{y}_\pm)$ is a non-linear function of $\delta\eta_*$, since, according to (93), $\mathbf{y}_\pm$ depend on $\delta\eta_*$ through r. Another qualification is that when calculating the power spectrum $\mathcal{P}_\theta$ at momentum k, we have to impose a restriction $p < k$ on the momentum p of modes of the field $\delta\eta_*$.

Since we treat the velocity $\mathbf{v}$ as constant in space, we can obtain the solution to the Cauchy problem explicitly, in a way similar to that of Section 4.3.3. However, we need the solution to the second order in v. The initial condition for the Minkowskian evolution is thus given by (65). Let us define the Lorentz-boosted coordinates $\mathbf{z}$ and τ:

$$z_{||} = \gamma(x_{||} + v\eta) \ , \qquad \mathbf{z}_T = \mathbf{x}_T \ , \qquad \tau = \gamma(\eta + vx_{||}) \ ,$$

where $||$ and T refer to components parallel and normal to velocity. Then the initial data are specified at the hypersurface $\tau = \tau_\pm = \text{const}$, and $\partial_\tau\theta = 0$ at this hypersurface. We re-express $\mathbf{x}$ and η in terms of $\mathbf{z}$ and τ and insert them into (65). Omitting the overall phase factor independent of $\mathbf{z}$ that cancels out in the two-point function, we write the initial conditions as

$$\theta(\mathbf{z}, \tau_\pm) \propto \int \frac{1}{\gamma(k + \mathbf{kv})} \mathrm{e}^{i\mathbf{qz}} A_{\mathbf{k}} \frac{d^3k}{\sqrt{2k}} + h.c. \ , \qquad \partial_\tau\theta = 0 \ , \tag{111}$$

where

$$q_{||} = \gamma(k_{||} + kv) \ , \qquad \mathbf{q}_T = \mathbf{k}_T \ .$$

The solution to the massless field equation in Minkowski space with this initial condition is

$$\theta \propto \int \frac{1}{\gamma(k+\mathbf{kv})} \mathrm{e}^{i\mathbf{qz}} \cos\left[q(\tau-\tau_{\pm})\right] A_{\mathbf{k}} \frac{d^3k}{\sqrt{2k}} + h.c. \,, \tag{112}$$

where $q = \gamma(k + k_{||}v)$. This solution again describes two waves propagating in opposite directions, which do not interfere at $\eta = \eta_1$. Let us consider the two waves separately.

At time η_1, we have for the first wave, moving in direction opposite to $\mathbf{k}$,

$$\mathrm{e}^{i\mathbf{qz}+iq\tau} = \mathrm{e}^{i\gamma^2(k_{||}+2kv+k_{||}v^2)x_{||}+i\mathbf{k}_T\mathbf{x}_T+i\varphi} \,, \tag{113}$$

where φ is a phase, irrelevant for the two-point function of $\delta\theta$. So, the actual momentum is

$$\tilde{k}_{||} = \gamma^2(k_{||} + 2kv + k_{||}v^2) \,, \qquad \tilde{\mathbf{k}}_T = \mathbf{k}_T \,.$$

Note that to order v^2 we have $\tilde{k}_{||} = \gamma_{2v}(k_{||} + 2kv)$, where $\gamma_{2v} = (1-4v^2)^{-1/2}$ is the Lorentz-factor for velocity $2v$. Hence, $\tilde{\mathbf{k}}$ again differs from momentum $\mathbf{k}$ by the Lorentz-boost with velocity $2\mathbf{v}$. We recall that $A_{\mathbf{k}}d^3k/\sqrt{2k}$ is Lorentz-invariant, and obtain for the contribution of the first wave at point $\mathbf{x}$ (again omitting the phase factor, irrelevant for the two-point function)

$$\theta(\mathbf{x}) \propto \int \frac{1}{\gamma(k+\mathbf{kv})} \mathrm{e}^{i\tilde{\mathbf{k}}\mathbf{x}} A_{\tilde{\mathbf{k}}} \frac{d^3\tilde{k}}{\sqrt{2\tilde{k}}} + h.c. \,,$$

where $k_{||} = \gamma_{2v}(\tilde{k}_{||} - 2\tilde{k}v)$, $k = \gamma_{2v}(\tilde{k} - 2\tilde{k}_{||}v)$. Expanding in $\mathbf{v}$ to the second order, we obtain the following form of the first contribution to the power spectrum

$$\mathcal{P}_\theta(\tilde{k}) \propto 1 + 2\left(\frac{\tilde{k}_i}{\tilde{k}}\langle v_i\rangle + \frac{\tilde{k}_i\tilde{k}_j}{\tilde{k}^2}\langle v_iv_j\rangle - \frac{1}{2}\langle v^2\rangle\right) + \frac{\tilde{k}_i\tilde{k}_j}{\tilde{k}^2}\langle v_iv_j\rangle \,.$$

Here the term in parentheses comes from $\langle\theta^{(0)}\theta^{(1)}\rangle$, where $\theta^{(0)}$ is the zeroth order phase perturbation and $\theta^{(1)}$ the correction (that includes linear and quadratic terms in $\mathbf{v}$), while the last term in the right hand side is due to the correlator $\langle\theta^{(1)}\theta^{(1)}\rangle$. We see that the explicitly quadratic terms cancel out and find (at this point we can set $\tilde{\mathbf{k}} = \mathbf{k}$)

$$\mathcal{P}_\theta \propto 1 + 2\hat{k}_i\langle v_i\rangle \,.$$

We now recall that the velocity is to be evaluated at the point $\mathbf{y}_+ = \mathbf{x} + \hat{\mathbf{k}}r$, where $r = \eta_1 - \eta_* - \delta\eta_*(\mathbf{x} + \hat{\mathbf{k}}r)$, so that

$$v_i(\mathbf{y}_+) = v_i[\mathbf{x} + \hat{\mathbf{k}}(\eta_1 - \eta_*)] - \partial_j v_i \cdot \hat{k}_j\delta\eta_* \,.$$

The expectation value of the first term on the right hand side vanishes, while the second term gives

$$\langle v_i(\mathbf{y}_+)\rangle = -\hat{k}_j \int \frac{d^3p}{4\pi p^3} p_ip_j\mathcal{P}_{\delta\eta_*}(p) = -\hat{k}_i \cdot \frac{3h^2}{8\pi^2}\log(kr) \,,$$

where we recalled that the relevant range of momenta is $r^{-1} \ll p \ll k$. Thus, the contribution due to the first wave has the form

$$\mathcal{P}_\theta \propto 1 - \frac{3h^2}{4\pi^2} \log(kr) \ . \tag{114}$$

Let us now consider the second wave that moves along $\mathbf{k}$. We have at time η_1

$$\mathrm{e}^{i\mathbf{p}\mathbf{y} - ip\tau} = \mathrm{e}^{i\mathbf{k}\mathbf{x} + i\varphi} \ , \tag{115}$$

so the actual momentum is equal to $\mathbf{k}$. Hence, the contribution of this wave is

$$\theta(\mathbf{x}) \propto \int \frac{1}{\gamma(k + \mathbf{k}\mathbf{v})} \mathrm{e}^{i\mathbf{k}\mathbf{z}} A_{\mathbf{k}} \frac{d^3k}{\sqrt{2k}} + h.c. \ .$$

Proceeding as before, we obtain the contribution of this wave to the power spectrum,

$$\mathcal{P}_\theta \propto 1 - 2\hat{k}_i \langle v_i \rangle \ ,$$

where the velocity is to be evaluated at the point $\mathbf{y}_- = \mathbf{x} - \hat{\mathbf{k}} r$ with $r = \eta_1 - \eta_*^{(0)} - \delta\eta_*(\mathbf{x} - \hat{\mathbf{k}} r)$. The resulting contribution again has the form (114), so we conclude that the shape of the entire power spectrum is given by (114).

The result (114) shows that the power spectrum of $\delta\theta$, and hence of the adiabatic perturbations, is tilted. If this is the only reason for the tilt, the scalar spectral index in our model is equal to $n_s = 1 - \frac{3h^2}{4\pi^2}$. As pointed out in Section 1, however, there may be other sources for the tilt, so we cannot insist on attributing the entire scalar tilt to the effect discussed in this Section.

To end up this Section, we sketch an alternative way of calculating the correction to the power spectrum $\mathcal{P}_\theta$. One makes use of the exact formula (92) with θ in the integrand given by (65) and evaluated at $\mathbf{y} = \mathbf{x} + \mathbf{n}r$, where r obeys Eq. (93). The dependence of the integrand in (92) on the integration variable $\mathbf{n}$ is fairly non-trivial, since the vector $\mathbf{n}$ enters the argument of η_* both explicitly and through $r(\mathbf{n})$. We know, however, that the integral (92) is saturated in regions near the two points on unit sphere, $\mathbf{n} = \hat{\mathbf{k}}$ and $\mathbf{n} = -\hat{\mathbf{k}}$. Consider the first region for definiteness. The idea is to write

$$\eta_*[\mathbf{x} + \mathbf{n}r(\mathbf{n})] = \eta_*[\mathbf{x} + \hat{\mathbf{k}} r(\hat{\mathbf{k}})] + \Big\{ \delta\eta_*[\mathbf{x} + \mathbf{n}r(\mathbf{n})] - \delta\eta_*[\mathbf{x} + \hat{\mathbf{k}} r(\hat{\mathbf{k}})] \Big\} \ ,$$
$$r(\mathbf{n}) = r(\hat{\mathbf{k}}) - \Big\{ \delta\eta_*[\mathbf{x} + \mathbf{n}r(\mathbf{n})] - \delta\eta_*[\mathbf{x} + \hat{\mathbf{k}} r(\hat{\mathbf{k}})] \Big\} \ ,$$

express these functions iteratively through

$$\delta\eta_*[\mathbf{x} + \mathbf{n}r(\hat{\mathbf{k}})] - \delta\eta_*[\mathbf{x} + \hat{\mathbf{k}} r(\hat{\mathbf{k}})]$$

and systematically expand the integrand in (92) in a series in the latter quantity, up to quadratic order. Then one has to deal with angular integrals, in which the integration

variable $\mathbf{n}$ enters either in combination $e^{i\mathbf{k}\mathbf{n}r(\hat{\mathbf{k}})}$ or via $e^{i\mathbf{k}\mathbf{n}r(\hat{\mathbf{k}})}\delta\eta_*[\mathbf{x}+\mathbf{n}r(\hat{\mathbf{k}})]$ (the integral with $\delta\eta_*^2$ is trivial after ensemble averaging). The former integral is straightforwardly evaluated by the saddle point method. To evaluate the latter integral, one writes $\delta\eta_*[\mathbf{x}+\mathbf{n}r(\hat{\mathbf{k}})]$ in the Fourier representation and arrives at the angular integral with $e^{i(\mathbf{k}+\mathbf{p})\mathbf{n}r(\hat{\mathbf{k}})}$, where $\mathbf{p}$ is still the momentum of a mode of $\delta\eta_*$. The latter integral is again evaluated by the saddle point method; the rest of the calculation is straightforward. We have performed the calculation of the power spectrum in this way; it is tedious, but does yield the result (114).

At this point we finish our discussion of the sub-scenrio B. Signatures of the latter combined with ones of the sub-scenario A, complete the full set of predictions in the model with conformal rolling. Shortly, we will see that these predictions are in fact generic ones and calculations of last two Chapters serve as the ansatz in a much broader class of models, like those of the (pseudo)-Conformal Universe [26].

5 Models of (pseudo)-Conformal Universe

5.1 Assumptions

By far, we studied the properties of the primordial scalar perturbations using the particular example of the conformal rolling scenario. Thus, one may think that the flatness of their spectrum is due to the particular choice of the model rather than due to the conformal symmetry inherent in it. In this Chapter, we will show following [26] that this is not so. In particular, we will see that there is in fact a broad range of models obeying a few assumptions, under which the spectrum of relevant perturbations is promised to be flat. Let us try to guess these assumptions. For this purpose, we turn back to the discussion of the conformal rolling scenario [18] in the beginning of the Chapter 3. There we considered the action for the complex massless field ϕ conformally coupled to gravity. After the appropriate field redefinition, namely $\chi = a\phi$, we were led to the Minkowskian evolution for χ. As it follows, the conformal coupling to gravity is irrelevant if the background evolution of the Universe is described by the nearly Minkowski metric at rather early times. Shortly it will turn to be one of the conditions ensuring the flat spectrum of the relevant perturbations.

In the conformal rolling scenartio, the self-interaction is described by the negative quartic potential, $V(\chi) = -h^2|\chi|^4$. Under this assumption, the radius of the field χ acquired the time-dependent profile, real without loss of generality, since the $U(1)$-symmetry of the model,

$$\chi_c \sim -\frac{1}{\eta} \, . \tag{116}$$

Here we omit the constant of the integration $\eta_\star$, which has meaning of the end-of-roll time in the conformal rolling scenario. This we do envisioning the dynamical picture of the Universe, where the end of roll is associated with the beginning of the hot epoch. The $U(1)$-symmetry also fixes the interaction between the phase θ of the field χ and its radius χ_c,

$$\mathcal{L}_{int} = \frac{1}{2}\chi_c^2(\partial_\mu\theta)^2 \, , \tag{117}$$

so that the phase perturbations evolving on the classical background (116) acquire the flat spectrum. Obviously, the self-interaction in the form of the negative quartic potential is not important as it is. Important is the background solution with the profile given by (116). The latter may appear as the solution from the Lagrangians, which are completely different from one of the conformal rolling scenario. Let us clarify its meaning from the viewpoint of the conformal algebra in 4 dimensions. For this purpose, it is convenient to decompose the field χ and view the radius and the phase θ as two separate fields. The basis of the conformal algebra in 4 dimensions is the set of 15 generators: 4 operators P_μ corresponding to Poincare translations, 6 generators $J_{\mu\nu}$ of the space-time rotations, the dilaton operator D and 4 generators of special conformal transformations K_μ. With respect to these transformations,

the field ρ is the conformal field with the weight $\Delta = 1$. We envision the situation with more than one conformal field, namely some set $\{\phi_I\}$, and each of them has the non-trivial profile, and each has some weight Δ_I. They transform under the conformal symmetries as follows,

$$P_\mu\phi_I = -i\partial_\mu\phi_I, \quad J^{\mu\nu}\phi_I = i(x^\mu\partial^\nu - x^\nu\partial^\mu)\phi_I$$
$$D\phi_I = -i(\Delta_I + x^\mu\partial_\mu)\phi_I, \quad K_\mu\phi_I = i(-2x_\mu\Delta_I - 2x_\mu x^\nu\partial_\nu + x^2\partial_\mu)\phi_I \ .$$

It is well-known, that the conformal group can be viewed as the group of rotations operating on the flat space-time with two time directions. To see this explicitly, let us write the commutation relations for the generators of the conformal group,

$$[D, P_\mu] = iP_\mu, \quad [D, K_\mu] = -iK_\mu, \quad [K_\mu, P_\nu] = -2i(J_{\mu\nu} - \eta_{\mu\nu}D),$$
$$[K_\lambda, J_{\mu\nu}] = i(\eta_{\lambda\mu}K_\nu - \eta_{\lambda\nu}K_\rho), \quad [P_\sigma, J_{\mu\nu}] = i(\eta_{\sigma\mu}P_\nu - \eta_{\sigma\nu}P_\mu) \ ,$$
$$[J_{\mu\nu}, J_{\rho\sigma}] = i(\eta_{\mu\sigma}J_{\nu\rho} - \eta_{\nu\sigma}J_{\mu\rho} + \eta_{\nu\rho}J_{\mu\sigma} - \eta_{\mu\rho}J_{\nu\sigma}) \ .$$

By redefining $\delta_{J_{-2,-1}} = \delta_D$, $\delta_{J_{-2,\mu}} = (\delta_{P_\mu} - \delta_{K_\mu})/2$ and $\delta_{J_{-1,\mu}} = (\delta_{P_\mu} + \delta_{K_\mu})/2$, we can assemble all the conformal generators into an anti-symmetric matrix $\delta_{J_{AB}}$, with A, B taking the six values $(-2, -1, \mu)$. The commutation relation then takes the form

$$[J_{AB}, J_{CD}] = i(\eta_{AC}\delta_{J_{BD}} - \eta_{BC}\delta_{J_{AD}} + \eta_{BD}\delta_{J_{AC}} - \eta_{AD}\delta_{J_{BC}}) \ ,$$

where $\eta_{AB} = \mathrm{diag}(1, -1, \eta_{\mu\nu})$ is a 6d Minkowskian metric with two time directions. These are the commutation relations of $SO(4, 2)$.

Now, we note that there are ten generators, which annihilate the time-dependent background value, namely

$$P_i, \quad D, \quad J_{ij}, \quad K_i, \quad i = 1, 2, 3 \ .$$

These ten unbroken generators can be assembled into an anti-symmetric matrix J_{ab}, with a and b taking the five values $(-2, -1, i)$, by defining $J_{-2,-1} = D, \quad J_{-2,i} = (P_i - K_i)/2$ and $J_{-1,i} = (P_i + K_i)/2$. The commutation relations then take the form

$$[J_{ab}, J_{cd}] = i(\eta_{ac}J_{bd} - \eta_{bc}J_{ad} + \eta_{bd}J_{ac} - \eta_{ad}J_{bc}),$$

where $\eta_{ab} = \mathrm{diag}(1, -1, -\delta_{ij})$ is a 5d Minkowski metric with one time direction. The remaining five generators do not annihilate χ. Thus, we deal with the symmetry breaking pattern $SO(4, 2) \to SO(4, 1)$.

The generalization to the case with more than one field with the non-trivial background is straightforward. If there is a set of fields $\{\phi_I\}$ each having the conformal weight Δ_I, then the non-trivial background for each of the fields is given by [26],

$$\bar{\phi}_I(t) = \frac{c_I}{(-t)^{\Delta_I}}$$

The power standing here is dictated by the invariance under the transformations induced by the dilaton operator D. The 5 broken generators act on the background solution as

$$\delta_{P_0}\bar{\phi}_I = \frac{i\Delta_I\bar{\phi}_I}{t}, \quad \Delta_{J_{0i}}\bar{\phi}_I = -\frac{i\Delta_I x_i}{t}\bar{\phi}_I, \quad \delta_{K_0}\bar{\phi}_I = -\frac{i\Delta_I x_\mu x^\mu}{t}\bar{\phi}\,.$$

As it follows, the zeroth weight conformal field cannot stand for the $SO(4,2) \to SO(4,1)$ symmetry breaking pattern. However, their role is of particular importance in our discussion. Indeed, the phase θ of the conformal rolling scenario is the weight-0 field, while the term (117) represents the minimal way of coupling the phase to the field ρ, so that the conformal symmetry of the model is preserved. The phase perturbations were most relevant for our discussion in the Chapter 3, since they served as the source of the primordial scalar perturbations with the flat spectrum.

Now, we are in the position to write down the assumptions, under which the scale invariance of relevant perturbations is guaranteed [26]:
a) the background evolution of the Universe is described by the Minkowski metric with a high accuracy;
b) the Universe is in the CFT state at these times, and among the field content there is a set of conformal fields $\{\phi_I\}$ with different conformal weights;
c) the conformal group $SO(4,2)$ is spontaneously broken down to the de Sitter group $SO(4,1)$ by the time-dependent background(s) of the field(s) ϕ_I;
d) there is at least one field with the zeroth conformal weight evolving on the spontaneously broken background.
If these conditions are obeyed, then the zeroth weight conformal field acquires the flat spectrum. The elegance of these conditions is that they allow to build the effective Lagrangian fixed up to some constants. We do it in the following Section (at the quadratic level). In parallel, we will give the proof of the statement made here.

The assumptions written represent the idea of the (pseudo)-Conformal Universe. In the treatment of Hinterbichler and Khoury, they imply that the matter dominating the evolution of the Universe is in the CFT state. Sure, one can relax this claim and deal with the spectator models *a la* conformal rolling scenario. In this case, only the part of the field content of the Universe is in the CFT state at very early times, while the presense of the background matter and the gravity can strongly violate the conformal symmetry. The effective Minkowski metric is then obtained by introducing the conformal coupling with the gravity. This is not necessary for the dynamical models. Indeed, as we will see in what follows, the Minkowskian evolution is the dynamical attractor in the Universe driven by the CFT state. Thus, the assumption a) is guaranteed, once the condition b) is satisfied. The Galilean Genesis [25] is the well-known example of the dynamical model, which satisfies all the conditions of the (pseudo)-Conformal Universe. Though basing on the drastically different Lagrangian, the authors of [25] resulted with the flat spectrum of the weight-0 conformal field.

5.2 Effective Lagrangian

The basic principles of constructing the Lagrangian, which respects the symmetry breaking pattern $G_1 \to G_2$, where the G_2 is some subgroup of G_1, have been established long time ago in [109]. Though this techniques is applied to the internal symmetries, it has been generalized by Volkov [110] on the case of space-time symmetries. He considered the particular case of the conformal group spontaneously broken down to the Lorentz group $SO(3,1)$, while the authors of [120] derived the effective Lagrangian respecting the symmetry breaking pattern of interest: $SO(4,2) \to SO(4,1)$. They constructed the effective Lagrangian up to the fourth derivative of the Goldstone field. For our purposes, it will be enough to consider the quadratic Lagrangian. The reason is that we interested in the leading order effects, and, in particular, in the flat spectrum of the zeroth weight fields perturbations. The quadratic Lagrangian was derived in [26]. Here we repeat the calculations made there (in a bit more details, however) and also consider the consequences for the perturbations of the fields.

The unbroken $SO(4,1)$ subalgebra acts linearly on the perturbations $\varphi_I = \phi_I - \bar{\phi}_I$,

$$
\begin{aligned}
&P_i\varphi_I = -i\partial_i\varphi_I \ , \quad J^{ij} = i(x^i\partial^j - x^j\partial^i)\varphi_I \ , \\
&D\varphi_I = -i(\Delta_I + x^\mu\partial_\mu)\varphi_I \ , \quad K_i = i(-2x_i\Delta_I - 2x_i x^\nu\partial_\nu + x^2\partial_i)\varphi_I \ ,
\end{aligned}
$$

whereas the 5 broken generators act non-linearly,

$$
\begin{aligned}
&P_0\varphi_I = \frac{\Delta_I}{t}\bar{\phi}_I - \dot{\phi}_I \ , \quad J^{0i}\varphi_I = -\frac{\Delta_I x^i}{t}\bar{\phi}_I + (t\partial_i + x^i\partial_t)\phi_I \ , \\
&K_0\varphi_I = -\frac{\Delta_I x^2}{t}\bar{\phi}_I + (2t\Delta_I + 2tx^\nu\partial_\nu + x^2\partial_t)\phi_I \ .
\end{aligned}
\tag{118}
$$

At the quadratic two derivative level, the most general lagrangian consistent with spatial rotations and translations is

$$
\mathcal{L}_{quad} = \frac{1}{2}M_1^{IJ}(t)\dot{\varphi}_I\dot{\varphi}_J - \frac{1}{2}M_2^{IJ}(t)\nabla\varphi_I\nabla\varphi_J - \frac{1}{2}M_3^{IJ}(t)\varphi_I\varphi_J \ , \tag{119}
$$

where the summation over I and J is implicit, and where $M_{\mathcal{I}}^{IJ}(t)$, $\mathcal{I} = 1,2,3$, are symmetric time-dependent matrices. First we impose the linearly realized symmetries. Since the Lagrangian (119) is manifestly invariant under spatial rotations and translations, we are left with dilatations δ_D and the spatial conformal transformations δ_{K_i}. The dilatation invariance implies that

$$
\frac{\delta\mathcal{L}^{EL}}{\delta\varphi_J}D\varphi_J = 0 \ , \tag{120}
$$

where EL means the Euler-Lagrange derivative, i.e.

$$
\frac{\delta\mathcal{L}^{EL}}{\delta\varphi_J} = -\frac{d}{dt}(M_1^{IJ}\dot{\varphi_J}) + M_2^{IJ}\nabla^2\varphi_J - M_3^{IJ}\varphi_J \ .
$$

For the time being we take for granted that the functional on the left hand side of (120) has the form

$$\frac{\delta\mathcal{L}^{EL}}{\delta\varphi_J}D\varphi_J = A^{IJ}(t,\mathbf{x})\dot{\varphi}_I\dot{\varphi}_J + B^{IJ}(t,\mathbf{x})\varphi_I\nabla^2\varphi_J + C^{IJ}(t,\mathbf{x})\varphi_I\varphi_J \ , \tag{121}$$

up to the terms appearing due to the integration by parts. We also assume that A^{IJ}, B^{IJ} and C^{IJ} are the functions of the matrices M_1^{IJ}, M_2^{IJ} and M_3^{IJ}, respectively. This will become clear from what follows. For the arbitrary function $\varphi_I(t,\mathbf{x})$, the equality (120) is satisfied provided that

$$A^{IJ}(t,\mathbf{x}) = 0 \ , \quad B^{IJ}(t,\mathbf{x}) = 0 \ , \quad C^{IJ}(t,\mathbf{x}) = 0 \ .$$

Let us focus on the second condition here, i.e. on $B^{IJ} = 0$. This condition imposes the restrictions on the elements of M_2^{IJ} and has nothing to do with the matrices M_1^{IJ} and M_3^{IJ}, so that we can omit the first and the third terms in the (119). Thus, we write

$$M_2^{IJ}\nabla^2\varphi_I(\Delta_J + x^\mu\partial_\mu)\varphi_J = 0 \ . \tag{122}$$

The first term here, i.e. one with the conformal weight Δ_J, already has the appropriate form. Thus, we need only discuss the second term. Intergrating it by parts, we obtain,

$$M_2^{IJ}\nabla^2\varphi_I x^\mu\partial_\mu\varphi_J = -\dot{M}_2^{IJ}t\nabla^2\varphi_I\varphi_J - M_2^{IJ}\partial_\mu\varphi_I\nabla^2(x^\mu\varphi_J) - 4M_2^{IJ}\nabla^2\varphi_I\varphi_J \tag{123}$$

Integrating further the second term on the right hand side by parts, one expresses it as follows

$$-M_2^{IJ}\partial_\mu\varphi_I\nabla^2(x^\mu\varphi_J) = 2M_2^{IJ}\nabla^2\varphi_I\varphi_J - M_2^{IJ}x^\mu\partial_\mu\varphi_I\nabla^2\varphi_J \ . \tag{124}$$

The second term on the right hand side here corresponds to the term on the left handside of (123) taken with the opposite sign. Thus, substituting (123) into (124), one writes

$$M_2^{IJ}x^\mu\partial_\mu\varphi_I\nabla^2\varphi_J = -\frac{1}{2}\dot{M}_2^{IJ}t\nabla^2\varphi_I\varphi_J + M_2^{IJ}\nabla^2\varphi_I\varphi_J - 2M_2^{IJ}\nabla^2\varphi_I\varphi_j \ .$$

Note also that the structure of the expression on the right hand side here and, consequently, the structure on the left hand side of (122) coincides with one conjectured in (121). This is a cross-check of the validity of our assumption made above. Combining altogether, we obtain the equation for the matrix M_2^{IJ} [26],

$$\dot{M}_2^{IJ} = \frac{2(\Delta_J - 1)}{t}M_2^{IJ} \ . \tag{125}$$

The similar manipulations lead to the equations for the matrices M_1^{IJ} and M_3^{IJ} [26],

$$\dot{M}_1^{IJ} = \frac{2(\Delta_I - 1)}{t}M_1^{IJ} \ , \quad \dot{M}_3^{IJ} = \frac{2(\Delta_I - 2)}{t}M_3^{IJ} \ . \tag{126}$$

Since these matrices are symmetric, it follows that $0 = \dot{M}^{IJ}_{\mathcal{I}} - \dot{M}^{JI}_{\mathcal{I}} = 2(\Delta_I - \Delta_J)M^{IJ}_{\mathcal{I}}/t$, and, hence, $M^{IJ}_{\mathcal{I}} = 0$ for $\Delta_I \neq \Delta_J$. In other words, fields with different conformal weights do not mix with each other. Moreover, the Eqs. (125) and (126) fix the time-dependence within each block:

$$M^{I,J}_{1,2}(t) = \tilde{M}^{IJ}_{1,2}(-t)^{2(\Delta_I - 1)} \ , \quad M^{IJ}_3(t) = \tilde{M}^{IJ}_3(-t)^{2(\Delta_I - 2)} \ .$$

Now let us impose the invariance under the special conformal transformations K_i. One can show that this symmetry does not lead to any further restrictions on the form of the matrix M^{IJ}_3. Indeed, providing the manipulations analogous to ones given above, one can show that

$$M^{IJ}_3 \varphi_I K_i \varphi_J \sim (\dot{M}^{IJ}_3 t - 2\Delta_I M^{IJ}_3 + 4M^{IJ}_3) x_i \varphi_I \varphi_J \ .$$

Therefore, it is always zero provided that the matrix M^{IJ}_3 satisfies the Eq. (126). Further one can show that

$$\frac{\delta \mathcal{L}^{EL}}{\delta \varphi_J} K_i \varphi_J = \tilde{A}^{IJ}_i \dot{\varphi}_I \dot{\varphi}_J + \tilde{B}^{IJ}_i \nabla \varphi_I \nabla \varphi_J + \tilde{F}^{IJ} \partial_i \varphi_I \partial_0 \varphi_J \ .$$

The matrices $\tilde{A}^{IJ}_i$ and $\tilde{B}^{IJ}_i$ depend on the matrices M^{IJ}_1 and M^{IJ}_2 separately, while the matrix $\tilde{F}^{IJ}$ depends on both matrices. It is straightforward to show that $\tilde{A}^{IJ}_i$ and $\tilde{B}^{IJ}_i$ vanish provided that the matrices M^{IJ}_1 and M^{IJ}_2 satisfy the Eqs. (125) and (126). The condition $\tilde{F}^{IJ} = 0$ then leads to the following restriction,

$$\tilde{M}^{IJ}_2 = \tilde{M}^{IJ}_1 \ .$$

Therefore, the most general form of the Lagrangian consistent with the linearly realized symmetries is [26]

$$\mathcal{L}_{quad} = \frac{1}{2}\tilde{M}^{IJ}_1 (-t)^{2(\Delta_I - 1)} \eta^{\mu\nu} \partial_\mu \varphi_I \partial_\nu \varphi_J - \frac{1}{2}\tilde{M}^{IJ}_3 (-t)^{2(\Delta_I - 2)} \varphi_I \varphi_J \ .$$

We now impose the 5 non-linear transformations assotiated with the broken symmetries. Let us focus on the conformal block of weight Δ. At the quadratic level, we need only impose the non-linear part of the transformations (118),

$$P_0 \varphi_I = i\Delta_I \frac{\bar{\phi}_I}{t} \ , \quad J^{0i}\varphi_I = -i\Delta_I \frac{x^i}{t}\bar{\phi}_I \ , \quad K_0 \varphi_I = -i\Delta_I \frac{x^2}{t}\bar{\phi}_I \ .$$

Invariance under P^0 yields the following condition

$$\Delta \tilde{M}^{IJ}_3 c_J = \Delta(\Delta + 1)(\Delta - 4)\tilde{M}^{IJ}_1 c_J \ , \tag{127}$$

By redefining the fields, we may diagonalize the kinetic matrix within each block, setting $\tilde{M}^{IJ}_1 = \delta_{IJ}$ and $\tilde{M}^{IJ}_3 \equiv M^{IJ}$. The condition (127) then takes the form

$$\Delta M^{IJ} c_J = \Delta(\Delta + 1)(\Delta - 4) c^I \ .$$

Finally, we write the quadratic Lagrangian for fluctuations, which respects the desired symmetry breaking pattern [26],

$$\mathcal{L}_{quad} = \sum_{blocks} \left(\frac{1}{2}(-t)^{2(\Delta-1)} \eta^{\mu\nu} \partial_\mu \varphi_I \partial_\nu \varphi_I - \frac{1}{2}(-t)^{2(\Delta-2)} M^{IJ} \varphi_I \varphi_J \right) . \tag{128}$$

Starting from this effective Lagrangian, one can prove the main statement made in the previous Section.

5.2.1 Flat spectrum of zeroth weight fields

The source of scale invariant perturbations will be conformal weight-0 fields, which we denote by θ_I. This field has a trivial background $\bar{\theta}_I = const$. The form of the quadratic action for $\Delta = 0$,

$$\mathcal{L}_{quad} = \frac{1}{2}(-t)^{-2} \eta^{\mu\nu} \partial_\mu \theta_I \partial_\nu \theta_I - \frac{1}{2} M^{IJ} (-t)^{-4} \theta_I \theta_J . \tag{129}$$

The first term in the right handside of the Lagrangian is quite the same as the phase term in the analogous Lagrangian of the conformal rolling scenario. The second term in (129). indicates that generically the weight-0 fields have mass mixing. Making the field redefinition, $\hat{\theta} = \theta/(-t)$, we obtain the equation of motion

$$\ddot{\hat{\theta}} + \left(k^2 - \frac{2 - M}{t^2} \right) \hat{\theta} = 0 ,$$

Not surprisingly that this equation is essentially the same as the equation for the perturbations of the imaginary part of the field χ discussed in the context of the conformal rolling scenario. There is, however, also the contribution due to the mass mixing characterized by the mass element M. Neglecting the latter and following the same steps as in the case of the conformal rolling scenario, we arrive at the flat power spectrum [26],

$$k^{3/2} |\theta| = \text{const} .$$

Taking into account the mass element M and keeping the latter a small quantity, $M \ll 1$, we obtain the small negative tilt. This is a novelty as compared to the conformal rolling scenario.

5.2.2 Weight $\Delta \neq 0$ modes

Take for simplicity the case, where there is one conformal field for each $\Delta \neq 0$, and that each has non-vanishing background, so that we may use the action (128) for each field. In the Fourier space, the equation of motion for perturbation φ takes the form,

$$\ddot{\varphi} + p^2 \varphi_p + \frac{2(\Delta - 1)}{t} \dot{\varphi} + \frac{(\Delta + 1)(\Delta - 4)}{t^2} \varphi = 0 .$$

With the field redefinition to the canonical variable, $\hat{\varphi} = (-t)^{\Delta-1}\varphi$, the equation reads

$$\ddot{\hat{\varphi}} + \left(p^2 - \frac{6}{t^2}\right)\hat{\varphi} = 0 \,. \tag{130}$$

This is essentially the same equation, which we had for the radial perturbations in the context of the conformal rolling scenario. Thus, following the same steps we arrive at the perturbations with the red power spectrum [26],

$$p^{3/2}|\hat{\varphi}| \sim \frac{1}{pt^2} \,.$$

Transforming back to the field φ, we obtain

$$p^{3/2}|\varphi| \sim \frac{1}{p(-t)^{\Delta+1}} \,. \tag{131}$$

Thus, all rolling fields no-vanishing profile and $\Delta \neq 0$ acquire a universal spectrum for their perturbations. As is in the case of the conformal rolling scenario, the perturbation (131) may be absorbed into the redefinition of the end-of-roll time. Though the obvious similarity, the "time delay" mode appears in the different light, if the rolling field dominates the evolution of the Universe. In this case, the gravitational effects become important. Consequently, the red perturbations become gauge-dependent, and the appropriate quanity describing the adiabatic perturbations is not the perturbation φ itself, but the gauge-invariant curvature ζ. The latter has the blue spectrum and completely irrelevant on the large scales [26, 25]. We discuss these issues in the following Section.

5.3 Turning on gravity: Hinterbichler–Khoury model

5.3.1 Background evolution

So far we discussed the field perturbations neglecting the gravitational degrees of freedom. Strictly speaking, this approximation is valid provided that the conformal fields $\{\phi_I\}$ are spectators during the evolution of the Universe at very early times. Let us assume the other opportunity. Namely, let one of the fields from the set $\{\phi_I\}$ or one of them drive the evolution of the Universe at very early times. Once this is said, one cannot neglect the effects associated with gravitational degrees of freedom anymore. Naively, one expects that the picture given in the previous Section is going to be roughly spoiled with turning on the gravity. In fact, this is not true. Following [25, 26, 111], we will show that in dynamical models of the Conformal Universe the gravitational effects are highly suppressed. This suppression holds on the classical level as well as at the level of perturbations. In particular, we will see that the Minkowski background netric is the dynamical attractor of the Universe passing through the CFT state. So, one should not include the conformal coupling of the

CFT fields to gravity as in the case of the conformal rolling scenario. Second, the predictions of the statistical anisotropy obtained in the spectator model hold for a quite generic class of dynamical models.

Let us first concentrate on the classical evolution. For the concreteness, we choose to work with the model akin to the conformal rolling scenario. Namely, we consider the model with two conformal fields, one of which, ϕ, has the conformal field one, and the second, θ, has the conformal weight zero. Again, the symmetry breaking pattern $SO(4,2) \to SO(4,1)$ is realized by introducing the negative quartic potential, $V(\phi) = -\frac{\lambda}{4}\phi^4$, where the coupling constant $\lambda > 0$. As compared to the case of the conformal rolling scenario, we assume that the field ϕ is minimally coupled to gravity. The action for the field ϕ is then given by [26]

$$S = \int d^4x\sqrt{-g}\left(\frac{1}{2}g^{\mu\nu}\partial_\mu\phi\partial_\nu\phi + \frac{\lambda}{4}\phi^4\right) .$$

The equation of motion following from this action is given by

$$\ddot{\phi} + 3H\dot{\phi} = \lambda\phi^3 . \tag{132}$$

Here we *a priori* assume that the effects of gravity are negligible, and the flat space-time description is a good approximation to the scalar field dynamics. Dropping the Hubble parameter from the Eq. (132) we obtain that the solution tends to the dynamical attractor,

$$\phi(t) = -\frac{\sqrt{2}}{\sqrt{\lambda}t} .$$

Here we drop the integration constant analogous to the the time $\eta_\star$ in the context of the conformal rolling scenario. The reason is that the beginning of the hot epoch is associated with the end of rolling in the dynamical picture. The Hubble parameter is obtained from the equation,

$$\dot{H} = -4\pi G(\rho + p) = -\frac{4\pi}{M_{Pl}^2}\dot{\phi}^2 .$$

To solution to the latter reads

$$H(t) = \frac{8\pi}{3\lambda M_{Pl}^2 t^3} .$$

Now, let us check the validity of neglecting gravity in the evolution of the field ϕ. This ammounted to the approximation $|\ddot{\phi}| \gg |3H\dot{\phi}|$, or

$$\lambda t^2 M_{Pl}^2 \gg 1 .$$

Hence, the approximation made is valid as long as $t \ll t_{end}$, where

$$t_{end} \sim -\frac{1}{\sqrt{\lambda}M_{Pl}} .$$

This corresponds to

$$t_{end} \sim M_{Pl} \ .$$

The natural expectation is that the potential becomes regularized at such large field values. The scalar field energy density follows from the Friedmann equation

$$\rho_\phi = \frac{3M_{Pl}^2 H^2}{8\pi} = \frac{8\pi}{3M_{Pl}^2 \lambda t^6} \ .$$

$$p_\phi \equiv \frac{1}{2}\dot{\phi}^2 - V(\phi) = \frac{2}{\lambda t^4} \ . \tag{133}$$

The scale factor is slowly contracting in the regime $t \ll t_{end}$:

$$a(t) = 1 - \frac{4\pi}{3M_{Pl}^2 \lambda t^2} \ .$$

Thus, we have $a(t) \approx 1$ throughout the evolution, consistent with our assumption that the gravity is a negligible effect on the scalar field dynamics.

Now, it becomes clear, why the contracting Universe dominated by the field ϕ is the dynamical attractor. Indeed, let us write the general Friedmann equation,

$$H^2 = \frac{8\pi}{M_{Pl}^2}\left(\frac{C_{mat}}{a^3} + \frac{C_{rad}}{a^4} + \frac{C_{aniso}}{a^6} + ... + \rho_\phi\right) - \frac{\kappa}{a^2} \ ,$$

which includes contributions from the spatial curvature ($\sim 1/a^2$), non-relativistic particles ($\sim 1/a^3$), radiation ($\sim 1/a^4$), and anisotropic stress of kinetic energy ($\sim 1/a^6$). We observe that since $a \approx 1$ throughout the evolution, the energy density in each of these components remains almost constant, while the energy density of the field ϕ rapidly grows in time. Thus, even with comparable initial density fractions for various components, the Universe quickly becomes flat, homogeneous, isotropic and empty [26]. For example, assume that the Universe starts out with $\Omega_K^i \lesssim \mathcal{O}(1)$ at some initial time t_i, the final value of Ω_K^{end} at t_{end} is therefore

$$\Omega_K^{end} \sim \frac{H^2(t_i)}{H^2(t_{end})} = \left(\frac{t_{end}}{t_i}\right)^2 \ .$$

Clearly, this can be made arbitrarily small by choosing $|t_i|$ suitably small.

To avoid the confusion, we note that the contracting stage is not generic for the models of the Conformal Universe. In the particular example of the Hinterbichler–Khoury model discussed here, the pressure corresponding to the conformal field ϕ is positive. Alternatively, one deals with the negative pressure, which results into the phase of (very slow) accelerated expansion. This opportunity is realized in the framework of the Galilean Genesis [25], which discussion we postpone until the end of this Chapter. Let us clarify this point. Since the background depends only on time and is invariant under dilatations, the pressure end and

energy density must both scale as $1/t^4$. But energy conservation implies $\rho \approx const$ at the zeroth order in $1/M_{Pl}$. Hence $\rho \approx 0$. Thus, the conformal symmetries fix the form of the energy density and pressure of the CFT,

$$\rho_{CFT} \approx 0 \ , \quad p_{CFT} \approx \frac{\beta}{t^4} \ . \tag{134}$$

Integrating then the equation

$$M_{Pl}^2 \dot{H} = -4\pi(\rho_{CFT} + p_{CFT})$$

gives the Hubble parameter

$$H(t) \approx \frac{4\pi\beta}{3M_{Pl}^2 t^3} \ ,$$

which corresponds to a contracting or an expanding Universe depending on the sign of β. Integrating Hubble parameter, one obtains the scale factor

$$a(t) \approx 1 - \frac{2\pi\beta}{3M_{Pl}^2 t^2} \ . \tag{135}$$

Thus, under rather general assumptions one concludes that the Universe is nearly static at early times. Depending on the sign of the constant β it undergoes either the contraction ($\beta > 0$) or the expansion ($\beta < 0$).

5.3.2 Perturbations in Hinterbichler–Khoury model

Now let us include the zeroth weight conformal fields in the model. The general conformally invariant action for these fields is given by [26],

$$\mathcal{L}_\theta = \frac{1}{2}\phi^2(\partial\theta)^2 - \kappa\lambda\phi^4 V(\theta) - \xi\phi\Box\phi F(\theta) \ , \tag{136}$$

here $V(\theta)$ and $F(\theta)$ are some functions of θ; κ and ξ are the constant, which we keep arbitrary for the time being. In the quadratic order, we write

$$V(\theta) = V(\theta)|_0 + \left.\frac{\partial V}{\partial\theta}\right|_0 \theta + \left.\frac{\partial^2 V}{\partial\theta^2}\right|_0 \theta^2 + \mathcal{O}(\theta^3)$$

and

$$F(\theta) = F|_0 + \left.\frac{\partial F}{\partial\theta}\right|_0 \theta + \frac{1}{2}\left.\frac{\partial^2 F}{\partial\theta^2}\right|_0 \theta^2 + \mathcal{O}(\theta^3) \ .$$

With no loss of generality, one can choose $F(0) = 0$ and $V(0) = 0$. This results into the irrelevant redefinition of the coupling constant λ. Then, choosing $\left.\frac{\partial V}{\partial\theta}\right|$ and $\left.\frac{\partial F}{\partial\theta}\right|_0$ to zero, one can tune the classical value of the field θ to zero. Thus, it may be non zero only due to

the quantum fluctuations, akin to the conformal rolling scenario. Finally, one can tune the second derivatives $\frac{\partial^2 V}{\partial\theta^2}\Big|_{\theta=0}$ and $\frac{\partial^2 F}{\partial\theta^2}\Big|_{\theta=0}$. This amounts into the redefinition of the constants κ and ξ. Now, one can write the action (136) in the form

$$\mathcal{L}_\theta = \frac{1}{2}\phi^2(\partial\theta)^2 - \frac{\kappa}{2}\lambda\phi^4 - \xi\phi\Box\phi \ .$$

Since we are working at the quadratic level, we replace the field ϕ by its background value. Then, the Lagrangian takes the form. The equations of motion for the canonical variable $\hat{\theta} = \theta/(-t)$ then reads

$$\ddot{\hat{\theta}} + \left(k^2 - \frac{2-\kappa-\xi}{t^2}\right)\hat{\theta} = 0 \ .$$

For rather small k and ξ one obtains approximately flat spectrum of the pertubations $\hat{\theta}$ in the late-time regime, $k(-t) \ll 1$. Account of κ and ξ results into the small scalar lilt [26],

$$n_s - 1 = \frac{4}{3}(\kappa + \xi) \ .$$

This is a novelty as compared to the conformal rolling scenario.

Note that the weight-zero fields are supposed to give the negligible contribution to the total energy density of the Universe. Thus, they are isocurvature ones and hence gauge-independent. As we will see in what follows, the effects of gravity can be safely neglected at the next to quadratic order as well. On the contrary, the perturbations of the weight-one field ϕ are gauge-dependent. Thus, strictly speaking, we cannot neglect the gravitational degrees of freedom in this case. Clearly with the gravity turned off, the perturbation of the weight-one field ϕ, i.e. $\varphi = \phi - \bar{\phi}$, behave literally in the same way as the perturbation of the radius of the field χ of the conformal rolling scenario. Namely, the quadratic Lagrangian for the perturbation φ of the Hinterbichler–Khoury model reads

$$\mathcal{L}_\varphi = \frac{1}{2}(\partial_\mu\varphi)^2 + \frac{3}{2}\lambda\bar{\varphi}^2\varphi^2 \ ,$$

and the equation of motion coincides with (130),

$$\ddot{\varphi} + \left(p^2 - \frac{6}{t^2}\right)\varphi = 0 \ .$$

The properly normalized late-time solution to this equation is given by

$$\varphi = \frac{3}{4\pi^{3/2}}\frac{1}{p^{5/2}t^2} \ .$$

Now we turn on the gravity. The proper description of perturbations in the dominating matter is given then in terms of the gauge-invariant curvature perturbation ζ. It is easy to

calculate the latter, once we remember the lessons learnt from the inflation. For the time being we fix the Newtonian gauge,

$$ds^2 = a^2(\eta)((1+2\Phi)d\eta^2 - (1+2\Psi)d\mathbf{x}^2) \ .$$

One further employs the Mukhanov–Sasaki variable u, which recall reads for the canonically normalized scalar field,

$$\frac{u}{a} = \left(\varphi - \frac{a\phi'}{a'}\Psi\right) \tag{137}$$

and satisfies the equation of motion in the momentum representation,

$$u'' + p^2 u - \frac{z''}{z}u = 0 \ , \tag{138}$$

where remind $z = \frac{a^2\phi'}{a'}$. On the nearly Minkowskian background, the last term in the Eq. [**?**] is negligible, and the quantity u essentially behaves as the free scalar field in the flat space-time. This results into the blue spectrum of the variable u, which translates into the blue spectrum of the curvature perturbation ζ, since the relation

$$\zeta = -\frac{a'}{a^2\phi'} \cdot u \ .$$

Consequently, the dominant adiabatic mode is completely irrelevant at the cosmological scales. Analogous result has been obtained in the context of Galilean Genesis [25].

5.3.3 Phenomenology

Once the field perturbation φ is gauge-dependent in the dynamical picture and the invariant curvature ζ has blue spectrum, one may have doubts about the validity of the results obtained in the spectator model. This discrepancy between the dynamical and the spectator model is, however, a fake one. Indeed, the field pertubation φ can be given a gauge-invariant definition; this field is related to, but different from ζ. Furthermore, at early times, when the conformal mechanism operates in models of Refs. [26], the energy density and pressure of the rolling field are small, so the effects due to gravity are negligible. Let us see, how it works in the Newtonian gauge [111], see also [25].

In the Newtonian gauge, the action for the zeroth weight field θ including terms linear in metric excitations and the pertubation φ [111],

$$S_\theta^{(1)} = \int d^4x a^2\phi'^2 \left[\left(-\Phi + 3\Psi + 2\frac{\varphi}{\phi}\right)\theta'^2 - \left(\Phi + \Psi + 2\frac{\varphi}{\phi}\right)\partial_i\theta\partial_i\theta\right] \ . \tag{139}$$

In the spectator model one has $\Phi = \Psi = 0$, while the perturbation φ coincides with the Mukhanov–Sasaki variable v in the short wavelength regime $p|\eta| \gg 1$ and is given by

$$\varphi = -\frac{3}{p^2\eta^2}u \tag{140}$$

in the large wavelength regime $p|\eta| \gg 1$. Let us prove this. The application of the linearized cosmological perturbation theory to the single-field fluid leads to the following equation for the Newtonian potential Φ

$$\Delta\Phi = \frac{1}{2M_{Pl}^2}\phi'\frac{z}{a}\frac{\partial}{\partial\eta}\left(\frac{u}{z}\right) \ . \tag{141}$$

As it follows from the latter, in the short wavelength regime,

$$\frac{a\phi'}{a'}\Psi \sim \frac{1}{p\eta}u \ll u \ ,$$

so that φ indeed equals to v. In the large wavelength regime, one obtains

$$\Phi = -\Psi = \frac{1}{2M_{Pl}^2}\frac{\sqrt{2}}{\sqrt{\lambda}\eta^3 p^2}v \ .$$

Substituting the latter into the Eq. (137), we find that the leading part of φ is given by (140). Hence, gravity does not modify φ in the Newtonian gauge. Further, in the Newtonian gauge one always has

$$\Phi \ll \frac{\varphi}{\phi} \ .$$

Indeed, the gravitational potential is doubly suppressed as compared to φ/ϕ. In the short wavelength limit this follows from the estimate

$$\frac{\Phi}{\varphi/\phi} = \frac{\Phi\phi}{u} \sim \frac{1}{\lambda M_{Pl}^2\eta^2}\frac{1}{p\eta} \ ,$$

while in the large wavelength limit

$$\frac{\Phi}{\varphi/\phi} \sim \frac{1}{\lambda M_{Pl}^2\eta^2} \ .$$

Hence, the gravitational potential is subdominant in the action (139) as compared to φ. Thus, the calculations made in the spectator picture give correct results in the dynamical scenario.

Thus, the signatures of the dynamical model coincide with ones of the conformal rolling scenario (version A). This concerns the statistical anisotropy and the non-Gaussianity at the level of the trispectrum. In particular, the constraint on the parameter h^2 of the conformal rolling scenario obtained from the non-observation of the (cosmological) statistical anisotropy, is directly translated on the parameters of the Hinterbichler–Khoury model and the Galileon Genesis. Here two qualifications are in order. The first one concerns the spectral tilt. Remarkably, the general picture of Hinterbichler–Khoury provides us with the natural source of small tilt, which can be either blue or red. This source is absent in the sub-scenario A of the conformal rolling and requires the additional assumptions, e.g. the small violation

of the conformal invariance [19]. Second, the intrinsic non-Gaussianity at the level of the bispectrum is non-zero already at the level of the bispectrum in the general picture. This source is encoded in the terms $\mathcal{O}(\theta^3)$ in the Lagrangian (136). The coresponding bispectrum has been calculated in [120]. The symmetry breaking pattern $SO(4,2) \to SO(4,1)$ fixes the shape of the bispectrum, so that the latter peaks in the squeezed limit. This is, however, not a particularly strong signature, since the bispectrum with the same shape is obtained in the curvaton models [46] or during the conversion epoch.

5.4 Galilean Genesis

As pointed out in the end of the Subsection 5.3.1, the Universe being in the conformal state undergoes either the slow contraction or the slow expansion depending on the sign of the constant β in the Eq. (135). Let us consider the case of the negative constant β. As it follows from (134), this implies the negative pressure. Given that the absolute pressure is much larger than the energy density in the conformal Universe, we are led to the strong violation of the Null Energy Condition,

$$p \ll -\rho \ .$$

The inequality $p < -\rho$ is not new for us. Remind, it has been invoked to provide the smooth transition from the contracting stage to the conventional expansion. In particular, the new ekpyrotic models [94] are designed in such a way that the NEC is *mildly* violated near the bounce in terms of the ghost condensate models [11]. The interesting proposal on the *strong* violation of the NEC without pathologies appeared recently in the context of the Galileon theories [95, 96]. Originally designed as the local modification of gravity, they have been used to address the early Universe problems. For example, the Galilean-type self-interactions may provide the smooth transition from the contracting stage to the expanding phase [97]. Also, conformally invariant versions of the Galileon theories can play the role of the very early Universe theory, alternative to the inflationary one. The picture of the Universe in this framework is referred to as the Galilean Genesis [25]. Let us discuss the latter in a bit more details. The general Lagrangian of the Galileon Genesis is the linear combination of five terms $\mathcal{L}_i$,

$$\mathcal{L} = c_1\mathcal{L}_1 + c_2\mathcal{L}_2 + c_3\mathcal{L}_3 + c_4\mathcal{L}_4 + c_5\mathcal{L}_5 \ ,$$

each invariant under the Galilean and conformal transformations. The first term in the combination is trivial,

$$\mathcal{L}_1 = e^{\pi} \ .$$

The interesting cosmology comes, once we consider the second and the third terms,

$$\mathcal{L}_2 = \frac{1}{2}e^{2\pi}(\partial\pi)^2 \ ,$$

$$\mathcal{L}_3 = -\frac{1}{2}(\partial\pi)^2\Box\pi - \frac{1}{4}(\partial\pi)^2\Box\pi \ .$$

The structure of $\mathcal{L}_4$ and $\mathcal{L}_5$ is more complicated. Fortunately, the non-trivial cosmology can be derived without their use. Though the complicated higher derivative structure of the general Lagrangian, the resulting equations of motion contain the two-derivative terms at most [95]. This protects from the appearance of the new potentially dangerous degrees of freedom. Interestingly, the Lagrangian admits the de Sitter solution,

$$e^{\pi_{dS}} = -\frac{1}{H_0 t} \ ,$$

provided that the constants in the linear combination satisfy the equation,

$$c_2 - \frac{3H_0^2}{2}c_3 + \frac{3H_0^4}{2}c_4 - \frac{3H_0^5}{4}c_5 = 0 \ . \tag{142}$$

Further, the system is free of ghosts, if the following inequality is obeyd,

$$c_2 - 3H_0^2 c_3 + \frac{9}{2}H_0^4 c_4 - 3H_0^6 c_5 > 0 \ . \tag{143}$$

Setting $c_4 = c_5 = 0$, the Eq. (142) gives us $c_3 = \frac{2}{3H_0^2}c_2$. Substituting the latter into the Eq. (143), we obtain that $c_2 < 0$, and hence the negative sign of the leading kinetic term. This results into the ghost instabilities around the solution $\pi = 0$.

It is convenient to write the action of the Galilean Genesis as follows,

$$S_\pi = \int d^4x\sqrt{-g}\left[-f^2e^{2\pi}(\partial\pi)^2 + \frac{f^3}{\Lambda^3}(\partial\pi)^2\Box\pi + \frac{f^3}{2\Lambda^3}(\partial\pi)^4\right] \ ,$$

where the coefficients f, Λ and H_0 are related between each other as follows

$$H_0^2 = \frac{2\Lambda^3}{3f} \ .$$

The novelty of the Galilean Genesis as compared to all the previous cosmologies becomes clear once we turn on the gravity. Let us calculate the energy-momentum tensor, $T_{\mu\nu} = \frac{\delta S}{2\sqrt{-g}\delta g^{\mu\nu}}$, see [25]

$$\begin{aligned} T_{\mu\nu} = &-f^2e^{2\pi}[2\partial_\mu\pi\partial_\nu\pi - g_{\mu\nu}(\partial\pi)^2] \\ &- \frac{f^3}{\Lambda^3}[2\partial_\mu\partial_\nu\Box\pi - (\partial_\mu\partial_\nu(\partial\pi)^2 + \partial_\nu\pi\partial_\mu(\partial\pi)^2) + g_{\mu\nu}\partial_\alpha\pi\partial^\alpha(\partial\pi)^2] \\ &- \frac{f^3}{2\Lambda^3}[4(\partial\pi)^2\partial_\mu\pi\partial_\nu\pi - g_{\mu\nu}(\partial\pi)^2] \ . \end{aligned} \tag{144}$$

Turning off the gravity for the instance, i.e. plugging $g_{\mu\nu} = \eta_{\mu\nu}$, we find that the Eq. (144) leads to the vanishing energy density and to the negative pressure, $p \sim -\frac{1}{t^4}$. This implies

the strong violation of the NEC. The Hubble parameter is negative and given at the early times by

$$H \approx -\frac{1}{3}\frac{f^2}{M_{Pl}^2} \cdot \frac{1}{H_0^2 t^3} \ .$$

The latter shows that the Hubble parameter grows with time with a rate $\dot{H} \gg H^2$.

At the quadratic level in perturbations of the field π, our discussion is essentially the same as one of the Hinterbichler–Khoury model. This is not a surprise for, since the Galilean Genesis contains all the necessary ingredients of the (pseudo)-Conformal Universe. Thus, without the tedious calculations we can already conclude with the red spectrum of the Galileon field perturbations. Including the gravitational degrees of freedom, the dominant adiabatic mode acquires the blue spectrum, as in the Hinterbichler–Khoury model. Hence, it cannot serve as the source of primordial scalar perturbations. From the previous analysis, we, however, know, how to achieve the flat spectrum of relevant perturbations. This is to add the zero conformal weight field,

$$S_\theta = \frac{1}{2}\int d^4x\sqrt{-g}e^{2\pi}(\partial_\mu\theta)^2 \ .$$

Remarkably, this simplest way of coupling of the zeroth conformal weight θ, fixes the phenomenological properties of the Galilean Genesis. These are ones of the sub-scenario A of the conformal rolling model, i.e. the non-Gaussianity at the level of the trispectrum and the statistical anisotropy [20, 21, 22].

5.5 Sub-scenario B in the picture of (pseudo)-Conformal Universe

As it follows, the sub-scenario A of the conformal rolling is easily generalized to the dynamical picture. This is not the case of the alternative sub-scenario, i.e. one with the intermediate stage. It should be considered on the equal footing with the sub-scenario A in the spectator picture, but is not particularly natural in the dynamical picture. One can imagine, however, the marginal scenario both dynamical and incorporating the long evolution at the intermediate stage. This may occur, e.g. in the Galileon Genesis, if the effective scale factor $\rho(\pi)$ is a non-trivial function of the galileon field π, such that $\rho \propto e^\pi$ at π smaller than some value of the π_0 and $\rho = \text{const}$ at larger π see [22].

Clearly, it is more reasonable to treat the version with the intermediate stage as the spectator model. Remarkably, the natural choice of the background in this case is one of the (pseudo)-Conformal Universe. Let us give a possible cosmological scenario incorporating the intermediate stage. Indeed, we can easily imagine the situation, when there are at least two fields with conformal weights $\Delta \neq 0$ and with the non-trivial time-dependent backgrounds. Assume that one of these fields drives the evolution of the Universe, while the second is a spectator. Coupling the latter with the zeroth conformal weight field, we return to the

picture of the conformal rolling scenario with the intermediate stage. The only qualification here is that there should be the hierarchy of scales of the explicit breaking of the conformal invariance. As we discussed in the Section 4.2, the scale of the explicit breaking of the conformal invariance in the scenario with the intermediate stage is naturally not larger than $10^{-6}M_{Pl}$, but is allowed to be as low as, say, 1 TeV. On the other side, the scale of breaking in the dynamical picture can be as large as M_{Pl}. With these scales of breaking, we naturally obtain the large intermediate stage. It is interesting to speculate about the relation between the hierarchy of scales of the conformal invariance breaking and the same in the high-energy physics. In particular, one can refer the violation of the conformal invariance in the spectator field to some low energy supersymmetry, while the breaking of the conformal invariance in the dynamical sector to the effects of the quantum gravity.

In either case, the sub-scenario B is of the special interest from the viewpoint of CMB experiments. The statistical anisotropy predicted there is a very clear signature, which will yield us the first interesting constraint on the unique parameter h^2 of the conformal rolling scenario. This is going to be the main subject of the next Chapter.

6 Statistical anisotropy of CMB

6.1 Sources of statistical anisotropy

Recent advances in the observational cosmology make it real to start probing the most intriguing aspects of the Universe. In particular, it is of importance to inquire whether the statistical isotropy of the scalar perturbations is exact or only approximate. This issue is of special interest because the statistical isotropy is one of the key assumptions of the six-parametric ΛCDM model and is favored by inflation. Thus, the violation of this property in the observed CMB would imply a highly non-trivial extension of the now standard cosmological model. An additional motivation to search for the statistical anisotropy is the possible presence of various anomalies in the CMB data, such as alignment of low multipoles, axis of evil, power assymetries, cold spots and others [28]–[36].

For the given distribution of the temperature anisotropies $\delta T(\mathbf{n})$ on the CMB sky, one defines the coefficients a_{lm} in the harmonic space,

$$a_{lm} = \int d\Omega \delta T(\mathbf{n}) Y^{\star}_{lm}(\mathbf{n}) \ . \tag{145}$$

Under the assumption of the statistical isotropy, the theoretical covariance $S_{lm;l'm'} = \langle a_{lm} a^{\star}_{l'm'} \rangle$, is diagonal in the harmonic space,

$$S_{lm;l'm'} = C_l \delta_{ll'} \delta_{mm'} \ , \tag{146}$$

where C_l's represent the standard CMB spectrum. This is not the case for the real CMB signal, which we denote by $\hat{a}_{lm}$. The latter incorporates the noise, the unavoidable feature of the experimental techniques. As a result, one naturally deals with the covariance

$$\mathbf{C}_{lm;l'm'} \equiv \langle \hat{a}_{lm} \hat{a}_{l'm'} \rangle = \mathbf{S}_{lm;l'm'} + \mathbf{N}_{lm;l'm'} \ ,$$

where $\mathbf{N}_{lm;l'm'}$ is the covariance, which corresponds to the instumental noise. In the real space this covariance is diagonal, i.e.

$$\mathbf{N}_{ij} \equiv \langle n_i n_j \rangle = \frac{\sigma_0^2}{N_{obs}(i)} \delta_{ij} \ .$$

The quantity σ_0 is the dispersion per pixel, while $N_{obs}(i)$ is the number of observations per pixel. The noise is inhomogeneous over the CMB sky. Hence, the non-diagonality in the harmonic space. Note, however, that since the the dispersion σ_0 and the number of observations per pixel $N_{obs}(i)$ are well established, the noise effects can be properly accounted and subtracted from the data.

Even in this case, one does not deal with the pure CMB signal. Indeed, the latter is highly contaminated by the emission coming from the foregrounds. The common way to deal with

the foregrounds is to mask the contaminated pixels. Clearly, this procedure immediately induces the statistical anisotropy. The other approach to the problem is based on the so called ILC (internal linear combination) full-sky maps. The latter are useful to study the CMB properties at the sufficiently low multipoles, e.g. the quadrupole-octupole alignment. We will employ the ILC maps in the Section 7.3., when discussing the quadrupole-octupole alignment. Note, however, that the range of trustful multipoles of the ILC maps has the cut-off at $l_{max} \sim 300$. Thus, the (current) ILC maps is not the appropriate tool for studies of the statistical anisotropy effects relevant at the overall CMB range. This is the case, e.g. of the primordial statistical anisotropy, to which discussion we turn shortly.

Before that, let us make one remark. In principle, the cosmological violation of the statistical isotropy is not necessarily rooted in the primordial physics. Several proposals have been made in the context of the dark energy models [143]. or the non-trivial topologies of the Universe (see, e.g. [144] and references therein). Note, however, that these sources can at best affect the lowest multipoles of the CMB. Indeed, the characteristic size of the non-trivial topologies is highly constrained by the present experiments [145]. Therefore, the corresponding effects are strongly suppressed. The dark energy based violation of the statistical isotropy relies on the super-horizon modulation of the homogeneous quintessence field. Thus, the associated effects fall down rapidly with the CMB multipole number, though being potentially interesting from the viewpoint of the lowest multipoles. In what follows, we will neglect these sources.

6.2 Statistical anisotropy as a probe of primordial physics

In the statistically anisotropic but spatially homogeneous Universe, the power spectrum of the primordial scalar perturbations $\zeta(\mathbf{k})$ depends on the direction of the wave vector $\mathbf{k}$. The power spectrum can then be written as follows,

$$\mathcal{P}_\zeta(\mathbf{k}) = \mathcal{P}_0(k)\left[1 + a(k)\sum_{LM} q_{LM} Y_{LM}(\hat{\mathbf{k}})\right] , \tag{147}$$

where $\hat{\mathbf{k}} = \mathbf{k}/k$. The coefficients q_{LM} parametrize the direction-dependent part, which one expands in spherical harmonics $Y_{LM}(\hat{\mathbf{k}})$. Unlike in Ref. [115], we assume here that the dependence on the wavenumber k may be absorbed into one function $a(k)$. Commutativity of the classical field $\zeta(\mathbf{x})$ yields $\mathcal{P}_\zeta(\mathbf{k}) = \mathcal{P}_\zeta(-\mathbf{k})$ and hence $q_{LM} = 0$ for odd L.

The generic prediction of the inflationary theory is that the power spectrum is isotropic, $a(k) = 0$. However, the statistical anisotropy can be generated in models of inflation involving vector fields [79, 81, 80, 89, 82]. Somewhat more exotic examples are given by introducing the noncommutative field theory [92, 93]. The most common feature of these models is the statistical anisotropy of a special quadrupole type (the only non-vanishing coefficient in a certain reference frame on the celestial sphere is q_{20}). This prediction arises, e.g., in the model

with the rotational invariance broken by a space-like vector [79]. However, higher multipoles q_{LM} can also emerge within the inflationary framework, see, e.g., Refs. [90] and [91]..

Motivated by the ACW model [79], Groeneboom and Eriksen [116] discovered the evidence for the quadrupole statistical anisotropy in the five-year WMAP data. However, it was found tob nearly aligned with the ecliptic poles. Using quadratic maximum likelihood estimator, Hanson and Lewis [117] extended the analysis to higher multipoles. They also included the relevant prefactor in the covariance neglected in [79] and [116]. Hanson and Lewis [117] confirmed the result on the large quadrupole q_{2M} lying nearly in the ecliptic plane. The strongest indication of the statistical anisotropy violation, non-zero at the 9σ confidence level was found in the W band of the five-year data in Ref. [118]. These findings have been confirmed by the WMAP team [37] in their analysis of the seven-year data. One possible explanation of the anomalous quadrupole is the systematics inherent in the WMAP data. As argued in [119], large observed statistical anisotropy may result from beam asymmetries rather than have the cosmological origin.

At the conformal rolling stage, the properties of perturbations to both linear and leading non-linear orders are uniquely determined by the underlying conformal symmetry [26], modulo the overall amplitude and a single dimensionless parameter h^2. This parameter governs the non-Gaussianity and statistical anisotropy. The statistical anisotropy generated in the conformal rolling scenario is quite different from the predictions of inflation. In particular, the coefficients q_{LM} parametrizing the power spectrum (147) are the random variables rather than fixed parameters of the model. For the convenience of future reference, we reming here their properties. In the case of the sub-scenario with the intermediate stage, coefficients q_{LM} are random Gaussian variables with zero means and variances

$$\langle q_{LM} q^{\star}_{L'M'} \rangle = \frac{3h^2}{\pi(L-1)(L+2)} \ , \quad a(k) = 1 \ . \tag{148}$$

In the sub-scenario A, there are two sets of coefficients $\{q_{2M}\}$ and $\{q'_{2M}\}$. The former parametrizes the statistical anisotropy of the general quadrupole type. In this case, the coefficients q_{2M} are again the Gaussian variables with zero means and variances

$$\langle q_{2M} q^{\star}_{2M'} \rangle = \frac{\pi h^2 H_0^2}{25} \delta_{MM'} \ , \quad a(k) = \frac{1}{k} \ . \tag{149}$$

The set q'_{2M} corresponds to the statistical anisotropy of the special quadrupole type. The coefficients q'_{2M}, which are not Gaussian in this case are given by

$$q_{2M} = -\frac{4\pi v^2}{5} Y^{\star}_{2M}(\hat{\mathbf{v}}) \ , \quad a(k) = 1 \ . \tag{150}$$

In this Chapter, we constrain the parameter h^2 of the conformal rolling scenario from the non-observation of the cosmological statistical anisotropy in the seven-year WMAP data as

discussed in our article [23]. We follow the general method proposed by Hirata and Seljak for the purpose of studying CMB lensing and known as the quadratic maximum likelihood (QML) estimation [124]. As discussed in Ref. [117], the same idea can be applied to the study of the statistically anisotropic properties of CMB. In this case one assumes that the coefficients q_{LM} are small and expands the log-likelihood of the observed CMB to the second order in these parameters. By maximizing the log-likelihood with respect to the coefficients q_{LM}, one obtains the estimator. Results derived within the QML approximation are in a good agreement with the exact likelihood methods.

We apply this method to construct the estimator for the parameter h^2. In view of the results quoted, the estimated values are expected to be inconsistent with the statistical isotropy because of the alleged systematics present in the WMAP data. Assuming that the interpretation in terms of systematics is correct, we set the upper limits on the parameter h^2 in the following way. For each value of h^2, we simulate the parameter sets $\{q_{LM}\}$, and then generate a number of anisotropic maps for each set $\{q_{LM}\}$. From the maps generated, we estimate the values of the parameter h^2. We require that in 95% cases they should not exceed the value estimated from the observed CMB. In this way we constrain the conformal rolling sub-scenario with the intermediate stage [23],

$$h^2 < 0.045$$

at the 95% confidence level. The constraint is much weaker in the framework of the alternative sub-scenario. The reason is that the amplitude of the leading order quadrupole decreases as k^{-1}. This translates into the suppression of the statistical anisotropy effects at high CMB multipoles. Thus, the data useful for the analysis are effectively limited, statistical errors are large and the constraint is [23] $h^2 < 190$ at the 95% confidence level. The constraint is improved significantly, once we take into account the subleading contribution to the statistical anisotropy. This contribution is of the special quadrupole type, and has the amplitude $a(k)$, which is independent of the wavenumber k. Thus, the number of CMB multipoles useful in the analysis is much larger. This somewhat compensates the smallness of the constant h, and we obtain the stronger constraint [23],

$$h^2 \ln \frac{H_0}{\Lambda} < 7$$

at the 95% confidence level. Here H_0 is the present value of the Hubble parameter, which plays the role of the ultraviolet cutoff, and Λ is the infrared cutoff. Without going into speculation on the value of the constant Λ, we point out that this constraint is still very weak, in view of the fact that the conformal rolling scenario is self-consistent only at $h^2 \ll 1$ anyway.

We conclude that the statistical anisotropy is the relevant signature of the conformal rolling with the intermediate stage. It is of particular interest in view of the upcoming

Planck data. Hopefully, the latter will be free of the quadrupole anomaly. The other expected advantage of the Planck data is the larger range of the CMB multipoles, which translates into smaller statistical errors. These two factors are expected to improve the sensitivity of the data to the parameter h^2 by more than an order of magnitude. On the other hand, statistical anisotropy appears to be a weak signature of the alternative sub-scenario, and the Planck data are not expected to improve the situation significantly. Thus, it makes sense to focus on the other prediction of this sub-scenario, the non-Gaussianity [21, 22]. At the level of bispectrum, the non-Gaussianities in the conformal scenario are not particularly special. The shape of the intrinsic bispectrum is dictated [120] by the symmetry breaking pattern $SO(4,2) \to SO(4,1)$ and coincides with the bispectrum of a spectator massless scalar field in inflationary theory [121, 122] (in fact, the intrinsic bispectrum may vanish for symmetry reasons, as in the conformal rolling scenario). The non-Gaussianity generated at the conversion epoch is not specific to the conformal scenario either. So, bispectrum alone cannot discriminate between the conformal scenario and, say, inflation equipped with the curvaton mechanism. On the other hand, the non-Gaussianity of a rather peculiar form arises in the trispectrum. Existing constraints (see, e.g. Ref. [123]) are model-dependent and cannot be directly applied to our model. We leave for the future the analysis of the CMB data aiming at the search for the non-Gaussianity characteristic of the conformal scenario.

6.2.1 Model-independent analysis

Let us first apply the quadratic maximum likelihood (QML) method to construct the estimators for the coefficients q_{ML}. Here we define the latter in a model-independent way, assuming only that the dependence on the wavenumber k can be factorized as in Eq. (147). We closely follow the technique developed in Ref. [117]. In Section 7.2.2, we use the same ideas when constructing the estimator for the parameter h^2.

In what follows we use the harmonic representation for the temperature fluctuations and their covariances unless the opposite stated. The log-likelihood of the observed CMB temperature map $\hat{\mathbf{a}}$ is given by

$$-\mathcal{L}(\hat{\mathbf{a}}|\mathbf{q}) = \frac{1}{2}\hat{\mathbf{a}}^\dagger \mathbf{C}^{-1}\hat{\mathbf{a}} + \frac{1}{2}\ln\det\mathbf{C}\,, \tag{151}$$

where $\mathbf{q}$ is the vector of coefficients q_{LM}; the covariance matrix $\mathbf{C}$ incorporates the theoretical covariance corresponding to the signal as well as the instrumental noise, $\mathbf{C} = \mathbf{S} + \mathbf{N}$. The theoretical covariance is given by

$$S_{lm;l'm'} = \langle a_{lm} a^\star_{l'm'}\rangle = i^{l-l'}\frac{2}{\pi}\int d\mathbf{k}\Delta_l(k)\Delta_{l'}(k)P_\zeta(\mathbf{k})Y^\star_{lm}(\hat{\mathbf{k}})Y_{l'm'}(\hat{\mathbf{k}})\,.$$

Here a_{lm} are the theoretical temperature fluctuations of the CMB sky $\delta T(\mathbf{n})$ in the harmonic representation, see the Eq. (145); $P_\zeta(\mathbf{k})$ is the power spectrum of the primordial perturba-

tions; $\Delta_l(k)$ are transfer functions. Under the assumption of the statistical anisotropy, we write the theoretical covariance as follows,

$$\mathbf{S} = \mathbf{S}^i + \delta\mathbf{S} \,,$$

where the leading contribution $\mathbf{S}^i$ comes from the isotropic signal well fitted by the ΛCDM model; the effects of the statistical isotropy violation are incorporated into $\delta\mathbf{S}$. The matrix $\mathbf{S}^i$ is diagonal in the harmonic representation and given by the Eq. (146). The matrix $\delta\mathbf{S}$ is given by

$$\delta S_{lm;l'm'} = i^{l'-l} C_{ll'} \sum_{LM} q_{LM} \int d\Omega_{\mathbf{k}} Y^{\star}_{lm}(\hat{\mathbf{k}}) Y_{l'm'}(\hat{\mathbf{k}}) Y_{LM}(\hat{\mathbf{k}}) \,, \tag{152}$$

where

$$C_{ll'} = 4\pi \int d\ln k \Delta_l(k) \Delta_{l'}(k) a(k) \mathcal{P}_\zeta(k) \,. \tag{153}$$

The integral of three spherical harmonics reads

$$\int d\Omega_{\mathbf{k}} Y^{\star}_{lm}(\hat{\mathbf{k}}) Y_{l'm'}(\hat{\mathbf{k}}) Y_{LM}(\hat{\mathbf{k}}) = (-1)^{m'} G^L_{ll'} C^{LM}_{lm;l'-m'} \,, \tag{154}$$

where $C^{LM}_{lm;l',-m'}$ are the Clebsch-Gordan coefficients and

$$G^L_{ll'} \equiv \sqrt{\frac{(2l+1)(2l'+1)}{4\pi(2L+1)}} C^{L0}_{l0l'0} \,.$$

Normally, the estimators for the coefficients q_{LM} are determined by equating the derivative of the log-likelihood to zero,

$$\frac{\partial \mathcal{L}}{\partial \mathbf{q}^\dagger} = 0 \,.$$

However, the covariance matrix $\mathbf{C}$ is not sparse and direct calculations are too costly. Thus, we need an appropriate approximation to work with. At this point we make use of the QML approach. Assuming that the statistical anisotropy is weak, we expand the log-likelihood derivative to the linear order in $\mathbf{q}$,

$$\frac{\partial \mathcal{L}}{\partial \mathbf{q}^\dagger} = \left.\frac{\partial \mathcal{L}}{\partial \mathbf{q}^\dagger}\right|_0 + \left.\frac{\partial^2 \mathcal{L}}{\partial \mathbf{q}^\dagger \partial \mathbf{q}}\right|_0 \mathbf{q} \,. \tag{155}$$

We replace the second derivative of the log-likelihood in this expansion by its expectation value [117],

$$\left\langle \frac{\partial^2 \mathcal{L}}{\partial \mathbf{q} \partial \mathbf{q}^\dagger} \right\rangle = -\left\langle \frac{\partial \mathcal{L}}{\partial \mathbf{q}} \frac{\partial \mathcal{L}}{\partial \mathbf{q}^\dagger} \right\rangle = -\mathbf{F} \,, \tag{156}$$

where $\mathbf{F}$ is the Fisher matrix. The first equality in Eq. (156) follows from the normalization condition

$$\int \exp(\mathcal{L})\, d\hat{\mathbf{a}} = 1 \,.$$

In what follows we use the derivatives of the log-likelihood calculated under the assumption of the statistical isotropy unless the opposite stated, and omit the subscript "0". The first derivative of the log-likelihood is then given by

$$\frac{\partial \mathcal{L}}{\partial \mathbf{q}^\dagger} = \frac{1}{2}\hat{\mathbf{a}}^\dagger \left(\mathbf{C}^i\right)^{-1} \frac{\partial \mathbf{C}}{\partial \mathbf{q}^\dagger} \left(\mathbf{C}^i\right)^{-1} \hat{\mathbf{a}} - \frac{1}{2}\mathrm{Tr}\left(\left(\mathbf{C}^i\right)^{-1} \frac{\partial \mathbf{C}}{\partial \mathbf{q}^\dagger}\right) ,$$

where $\mathbf{C}^i$ is the statistically isotropic covariance incorporating the noise, $\mathbf{C}^i = \mathbf{S}^i + \mathbf{N}$. The second term in the right hand side of this equation is, in fact, the average of the first term over the realizations of CMB. This follows from the identity $\mathrm{Tr}\mathbf{A} = \langle \bar{\mathbf{x}}^\dagger \mathbf{A}\mathbf{C}^{-1}\bar{\mathbf{x}}\rangle$, where $\mathbf{A}$ is any matrix and $\mathbf{x}$ is a vector of Gaussian random variables with the covariance $\mathbf{C}$. Thus, one writes

$$\frac{\partial \mathcal{L}}{\partial \mathbf{q}^\dagger} = \mathbf{h} - \langle \mathbf{h} \rangle , \tag{157}$$

where

$$\mathbf{h} = \frac{1}{2}\bar{\mathbf{a}}^\dagger \frac{\partial \mathbf{C}}{\partial \mathbf{q}^\dagger}\bar{\mathbf{a}} , \tag{158}$$

and the quantities $\bar{\mathbf{a}}$ are the inverse-variance filtered CMB harmonics calculated in the absence of the statistical anisotropy,

$$\bar{\mathbf{a}} = \left(\mathbf{S}^i + \mathbf{N}\right)^{-1} \hat{\mathbf{a}} . \tag{159}$$

By substituting Eqs. (156) and (157) into Eq. (155) and equating the result to zero, we obtain the QML estimator,

$$\mathbf{q} = (\mathbf{F})^{-1}(\mathbf{h} - \langle \mathbf{h} \rangle) . \tag{160}$$

In what follows we use the Fisher matrix calculated in the full sky and homogeneous noise approximation [117]. It has only diagonal elements, which do not depend on M,

$$F_{LM;L'M'} = \delta_{LL'}\delta_{MM'} w \sum_{l,l'} \frac{(2l+1)(2l'+1)}{8\pi} \begin{pmatrix} L & l & l' \\ 0 & 0 & 0 \end{pmatrix}^2 \frac{C_{ll'}^2}{C_l^{tot} C_{l'}^{tot}} , \tag{161}$$

where C_l^{tot} is the sum of the standard CMB spectrum C_l and the noise spectrum N_l. The constant w denotes the uncut fraction of the sky. We include this factor to achieve better agreement between the approximate Fisher matrix and the exact one defined as the average over the ensemble of simulated maps with the real sky coverage and inhomogeneous noise.

6.2.2 Application to conformal rolling scenario

In the framework of the conformal rolling scenario, the coefficients q_{LM} are random variables with zero expectation values. To the linear order in h they are Gaussian and have variances given by Eq. (148) or (149). The variances depend on the constant h^2, which is the only

parameter of the model. This makes it possible to constrain the conformal rolling scenario from the non-observation of the cosmological statistical anisotropy. We again use the QML method to construct the estimator for the parameter h^2. We do that starting from the Gaussian hypothesis about the coefficients q_{LM}. This hypothesis is particularly appropriate in the context of the sub-scenario B. The non-Gaussian q_{2M}'s appear in the sub-scenario A to the subleading order; we comment on this case in the end of this Section.

The probability density of the coefficients q_{LM} for a given value of h^2 is

$$\mathcal{W}(\mathbf{q}|h^2) \sim \frac{1}{\sqrt{\det \mathbf{Q}}} \exp\left(-\frac{1}{2}\mathbf{q}^\dagger \mathbf{Q}^{-1}\mathbf{q}\right) .$$

Here the matrix $\mathbf{Q}$ is the covariance of the anisotropy parameters, $Q_{LM;L'M'} \equiv \langle q_{LM} q^\star_{L'M'}\rangle$. To obtain the likelihood of the observed CMB with respect to the parameter h^2, one integrates the product of two probability densities over the set of the parameters q_{LM},

$$\mathcal{W}(\hat{\mathbf{a}}|h^2) = \int \mathcal{W}(\hat{\mathbf{a}}|\mathbf{q})\mathcal{W}(\mathbf{q}|h^2) d\mathbf{q} , \tag{162}$$

where $\mathcal{W}(\hat{\mathbf{\Theta}}, \mathbf{q}) = \exp[\mathcal{L}(\hat{\mathbf{\Theta}}, \mathbf{q})]$ and $\mathcal{L}$ is the log-likelihood introduced in Eq. (151). Following the main idea of the QML estimation, we expand the log-likelihood to the second order in $\mathbf{q}$,

$$\mathcal{L} = \mathcal{L}_0 + \frac{\partial \mathcal{L}}{\partial \mathbf{q}}\mathbf{q} - \frac{1}{2}\mathbf{q}^\dagger \mathbf{F}\mathbf{q} ,$$

where we again replaced the second derivative by its expectation value over the CMB isotropic realizations. Now the integral in Eq. (162) takes a simple Gaussian form and can be straightforwardly evaluated,

$$\mathcal{W} \sim \frac{1}{\sqrt{\det(\mathbf{F}\mathbf{Q} + \mathbf{I})}} \exp\left(\frac{1}{2}\frac{\partial \mathcal{L}}{\partial \mathbf{q}^\dagger}(\mathbf{F} + \mathbf{Q}^{-1})^{-1}\frac{\partial \mathcal{L}}{\partial \mathbf{q}}\right) . \tag{163}$$

Maximizing (163) with respect to the parameter h^2,

$$\frac{\partial \ln \mathcal{W}(\hat{\mathbf{a}}|h^2)}{\partial h^2} = 0 ,$$

we obtain the equation for the estimator of h^2,

$$\mathrm{Tr}\left((\mathbf{F}\mathbf{Q} + \mathbf{I})^{-1}\mathbf{F}\frac{\partial \mathbf{Q}}{\partial h^2}\right) = \frac{\partial \mathcal{L}}{\partial \mathbf{q}^\dagger}(\mathbf{F}\mathbf{Q} + \mathbf{I})^{-1}\frac{\partial \mathbf{Q}}{\partial h^2}(\mathbf{F}\mathbf{Q} + \mathbf{I})^{-1}\frac{\partial \mathcal{L}}{\partial \mathbf{q}} .$$

In the full sky and homogeneous noise approximation, the Fisher matrix (161) is diagonal,

$$F_{LM;L'M'} = F_L \delta_{LL'}\delta_{MM'} .$$

The matrix Q has the same property,

$$Q_{LM;L'M'} = \tilde{Q}_L h^2 \delta_{LL'} \delta_{MM'} \,,$$

where we introduce the quantities $\tilde{Q}_L$ which do not depend on the parameter h^2. Then the equation determining the estimator takes the form

$$h^2 \sum_L \frac{(2L+1)F_L^2 \tilde{Q}_L^2}{(1+F_L \tilde{Q}_L h^2)^2} = \sum_L \frac{(2L+1)F_L \tilde{Q}_L}{(1+F_L \tilde{Q}_L h^2)^2} (F_L C_L^q - 1) \,, \tag{164}$$

where we use the same notation h^2 for the estimator as for the parameter of the model. The quantities C_L^q entering Eq. (164) are given by

$$C_L^q = \frac{1}{2L+1} \sum_M |q_{LM}|^2 \,, \tag{165}$$

where the coefficients q_{LM} are defined by Eq. (160).

Note that it follows from Eq. (164) that if the predicted statistical anisotropy is of the quadrupole form, i.e., with non-zero q_{2M}'s only, then the parameter h^2 can be estimated simply as $h^2 = C_2^q$, modulo obvious additive and multiplicative constants. This is also clear on general grounds. Indeed, the rotational invariance requires that the estimator should be some function of C_2^q, i.e. $h^2 = f(C_2^q)$. In the small statistical anisotropy approximation, we keep only linear terms in the Taylor expansion of the function $f(C_2^q)$. This immediately implies the quoted relationship between h^2 and C_2^q. Since no assumptions about the properties of the random quantities q_{2M} have been used in the latter argument, it holds for non-Gaussian q_{2M}'s, which describe the quadrupole of the special type, see Eq. (150). The only qualification is that the statistical anisotropy is of the order $h^2 \ln \frac{H_0}{\Lambda}$ in that case. Hence, the corresponding estimator reads $h^4 \ln^2 \frac{H_0}{\Lambda} = C_2^q$, up to multiplicative and additive constants.

6.2.3 Implementation and results

We search for the statistical anisotropy using WMAP seven-year maps [125, 1]. We study the V and W band data at 61 and 94 GHz. The first step is to implement inverse-variance filtering defined by Eq. (159). We write that equation in the form appropriate for applying the conjugate gradient technique,

$$[\left(\mathbf{S}^i\right)^{-1} + \tilde{\mathbf{Y}}^\dagger \mathbf{N}^{-1} \tilde{\mathbf{Y}}] \mathbf{S}^i \bar{\mathbf{a}} = \tilde{\mathbf{Y}}^\dagger \mathbf{N}^{-1} \hat{\mathbf{a}} \,. \tag{166}$$

Here we use the *pixel* representation for the noise covariance $\mathbf{N}$ and the observed CMB temperature $\hat{\mathbf{\Theta}}$. The matrix $\tilde{\mathbf{Y}}$ relates the harmonic space covariance and the observed map,

$$\tilde{Y}_{i,lm} = B_l Y_{lm}(\vartheta_i, \varphi_i) \,,$$

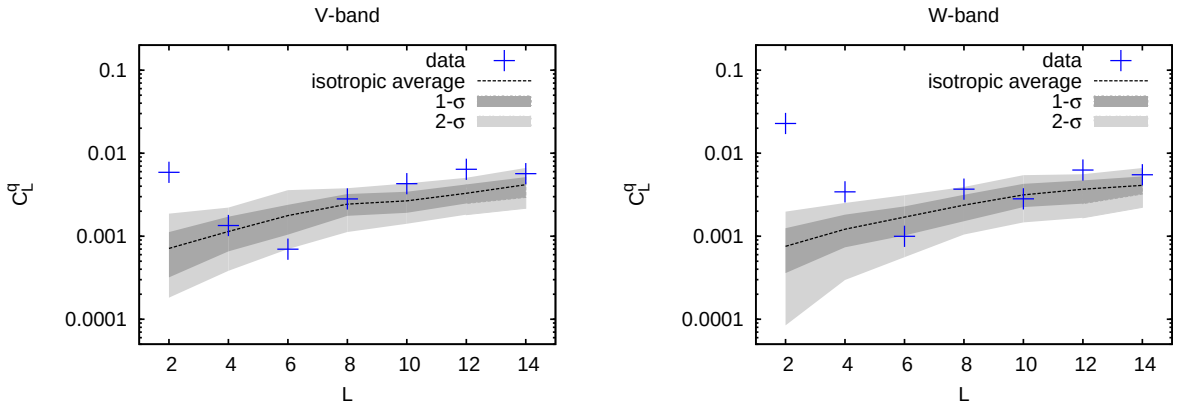

Figure 8: C_L^q of the q_{LM} reconstruction for the V (left) and W (right) bands of the seven-year WMAP data. This analysis assumes $a(k) = 1$ in Eq. (147). The 1σ (dark grey) and 2σ (light grey) confidence intervals are calculated using MC simulated statistically isotropic maps. The analysis is performed with the WMAP temperature analysis mask and $l_{max} = 400$.

where B_l are the beam transfer functions and i labels pixels. We use the foreground reduced V and W seven-year maps [126] provided in HEALPix format [127] with $N_{side} = 512$. For the beam transfer function we use the average of $V1$ and $V2$ functions for V band and the average of $W1$, $W2$, $W3$ and $W4$ for W band.

We consider the noise of the pixels uncorrelated and having the variance σ_0^2/n_{obs}, where σ_0 is 3.137 mK and 6.549 mK for V and W bands, respectively, and n_{obs} is specific to each pixel and tabulated in the maps. To remove foreground contaminated pixels we use the WMAP temperature analysis mask which leaves us with $w = 78\%$ of the sky. We take the noise covariance to be infinite (inverse noise is zero) for masked pixels. The noise model $\mathbf{N}^{-1}$ is constructed using noise covariance and template maps for removing monopole and dipole contributions.

To evaluate the confidence intervals, inverse filtering should be performed on both data and large number of simulated maps. Thus, the system (166) must be well preconditioned. Following Ref. [117], we make use of the multigrid preconditioner, first proposed by Smith et. al. in Ref. [129]. It is known to be the fastest to date and has a typical cost of ten minutes when evaluated to $l_{max} = 1000$.

Next, we compute the quantities h_{LM} given by Eq. (158). Using Eqs. (152) and (154), we write them as follows,

$$h_{LM} = \frac{1}{2} \sum_{lm;l'm'} (-1)^{m'} i^{l'-l} \bar{a}^{\star}_{lm} \bar{a}_{l'm'} C_{ll'} G^L_{ll'} C^{LM}_{lm;l'-m'} \ . \tag{167}$$

We calculate the Clebsch-Gordan coefficients using the GSL [130] and Slatec [131] libraries.

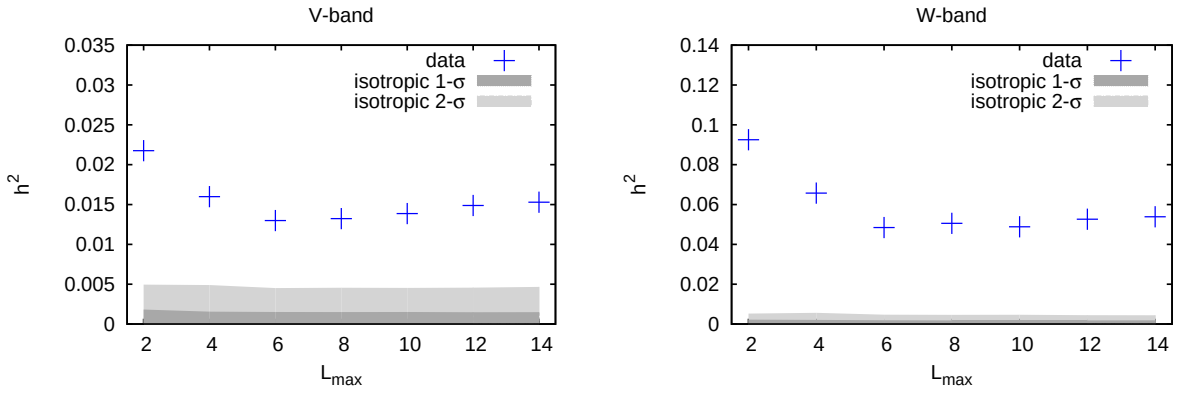

Figure 9: Parameter h^2 of the sub-scenario B reconstructed from the WMAP V band (left) and W band (right). The 1σ (dark grey) and 2σ (light grey) confidence intervals obtained from MC simulations are also shown.

The summation in (161) and (167) is performed up to $l_{max} = 400$. We use the publicly available Boltzman code (CAMB) [132] to compute the quantities $C_{ll'}$.

We have simulated large number of statistically isotropic Monte-Carlo (MC) realizations of the field $\hat{\mathbf{\Theta}}$ using WMAP noise covariance and beam transfer functions. We store the MC maps in the same format as the original map, and the analysis procedure explained in this Section is applied to both data and MC maps on equal footing.

Now we can check the consistency of the observed CMB with the hypothesis of the statistical isotropy. We begin with the model-independent analysis, as outlined in Section 6.2.1. We reconstruct coefficients C_L^q, defined by Eq. (165), from the seven-year WMAP data as well as from the MC maps. The results are presented in Fig. 8. They are in a good agreement with the results obtained by Hanson and Lewis [117] for the five-year maps. In particular, we confirm the result on the large quadrupole for the V and W bands. As discussed in Refs. [116]–[118], the preferred quadrupole direction lies very close to the ecliptic poles. Another suspicious thing is the frequency dependence of the signal. Namely, it is non-zero in the W band at much higher confidence level than in the V band. This indicates a systematic effect rather than the cosmological origin. As discussed in Ref. [119], the account of beam asymmetries can provide a complete explanation of the anomaly.

Let us turn to the conformal rolling scenario. First, we consider the version of the model with the intermediate stage (sub-scenario B). The statistical anisotropy is determined by Eq. (148). Having the set of the coefficients C_L^q reconstructed from the observed CMB, we solve Eq. (164) and estimate the value of h^2. We perform the analysis for the multipole numbers starting from $L_{min} = 2$ and ranging up to $L_{max} = 2 - 14$. The results are presented in Fig. 9. To evaluate the statistical errors we use about one hundred MC simulated isotropic

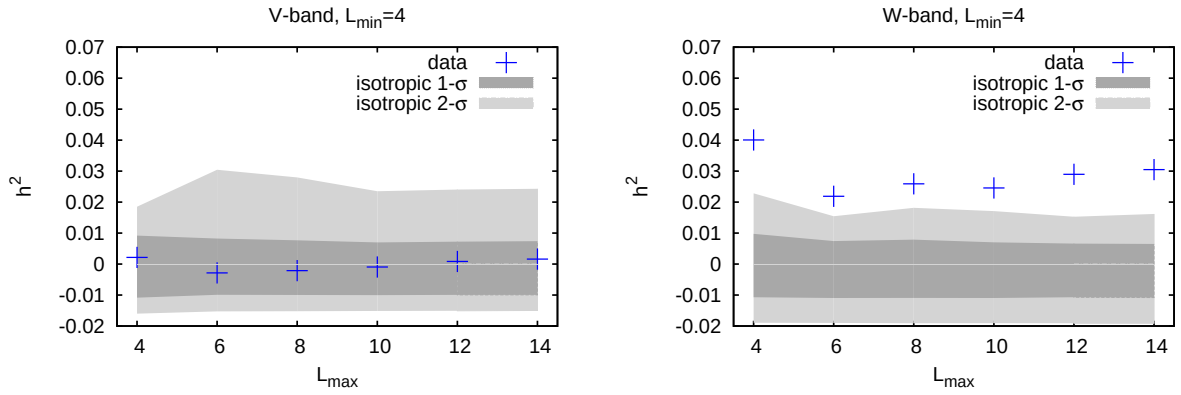

Figure 10: Parameter h^2 of the sub-scenario B reconstructed from higher multipoles ($L_{min} = 4$). Results are plotted for the WMAP V band (left) and W band (right). Shown are the 1σ (dark grey) and 2σ (light grey) confidence intervals obtained from MC simulations.

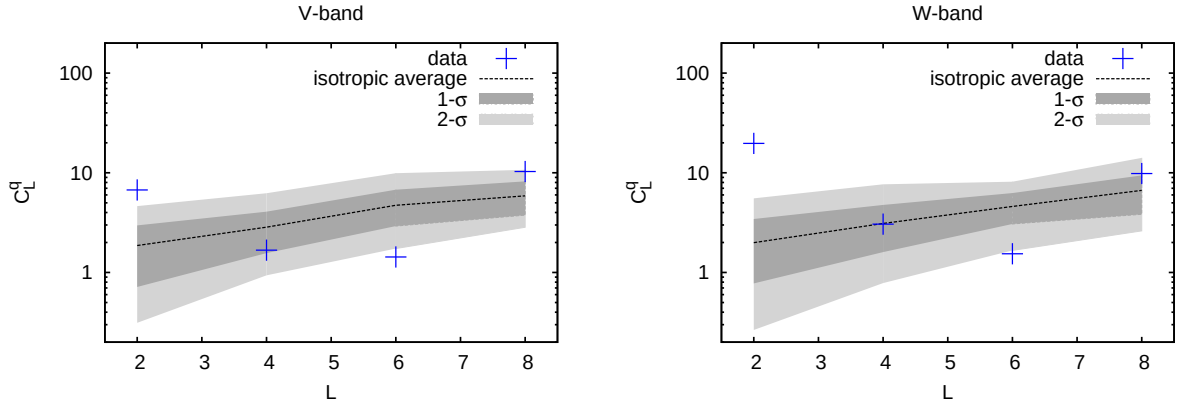

Figure 11: C_L^q of the q_{LM} reconstruction for the V (left) and W (right) bands of the seven-year WMAP. The momentum dependence of the statistical anisotropy is $a(k) = H_0 k^{-1}$. The 1σ (dark grey) and 2σ (light grey) confidence intervals are calculated using MC simulated statistically isotropic maps.

maps. We see that the isotropic model is ruled out at more than 3σ confidence level even in the V band. However, the large value of h^2 (e.g., $h^2 \approx 0.015$ at $L_{max} = 14$) is due to the anomalous quadrupole anisotropy, which is argued to have non-cosmological origin.

Aiming at constraining the parameter h^2, we simulate a large number of anisotropic maps for each value of this parameter. We adapt the approach of Ref. [117], and use the following procedure, adequate in the case of small statistical anisotropy.

We first simulate a seed map $\mathbf{a}^i$ with a covariance $\mathbf{S}^i$ given by Eq. (146). Then we generate

a set of coefficients $\{q_{LM}\}$ based on the value of h^2. The map

$$\mathbf{a^a} = \left(\mathbf{I} + \delta\mathbf{S}\left[\mathbf{S}^i\right]^{-1}\right)^{1/2}\mathbf{a}^i \ ,$$

has covariance $\mathbf{S}^i + \delta\mathbf{S}$, where $\delta\mathbf{S}$ is given by Eq. (152). To the linear order in the anisotropic effects we have

$$\mathbf{a^a} = \mathbf{a}^i + \frac{1}{2}\delta\mathbf{S}[\mathbf{S}^i]^{-1}\mathbf{a}^i \ .$$

Finally, we multiply the map by the beam transfer function in the harmonic space, convert it to coordinate space and add pixel noise to get statistically anisotropic simulated map $\hat{\mathbf{\Theta}}^{\mathbf{a}}$ similar to that observed by WMAP. To set an upper limit, we allow h^2 to be so large that for 95% of simulated anisotropic maps the value of the estimated parameter exceeds the value estimated from the observed CMB map. In this way we obtain the upper limit, which reads

$$h^2 < 0.045 \tag{168}$$

at the 95% confidence level.

In view of the likely non-cosmological origin of the anomalous quadrupole in the statistical anisotropy of the WMAP data, one would like to constrain the parameter h^2 from the non-observation of higher multipoles only. One way to do that would be to follow the same procedure as discussed in Sections 6.2.1 and 6.2.2 but keep the set $\{q_{2M}\}$ of the quadrupole coefficients fixed and taken from the observational data. In practice, things are simpler. Indeed, the effects of the statistical anisotropy corresponding to different multipole numbers L, M do not interfere with each other, at least in the approximation of small coefficients q_{LM}. To see this, we note that the theoretical reconstruction of the Fisher matrix (161) is diagonal. The covariances of the quantities q_{LM} are diagonal as well. As a consequence, it is straightforward to neglect the effect of the quadrupole modulation by using the estimator for the parameter h^2 as in (164) but with the summation starting from $L_{min} = 4$. The values of h^2 estimated in this way are plotted in Fig. 10. We restrict our analysis to $L_{max} = 14$ and obtain that h^2 is consistent with zero for the V band. Making use of the statistical uncertainty inferred from isotropic MC maps, we obtain the upper limit

$$h^2 < 0.040$$

at the 95% confidence level. Even though omitting the anomalous quadrupole makes the situation cleaner (at least in the V band), this constraint is similar to Eq. (168). The reason is twofold. First, according to Eq. (148), the predicted statistical anisotropy spectrum C_L^q decreases with L as

$$C_L^q \propto \frac{2L+1}{(L-1)(L+2)} \ .$$

Second, the errors grow with the multipole number roughly as L, see Fig. 8.

With the Planck data available, we expect substantial improvement of the constraint (168). The reason is twofold. Hopefully, the quadrupole anomaly will be absent in the Planck data. Also, the range of the CMB multipoles useful in the analysis will be considerably extended. The error bars, whch can be roughly estimated by making use of the inverse Fisher matrix, scale with the number of multipoles as l_{max}^{-2}. This is clear from the Eq. (161). Taking, e.g., $l_{max} = 1200$, one would be able to reduce the error bars by about an order of magnitude. Hence, the non-observation of the statistical anisotropy will give the constraint as strong as $h^2 \lesssim 0.001$. We conclude that the statistical anisotropy is a promising signature from the viewpoint of the CMB observations in the case of the sub-scenario B.

Finally, we consider the sub-scenario A. To the linear order in constant h, the statistical anisotropy is of the general quadrupole type with decreasing amplitude, $a(k) \propto k^{-1}$. This fact is crucial for the search for the statistical anisotropy in the CMB sky. Indeed, the contribution to the signal $\delta\mathbf{S}$ is additionally suppressed by the CMB multipole number l. This suppression is due to the fact that the integral in Eq. (153) is saturated, roughly speaking, at $k \sim lH_0$. Effectively, it results in low statistics of the relevant CMB multipoles and large statistical errors, which severely restrict the opportunity to observe the (cosmological) statistical anisotropy of the type predicted. Somewhat loosely we apply the QML estimator to the seven-year WMAP data. In Fig. 11 we show the results for C_L^q of the WMAP reconstructed coefficients q_{LM}, assuming $a(k) = H_0 k^{-1}$, but not restricting yet to the quadrupole-only q_{LM}. We apply the procedure used in the case of the sub-scenario with the intermediate stage, to constrain the sub-scenario A; to this end, the quadrupole point $L = 2$ in Fig. 11 is relevant only. The limit on the parameter h^2 then reads

$$h^2 < 190$$

at the 95% confidence level. Note, however, that for large values of h^2, the QML procedure is questionable. This limit can be viewed merely as an indication that the leading order contribution to the statistical anisotropy is in fact negligible. The stronger constraint comes from the subleading contribution encoded in (150). The reason is that the amplitude $a(k)$ is independent of the wavenumber k in this case. Thus, the suppression at high CMB multipoles is absent, and the range of relevant l's is extended up to $l_{max} = 400$. Since the quantities q_{2M} are non-Gaussian in this particular case, the constraining procedure is somewhat different. First, we generate the components of the "velocity" $\mathbf{v}$ starting from a given value of the effective constant $h^2 \ln \frac{H_0}{\Lambda}$. Then, using (150), we calculate the coefficients q_{2M}. The quantity $C_2^q = \frac{1}{5}\sum_M |q_{2M}|^2$ constructed out of these q_{2M} is compared with the one estimated from the seven-year WMAP data. In this way we obtain the constraint, which reads

$$h^2 \ln \frac{H_0}{\Lambda} < 7 \tag{169}$$

at the 95% confidence level. Assuming that the logarithmic enhancement is not particularly

strong, we conclude that this constraint is still weak. Note also that the statistical anisotropy predicted by the sub-scenario A is of the same type as in some inflationary models [79, 81, 80, 82, 89]. Thus, it cannot be used to descriminate our model from other models of the generation of primordial perturbations. Fortunately, the sub-scenario A gives rise to the non-Gaussianity in the trispectrum [21, 22], which is in the sharp contrast with the inflationary predictions. We leave for the future search for the corresponding signatures in the CMB sky.

6.3 Low CMB multipoles alignment and parity asymmetry

It seems that the statistical anisotropy predicted by the conformal rolling scenario or the inflation, can be in principle large enough. Still, the direction dependence of the primordial power spectrum is unlikely to be the source of the strong correlations between the lowest multipoles. Up to the cosmic variance, the non-zero correlations in this case are only ones of the anisotropy coefficients a_{lm} with the multipole values l differing by some even number l. This is a quite generic statement, since it relies solely on the assumption of the Lorentz invariance inherent in the very early Universe models. If this holds, then the primordial physics fails to explain the strong quadrupole-octupole correlations detected first in [28] and further elaborated in [155, 135, 154]. Therefore, we turn to the study of the possible non-primordial sources of the statistical anisotropy. One's natural desire in this way is to give the unique explanation for two or more of the CMB anomalies. The model proposed in this Section, though being the subject of the future tests, addresses also the so called parity asymmetry detected recently in the WMAP data.

6.3.1 Uncounted foregrounds as the source of CMB anomalies

The potential contribution of foregrounds to the strong quadrupole-octupole alignment has been discussed widely in literature. In [38] it was concluded that the low multipoles are significantly contaminated by the foregrounds. The authors of the Ref. [133], however, result with the statement that the foregrounds are not statistically important to the large-scale modes of CMB. In particular, making use of the ILC maps does not change the situation significantly. Moreover, it is believed (see, e.g. [134]) that the true alignment is degraded by the foregrounds rather than created by the latter. There is, however, the loophole in this discussion. Namely, one should be aware of the situation, when some new foregrounds uncounted in the previous analyses can play a profound role in explaining the CMB anomalies. In this Section we argue that this might be the case of the Kuiper belt. We give a quantitative description of the Kuiper belt in the following Subsection. Here we just state that it can be modelled as a very symmetric foreground in the outer Solar System. An illustration is given in the Fig. 13, where the models of the Kuiper belt objects (hereafter, KBO) emmisivity are shown in Galactic and Ecliptic coordinates for different angular heights of

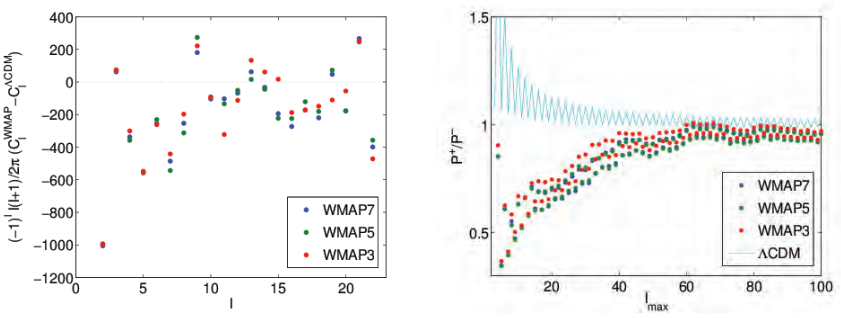

Figure 12: Left figure. $(-1)^l \times$difference between WMAP power spectrum data and ΛCDM model. Right figure. The estimator $g_p(l) \equiv \frac{P_+}{P_-}$ value of WMAP data and ΛCDM. These pictures are reproduced with the permission of the authors [35, 36]

the KBO, namely, $H = \pi/12, \pi/6$ and $7\pi/180$.

On the other hand, the residuals of the foregrounds are able to provide the explanation of the other CMB anomaly, i.e. the parity asymmetry. The latter is nothing but the preference of the odd multipoles upon the even ones in the CMB multipole range $2 \leq l \leq 23$ [36, 35] see also [148]. The estimator for testing the parity asymmetry has been proposed therein. It reads

$$g(l) \equiv \frac{P_+}{P_-} = \frac{\sum_{l_{min}}^{l_{max}} l(l+1)C(l)\Gamma^+(l)}{\sum_{l_{min}}^{l_{max}} l(l+1)C(l)\Gamma^-(l)} \,.$$

Applied to the WMAP data, it showed the odd preference exhibiting 4 maps out of 1000, see the Fig. 12. As claimed in the Ref. [154], the uncounted foregrounds, like emissivity of dust from the Kuiper belt, could explain the detected parity asymmetry of the CMB. The main idea of the method proposed in [136] is that a very symmetric foreground, when taken into account and subtracted from the WMAP whole-sky ILC map, could amplify the CMB power stored in even multipoles, increasing the parity parameter $g(l)$ (i.e. mitigating the observed parity asymmetry) for the multipole range $2 \leq l \leq 23$.

Besides the Kuiper belt, the other important ingredient of the model we consider in this Section, is the dipole modulation of the CMB sky. The evidence for a large-scale hemispherical asymmetry of the WMAP data was found first in [140] at the $95\% - 99\%$ confidence level depending on the range of multipoles under study. In what follows, we prefer to distinguish between the hemispherical asymmetry usually referred to the situation of the discontinuous jump in the power of the northern and southern hemispheres, and the dipole power asymmetry dealing with the smooth change of the power. Usually the data analysis techniques is applied to the second type of the anomaly. Thus, we specify to the latter in all our discussions in this Section. In this case, the large-scale CMB is assumed to

be of the form

$$T_{mod}(\mathbf{n}) = (1 + A(\mathbf{qn}))T_{unmod}(\mathbf{n}) \ ,$$

where A is the amplitude of the dipole modulation characterized by the unit vector $\mathbf{q}$.

The exact likelihood analysis of this anomaly has been made in [153, 150, 141], and recently the Refs. [152, 151] have extended the analysis of the dipole power asymmetry to the smaller angular scales arguing for the increased detection as more data is included. However, as it has been in the Ref. [117] by making use of the quadratic maximum likelihood method, the evidence for the dipole power asymmetry decreases at multipoles higher than $l > 60$. The results of the seven-year WMAP team are in the agreement with this statement [37]. This decrease is, however, not particularly important for us. We assume that the dipole modulation has the systematic rather than the primordial origin. In this case, it affects not only the primordial CMB signal but all the measurements of the foregrounds as well, including the Kuiper Belt.

6.3.2 Kuiper belt as a new foreground

Let us establish the main properties of the Kuiper belt on a bit more quantitative grounds. The blackbody-like radiation from the KBO affects the intensity of the microwave sky as follows:

$$I(\nu, \hat{\mathbf{r}}) = (B(\nu, T_{KBO}) - B(\nu, T_{CMB}))\tau(\hat{\mathbf{r}}) \ , \tag{170}$$

where ν is the observation frequency and $B(\nu, T)$ is the blackbody radiation spectrum at T, and $\tau(\hat{\mathbf{r}})$ is the optical depth of KBOs as the function of the direction on the sky $\hat{\mathbf{r}}$. The second term on the right hand side of the Eq. (170) arises from the occultation of the CMB photons by the KBO. The FIRAS data imposed the most stringent constraint on the sky-averaged optical depth of the KBOs, which reads $\tau \lesssim 3 \times 10^{-7}$ [156, 157, 158, 159].

The heating is mainly due to the radiation from the Sun. Therefore, it is possible to calculate the temperature of these objects at the equilibrium, assuming that it arises from the conversion of the solar radiation absorbed by the object into the microwave emission. At a distance of 40AU, where KBO's are most widely populated, we find an equilibrium temperatures of ~ 43.7K. Notably, the frequency spectrum of KBO's does not vary significantly within the range of the WMAP frequencies:

$$(f(\nu_K) - f(\nu_W))/f(\nu_K) \lesssim 0.22 \ ,$$

where $f(\nu)$ is the frequency spectrum of the Kuiper belt, ν_K and ν_W are the frequencies of the K- and W-bands, respectively. Therefore, the emisson may be confused with the intrinsic CMB anisotropy, even when the contribution to the microwave sky emission is sizeable. For the allowed values of the optical depth, $\tau \lesssim 3 \times 10^{-7}$, the KBO's may have an averaged effect on the CMB data as big as 15μK. Provided the KBO's have certain large-scale patterns,

KBO's may have an effect large enough to be the culprits of the reported large-scale CMB anomalies.

To investigate the emissivity of the Kuiper belt, we adopt the model of [136], where the Kuiper belt covers a symmetrical band in the Ecliptic plane of constant disk height H, with uniform temperature distribution. Following [136], we pick three models, defined by the angle $\pm H/2$ from the Ecliptic plane, where we choose $H_{KBO} = \pi/12, \pi/6$ and $7\pi/18$, respectively. For the three values of H_{KBO}, we set the temperature inside the Kuiper belt, so that it agrees with the upper bound of 15μK for the entire sky. In practice, we do this by the calculating the respective fractions of the total sky area, for each value of H_{KBO}, and finding the required temperature inside the band from the value:

$$T_{KBO}(\theta,\phi) = B\Theta\left[\theta - \frac{1}{2}(\pi - H)\right]\Theta\left[\frac{1}{2}(\pi + H) - \theta\right] ,$$

where B is the normalization constant and $\Theta(x)$ is the Heaviside-function. It is natural to use the average of the temperature of the KBO emission as normalization of B:

$$T_{KBO} = \frac{1}{4\pi}\int_0^{2\pi} d\phi \int_0^{\pi} d\theta \sin\theta T_{KBO}(\theta,\phi) = B\sin\left(\frac{H}{2}\right) .$$

Now, we decompose the KBO signal into spherical harmonics and get the following coefficients of decomposition

$$f_{lm} = \sqrt{\frac{(2l+1)}{4\pi}} B\Gamma^{+}(l)\delta_{m0}\int_{(\pi-H)/2}^{(\pi+H)/2} d\theta \sin\theta P_l\cos\theta .$$

For $H \ll \pi/2$ we can use the Taylor series representation: $P_l(x) \approx P_l(0) + \frac{1}{2}P_l''(0)x^2$. The first derivative vanishes for even $l = 2n$ due to the symmetry of the model. This gives

$$P_l(0) = \sqrt{\pi}\left[\Gamma\left(\frac{l}{2}+1\right)\Gamma\left(1/2 - l/2\right)\right]^{-1} , \quad P_l''(0) = -l(l+1)P_l(0) .$$

Here $\Gamma(x)$ is the Gamma-function. For $l(l+1)H^2/24 \ll 1$ one can get

$$f_{l,0} \approx \sqrt{\frac{2l+1}{\pi}} B\sin\left(\frac{H}{2}\right) P_l(0)\Gamma^{+}(l)\left[1 - \frac{l(l+1)}{24}H^2\right] .$$

Thus, for $l \ll 35\left(\frac{15}{H(deg)}\right)$ the coefficients of the expansion $f_{l,0}$ have the following analytical representation

$$f_{l0} \approx \sqrt{\frac{2l+1}{\pi}} T_{KBO}(-1)^n \frac{(2n-1)!!}{2^n n!} , \quad l = 2n .$$

In order to test the influence of the models on the lowest multipoles, we find the power spectrum for each value of H_{KBO} and compare them with the ILC power spectrum. The results are presented in Fig. 14. It is clear that for all 3 values the power of the KBO quadrupole is strong enough to affect the ILC quadrupole. For higher multipoles, $H_{KBO} = 15$ can affect the even multipoles up to $l = 19$.

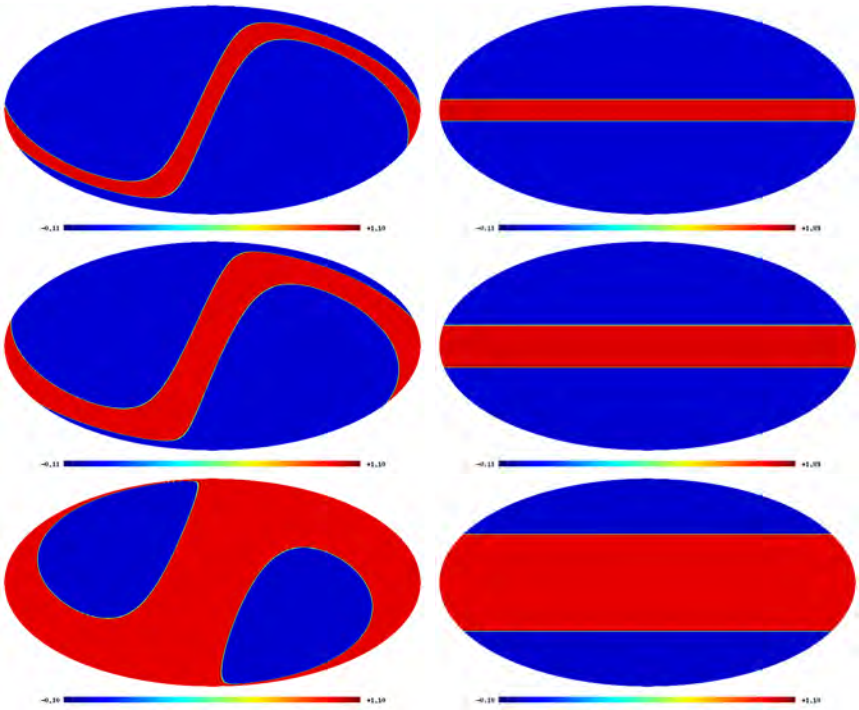

Figure 13: Left column. Model for the KBO emissivity distribution (arbitrary units) in Ecliptic coordinates for $H = \pi/12$ (top), for $H = \pi/6$ (the middle panel) and $H = 7\pi/18$ (the bottom panel). The same but in the Galactic coordinates is shown in the right column. All maps carry equal power.

6.3.3 Model of CMB-KBO cross-correlation

To assess the problem of a possible contamination of the ILC by the KBO-foreground, we will use the model of the CMB signal for a given direction on the sky $\mathbf{n}$:

$$T_c(\mathbf{n}) = T_{ILC}(\mathbf{n}) - [1 + A(\mathbf{qn})]\chi_{KBO}(\mathbf{n}) \ , \tag{171}$$

where $T_c(\mathbf{n})$ and $T_{ILC}(\mathbf{n})$ are the temperature of the intrinsic CMB signal and the ILC, $\chi_{KBO} \sim T_{KBO}(\mathbf{n})$ corresponds to the residuals of the KBO emmisivity. The second term in (171), the residuals of the KBO emmisivity is symmetric with respect to inversion: $\chi_{KBO}(\mathbf{n}) = \chi_{KBO}(-\mathbf{n})$, while the last term, dependent on the dipole, is anti-symmetric: $\epsilon(-\mathbf{n}) = -\epsilon(\mathbf{n})$. In the multipole domain, these two components contribute to the coefficients of the spherical harmonic decomposition additively:

$$a_{lm} = \hat{a}_{lm} - f_{lm}\Gamma^{+}(l) - \epsilon_{lm}\Gamma^{-}(l) \equiv \hat{a}_{lm} - \Pi_{lm} \ ,$$

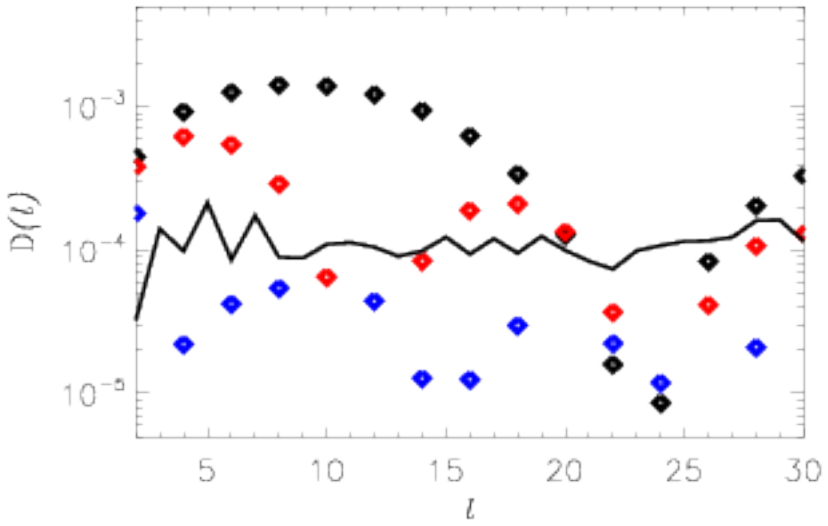

Figure 14: Power spectrum $D(l) = \frac{l(l+1)}{2\pi}C(l)$ (in units of mK) for the three KBO models, with $H = \pi/12$ (black), $\pi/6$ (red) and $7\pi/18$ (blue), compared to the ILC power spectrum (black line).

where a_{lm} is the primordial coefficient of decomposition. Coefficients ϵ_{lm} can be expressed as

$$\epsilon_{lm} = \sum_{m'=-1}^{1} \sum_{l''=0}^{\infty} \sum_{m''=-l''}^{l''} (-1)^m (b_{1m'} f_{l''m''}) = \sqrt{\frac{3(2l''+1)(2l+1)}{4\pi}} \begin{pmatrix} l'' & 1 & l \\ 0 & 0 & 0 \end{pmatrix} \begin{pmatrix} l'' & 1 & l \\ m'' & m' & -m \end{pmatrix} \tag{172}$$

Here b_{lm} relates to the parameters A and $\mathbf{n}$ by the relation $b_{lm} = \frac{4\pi A}{3} Y^{\star}_{lm}(\mathbf{n})$. As stated earlier, for the given model of the KBO we have $f_{lm} = f(l)\Gamma^{+}(l)\delta_{m0}$, and, thus, in Ecliptic coordinates can be simplified as follows:

$$\epsilon_{lm} = \sum_{m'=-1}^{1} \sum_{l''=2}^{\infty} (-1)^m \Gamma^{+}(l'') b_{1m'} f_{l''} = \sqrt{\frac{3(2l''+1)(2l+1)}{4\pi}} \begin{pmatrix} l'' & 1 & l \\ 0 & 0 & 0 \end{pmatrix} \begin{pmatrix} l'' & 1 & l \\ 0 & m' & -m \end{pmatrix} \tag{173}$$

6.3.4 Suppression of odd multipoles

We would like to show that our model can work if, and only if, the primordial CMB signal just by chance has a strong cross-correlations with uncounted foregrounds. For this purpose, let us define the coefficients of the cross-correlations between the ILC map and the Kuiper belt,

$$K(l) = \frac{\sum_m [a_{lm}\Pi^{\star}_{lm} + a^{\star}_{lm}\Pi_{lm}]}{2(\sum_m |a_{lm}|^2 \sum_{m'} |\Pi_{lm'}|^2)^{1/2}} \ . \tag{174}$$

and between the pure CMB signal and the Kuiper belt,

$$\zeta(l) = \frac{\sum_m [c_{lm}\Pi^{\star}_{lm} + c^{\star}_{lm}\Pi_{lm}]}{2(\sum_m |c_{lm}|^2 \sum_{m'} |\Pi_{l'm}|^2)^{1/2}} \ . \tag{175}$$

Starting from (174) and (175), one can define the power spectrum of the primordial CMB as:

$$C_p(l) = \frac{1}{2l+1} \sum_m |c_{lm}|^2 = V(l) C_{ilc}(l) \ ,$$

where $C_{ilc}(l)$ is the power of the ILC 7 map, and

$$V(l) = \frac{1 - K^2(l)}{1 - \zeta^2(l)} \tag{176}$$

is the factor of modulation of the ILC 7 power. Using (176), we can estimate the parity parameter for the primordial CMB as

$$g_p(l) = \frac{\sum_{m=2}^{l} n(n+1) V(n) \Gamma^{+}(n) C_{ilc}(n)}{\sum_{n=2}^{l} n(n+1) V(n) \Gamma^{-}(n) C_{ilc}(n)} \ .$$

In order to increase the contribution of even multipoles in parity parameter $g_p(l)$, the functions $V^{+}(l) = V(l)\Gamma^{+}(l)$ and $V^{-}(l) = V(l)\Gamma^{-}(l)$ should satisfy the following conditions: $V^{+}(l) \gg V^{-}(l)$. This means that there are only two variants: $\zeta^{+}(l) \to 1$ or $K^{-} \to 1$, where the $+$ and $-$ in the superscript symbolizes that the ζ or the K is drawn from either V^{+} or V^{-} respectively. The first case (with $|\zeta^{+}| \to 1$ and symmetric foreground) was discussed in [136], and it requires a significant coupling between the priomordial CMB and KBO-foreground. Due to clearly established non-Gaussian properties of the KBO foreground, a high correlation between it and the primordial CMB temperature anisotropy, is in contradiction with the assumption about a statistical isotropic and Gaussian intrinsic CMB signal. Thus, the improvement of the parity parameter by an increase of ζ^{+} loses its theoretical basis. In contrast, for $|\zeta^{\pm}| \ll 1$, the only way to increase $g_p(l)$, keeping the assumption about the Gaussianity and statistical isotropy of the intrinsic CMB signal, is to get $|K^{-}| \to 1$ and $K^{+} < 1$. That is a high correlation between the ILC signal and the KBO-foreground for odd

m	$Re^{l_3}(\hat{a}_{2m})$	$Im^{l_3}(\hat{a}_{2m})$	$Re^{l_5}(\hat{a}_{2m})$	$Im^{l_5}(\hat{a}_{2m})$
0	$1.3576 \cdot 10^{-2}$	0	$1.3576 \cdot 10^{-2}$	0
1	$-1.5904 \cdot 10^{-3}$	$-1.1121 \cdot 10^{-3}$	$-1.5904 \cdot 10^{-3}$	$-1.1121 \cdot 10^{-3}$
2	$-7.8456 \cdot 10^{-3}$	$-1.9363 \cdot 10^{-2}$	$-7.8456 \cdot 10^{-3}$	$-1.9363 \cdot 10^{-2}$
m	$Re^{l_3}(\hat{a}_{3m})$	$Im^{l_3}(\hat{a}_{3m})$	$Re^{l_5}(\hat{a}_{3m})$	$Im^{l_5}(\hat{a}_{3m})$
0	$-2.3688 \cdot 10^{-2}$	0	$-8.5516 \cdot 10^{-3}$	0
1	$-1.1804 \cdot 10^{-2}$	$5.4817 \cdot 10^{-3}$	$-1.4239 \cdot 10^{-2}$	$-8.4113 \cdot 10^{-3}$
2	$2.3844 \cdot 10^{-3}$	$5.0355 \cdot 10^{-3}$	$2.1783 \cdot 10^{-2}$	$-9.7430 \cdot 10^{-3}$
3	$-1.6411 \cdot 10^{-2}$	$2.0018 \cdot 10^{-2}$	$-2.8771 \cdot 10^{-3}$	$2.6001 \cdot 10^{-2}$

Table 1: Quadrupole and octupole temperature coefficients in two models with the different choice of the maximization of the parameter K.

multipoles, and at the same time, a relatively low correlation between the ILC signal and the KBO-foreground for even multipoles.

The contribution from the KBO emissivity into the coefficient of cross-correlations $K^- = K(l)\Gamma^-(l)$ is given by

$$K^-(l) = \frac{\sum_m [a_{lm}\epsilon^\star_{lm} + a^\star_{lm}\epsilon_{lm}]}{2(\sum_m |a_{lm}|^2 \sum_{m'} |\epsilon_{lm'}|^2)^{1/2}} \ .$$

As it follows from the formulas in the Appendix F, the coefficient of cross-correlations depends on the orientation of the dipole in the Ecliptic coordinates (Θ, Φ). Let us discuss one particular choice of Θ and Φ, which maximizes the coefficient of cross-corrlations $K_3 \equiv K^-(3)$. Let us show at the qualitative level, how the model resolves the quadrupole-octupole alignment. This is due to the coupling between even and odd components of ϵ_{lm}. In particular, the octupole component of ϵ_{lm} depends on the linear combination of the quadrupole and $l = 4$-components of f_{lm}. Due to the azimuthal symmetry of the KBO emissivity, these components have opposite phases. Thus, the coefficient of the KBO quadrupole and octupole cross-correlation depends only on Θ and Φ. Since the KBO quadrupole and octupole components could correlate with the corresponding components of the ILC, maximizing correlations between the ILC octupole and ϵ_{3m}, will provide the optimal way for a disalignment of the intrinsic quadrupole and octupole. As one can see from the Table 1, the phase of the $(3,1)$-th component of the octupole is $\phi_{3,1} = 1.227$, which means that in order to maximize the the K_3-coefficient, the azimuthal angle Φ should satisfy the following equation: $\Phi = -\phi_{3,1}$. Then, the coefficient of cross-correlations K_3 is given by

$$\begin{aligned} K_3(\Theta) &= \frac{a_{3,0} b \cos\Theta + 2|a_{3,1}| c \sin\Theta}{\sqrt{7C_3[b^2\cos^2\Theta + 2c^2\sin^2\Theta]}} \\ &= \Big(\frac{a^2_{3,0}b^2 + 4c^2|a_{3,1}|^2}{7C_3}\Big)^{1/2} \frac{\cos(\Theta - \eta)}{\sqrt{b^2\cos^2\Theta + 2c^2\sin^2\Theta}} \ , \end{aligned} \tag{177}$$

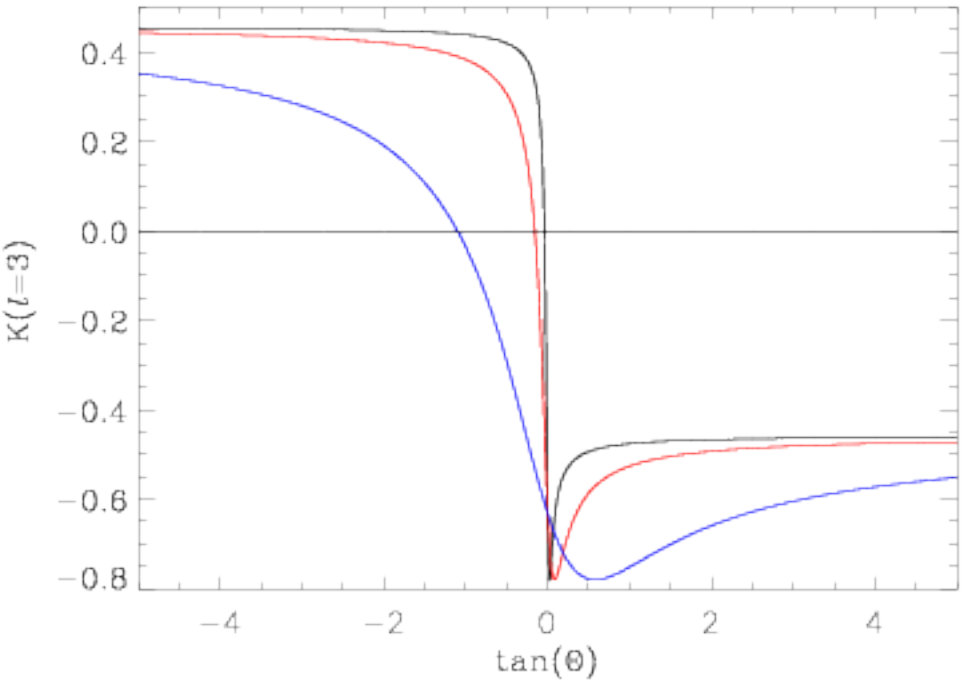

Figure 15: The coefficient $K_3(\Theta)$ versus $\tan(\Theta)$ in Ecliptic coordinates. Black line corresponds to $H = \pi/12$, the red line indicates the model with $H = \pi/6$, and the blue line corresponds to the model with the model with $H = 7\pi/18$.

where we used the following definitions: $\epsilon_{3,0} = b\cos\Theta$ and $|\epsilon_{3,1}| = c\sin\Theta$, and C_3 is the power of the ILC octupole and

$$\eta = \tan^{-1}\left(\frac{2|a_{3,1}|c}{a_{3,0}b}\right) .$$

As it follows from the Table 1, the amplitudes of the octupole in the Ecliptic coordinates are at the same order of magnitude, while the parameters b and c depend on the power spectrum of the Kuiper Belt angular anisotropy. This is why we will focus on two asymptotics, $|b| \gg |c|$, and $|b| \ll |c|$, in order to investigate the dependency of the cross-correlations on the particular choice of these parameters. In the case $|b| \gg |c|$, all the power of the ϵ_{lm}-signal would be concentrated at $m = 0$ mode, and

$$K_3(\Theta) \approx \frac{a_{30}}{\sqrt{7C_3}} \approx -0.65 , \quad \Theta \ll \frac{\pi}{2} .$$

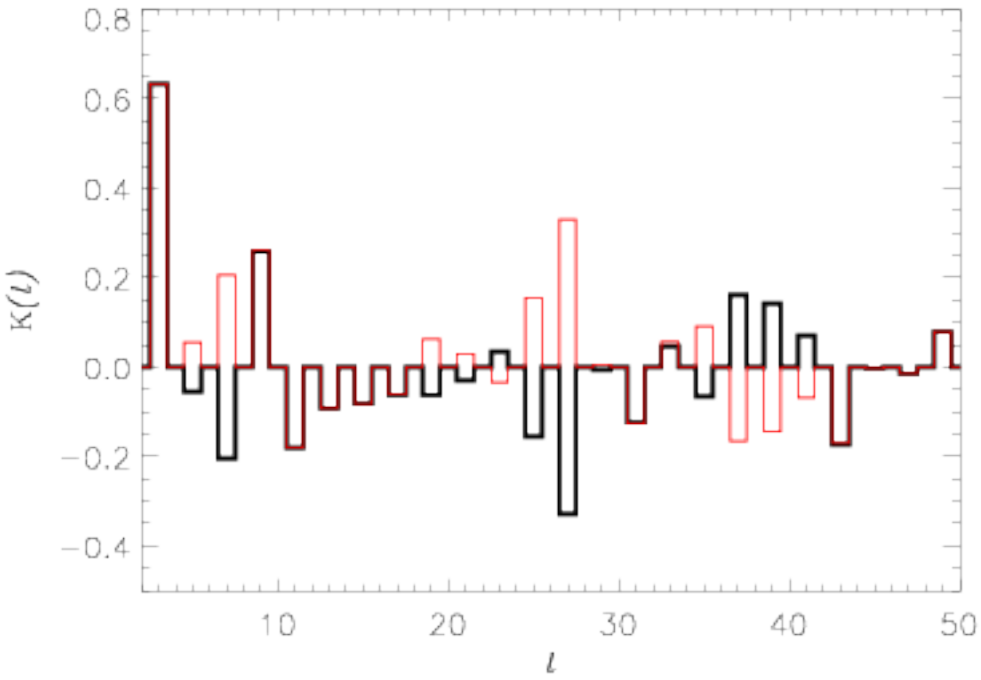

Figure 16: The coefficient $K_l^-(\Theta)$ versus l. Black line corresponds to $H = \pi/12$, and the red line indicates the model with $H = \pi/6$.

In the opposite case, when $|b| \gg |c|$, the coefficient of cross-correlation is given by

$$K_3(\Theta) \approx \frac{\sqrt{2}|a_{3,1}|}{\sqrt{7C_3}} \approx 0.46 \ , \quad \Theta \gg \tan^{-1}\left(\frac{a_{30}b}{2c|a_{31}|}\right)$$

Alternatively, one can minimize the power for the $l = 5$ multipole in the intrinsic CMB. The $l = 5$ mode of the power spectrum is one of the major sources of the parity asymmetry, as it is clearly seen in the Fig. 12. Again, we exploit the fact that only the $\epsilon_{5,0}$ and $\epsilon_{5,1}$ components of the modulation are non-zero. Taking under the consideration that the phase of the $(5,1)$-th component of the ILC 7 is $\phi_{5,1} = -2.23845$, we have adopted $\Phi = -\phi_{5,1}$ for the azimuthal angle Φ, maximizing the correlations between the $(5,1)$-th component of the ILC and $\epsilon_{5,1}$. Then, we obtain

$$K_5(\Theta) = \frac{a_{50}\mu\cos\Theta + 2|a_{51}|\nu\sin\Theta}{\sqrt{11C(l=5)[\mu^2\cos^2\Theta + 2\nu^2\sin^2\Theta]}} \ , \tag{178}$$

where $\epsilon_{50} = \mu\cos\Theta$ and $\epsilon_{51} = \nu\sin\Theta$ is the power of ILC and the $l = 5$ mode. From the Eq. (178), one finds that the maximum value of $K^-(l=5)(\Theta) \approx 0.28$ can be achieved, if $\Theta \approx \pi/2$.

	M_1	M_2	M_3	mean
Oct.-Quadr.(l_3)	0.1860	0.4433	0.4658	0.36505
Oct.-Quadr.(l_5)	0.41576	0.32210	0.3879	0.3752
Oct.-Quadr. (ilc)	0.7478	0.7037	0.7569	0.7361

Table 2: Quadrupole-octupole correlation estimated using the multipole vector analysis.

6.3.5 De-correlation of ILC and KBO

Now, we are in the position to discuss the possible changes in the morphology of the ILC map after removal of modulations, associated with the KBO emission. We will concentrate on one particular model of the KBO emission, $H = \pi/6$, using the model of the normalization from the previous Section.

We would like to point out that our de-correlation technique is generally unstable, since we cannot recover all the chance-correlations of the intrinsic CMB and KBO, which are sufficient for the low multipole range of the power spectrum. This is why de-correlation of the ILC and KBO could only demonstrate the tendency of the changes in the morphology of the ILC, pointing at some general properties of the reconstructed (de-correlated) signal. Assume that the intrinsic CMB associated with the de-correlated ILC map, has zero correlations with the KBO emmisivity map, which allows us to set $\zeta(l) = 0$. Now, taking the particular models for f_{lm} and ϵ_{lm}, we estimate the reconstructed signal from ILC 7, shown in the Figs. 17 and 18.

We now perform a test of the alignment between the quadrupole and octupole for the decorrelated CMB signals using the publicly available code from [142]. Our goal is to test the the orientation between the quadrupole and the octupole, and in particular to test the difference between the alignment for the pure ILC 7 and for our KBO-foreground cleaned maps. In [142], the authors introduce different approaches for comparing vectors associated with two different multipoles. We use the statistics of the oriented area, following the definition of [142], namely we consider the quantity

$$|\hat{v}^{l_1,i} \times \hat{v}^{l_1,j}|\big|\hat{v}^{l_2,k} \times \hat{v}^{l_2,m}| \ ,$$

That is, we cross the the i'th and the j'th vector from the multipole l_1, and the k'th and m'th vectors from the multipole l_2, before we take the dot product between these two surfaces. Values close to the unity are assotiated with a high level of alignment between two planes. Generally, for a given l_1 and l_2, and $i \neq j$ and $k \neq m$, there are $M = l_1(l_1-1)l_2(l_2-1)/4$ different products, meaning that for the comparison of the quadrupole and the octupole, we have three oriented areas, namely M_1, M_2 and M_3. In Table 2, we have summarized the result of the quadrupole-octupole alignment test for the de-correlated CMB signal, including the standard result for the ILC 7 map for the comparison. Clearly, for the KBO-foreground

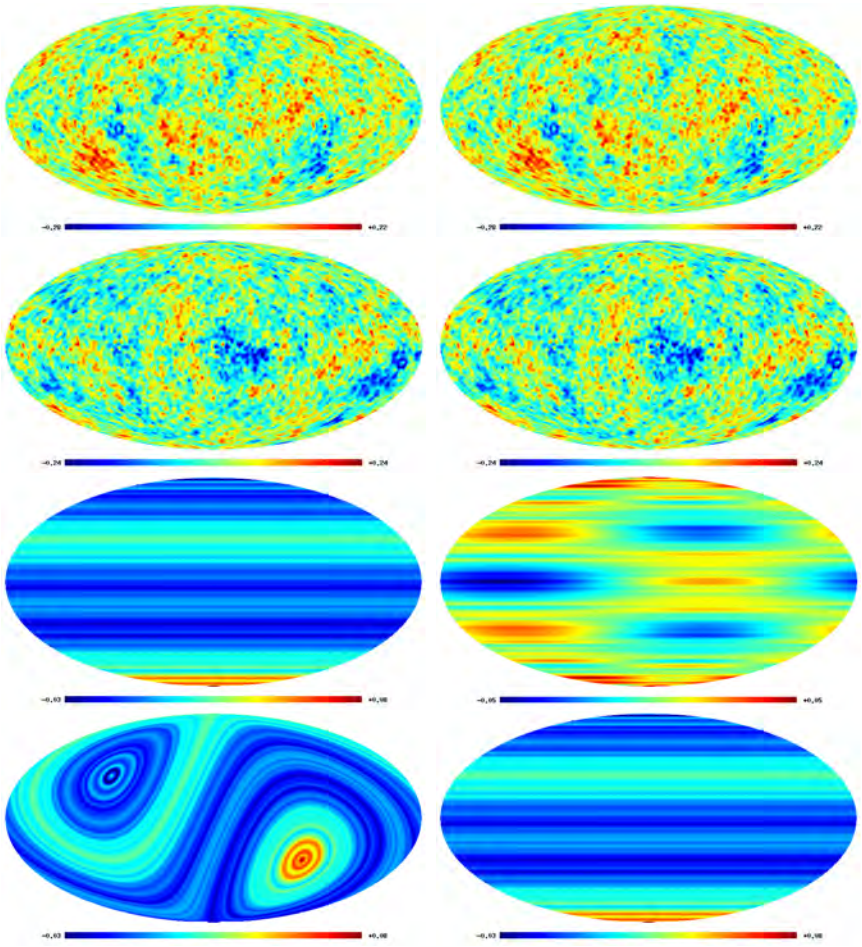

Figure 17: Left column. Reconstructed ILC for the model with $H = \pi/6$ (in Ecliptic coordinates, top panel). Second from the top is the same signal as the first, but in the Galactic coordinates. The second from the bottom panel, is the map of ILC modulated by the KBO (in Ecliptic coordinates). The bottom panel is the same map as above, just in Galactic coordinates. All the maps correspond to the normalization $\Theta = \pi, \Phi = -1.227$rad. Right column. The same as left, but for the normalization on the $l = 5$ harmonic with $\Theta = \pi/2, \Phi = 2.2384$rad.

cleaned map, we see significantly reduced alignments among the three oriented areas. In summary, when we remove the KBO contribution from the ILC signal, to reduce the the parity asymmetry, we see a weaker (statistically negligible) correlation between the quadrupole and the octupole, than in the case of the ILC 7 map.

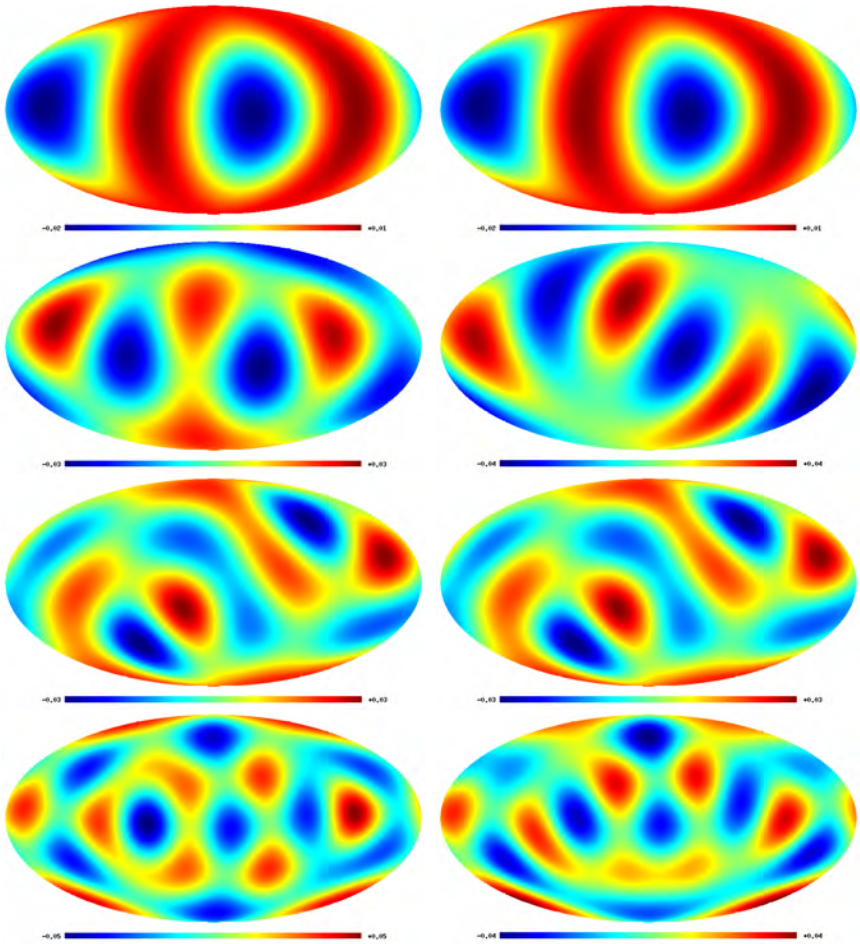

Figure 18: Left column. The map from the top left of the Fig. 17, but for $l = 2, 3, 4, 5$ (from the top to bottom). Right column. The map from the top right of the Fig. 17, but for $l = 2, 3, 4, 5$ (from the top to the bottom).

7 Conclusions

In the present thesis we mostly concentrated on theoretical and observational properties of the conformal rolling scenario. Basing on this particular example, one can show that conformal symmetries inherent in the underlying theory of Nature at very early times, can explain the flat spectrum of primordial scalar perturbations. In particular, the latter can be sourced by the phase perturbations of the conformal complex scalar field ϕ rolling down the negative quartic potential, $V(\phi) = -h^2|\phi^4|$. The coupling constant h is the unique parameter of the conformal rolling scenario, essentially unconstrained at the theoretical level, i.e. it can be as large as $h \sim 1$ and arbitrarily small. In the leading order, the predictions of the

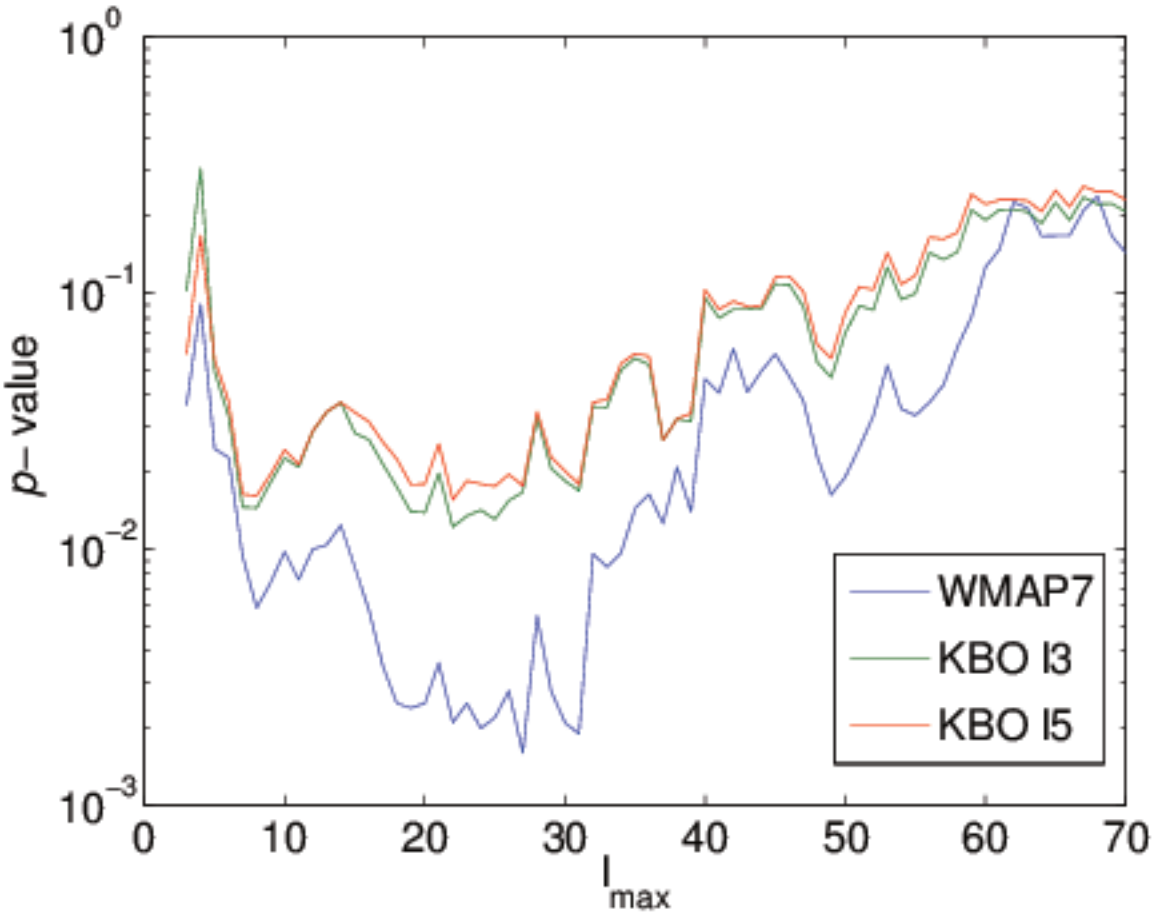

Figure 19: P-value for the reconstructed CMB in the model with $H = \pi/6$ and the normalization on the constant $l = 3$ (the green line), the normalization on $l = 5$ (the red line) and for ILC 7 map (the blue line).

conformal rolling scenario are ones of the minimal inflation, i.e. the flat spectrum and the Gaussianity of primordial scalar perturbations.

The degeneracy with the inflation is broken, once we account for the subleading orders in the coupling constant. The most interesting predictions of the conformal rolling scenario are the non-Gaussianity at the level of the trispectrum and the statistical anisotropy. The former is more prominent in the sub-scenario A, i.e. one with the cosmological modes superhorizon by the end of the conformal rolling. The distinctive feature of the trispectrum generated in this case as compared to predictions of the single-field inflation is the singularity in the folded limit. On the other hand, the statistical anisotropy is rather weak in the sub-scenario A being suppressed either by the momentum scale of the cosmological modes or by the

power of the constant h. The situation is different in the sub-scenario with cosmological modes subhorizon by the end of the conformal rolling. In that case, the evolution of the phase perturbations at the intermediate stage is required. This evolution with the initial conditions encoding the the dynamics at the conformal stage, results into the statistical anisotropy of all even multipoles starting from the quadrupole of the general type. This is in sharp contrast to predictions of inflation.

The deep insight into the conformal rolling scenario has been made from the positions of the (pseudo)-Conformal Universe, which we reviewed in this thesis. This is the novel picture of the cosmological evoltuion at very early times. Its main ingredient is the conformal symmetry spontaneously broken down to the de Sitter symmetry by the time-dependent background values of the conformal weight $\Delta \neq 0$ fields. The zeroth conformal weight fields evolving on this spontaneously broken background acquire the flat spectrum. Remarkably, the conformal rolling scenario and the Galilefn Genesis are just the particular realizations of this general idea. This, however, does not downgrade the predictions made in the simple model with the negative quartic potential. In particular, the statistical anisotropy and non-Gaussianity there are generic for a much broader class of models.

Basing on the prediction of the statistical anisotropy, we searched for the signatures of the conformal rolling scenario in the seven-year WMAP data. In particular, we repeated the result of the large statistical anisotropy quadrupole recently observed in the V and W channels of the five-year data. The anomalous quadrupole has been argued, however, to originate from the systematics rather than have the primordial origin. We estimated the parameter h^2 from the seven-year data and compared it with estimates obtained from the Monte–Carlo generated anisotropic maps. We resulted with the constrint $h^2 < 0.045$ at the 95% CL.

In this thesis, we also considered the statistical anisotropy of low CMB multipoles. The latter is unlikely to be explained by the primordial physics. The natural approach to the problem is to consider the uncounted foregrounds, e.g. the Kuiper belt. De-correlating the Kuiper belt and the seven-year ILC map, one can decrease the level of the quadrupole-octupole correlation. Simultaneously, the problem of the parity asymmetry is addressed, namely the de-correlation leads to the increase of even multipoles, thus mitigating the detected odd preference of low multipoles.

Now we are moving towards a very interesting epoch in cosmology, when predictions of very early Universe models will become the subject of the rigorous experimental tests. Hopefully, the forthcoming PLANCK data will shed the light on the origin of the Universe and/or the mechanism standing for the primordial perturbations creation.

Appendix A. Cosmological perturbation theory

Fixing the gauge

The results presented in this Appendix are very well-known and can be found in the reviews and textbooks [39, 40, 41, 42]. We prefer to use the books by Gorbunov and Rubakov [41, 42] as our guideline in what follows. The results of cosmological perturbation theory are quite generic and applied to study the evolution of perturbations during the Big Bang and at the earlier epochs (not necessarily inflation!). The qualification here is that the perturbations of the energy-momentum tensor $T^{\mu\nu}$ and the associated perturbations of the metric $g^{\mu\nu}$ are small enough, so that we can work in the linear approximation in these perturbations.

When study the cosmological perturbation theory, it is convenient to work in terms of the conformal time defined as $a(\eta)d\eta = dt$. In this case, the perturbed metric takes the form

$$g^{\mu\nu} = \frac{1}{a^2}(\eta^{\mu\nu} - h^{\mu\nu}) \ .$$

The indices of the metric excitation $h^{\mu\nu}$ are raised and lowered with the Minkowski metric $\eta^{\mu\nu}$. We also choose to work with the Fourier transform of the perturbation $h_{\mu\nu}(\mathbf{x})$,

$$h_{\mu\nu} = \int d^3k e^{i\mathbf{kx}} h_{\mu\nu}(\mathbf{k}) \ .$$

Now, let us fix the vector $\mathbf{k}$ and consider the rotations in the plane orthogonal to the vector $\mathbf{k}$. Since the background metric is invariant under spatial rotations, one can decompose the perturbation $h_{\mu\nu}$ into the irreducible representations of the rotation group $SO(2)$, namely

$$h_{00} = 2\Phi \ , \quad h_{0i} = ik_i Z + Z_i^T \ ,$$

$$h_{ij} = -2\Psi\delta_{ij} - 2k_i k_j E + i(k_i W_j^T + k_j W_i^T) + h_{ij}^{TT} \ ,$$

where Φ, Ψ, Z and E are the scalars with respect to the group of rotations, Z_i^T and W_i^T are vectors, while the transversal symmetric traceless structure h_{ij}^{TT} stands for the tensor perturbations. Not all of these degrees of freedom are physical. Some of them can be eliminated due to the invariance of the General Relativity under the transformations of the coordinates

$$x^\mu \to \tilde{x}^\mu = x^\mu + \zeta^\mu(x^\nu) \ ,$$

which induces the following transformation of the metric,

$$g^{\mu\nu} \to \tilde{g}^{\mu\nu} = g^{\mu\nu} + \nabla^\mu\zeta^\nu + \nabla^\nu\zeta^\mu \ .$$

Here $\zeta^\mu(x^\nu)$ is the arbitrary function of the space-time coordinates, and ∇^μ denotes the covariant derivative. The linear pertubation $h^{\mu\nu}$ then transforms as to

$$\tilde{h}_{\mu\nu} = h_{\mu\nu} + \partial_\mu\zeta_\nu + \partial_\nu\zeta_\mu + 2\eta_{\mu\nu}\zeta^\lambda\frac{\partial_\lambda a}{a} \ .$$

First, it is convenient to get rid off the functions Z and Z_i^T by applying the gauge

$$h_{0i} = 0 \; . \tag{179}$$

Still, we are free to perform the transformation with the function ζ_μ obeying the condition $\partial_i \zeta_0 + \partial_0 \zeta_i = 0$. Choosing in particular

$$\zeta_i = -\partial_i \sigma(\eta, \mathbf{x}), \quad \zeta_0 = \partial_0 \sigma(\eta, \mathbf{x}) \; ,$$

and taking $\sigma = E$, we eliminate the function E. This way of fixing the gauge freedom is known as the conformal Newtonian gauge, to which we specify in what follows, unless the opposite is stated. Let us write the metric perturbation in this gauge

$$h_{00} = 2\Phi \; , \quad h_{0i} = 0 \; ,$$

$$h_{ij} = -2\Psi + i(k_i W_j^T + k_j W_i^T) + h_{ij}^{TT} \; . \tag{180}$$

Still, we have the residual gauge freedom. Indeed, the gauge choice $\zeta_0 = 0$ and $\zeta_i = f_i(\mathbf{x})$ leaves the Newtonian gauge unaffected. We can use the residual gauge freedom to eliminate the vector modes. Note without the derivation that the latter are the pure gauge if not sourced by the matter, and, therefore, can be removed by the appropriate choice of the gauge function $f_i(\mathbf{x})$. In the opposite case, they rapidly fall with the scale factor a in the expanding Universe and quickly become negligible.

Linearized Einstein equations

For the future purposes, we need to obtain the linearized Einstein equations. The latter follow from the Einstein–Hilbert action and are given by

$$G_\nu^\mu = 4\pi G T_\nu^\mu \; ,$$

where $G^{\mu\nu}$ is the Einstein tensor,

$$G_\nu^\mu = R_\nu^\mu - \frac{1}{2}\delta_\nu^\mu R \; .$$

It is convenient to work with the (00)-th, the $(0i)$-th and the (ij)-th components of the Einstein equations separately, i.e. we write

$$\delta G_0^0 = 4\pi G \delta T_0^0 \; , \quad \delta G_i^0 = 4\pi G \delta T_i^0 \; , \quad \delta G_j^i = 4\pi G \delta T_j^i \; . \tag{181}$$

First, it is easy to linearize the energy-momentum tensor T_ν^μ. Assume that the latter is one of the perfect fluid,

$$T_\nu^\mu = (\rho + p) u^\mu u_\nu - \delta_\nu^\mu p \; .$$

Here $\rho = \rho_0 + \delta\rho$ and $p = p_0 + \delta p$ are the energy density and the pressure of the fluid; ρ_0 and p_0 are their background values, while $\delta\rho$ and δp are the linear perturbations. The 4-vector u^μ and u_μ are the 4-velocities, which unperturbed components are given by

$$\bar{u}^0 = \frac{1}{a} \, , \bar{u}_0 = a \, , u^i = u_i = 0 \, ,$$

while the linear perturbations are given by

$$u^0 = \frac{1}{a}(1 + \delta u^0) \, , u^i = \frac{1}{a} v^i \, .$$

In the linear approximation, the perturbation of the zeroth component of the 4-velocity, δu_0, is simply related to the perturbation of the (00)-th component of the metric, h_{00}. This follows from the normalization condition $g^{\mu\nu} u_\mu u_\nu = 1$, which gives

$$\delta u_0 = -\frac{1}{2} h_{00} \, .$$

The linear perturbation of the energy-momentum tensor reads

$$\delta T^0_0 = \delta\rho \, , \quad \delta T^0_i = -(\rho + p) v_i \, , \quad \delta T^i_j = -\delta^i_j \delta p \, . \tag{182}$$

It is convenient to decompose the velocity into the sum of the collinear and transverse components,

$$v_i = V^T_i + i k_i v \, .$$

The reason to perform this decomposition is that the transverse component of the velocity sources the vector modes of the metric perturbation, while the collinear part sources the scalar excitations. Note also that the energy-momentum tensor of the perfect fluid does not source the tensor modes.

To obtain the linearized Einstein equations, we also need to linearize the Einstein tensor in metric fluctuations. Note that in the linear approximation scalar, vector and tensor modes evolve independently from each other. First, we focus on the scalar sector. The linear perturbation of the Einstein tensor for the (00)-th, $(0i)$-th and (ij)-th components is given by

$$\begin{aligned}
\delta G^0_0 &= \frac{2}{a^2}\left(k^2\Psi + 3\frac{a'}{a}\Psi' - 3\frac{a'^2}{a^2}\Phi\right) \\
\delta G^0_i &= \frac{2}{a^2}\left(-ik_i\Psi' + \frac{a'}{a} ik_i \Phi\right) \qquad (183) \\
\delta G^i_j &= -\frac{1}{a^2} k_i k_j (\Phi + \Psi) - \frac{2}{a^2}\delta_{ij}\left[-\Psi'' - \frac{1}{2}k^2(\Phi + \Psi) + \frac{a'}{a}(\Phi' - 2\Psi') + 2\frac{a''}{a}\Phi - \frac{a'^2}{a^2}\Phi\right]
\end{aligned}$$

We can simplify these formulae if we note that the structure $k_i k_j$ present in the last equation of (183) is absent in the linearized energy-momentum tensor of the perfect fluid. Hence, in the approximation of the perfect fluid we have the following constraint,

$$\Phi = -\Psi \ .$$

Using the latter, we substitute (183) and (182) into the Eqs. (181) and obtain

$$k^2\Phi + 3\frac{a'}{a}\Phi' + 3\frac{a'^2}{a^2}\Phi = -4\pi G a^2 \delta\rho \quad (00) \tag{184}$$

$$\Phi' + \frac{a'}{a}\Phi = -4\pi G a^2 [(\rho + p)v] \quad (0i) \tag{185}$$

$$\Phi'' + 3\frac{a'}{a}\Phi' + \left(2\frac{a''}{a} - \frac{a'^2}{a^2}\right)\Phi = 4\pi G a^2 \delta p \quad (ij) \tag{186}$$

To complete this system of equations, one should also know the linearized energy-momentum tensor conservation. We split the latter as follows

$$\nabla^\nu T^0_\nu = 0 \ , \quad \nabla^\nu T^i_\nu = 0 \ .$$

Linearizing these two equations separately in metric and energy-momentum tensor perturbations, one has

$$\delta\rho' + 3\frac{a'}{a}(\delta\rho + \delta p) - (\rho + p)(k^2 v + 3\Phi') = 0 \tag{187}$$

and

$$[(\rho + p)v]' + 4\frac{a'}{a}(\rho + p)\Phi = 0 \ . \tag{188}$$

If we deal with the multi-component fluid, then the above equations hold for each component separately.

Since the tensor perturbations are not sourced by the matter, the Einstein equations in this case reads simply $\delta G^i_j = 0$, where the linearization over the tensor excitations is understood. Let us write the equation of motion for the tensor perturbations,

$$\partial^2_\eta h^{TT}_{ij} + 2\frac{a'}{a}\partial_\eta h^{TT}_{ij} - \Delta h^{TT}_{ij} = 0 \ .$$

It is convenient to expand the tensor perturbation h^{TT}_{ij} over the basic tensors e^A_{ij},

$$h^{TT}_{ij} = \sum_A e^A_{ij} h^A \ .$$

where h^A are the coordinates in the chosen basis. The tensors e^A_{ij}, $A = +, \times$, are constructed out of the unit vectors $\mathbf{e}^1_i$ and $\mathbf{e}^2_i$ orthogonal to each other and to the momentum $\mathbf{k}$,

$$e^+_{ij} = \frac{1}{\sqrt{2}}(e^1_i e^1_j - e^2_i e^2_j) \ ,$$

$$e_{ij}^{\times} = \frac{1}{\sqrt{2}}(e_i^1 e_j^2 + e_i^2 e_j^1) \ .$$

Further, one can build two linear combinations out of the vectors e_{ij}^A, i.e. $e_{ij}^{\pm 2}$ transforming under the rotations in the plane orthogonal to the momentum $\mathbf{k}$ as follows

$$e_{ij}^{\pm 2\prime} = e^{\pm 2i\alpha} e_{ij}^{\pm 2} \ ,$$

where α is the angle of the rotation. Clearly, the arbitrary transversal symmetric traceless tensor can be performed as the linear combination of the chirality-2 tensors. Note that the fields h^A are not the canonically normalized one. This is clear from the quadratic action for the tensor perturbations,

$$S_{TT} = \frac{1}{64\pi G} \int d^4x a^2 [(\partial_\eta h^A)^2 - \partial_k h^A \partial_k h^A] \ .$$

One can, however, define a new variable

$$\phi^A = \sqrt{\frac{M_{Pl}^2}{32\pi}} \ .$$

The action for the field ϕ^A is canonically normalized, and therefore it is a convenient variable to describe the evolution of tensor perturbations. This shows that the tensor h_{ij}^{TT} belongs to the irreducible represntation of the group $SO(2)$ and, thus, its evolution can be considered independently.

As pointed out earlier, vector modes can be safely omitted from our discussion. In particular, if the Universe is driven by the scalar field with the standard kinetic term, the corresponding energy-momentum tensor does not source vector modes at all, and the latter can be reduced by the appropriate gauge choice.

Adiabatic initial conditions

To solve the linearized Einstein equations supplemented by the linearized energy-momentum tensor conservation, one needs to know the initial conditions for this system. It is natural to separate the possible initial conditions into adiabatic and isocurvature ones. The former corresponds to the situation, when the Universe is described uniquely by the energy density ρ. In particular, the adiabaticity implies that the pressure is the unique function of the energy density, i.e. $p = p(\rho)$. Note, however, that the energy density perturbation is, generally speaking, gauge-dependent, and, thus, may not be the appropriate variable to describe adiabatic initial conditions. The gauge-independent description of the primordial perturbations has been established in the seminal article [43]. Shortly, we will turn to the gauge-independent description, but for the time being we specify to the Newton gauge.

Linearizing the pressure as the function of the energy density in the perturbation of the latter, one has

$$\delta p = \frac{dp}{d\rho}\delta\rho = \frac{p'}{\rho'}\delta\rho \ . \tag{189}$$

Substituting this into the linearized energy-momentum conservation law (187), one obtains

$$\Phi' = \frac{\delta\rho'}{3(\rho+p)} + \frac{a'}{a}\frac{\rho'+p'}{\rho+p}\delta\rho \ .$$

Then, using the conservation law for the unperturbed energy density,

$$\rho' + 3\frac{a'}{a}(\rho+p) = 0 \ ,$$

one obtains

$$\left(-\Phi + \frac{\delta\rho}{3(\rho+p)}\right)' = 0 \ .$$

From the latter it follows that the combination in the brackets is time-independent on the superhorizon scales. Commonly, this quantity denoted by ζ is written as follows

$$\zeta = \Psi - H\frac{\delta\rho}{\dot\rho} \ .$$

First it has been introduced in [8, 44]. Here we used the constraint $\Phi = -\Psi$ valid in the approximation of the perfect fluid. In literature, the quantity ζ is referred to as the curvature perturbation. The reason for this name will become clear shortly. In the case of the multi-component fluid, one can define the curvature perturbation ζ_λ for each component separately,

$$\zeta_\lambda = \Psi - H\frac{\delta\rho_\lambda}{\dot\rho_\lambda} \ . \tag{190}$$

Note that each ζ_λ is conserved on the superhorizon scales provided that the corresponding pressure is adiabatic, i.e.

$$\delta p_\lambda = \frac{p'_\lambda}{\rho'_\lambda}\delta\rho_\lambda \ .$$

The latter may be written as follows,

$$\delta\rho_\lambda = \rho'_\lambda\epsilon_\lambda \ ,$$
$$\delta p_\lambda = p'_\lambda\epsilon_\lambda \ ,$$

Further, the adiabaticity implies that the function ϵ_λ does not depend on the choice of the component, i.e. $\epsilon_\lambda = \epsilon$ is the unique function for all the components of the fluid. In this case, the function ϵ is related to the total energy density perturbation,

$$\epsilon = \frac{\delta\rho}{\rho'} \ .$$

In particular, this implies that the partial and the total curvature perturbations are equal between each other,

$$\zeta = \zeta_{\lambda_1} = ... = \zeta_{\lambda_n} \ . \tag{191}$$

Before we complete our discussion, let us prove that the curvature perturbation ζ is gauge-independent. To do that, let us turn from the Newtonian gauge to the gauge, where the energy density stays spatially constant at each time, but the condition $h_{0i} = 0$ is preserved. From the transformation law of the energy-momentum tensor,

$$\tilde{T}^{\mu\nu} = T^{\mu\nu} + \nabla^\mu \xi^\nu + \nabla^\nu \xi^\mu \ .$$

it follows that

$$(\rho + \tilde{\delta\rho})(\tilde{x}) = (\rho + \delta\rho)(x) \ .$$

Linearizing the latter we obtain

$$\tilde{\delta\rho}(x) = \delta\rho(x) - \rho' \xi^0 \ .$$

This fixes the transformation parameter ξ^0,

$$\xi^0 = \frac{\delta\rho}{\rho'} \ .$$

This transformation induces the non-zero $E(x)$ and also leads to the transformation of $\Psi(x)$, so that the latter takes the form

$$\tilde{\Psi} = \Psi + \frac{\delta\rho}{3(\rho + p)} \ .$$

Comparing the latter and the Eq. (190), we see that the curvature perturbation ζ coincided with the potential $\tilde{\Psi}$ evaluated on the hypersurface of the uniform density. Further we note without the derivation that the potential $\tilde{\Psi}$ defines the spatial curvature calculated on the corresponding hypersurfaces,

$$R^{(3)} = -\frac{4}{a^2}\Delta\zeta \ .$$

Here one important remark is in order. In literature it is quite common to use the quantity $\mathcal{R}$ defined by

$$\mathcal{R} = \Psi + \frac{a'}{a} v \ ,$$

where

$$v = \frac{\sum(\rho_\lambda + p_\lambda) v_\lambda}{\sum(\rho_\lambda + p_\lambda)} \ .$$

However, for the superhorizon modes the quantities ζ and $\mathcal{R}$ are equal. It follows from the linearized Einstein equations (184) and (185),

$$\zeta - \mathcal{R} = \frac{\delta\rho}{3(\rho + p)} - \frac{a'}{a} v = -\frac{1}{12\pi G a^2 (\rho + p)} k^2 \Phi \ .$$

This difference is negligibly small in the superhorizon regime, i.e. in the formal limit $k \to 0$.

Isocurvature initial conditions

Once the condition (191) is not satisfied, one deals with the adimixture of the isocurvature parturbations. It is convenient to define the set the isocurvature initial conditions in terms of the differences between the partial perturbations ζ_λ, namely,

$$S_{\lambda\lambda'} = 3(\zeta_\lambda - \zeta_{\lambda'}) \ .$$

Further, the natural chocie is to define the differences $S_{\lambda\lambda'}$ relatively to the dominant component, radiation at the conventional at the conventional hot epoch. It may happen so that the dominant component carries the negligible parturbation at the time, when the initial conditions are set, i.e. $\zeta_{tot} = 0$. In this case, one deals with the purely isocurvature perturbations. As it follows, the spatial curvature defined at the slices of the uniform energy density tends to zero in this situation, Hence, the name "isocurvature". We will encounter this situation in the context of the curvaton models and frameworks alternative to the inflation. Note that the separation of the initial conditions into the adiabatic and isocurvature ones is well motivated from the viewpoint of the CMB experiments. Starting from these two different types of the initial conditions, cosmological perturbations follow different evolution and, consequently, make the imprint on the CMB sky, which can be easily distinguished. Accordingly to the current experimantal data, the admixture of the isocurvature initial conditions is highly constrained. Thus, for the cosmological model to be successful, one should guarantee that the cosmological perturbations are of the adiabatic type at the beginning of the conventional hot epoch.

Application to single-field fluid

Basing on the cosmological perturbation theory, let us study the evolution of fluctuations in the Universe driven by the unique scalar field ϕ. Provided that the latter has the canonically normalized kinetic term, the energy-momentum tensor of the matter is fixed by the Eq.... . As usually, we employ the Newtonian gauge. With this choice, the metric takes the form

$$ds^2 = a^2(\eta)[(1+2\Phi)d\eta^2 - (1-2\Phi)d\mathbf{x}^2] \ ,$$

where we omit vector and tensor exitations, which can be considered separately. We linearize the energy-momentum tensor with respect to the perturbation φ of the scalar field ϕ,

$$\phi(\mathbf{x}, t) = \phi_c(t) + \varphi(\mathbf{x}, t) \ ,$$

where ϕ_c is the background value of the field ϕ, assumed to be spatially homogeneous. The (00)-th and the $(0i)$-th components of the energy-momentum tensor perturbation read

$$\delta T^0_0 \equiv \delta\rho = \frac{1}{a^2}[-\Phi {\phi'_c}^2 + \phi'_c\varphi'] + \frac{dV(\phi_c)}{d\phi_c}\varphi \tag{192}$$

and

$$\delta T^0_i = \frac{1}{a^2}\phi'_c\partial_i\varphi \ . \tag{193}$$

Comparing the latter equation with (182), we conclude that the spatial derivative of the inflaton perturbation is intimately related to the 3-velocity of the perfect fluid,

$$\frac{\partial_i\varphi}{\phi'_c} = -v_i = -\partial_i v \ ,$$

where v is the velocity potential. Now we substitute the Eqs. (192) and (193) into the linearized Einstein equations. The (00)-th component of these equations takes the form

$$\Delta\Phi - 3\frac{a'}{a}\Phi' - 3\frac{a'^2}{a^2}\Phi = -4\pi G{\phi'_c}^2\Phi + 4\pi G\left[\phi'_c\varphi' - \left(\phi''_c + 2\frac{a'}{a}\phi'_c\right)\varphi\right] \ , \tag{194}$$

where we make use of the equation of motion for the unperturbed inflaton field, which in the conformal time takes the form

$$\phi''_c + 2\frac{a'}{a}\varphi'_c + a^2\frac{dV}{d\phi_c} = 0 \ .$$

The (0i)-th Einstein equation is given by

$$\Phi' + \frac{a'}{a}\Phi = 4\pi G\phi'_c\varphi \ . \tag{195}$$

In further calculations we will also need the equation

$$\frac{a''}{a} - 2\frac{a'^2}{a^2} = -4\pi G(\rho + p)a^2 = -4\pi G{\phi'_c}^2 \ . \tag{196}$$

Using the latter, one can transform the first term in the right handside of the Eq. (194). Then, the latter takes the form

$$\Delta\Phi - 3\frac{a'}{a}\Phi' - \left(\frac{a''}{a} + \frac{a'^2}{a^2}\right)\Phi = 4\pi G[\phi'_c\varphi' - (\phi''_c + 2\frac{a'}{a}\phi'_c)] \ . \tag{197}$$

Then, using the Eq. (195), we express the potential Φ through Φ' and φ_c and substitute into the Eq. (197). Again making use of the Eq. (196), we obtain

$$\Delta\Phi = 4\pi G\frac{a}{a'}{\phi'_c}^2\frac{d}{d\eta}\left(\Phi + \frac{a'}{a\phi'_c}\varphi\right) \ . \tag{198}$$

The quantity in brackets,

$$-\mathcal{R} = \Phi - \frac{a'}{a}v = \left(\Phi + \frac{a'}{a\phi_c'}\varphi\right) \ .$$

has a very clear physical meaning. In fact, $\mathcal{R}$ is nothing but the spatial curvature of the hypersurface defined in the comoving gauge, $v_i = 0$ (or, in other words, at the spatially constant value of the inflaton field). This all motivates us to use the variable

$$\tilde{\phi} = \frac{u}{a} \ ,$$

$$u = -z\mathcal{R} \ , \quad z = \frac{a^2\phi_c'}{a'} \ .$$

In the literature, the guage-invariant quantity u is referred to as the Mukhanov–Sasaki variable [45]. With this notation, the Eq. (198) takes the form,

$$\Delta\Phi = 4\pi G\phi_c'\frac{z}{a}\frac{d}{d\eta}\left(\frac{u}{z}\right) \ . \tag{199}$$

while the $(0i)$-th Einstein equation is given by

$$\frac{a'}{a^2}\frac{d}{d\eta}\left(\frac{a^3}{a'}\Phi\right) = 4\pi G\phi_c' u \ . \tag{200}$$

Finally, we express the potential Φ from the Eq. (199) and substitute it into the Eq. (200). This gives us

$$u'' - \Delta u - \frac{z''}{z}u = 0 \ . \tag{201}$$

This simple formula will serve us to derive the dominating scalar perturbations generated in the Universe at very early stages.

Appendix B. Corrections to phase perturbations of order $\partial_i\partial_j\eta_\star/k$

In this Appendix we calculate phase perturbations of the conformal rolling scenario including corrections of the order $\partial_i\partial_j\eta_\star/k$. We employ the Eq. (62) from the main body of the thesis, where the classical background is replaced the modified one. We search for the solution in the following form,

$$\delta\chi_2^{(-)}(\mathbf{k},\mathbf{x},\eta) = e^{i\mathbf{k}\mathbf{x}-ik\eta_\star(\mathbf{x})-i\mathbf{k}\mathbf{v}[\eta_\star(\mathbf{x})-\eta]}\cdot\left[F(q,\eta_\star(\mathbf{x})-\eta) + F^{(2)}(q,\eta_\star(\mathbf{x})-\eta)\right] \ ,$$

where the leading term F is defined by and $F^{(2)}$ is propotional to $\partial_i\partial_j\eta_\star$. Substituting this ansatz into the Eq. (62), we obtain to the linear order,

$$F^{(2)\prime\prime} + k^2 F^{(2)} - \frac{2}{\zeta^2} F^{(2)} = \partial_i\partial_i\eta_\star \cdot S + k_i k_j \partial_i\partial_j\eta_\star \cdot T \ ,$$

where $\zeta = \eta_\star - \eta$,

$$S = -ikF + \frac{\partial F(k,\zeta)}{\partial\zeta} + \frac{2}{3\zeta} F \ ,$$

$$T = -2F\zeta - 2i\frac{\partial F(k,\zeta)}{\partial k} = -\frac{2}{k^2\zeta} e^{ik\zeta} \ .$$

The solution $F^{(2)}$ should vanish as $\eta_\star - \eta \to \infty$. Hence, it is given in terms of the retarded Green's function (recall that $\zeta' > \zeta$ corresponds to $\eta' < \eta$),

$$G(\zeta,\zeta') = \frac{\pi\sqrt{\zeta\zeta'}}{2}\Theta(\zeta'-\zeta)\cdot\left[J_{3/2}(k\zeta)N_{3/2}(k\zeta') - N_{3/2}(k\zeta)J_{3/2}(k\zeta')\right] \ , \qquad (202)$$

where $J_{3/2}$ and $N_{3/2}$ are the Bessel functions. Namely,

$$F^{(2)}(\zeta) = \int_\zeta^\infty d\zeta' G(\zeta',\zeta)\left[\partial_i\partial_i\eta_\star S(\zeta') + k_i k_j \partial_i\partial_j\eta_\star T(\zeta')\right].$$

We are interested in the behavior of this solution in the super-"horizon" regime, $k\zeta \to 0$. Since the most singular behavior of S and T at small ζ is ζ^{-2}, the first term in the Eq. (202) is irrelevant and can be safely omitted.

$$Im\mathrm{F}^{(2)T}|_{\zeta\to 0} = -\frac{\pi\sqrt{\zeta}}{2} N_{3/2}(k\zeta)\int_0^\infty d\zeta'\sqrt{\zeta'}J_{3/2}(k\zeta')\left(-\frac{2\sin k\zeta'}{k^2\zeta'}\right)k_i k_j\partial_i\partial_j\eta_\star = -\frac{\pi}{2}\frac{1}{k^2\zeta}\cdot\frac{k_i k_j}{k^2}\partial_i\partial_j\eta_\star$$

Performing similar calculation for S-term, we obtain that in the super-"horizon" regime

$$F + F^{(2)} = \frac{i}{q(\eta_\star - \eta)}\left(1 - \frac{\pi}{2k}\cdot\frac{k_i k_j}{k^2}\partial_i\partial_j\eta_\star + \frac{\pi}{6k}\partial_i\partial_i\eta_\star\right) \ .$$

Now we can write the expression for the phase perturbations in the super-"horizon" regime [20],

$$\delta\theta(\mathbf{x}) = \int\frac{d\mathbf{k}}{\sqrt{k}4\pi^{3/2}q}e^{i\mathbf{kx}-ik\eta_\star(\mathbf{x})}\left[1 - \frac{\pi}{2k}\frac{k_i k_j}{k^2}\partial_i\partial_j\eta_\star + \frac{\pi}{6k}\partial_i\partial_i\eta_\star\right]A_{\mathbf{k}} + h.c. \qquad (203)$$

The correction $\mathcal{O}\left(\partial_i\partial_j\eta_\star/k\right)$ in the brackets serves as the source of the statistical anisotropy in the sub-scenario A of the conformal rolling, i.e. one with the cosmologically interesting modes superhorizon in the conventional sense by the end of the conformal rolling.

Appendix C. Derivation of the formula (92)

In this Appendix we consider the Cauchy problem for the Eq. (86) with initial data specified at the hypersurface

$$f(y) = \eta - \eta_*(\mathbf{y}) = 0 \,, \tag{204}$$

where y denotes a point with coordinates $y^\mu = (\eta, \mathbf{y})$. We simplify the notation and use $\theta(x)$ instead of $\delta\theta(x)$.

Let $\tilde{\theta}(x)$ be the solution to the D'Alembert equation (86), such that $\tilde{\theta}(y)$ and $\partial_N\tilde{\theta}(y)$ coincide with the Cauchy data $\theta(y)$ and $\partial_N\theta(y)$ at the Cauchy hypersurface (hereafter ∂_N denotes the normal derivative). Let us introduce

$$\theta(x) = \tilde{\theta}(x)\cdot\Theta[f(x)] \,,$$

where Θ is a step function. Then

$$\Box\,\theta = \partial_\mu\tilde{\theta}\,\partial^\mu f\cdot\delta(f) + \partial_\mu[\tilde{\theta}\,\partial^\mu f\cdot\delta(f)]$$

and, therefore,

$$\theta(x) = \int d^4y \,\left\{ D^{ret}(x,y)\,\partial_\mu\theta(y)\,\partial^\mu f(y)\cdot\delta[f(y)] - \left[\frac{d}{dy^\mu}D^{ret}(x,y)\right]\theta(y)\,\partial^\mu f(y)\cdot\delta[f(y)]\right\} \,, \tag{205}$$

where we omitted tilde over θ in the right hand side, since the integration runs over the Cauchy hypersurface. The second term in the integrand is obtained by integration by parts. The formula (205) is nothing but the general formula (90), and $\partial_\mu\theta\,\partial^\mu f \propto \partial_N\theta$.

In the case of interest, the normal derivative vanishes at the Cauchy hypersurface, and the first term in the integrand in (205) is absent. We make use of (91) and write

$$\frac{d}{dy^\mu}D^{ret}(x,y) = -\frac{1}{\pi}(x_\mu - y_\mu)\delta'[(x-y)^2] \,.$$

We use the explicit form (204) of $f(y)$, integrate over η in (205) and obtain for $x = (\eta_1, \mathbf{x})$

$$\theta(x) = \frac{1}{\pi}\int d^3y \,\left[\eta_1 - \eta_*(\mathbf{y}) + \mathbf{v}(\mathbf{x}-\mathbf{y})\right]\theta(\mathbf{y})\,\delta'\left([\eta_1 - \eta_*(\mathbf{y})]^2 - (\mathbf{x}-\mathbf{y})^2\right) \,, \tag{206}$$

where $v_i = -\partial_i\eta_*(\mathbf{y})$ and $\theta(\mathbf{y}) \equiv \theta[\mathbf{y}, \eta_*(\mathbf{y})]$ is the field value at the Cauchy hypersurface. We now introduce the integration variable $\mathbf{r}$ via $\mathbf{y} = \mathbf{x} + \mathbf{r}$, write $\mathbf{r} = \mathbf{n}r$, where $\mathbf{n}$ is a unit vector, and cast the integral (206) into the following form:

$$\theta(x) = \frac{1}{\pi}\int d\Omega_{\mathbf{n}}\, r^2 dr \,\left[\eta_1 - \eta_*(\mathbf{x}+\mathbf{n}r) - \mathbf{n}\mathbf{v}r\right]\theta(\mathbf{x}+\mathbf{n}r)\,\delta'\left([\eta_1 - \eta_*(\mathbf{x}+\mathbf{n}r)]^2 - r^2\right) \,. \tag{207}$$

Here $\mathbf{v} = \mathbf{v}(\mathbf{x} + \mathbf{n}r)$. Finally, we make use of the identity

$$\delta'\left([\eta_1 - \eta_*(\mathbf{x}+\mathbf{n}r)]^2 - r^2\right) = -\frac{1}{2\left\{r - \mathbf{nv}[\eta_1 - \eta_*(\mathbf{x}+\mathbf{n}r)]\right\}}\frac{\partial}{\partial r}\delta\left([\eta_1 - \eta_*(\mathbf{x}+\mathbf{n}r)]^2 - r^2\right) \ ,$$

which is obtained by evaluating the derivative over r of $\delta\left([\eta_1 - \eta_*(\mathbf{x}+\mathbf{n}r)]^2 - r^2\right)$. Since $r \neq 0$ at the Cauchy hypersurface, we can integrate over r in (207) by parts. We also use the fact that

$$\delta\left([\eta_1 - \eta_*(\mathbf{x}+\mathbf{n}r)]^2 - r^2\right) = \frac{1}{2r(1-\mathbf{nv})}\delta[r - r(\mathbf{n})] \ , \tag{208}$$

where $r(\mathbf{n})$ is the solution to Eq. (93). We get

$$\theta(x) = \frac{1}{\pi}\int d\Omega_{\mathbf{n}} dr \ \frac{\partial}{\partial r}\left(\frac{r^2}{2\left\{r - \mathbf{nv}[\eta_1 - \eta_*(\mathbf{x}+\mathbf{n}r)]\right\}}[\eta_1 - \eta_*(\mathbf{x}+\mathbf{n}r) - \mathbf{nv}r]\,\theta(\mathbf{x}+\mathbf{n}r)\right)$$
$$\times \frac{1}{2r(1-\mathbf{nv})}\delta[r - r(\mathbf{n})] \ .$$

The integration over r is now straightforward, and we obtain after some algebra (note the cancellation of the terms with derivative $\partial\mathbf{v}(\mathbf{x}+\mathbf{n}r)/\partial r$)

$$\theta(x) = \frac{1}{4\pi}\int d\Omega_{\mathbf{n}}\left[\theta + \frac{1}{1-\mathbf{nv}}r\partial_r\theta\right] \ , \tag{209}$$

where in the right hand side one has $\theta = \theta(\mathbf{y}, \eta_*(\mathbf{y}))$ with $\mathbf{y} = \mathbf{x} + \mathbf{n}r$. Let us emphasize that (209) is the exact result for the Cauchy problem with $\partial_N\theta = 0$. At large r, the second term in the integrand dominates, and we arrive at the formula (92) used in the text.

For completeness, let us derive the general formula for the solution to the Cauchy problem with non-vanishing $\partial_N\theta$. With the Cauchy hypersurface defined by Eq. (204), the derivative along the unit normal is given by

$$\partial_N\theta = \gamma\partial_\mu\theta\,\partial^\mu f \ , \tag{210}$$

where $\gamma = (1-v^2)^{-1/2}$. This expression can be obtained by performing local boost

$$d\tau = \gamma(d\eta + \mathbf{v}d\mathbf{x}) \ , \quad \text{etc.}$$

Then τ is the time coordinate along the normal, and

$$\partial_N\theta = \partial_\tau\theta = \gamma(\partial_\eta\theta - v_i\partial_i\theta) \ ,$$

which is precisely (210). Making use of (210) and (91) we write the first term in (205) as follows,

$$\int d^3y\frac{1}{2\pi}\delta\left([\eta_1 - \eta_*(\mathbf{y})]^2 - (\mathbf{x}-\mathbf{y})^2\right)\frac{1}{\gamma}\partial_N\theta \ .$$

We proceed as before, again use (208) and obtain for this term

$$\frac{1}{4\pi}\int d\Omega_{\mathbf{n}}\ \frac{r}{\gamma(1-\mathbf{nv})}\partial_N\theta\ .$$

Thus, the complete expression for the solution to the Cauchy problem is

$$\theta(x)=\frac{1}{4\pi}\int d\Omega_{\mathbf{n}}\left[\theta+\frac{1}{1-\mathbf{nv}}r\left(\partial_r\theta+\sqrt{1-v^2}\partial_N\theta\right)\right]\ . \tag{211}$$

The notations here are the same as in (209).

Appendix D. Details of saddle point calculation

Saddle point $\mathbf{n}\approx\hat{\mathbf{k}}$

To find the saddle points of the integral (95), we solve Eq. (97) with $\partial\psi/\partial\mathbf{n}$ given by (98). To the linear order in h, the first saddle point is

$$\mathbf{n}_+=\hat{\mathbf{k}}+2[\mathbf{v}-\hat{\mathbf{k}}\cdot(\hat{\mathbf{k}}\mathbf{v})]$$

with

$$\lambda=1+2\,\hat{\mathbf{k}}\mathbf{v}\ . \tag{212}$$

Let us evaluate the contribution to the integral (95) coming from the saddle point region near $\mathbf{n}_+$. Let ϑ, φ be angular coordinates in the frame with the third axis along $\mathbf{n}_+$. Then

$$\mathbf{n}=\mathbf{n}_+ +\mathbf{n}^{(1)}+\mathbf{n}^{(2)}\ ,$$

where $\mathbf{n}^{(1)}$ and $\mathbf{n}^{(2)}$ are of the first and second order in ϑ, respectively,

$$\mathbf{n}^{(1)}=(\sin\vartheta\cos\varphi,\sin\vartheta\sin\varphi,0)\ ,$$
$$\mathbf{n}^{(2)}=(0,0,\cos\vartheta-1)\ .$$

We have

$$\psi(\mathbf{n})=\psi(\mathbf{n}_+)+\psi^{(2)}\ ,$$

where

$$\psi^{(2)}=\frac{\partial\psi}{\partial n_i}n_i^{(2)}+\frac{1}{2}\frac{\partial^2\psi}{\partial n_i\partial n_j}n_i^{(1)}n_j^{(1)}$$

and the derivatives are evaluated at $\mathbf{n}=\mathbf{n}_+$. The first derivative is given by Eqs. (97) and (212), while to the linear order in v and ∂v (i.e., linear order in h), the second derivative is

$$\frac{\partial^2\psi}{\partial n_i\partial n_j}=r(k_iv_j+k_jv_i)+r^2(\mathbf{kn}_+ +k)\partial_iv_j\ .$$

The angular integral is now straightforwardly evaluated (one first integrates over ϑ near $\vartheta = 0$ with weight $\vartheta d\vartheta$, then expands in v and ∂v and integrates over φ), and to the linear order in h one finds

$$ir \int \frac{d\Omega_{\mathbf{n}}}{4\pi} \mathrm{e}^{i\psi^{(2)}} = \frac{1}{2k}[1 - 2(\hat{\mathbf{k}}\mathbf{v})][1 + r(\delta_{ij} - \hat{k}_i\hat{k}_j)\partial_i v_j] \ .$$

The pre-exponential factor in (95) is to be evaluated at $\mathbf{n} = \mathbf{n}_+$. Collecting all factors, we get the contribution of the first saddle point (to the first order in h):

$$I_+ = \frac{1}{2}\mathrm{e}^{i\psi(\mathbf{n}_+)} \frac{1 + r \cdot (\delta_{ij} - \hat{k}_i\hat{k}_j)\partial_i v_j}{k + \mathbf{kv}} \ .$$

Note a non-trivial cancellation between $\mathbf{v}$-dependent terms in the pre-exponential factor. Finally, we recall that

$$\psi(\mathbf{n}_+) = \mathbf{k}\mathbf{n}_+\eta_1 - (\mathbf{k}\mathbf{n}_+ + k)\eta_*(\mathbf{x} + \mathbf{n}_+ r) = k\eta_1 - 2k\eta_*(\mathbf{x} + \hat{\mathbf{k}}r) \ ,$$

where we still work to the linear order in h. Since $\delta\eta_*$ and $\mathbf{v}$ are already of order h, their argument is merely $\mathbf{y}^{(+)} = \mathbf{x} + \hat{\mathbf{k}}r$. In this way we arrive at the first term in (99).

Second saddle point

The second saddle point is precisely at

$$\mathbf{n}_- = -\hat{\mathbf{k}}$$

(this is exact result valid to all orders in v). At this saddle point we have

$$\psi(\mathbf{n}_-) = -k\eta_1 \ .$$

The same calculation as above gives for the contribution of the second saddle point

$$I_- = \frac{1}{2}\mathrm{e}^{i\psi(\mathbf{n}_-)} \frac{1}{k + \mathbf{kv}} \ .$$

So, the second term in (99) is obtained in a very straightforward way.

Appendix E. Multipoles of statistical anisotropy.

The field $\delta\eta_*(\mathbf{x})$ is an isotropic Gaussian field. Therefore, the multipole coefficients in (104) are independent,

$$\langle q_{LM} q^*_{L'M'} \rangle = Q_l \delta_{lL'} \delta_{MM'} \ .$$

We make use of the expression (105) and calculate the sum $\sum_M \langle |q_{LM}|^2 \rangle$. Since $\langle \delta\eta_*(\mathbf{p}) \delta\eta_*^*(\mathbf{p}') \rangle \propto \delta(\mathbf{p} - \mathbf{p}')$, this sum has the following form:

$$\sum_M \langle |q_{LM}|^2 \rangle = \int d^3p \, \frac{\mathcal{P}_{\delta\eta_*}}{4\pi p^3} \sum_M |q_{LM}(\mathbf{p})|^2 \, . \tag{213}$$

The integrand here is independent of the direction of $\mathbf{p}$ and therefore can be calculated in any reference frame. To simplify formulas, we choose, somewhat loosely, a reference frame one step earlier, in the inner integral in (105), so we calculate $q_{LM}(\mathbf{p})$ in a $\mathbf{p}$-dependent frame. This procedure is legitimate as long as one calculates the sum in the right hand side of (213). We choose the spherical frame with $\mathbf{p}$ directed along the third axis and write

$$\begin{aligned} q_{LM}(\mathbf{p}) &= -i \int d\Omega \; Y^*_{LM}(\vartheta, \varphi) \cdot p \cos\vartheta \cdot (\mathrm{e}^{ipr\cos\vartheta} - \mathrm{e}^{-ipr\cos\vartheta}) \\ &= -i\delta_{M0} \sqrt{(2l+1)\pi} \int\limits_{-1}^{1} dt P_L(t) \cdot pt \cdot (\mathrm{e}^{iprt} - \mathrm{e}^{-iprt}) \, , \end{aligned} \tag{214}$$

where P_l are the Legendre polynomials, ϑ is the angle between the momenta $\mathbf{p}$ and $\mathbf{k}$ and $t = \cos\vartheta$. Since the integrand in (214) is symmetric under $t \to -t$ (this is a consequence of the symmetry of the power spectrum $\mathcal{P}_{\delta\theta}(\mathbf{k})$ under $\mathbf{k} \to -\mathbf{k}$, see (103)), odd multipoles vanish. In what follows we consider even $l \neq 0$.

The standard way of calculating the integral (214) is to make use of the expansion of the oscillating exponent in Legendre polynomials,

$$\mathrm{e}^{iprt} = \sum_{L'=0}^{\infty} (2L'+1) i^{L'} j_{L'}(pr) P_{L'}(t),$$

where j_L are spherical Bessel functions. We make use of the normalization of the Legendre polynomials,

$$\int_{-1}^{1} dt P_L(t) P_{L'}(t) = \frac{2}{2L+1} \delta_{LL'} \, ,$$

and recurrence relation

$$tP_{L'}(t) = \frac{L' P_{L'-1}(t) + (L'+1) P_{L'+1}(t)}{2L'+1} \, .$$

Then the integral (214) is straightforwardly evaluated,

$$q_{LM}(\mathbf{p}) = 2\delta_{M0} \sqrt{\frac{4\pi}{2L+1}} \, i^L \, p \left[(L+1) j_{L+1}(y) - L j_{L-1}(y) \right] \, ,$$

where

$$y = rp \, .$$

We now insert this result into (213), recall that the power spectrum of $\delta\eta_*$ is given by (57) and get

$$\sum_M \langle |q_{LM}|^2 \rangle = \frac{18h^2}{\pi(2L+1)} \int_0^\infty \frac{dy}{y} \left[(L+1) j_{L+1}(y) - L j_{L-1}(y) \right]^2 \ . \tag{215}$$

Finally, we recall the relationship between the spherical and conventional Bessel functions,

$$j_L(y) = \sqrt{\frac{\pi}{2y}} J_{L+\frac{1}{2}}(y)$$

and perform integration by using

$$\int_0^\infty J_\nu(y) J_\mu(y) y^{-\lambda} dy = \frac{\Gamma(\lambda)\Gamma\left(\frac{\nu+\mu-\lambda+1}{2}\right)}{2^\lambda \Gamma\left(\frac{-\nu+\mu+\lambda+1}{2}\right)\Gamma\left(\frac{\nu+\mu+\lambda+1}{2}\right)\Gamma\left(\frac{\nu-\mu+\lambda+1}{2}\right)} \ .$$

After straightforward algebra this yields

$$\sum_M \langle |q_{LM}|^2 \rangle = \frac{3h^2}{\pi} \frac{2L+1}{(L-1)(L+2)} \ , \quad \text{even} \quad L > 0 \ ,$$

or, equivalently, the quoted result (106).

It is worth noting that the relevant integration region in the integral (215) is $y \equiv pr \sim L$ (the spherical Bessel function $j_L(y)$ is exponentially small at $y \ll L$ and decays as y^{-1} at $y \gg L$). This means that our approximation $p \ll (k/r)^{1/2}$ is justified for $kr \gg 1$, unless L is very large.

Appendix F. Distortion of odd multipoles

The coefficients ϵ_{lm} corrsponfing to the dipole modulated part of the KBO emission are given by

$$\begin{aligned} \epsilon_{lm} &= A \cos\Theta [\alpha_1(l,m) f_{l+1,m} + \beta_1(l,m) f_{l-1,m}] \\ &+ (A/2) \sin\Theta e^{i\Theta} [\alpha_2(l,m) f_{l-1,m+1} - \\ &- \beta_2(l,m) f_{l+1,m+1}] \\ &+ (A/2) \sin\Theta e^{-i\Theta} [\alpha_3(l,m) f_{l+1,m-1} - \\ &- \beta_3(l,m) f_{l-1,m-1}] \ , \end{aligned} \tag{216}$$

where

$$\alpha_1(l,m) = \left(\frac{(l+m+1)(l-m+1)}{(2l+1)(2l+3)} \right)^{1/2} , \quad \beta_1(l,m) = \left(\frac{(l+m)(l-m)}{(2l+1)(2l-1)} \right)^{1/2} \ ,$$

$$\alpha_2(l,m) = \left(\frac{(l-m)(l-m-1)}{(2l+1)(2l-1)}\right)^{1/2}, \quad \beta_2(l,m) = \left(\frac{(l+m+1)(l+m+2)}{(2l+1)(2l+3)}\right)^{1/2},$$
$$\alpha_3(l,m) = \left(\frac{(l-m+1)(l-m+2)}{(2l+1)(2l+3)}\right)^{1/2}, \quad \beta_3(l,m) = \left(\frac{(l+m-1)(l+m)}{(2l+1)(2l-1)}\right)^{1/2}.$$

Here Θ and Φ are the coordinates of the dipole modulation in the ecliptic system of coordinates. and $f_{lm} = f_l\Gamma^+(l)\delta_{m0}$ is the KBO foreground. Due to the high symmetricity of the KBO foreground, coefficients ϵ_{lm} in the Eq. (216) have only three non-vanishing components with odd $l = 2n+1$ and $m = 0, \pm 1$. Namely,

$$\epsilon_{2n+1,0} = A\cos\Theta[\alpha_1(2n+1,0)f_{2n+2} + \beta_1(2n+1,0)f_{2n}],$$
$$\epsilon_{2n+1,1} = (A/2)\sin\Theta e^{-i\Phi}[\alpha_3(2n+1,1)f_{2n+2} - \beta_3(2n+1,1)f_{2n}],$$
$$\epsilon_{2n+1,-1} = (A/2)\sin\Theta e^{i\Phi}[\alpha_2(2n+1,-1)f_{2n} - \beta_2(2n+1,-1)f_{2n+2}],$$

where $l = 2n+1$ and

$$\alpha_3^2(l,1) = \beta_2^2(l,-1) = \frac{l(l+1)}{(2l+1)(2l+3)},$$
$$\beta_3^2(l,1) = \alpha_2^2(l,-1) = \frac{l(l+1)}{(2l+1)(2l-1)},$$
$$\alpha_1^2(l,0) = \frac{(l+1)^2}{(2l+1)(2l+3)}, \quad \beta_1^2(l,0) = \frac{l^2}{(2l+1)(2l-1)}.$$

References

[1] E. Komatsu *et al.* [WMAP Collaboration], Astrophys. J. Suppl. **192**, 18 (2011) [arXiv:1001.4538 [astro-ph.CO]].

[2] A. A. Starobinsky, JETP Lett. **30** (1979), 682; [Pisma Zh. Eksp. Teor. Fiz. **30** (1979), 719]; Phys. Lett. B **91** (1980), 99.

[3] V. F. Mukhanov and G. V. Chibisov, JETP Lett. **33** (1981), 532; [Pisma Zh. Eksp. Teor. Fiz. **33** (1981), 549].

[4] A. H. Guth, Phys. Rev. D **23** (1981), 347.

[5] A. D. Linde, Phys. Lett. B **108** (1982) 389.
A. Albrecht and P. J. Steinhardt, Phys. Rev. Lett. **48** (1982), 1220.

[6] A. D. Linde, Phys. Lett. B **129** (1983) 177.

[7] S. W. Hawking, Phys. Lett. B **115** (1982), 295.
A. A. Starobinsky, Phys. Lett. B **117** (1982), 175.
A. H. Guth and S. Y. Pi, Phys. Rev. Lett. **49** (1982), 1110.

[8] J. M. Bardeen, P. J. Steinhardt and M. S. Turner, Phys. Rev. D **28** (1983), 679.

[9] L. Kofman, A. D. Linde and A. A. Starobinsky, Phys. Rev. Lett. **73** (1994) 3195 [hep-th/9405187].
L. Kofman, A. D. Linde and A. A. Starobinsky, Phys. Rev. D **56** (1997) 3258 [hep-ph/9704452].

[10] M. Gasperini and G. Veneziano, Phys. Rept. **373** (2003) 1 [hep-th/0207130].

[11] N. Arkani-Hamed, H. -C. Cheng, M. A. Luty and S. Mukohyama, JHEP **0405** (2004) 074 [hep-th/0312099].

[12] A. Adams, N. Arkani-Hamed, S. Dubovsky, A. Nicolis and R. Rattazzi, JHEP **0610** (2006) 014 [hep-th/0602178].

[13] P. Creminelli, M. A. Luty, A. Nicolis and L. Senatore, JHEP **0612** (2006) 080; hep-th/0606090.

[14] E. I. Buchbinder, J. Khoury and B. A. Ovrut, Phys. Rev. D **76** (2007) 123503; hep-th/0702154.
P. Creminelli and L. Senatore, JCAP **0711** (2007) 010; hep-th/0702165.

[15] J. Khoury, B. A. Ovrut, P. J. Steinhardt and N. Turok, Phys. Rev. D **64** (2001) 123522; hep-th/0103239.
J. Khoury, B. A. Ovrut, N. Seiberg, P. J. Steinhardt and N. Turok, Phys. Rev. D **65** (2002) 086007; hep-th/0108187.

[16] V. A. Belinsky, I. M. Khalatnikov and E. M. Lifshitz, Adv. Phys. **19** (1970) 525.

[17] J. K. Erickson, D. H. Wesley, P. J. Steinhardt and N. Turok, Phys. Rev. D **69** (2004) 063514; hep-th/0312009.
D. Garfinkle, W. C. Lim, F. Pretorius and P. J. Steinhardt, Phys. Rev. D **78** (2008) 083537; arXiv:0808.0542 [hep-th].

[18] V. A. Rubakov, JCAP **0909** (2009), 030; arXiv:0906.3693 [hep-th].

[19] V. Rubakov and M. Osipov, arXiv:1007.3417 [hep-th].

[20] M. Libanov and V. Rubakov, JCAP **1011** (2010), 045; arXiv:1007.4949 [hep-th].

[21] M. Libanov, S. Mironov and V. Rubakov, arXiv:1012.5737 [hep-th].

[22] M. Libanov, S. Mironov and V. Rubakov, Phys. Rev. D **84** (2011) 083502 [arXiv:1105.6230 [astro-ph.CO]].

[23] M. Libanov, S. Ramazanov and V. Rubakov, JCAP **1106** (2011) 010 [arXiv:1102.1390 [hep-th]].

[24] I. Antoniadis, P. O. Mazur and E. Mottola, Phys. Rev. Lett. **79** (1997) 14 [arXiv:astro-ph/9611208].

[25] P. Creminelli, A. Nicolis and E. Trincherini, JCAP **1011**, 021 (2010); arXiv:1007.0027 [hep-th].

[26] K. Hinterbichler and J. Khoury, arXiv:1106.1428 [hep-th].

[27] J. M. Maldacena, JHEP **0305** (2003) 013 [astro-ph/0210603].

[28] M. Tegmark, A. de Oliveira-Costa and A. Hamilton, Phys. Rev. D **68** (2003) 123523 [arXiv:astro-ph/0302496].

[29] P. Bielewicz, H. K. Eriksen, A. J. Banday, K. M. Gorski and P. B. Lilje, Astrophys. J. **635** (2005) 750 [arXiv:astro-ph/0507186].

[30] C. J. Copi, D. Huterer, D. J. Schwarz and G. D. Starkman, Mon. Not. Roy. Astron. Soc. **367** (2006) 79 [arXiv:astro-ph/0508047].

[31] K. Land and J. Magueijo, Phys. Rev. Lett. **95** (2005) 071301 [arXiv:astro-ph/0502237].

[32] F. K. Hansen, A. J. Banday, K. M. Gorski, H. K. Eriksen and P. B. Lilje, Astrophys. J. **704** (2009) 1448 [arXiv:0812.3795 [astro-ph]].

[33] H. K. Eriksen, F. K. Hansen, A. J. Banday, K. M. Gorski, and P. B. Lilje, Astrophys. J. **605**, 14 (2004), [arXiv:0307507 [astro-ph]].

[34] M. Cruz, L. Cayon, E. Martinez-Gonzalez, P. Vielva and J. Jin, Astrophys. J. **655** (2007) 11 [arXiv:astro-ph/0603859].

[35] J. Kim and P. Naselsky, Phys. Rev. D **82** (2010) 063002 [arXiv:1002.0148 [astro-ph.CO]].

[36] J. Kim and P. Naselsky, Astrophys. J. **714** (2010) L265 [arXiv:1001.4613 [astro-ph.CO]].

[37] C. L. Bennett, R. S. Hill, G. Hinshaw, D. Larson, K. M. Smith, J. Dunkley, B. Gold and M. Halpern *et al.*, Astrophys. J. Suppl. **192** (2011) 17 [arXiv:1001.4758 [astro-ph.CO]].

[38] L. -Y. Chiang, P. D. Naselsky and P. Coles, Mod. Phys. Lett. A **23** (2008) 1489 [arXiv:0711.1860 [astro-ph]].

[39] V. F. Mukhanov, H. A. Feldman and R. H. Brandenberger, Phys. Rept. **215** (1992) 203.

[40] V. Mukhanov, Cambridge, UK: Univ. Pr. (2005) 421 p

[41] D. S. Gorbunov and V. A. Rubakov, Hackensack, USA: World Scientific (2011) 473 p

[42] D. S. Gorbunov and V. A. Rubakov, Hackensack, USA: World Scientific (2011) 489 p

[43] J. M. Bardeen, Phys. Rev. D **22** (1980) 1882.

[44] J. M. Bardeen, DOE/ER/40423–01-C8 *Lectures given at 2nd Guo Shou-jing Summer School on Particle Physics and Cosmology, Nanjing, China, Jul 1988.*

[45] M. Sasaki, Prog. Theor. Phys. **76** (1986) 1036.
V. F. Mukhanov, Sov. Phys. JETP **67** (1988) 1297 [Zh. Eksp. Teor. Fiz. **94N7** (1988) 1].

[46] S. Mollerach, Phys. Rev. D **42**, 313 (1990);
A. D. Linde and V. F. Mukhanov, Phys. Rev. D **56** (1997), 535 [arXiv:9610219 [astro-ph]];
K. Enqvist and M. S. Sloth, Nucl. Phys. B **626** (2002), 395 [arXiv:0109214 [hep-ph]];
T. Moroi and T. Takahashi, Phys. Lett. B **522** (2001), 215 [Erratum-ibid. B **539** (2002), 303] [arXiv:0110096 [hep-ph]];

[47] D. H. Lyth and D. Wands, Phys. Lett. B **524** (2002), 5 [arXiv:0110002 [hep-ph]];

[48] K. Dimopoulos, D. H. Lyth, A. Notari and A. Riotto, JHEP **0307**, (2003), 053; hep-ph/0304050.

[49] D. H. Lyth, C. Ungarelli and D. Wands, Phys. Rev. D **67** (2003) 023503 [astro-ph/0208055].

[50] K. A. Malik, D. Wands and C. Ungarelli, Phys. Rev. D **67** (2003) 063516 [astro-ph/0211602].

[51] N. Bartolo, E. Komatsu, S. Matarrese and A. Riotto, Phys. Rept. **402** (2004) 103 [astro-ph/0406398].

[52] T. J. Allen, B. Grinstein and M. B. Wise, Phys. Lett. B **197** (1987) 66. T. Falk, R. Rangarajan and M. Srednicki, Astrophys. J. **403** (1993) L1 [astro-ph/9208001].

[53] A. Gangui, Phys. Rev. D **50** (1994) 3684 [astro-ph/9406014]. A. Gangui, F. Lucchin, S. Matarrese and S. Mollerach, Astrophys. J. **430** (1994) 447 [astro-ph/9312033].

[54] D. Babich, P. Creminelli and M. Zaldarriaga, JCAP **0408** (2004) 009 [astro-ph/0405356].

[55] G. Dvali, A. Gruzinov and M. Zaldarriaga, Phys. Rev. D **69** (2004), 023505; astro-ph/0303591.
L. Kofman, astro-ph/0303614.

[56] G. Dvali, A. Gruzinov and M. Zaldarriaga, Phys. Rev. D **69** (2004), 083505; astro-ph/0305548.

[57] F. Bernardeau and J. -P. Uzan, Phys. Rev. D **66** (2002) 103506 [hep-ph/0207295].

[58] P. Creminelli, JCAP **0310** (2003) 003 [astro-ph/0306122].

[59] C. Armendariz-Picon, T. Damour and V. F. Mukhanov, Phys. Lett. B **458** (1999) 209 [hep-th/9904075].

[60] N. Arkani-Hamed, P. Creminelli, S. Mukohyama and M. Zaldarriaga, JCAP **0404** (2004) 001 [hep-th/0312100].

[61] E. Silverstein and D. Tong, Phys. Rev. D **70** (2004) 103505 [hep-th/0310221].
M. Alishahiha, E. Silverstein and D. Tong, Phys. Rev. D **70** (2004) 123505 [hep-th/0404084].

[62] R. Holman and A. J. Tolley, JCAP **0805** (2008) 001 [arXiv:0710.1302 [hep-th]].

[63] P. Creminelli and M. Zaldarriaga, JCAP **0410** (2004) 006 [astro-ph/0407059].

[64] N. Bartolo, M. Fasiello, S. Matarrese and A. Riotto, JCAP **1009** (2010) 035 [arXiv:1006.5411 [astro-ph.CO]].

[65] T. Okamoto and W. Hu, Phys. Rev. D **66** (2002) 063008 [astro-ph/0206155].

[66] N. Kogo and E. Komatsu, Phys. Rev. D **73** (2006) 083007 [astro-ph/0602099].

[67] D. Seery, M. S. Sloth and F. Vernizzi, JCAP **0903** (2009) 018 [arXiv:0811.3934 [astro-ph]].
D. Seery, J. E. Lidsey and M. S. Sloth, JCAP **0701** (2007) 027 [astro-ph/0610210].
D. Seery and J. E. Lidsey, JCAP **0701** (2007) 008 [astro-ph/0611034].

[68] X. Gao, M. Li and C. Lin, JCAP **0911** (2009) 007 [arXiv:0906.1345 [astro-ph.CO]].
X. Gao and C. Lin, JCAP **1011** (2010) 035 [arXiv:1009.1311 [hep-th]]. S. Mizuno, F. Arroja and K. Koyama,
Phys. Rev. D **80** (2009) 083517 [arXiv:0907.2439 [hep-th]]. X. Chen, M.-x. Huang and G. Shiu, Phys. Rev. D **74** (2006) 121301 [hep-th/0610235].
F. Arroja and K. Koyama, Phys. Rev. D **77** (2008) 083517 [arXiv:0802.1167 [hep-th]].
F. Arroja, S. Mizuno, K. Koyama and T. Tanaka, Phys. Rev. D **80** (2009) 043527 [arXiv:0905.3641 [hep-th]].
K. Izumi and S. Mukohyama, JCAP **1006** (2010) 016 [arXiv:1004.1776 [hep-th]].

[69] X. Chen, B. Hu, M. -x. Huang, G. Shiu and Y. Wang, JCAP **0908** (2009) 008 [arXiv:0905.3494 [astro-ph.CO]].

[70] C. Cheung, P. Creminelli, A. L. Fitzpatrick, J. Kaplan and L. Senatore, JHEP **0803** (2008) 014 [arXiv:0709.0293 [hep-th]].

[71] C. Cheung, A. L. Fitzpatrick, J. Kaplan and L. Senatore, JCAP **0802** (2008) 021 [arXiv:0709.0295 [hep-th]].

[72] S. Weinberg, Phys. Rev. D **77** (2008) 123541 [arXiv:0804.4291 [hep-th]].

[73] K. M. Smith, L. Senatore and M. Zaldarriaga, JCAP **0909** (2009) 006 [arXiv:0901.2572 [astro-ph]].

[74] L. Senatore and M. Zaldarriaga, JHEP **1204** (2012) 024 [arXiv:1009.2093 [hep-th]].

[75] P. Creminelli, G. D'Amico, M. Musso, J. Norena and E. Trincherini, JCAP **1102** (2011) 006 [arXiv:1011.3004 [hep-th]].

[76] A. E. Gumrukcuoglu, C. R. Contaldi and M. Peloso, arXiv:astro-ph/0608405; JCAP **0711** (2007) 005; 0707.4179 [astro-ph].

[77] R. M. Wald, Phys. Rev. D **28** (1983) 2118.

[78] A. Maleknejad and M. M. Sheikh-Jabbari, Phys. Rev. D **85** (2012) 123508 [arXiv:1203.0219 [hep-th]].

[79] L. Ackerman, S. M. Carroll and M. B. Wise, Phys. Rev. D **75** (2007) 083502 [Erratum-ibid. D **80** (2009) 069901]; astro-ph/0701357.

[80] S. Yokoyama and J. Soda, JCAP **0808** (2008) 005 [arXiv:0805.4265 [astro-ph]].

[81] M. A. Watanabe, S. Kanno and J. Soda, Phys. Rev. Lett. **102** (2009) 191302; arXiv:0902.2833 [hep-th]; Prog. Theor. Phys. **123**, 1041 (2010); arXiv:1003.0056 [astro-ph.CO].

[82] J. Soda, arXiv:1201.6434 [hep-th].

[83] L. Parker, Phys. Rev. Lett. **21** (1968) 562.

[84] M. S. Turner and L. M. Widrow, Phys. Rev. D **37** (1988) 2743.

[85] B. Ratra, Astrophys. J. **391** (1992) L1.

[86] V. Demozzi, V. Mukhanov and H. Rubinstein, JCAP **0908** (2009) 025 [arXiv:0907.1030 [astro-ph.CO]].

[87] B. Himmetoglu, C. R. Contaldi and M. Peloso, Phys. Rev. D **79** (2009) 063517 [arXiv:0812.1231 [astro-ph]]. B. Himmetoglu, C. R. Contaldi and M. Peloso, Phys. Rev. D **80** (2009) 123530 [arXiv:0909.3524 [astro-ph.CO]].

[88] T. R. Dulaney and M. I. Gresham, Phys. Rev. D **81** (2010) 103532; arXiv:1001.2301 [astro-ph.CO].
A. E. Gumrukcuoglu, B. Himmetoglu and M. Peloso, Phys. Rev. D **81** (2010) 063528; arXiv:1001.4088 [astro-ph.CO].

[89] K. Dimopoulos, M. Karciauskas, D. H. Lyth and Y. Rodriguez, JCAP **0905** (2009) 013 [arXiv:0809.1055 [astro-ph]].
K. Dimopoulos, M. Karciauskas and J. M. Wagstaff, Phys. Lett. B **683** (2010) 298 [arXiv:0909.0475 [hep-ph]].
K. Dimopoulos, arXiv:1107.2779 [hep-ph].

[90] C. Armendariz-Picon, JCAP **0603** (2006) 002 [arXiv:astro-ph/0509893].

[91] G. V. Chibisov and Yu. V. Shtanov, Sov. Phys. JETP **69** (1989) 17 [Zh. Eksp. Teor. Fiz. **96** (1989) 32]; Int. J. Mod. Phys. A **5** (1990) 2625.
R. V. Buniy, A. Berera and T. W. Kephart, Phys. Rev. D **73** (2006) 063529; hep-th/0511115.
J. F. Donoghue, K. Dutta and A. Ross, Phys. Rev. D **80** (2009) 023526; astro-ph/0703455.
C. Armendariz-Picon, JCAP **0709** (2007) 014; arXiv:0705.1167 [astro-ph].
T. S. Pereira, C. Pitrou and J. P. Uzan, JCAP **0709** (2007) 006; arXiv:0707.0736 [astro-ph];
C. Pitrou, T. S. Pereira and J. P. Uzan, JCAP **0804** (2008) 004; arXiv:0801.3596 [astro-ph].
Y. Shtanov and H. Pyatkovska, Phys. Rev. D **80** (2009) 023521; arXiv:0904.1887 [gr-qc];
Y. Shtanov, Annalen Phys. **19** (2010) 332; arXiv:1002.4879 [astro-ph.CO].

[92] E. Akofor, A. P. Balachandran, S. G. Jo, A. Joseph and B. A. Qureshi, "Direction-Dependent CMB Power Spectrum and Statistical Anisotropy from Noncommutative Geometry," JHEP **0805**, 092 (2008) [arXiv:0710.5897 [astro-ph]].

[93] T. S. Koivisto and D. F. Mota, JHEP **1102** (2011) 061 [arXiv:1011.2126 [astro-ph.CO]].

[94] J. L. Lehners, Phys. Rept. **465** (2008) 223; arXiv:0806.1245 [astro-ph].

[95] A. Nicolis, R. Rattazzi and E. Trincherini, Phys. Rev. D **79** (2009) 064036 [arXiv:0811.2197 [hep-th]].

[96] A. Nicolis, R. Rattazzi and E. Trincherini, JHEP **1005** (2010) 095 [Erratum-ibid. **1111** (2011) 128] [arXiv:0912.4258 [hep-th]].

[97] D. A. Easson, I. Sawicki and A. Vikman, JCAP **1111** (2011) 021 [arXiv:1109.1047 [hep-th]].

[98] L. E. Allen and D. Wands, Phys. Rev. D **70** (2004) 063515; astro-ph/0404441.

[99] D. H. Lyth, Phys. Lett. B **524** (2002) 1; hep-ph/0106153.
R. Brandenberger and F. Finelli, JHEP **0111** (2001) 056; hep-th/0109004.
J. c. Hwang, Phys. Rev. D **65**, 063514 (2002), astro-ph/0109045.
A. J. Tolley, N. Turok and P. J. Steinhardt, Phys. Rev. D **69** (2004) 106005 [hep-th/0306109].

[100] J. Khoury and P. J. Steinhardt, Phys. Rev. Lett. **104** (2010) 091301 [arXiv:0910.2230 [hep-th]].

[101] A. Linde, V. Mukhanov and A. Vikman, JCAP **1002** (2010) 006 [arXiv:0912.0944 [hep-th]].

[102] J. Khoury and P. J. Steinhardt, Phys. Rev. D **83** (2011) 123502 [arXiv:1101.3548 [hep-th]].

[103] J. -L. Lehners, P. McFadden, N. Turok and P. J. Steinhardt, Phys. Rev. D **76** (2007) 103501 [hep-th/0702153 [HEP-TH]].

[104] A. J. Tolley and D. H. Wesley, JCAP **0705** (2007) 006 [hep-th/0703101].

[105] K. Koyama and D. Wands, JCAP **0704** (2007) 008 [hep-th/0703040 [HEP-TH]].

[106] J. -L. Lehners and P. J. Steinhardt, Phys. Rev. D **79** (2009) 063503 [arXiv:0812.3388 [hep-th]].

[107] S. Mukohyama, JCAP **0906** (2009), 001; arXiv:0904.2190 [hep-th].

[108] M. B. Voloshin and A. D. Dolgov, Sov. J. Nucl. Phys. **35** (1982) 120 [Yad. Fiz. **35** (1982) 213].

[109] S. R. Coleman, J. Wess and B. Zumino, Phys. Rev. **177** (1969) 2239. C. G. Callan, Jr., S. R. Coleman, J. Wess and B. Zumino, Phys. Rev. **177** (1969) 2247.

[110] D. V. Volkov, Fiz. Elem. Chast. Atom. Yadra **4** (1973) 3.

[111] M. Libanov and V. Rubakov, arXiv:1107.1036 [hep-th].

[112] S. R. Ramazanov and G. I. Rubtsov, JCAP **1205** (2012) 033 [arXiv:1202.4357 [astro-ph.CO]].

[113] D. Larson *et al.*, arXiv:1001.4635 [astro-ph.CO].

[114] E. Komatsu *et al.* [WMAP Collaboration], Astrophys. J. Suppl. **180** (2009) 330; arXiv:0803.0547 [astro-ph].

[115] A. R. Pullen and M. Kamionkowski, Phys. Rev. D **76** (2007) 103529 [arXiv:0709.1144 [astro-ph]].

[116] N. E. Groeneboom and H. K. Eriksen, Astrophys. J. **690** (2009) 1807 [arXiv:0807.2242 [astro-ph]].

[117] D. Hanson and A. Lewis, Phys. Rev. D **80** (2009) 063004 [arXiv:0908.0963 [astro-ph.CO]].

[118] N. E. Groeneboom, L. Ackerman, I. K. Wehus and H. K. Eriksen, Astrophys. J. **722** (2010) 452 [arXiv:0911.0150 [astro-ph.CO]].

[119] D. Hanson, A. Lewis and A. Challinor, Phys. Rev. D **81** (2010) 103003 [arXiv:1003.0198 [astro-ph.CO]].

[120] K. Hinterbichler, A. Joyce and J. Khoury, arXiv:1202.6056 [hep-th].

[121] M. Zaldarriaga, Phys. Rev. D **69** (2004) 043508 [astro-ph/0306006].

[122] P. Creminelli, Phys. Rev. D **85** (2012) 041302 [arXiv:1108.0874 [hep-th]].

[123] J. R. Fergusson, D. M. Regan and E. P. S. Shellard, arXiv:1012.6039 [astro-ph.CO].

[124] C. M. Hirata and U. Seljak, Phys. Rev. D **67** (2003) 043001 [arXiv:astro-ph/0209489].

[125] N. Jarosik, C. L. Bennett, J. Dunkley, B. Gold, M. R. Greason, M. Halpern, R. S. Hill and G. Hinshaw *et al.*, Astrophys. J. Suppl. **192**, 14 (2011) [arXiv:1001.4744 [astro-ph.CO]].

[126] http://lambda.gsfc.nasa.gov/

[127] K. M. Gorski, E. Hivon, A. J. Banday, B. D. Wandelt, F. K. Hansen, M. Reinecke and M. Bartelman, Astrophys. J. **622**, 759 (2005) [arXiv:0409513 [astro-ph]].

[128] S. P. Oh, D. N. Spergel, and G. Hinshaw, Astrophys. J. **510**, 551 (1999), [arXiv:9805339 [astro-ph]].

[129] K. M. Smith, O. Zahn, and O. Dore, Phys. Rev. D **76**, 043510 (2007), [arXiv:0705.3980 [astro-ph]].

[130] http://www.gnu.org/software/gsl/

[131] http://www.netlib.org/slatec/

[132] A. Lewis, A. Challinor and A. Lasenby, Astrophys. J. **538** (2000) 473 [arXiv:astro-ph/9911177].

[133] C. -G. Park, C. Park and J. R. Gott, III, Astrophys. J. **660** (2007) 959 [astro-ph/0608129].

[134] A. de Oliveira-Costa and M. Tegmark, Phys. Rev. D **74** (2006) 023005 [astro-ph/0603369].

[135] K. Land and J. Magueijo, Mon. Not. Roy. Astron. Soc. **357** (2005) 994 [astro-ph/0405519].

[136] M. Maris, C. Burigana, A. Gruppuso, F. Finelli and J. M. Diego, Mon. Not. Roy. Astron. Soc. **415** (2011) 2546 [arXiv:1010.0830 [astro-ph.CO]].

[137] P. D. Naselsky, A. G. Doroshkevich and O. V. Verkhodanov, Astrophys. J. **599** (2003) L53 [astro-ph/0310542].

[138] P. D. Naselsky, L. -Y. Chiang, P. Olesen and O. V. Verkhodanov, Astrophys. J. **615** (2004) 45 [astro-ph/0405181].

[139] P. D. Naselsky, A. G. Doroshkevich and O. V. Verkhodanov, Mon. Not. Roy. Astron. Soc. **349** (2004) 695 [astro-ph/0310601].

[140] F. K. Hansen, P. Cabella, D. Marinucci and N. Vittorio, Astrophys. J. **607** (2004) L67 [astro-ph/0402396].

[141] D. N. Spergel *et al.* [WMAP Collaboration], Astrophys. J. Suppl. **170** (2007) 377 [astro-ph/0603449].

[142] C. J. Copi, D. Huterer and G. D. Starkman, Phys. Rev. D **70** (2004) 043515 [astro-ph/0310511].

[143] C. Gordon, W. Hu, D. Huterer and T. M. Crawford, Phys. Rev. D **72** (2005) 103002 [astro-ph/0509301].

[144] J. J. Levin, Phys. Rept. **365** (2002) 251 [gr-qc/0108043].

[145] P. Bielewicz and A. J. Banday, arXiv:1012.3549 [astro-ph.CO].

[146] M. Hansen, J. Kim, A. M. Frejsel, S. Ramazanov, P. Naselsky, W. Zhao and C. Burigana, arXiv:1206.6981 [astro-ph.CO].

[147] P. D. Naselsky, P. R. Christensen, P. Coles, O. Verkhodanov, D. Novikov and J. Kim, Astrophys. Bull. **65** (2010) 101 [arXiv:0712.1118 [astro-ph]].

[148] M. Hansen, A. M. Frejsel, J. Kim, P. Naselsky and F. Nesti, Phys. Rev. D **83** (2011) 103508 [arXiv:1103.6135 [astro-ph.CO]].

[149] F. K. Hansen, A. J. Banday and K. M. Gorski, Mon. Not. Roy. Astron. Soc. **354** (2004) 641 [astro-ph/0404206].

[150] C. Gordon, Astrophys. J. **656** (2007) 636 [astro-ph/0607423].

[151] J. Hoftuft, H. K. Eriksen, A. J. Banday, K. M. Gorski, F. K. Hansen and P. B. Lilje, Astrophys. J. **699** (2009) 985 [arXiv:0903.1229 [astro-ph.CO]].

[152] H. K. Eriksen, A. J. Banday, K. M. Gorski, F. K. Hansen and P. B. Lilje, Astrophys. J. **660** (2007) L81 [astro-ph/0701089].

[153] F. K. Hansen, A. J. Banday, K. M. Gorski, H. K. Eriksen and P. B. Lilje, Astrophys. J. **704** (2009) 1448 [arXiv:0812.3795 [astro-ph]].

[154] K. Land and J. Magueijo, Phys. Rev. D **72** (2005) 101302 [astro-ph/0507289].

[155] D. J. Schwarz, G. D. Starkman, D. Huterer and C. J. Copi, Phys. Rev. Lett. **93** (2004) 221301 [astro-ph/0403353].

[156] D. J. Fixsen, E. S. Cheng, J. M. Gales, J. C. Mather, R. A. Shafer and E. L. Wright, Astrophys. J. **473** (1996) 576 [astro-ph/9605054].

[157] C. L. Bennett, A. Banday, K. M. Gorski, G. Hinshaw, P. Jackson, P. Keegstra, A. Kogut and G. F. Smoot *et al.*, Astrophys. J. **464** (1996) L1 [astro-ph/9601067].

[158] J. C. Mather, D. J. Fixsen, R. A. Shafer, C. Mosier and D. T. Wilkinson, Astrophys. J. **512** (1999) 511 [astro-ph/9810373].

[159] D. Babich, C. H. Blake and C. Steinhardt, arXiv:0705.0986 [astro-ph].